universität wien

DISSERTATION

Titel der Dissertation

Role of the β-propeller domain of low-density lipoprotein receptor in human rhinovirus infection

angestrebter akademischer Grad

Doktor/in der Naturwissenschaften (Dr. rer.nat.)

Verfasserin / Verfasser:	Mag. Tünde Konecsni
Matrikel-Nummer:	0014454
Dissertationsgebiet (lt. Studienblatt):	Molekulare Biologie
Betreuerin / Betreuer:	Univ.-Prof. Dr. Dieter Blaas

Wien, am 26. Februar 2010

Contents

1A. Abstract

Three members of the low-density lipoprotein receptor (LDLR) family, LDLR proper, very-LDLR (VLDLR) and LDLR-related protein (LRP) act as minor group human rhinovirus (HRV) receptors. Whereas ICAM-1, the receptor of the major group of HRVs, actively contributes to viral uncoating, minor group receptors were rather considered passive vehicles just delivering virus to the low pH environment of endosomes. However, the YWTD β-propeller domain of LDLR has been shown to be involved in the dissociation of bound LDL at acidic pH. We thus aimed to clarify whether it also actively contributes to HRV infection. No human cell line expressing LDLR in the absence of VLDLR or LRP is available. Therefore, CHO-*ldla7* cells which are deficient in endogenous LDLR and are stably transfected to express either wild-type or β-propeller negative human LDLR were used to investigate low pH-triggered conversion of HRV2 and its release from the receptor. Lower pH was required for conversion when HRV2 was attached to the propeller-negative LDLR, indicating that the high-avidity receptor-binding stabilizes the virus in its native conformation. Infection assays showed a delay in intracellular viral conversion, degradation, as well as in *de novo* viral synthesis in the absence of the β-propeller domain. We conclude that the function of the β-propeller at low pH is also significant when the ligand is a rhinovirus; it facilitates viral conversion within endosomes by decreasing the virus-stabilizing effect of the high avidity LDLR binding, and thereby promotes infection.

1B. Zusammenfassung

Drei Vertreter der *low-density* Lipoprotein Rezeptor Familie, *LDLR* selbst, *very-LDLR*, und *LDLR related protein* (LRP) werden von *minor group* Rhinoviren des Menschen (HRVs) als Rezeptoren verwendet. Während ICAM-1, der Rezeptor der *major group* der HRVs, aktiv am viralen *uncoating* beteiligt ist, wurden *minor group* Rezeptoren als passive Vehikel betrachtet, die das Virus in Endosomen transportieren, wo sie ein Milieu mit niedrigem pH vorfinden. Für die YWTD *β-Propeller* Domaine des LDL-Rezeptors wurde jedoch gezeigt, dass sie an der Abdissoziation gebundenen LDLs bei niedrigem pH beteiligt ist. Wir wollten daher herausfinden, ob sie auch aktiv an der Infektion mit HRVs teilnimmt. Es existiert keine humane Zell Linie, die *LDLR* in Abwesenheit von *VLDLR* oder *LRP* exprimiert. Daher wurden in unseren Untersuchungen CHO-*ldla7* Zellen verwendet, die keinen endogenen LDL-Rezeptor exprimieren. Diese waren stabil transfiziert um entweder Wildtyp oder *β-Propeller* negative humane LDL-Rezeptoren zu exprimieren. Mit Hilfe dieser Zellen untersuchten wir den möglichen Einfluss des β-Propellers auf die Konversion von HRV2 in subvirale Partikel als eine Funktion des niedrigen pH und die Freisetzung des Virus vom Rezeptor. Wenn HRV2 an propeller-negativen *LDLR* gebunden war ein niedrigerer pH wurde für die Konversion benötigt. Dies deutet darauf hin, dass die hoch-avide Rezeptorbindung das Virus in seiner nativen Konformation stabilisiert. Infektionsversuche zeigten eine zeitliche Verzögerung in der intrazellulären viralen Konversion, im Abbau und in der viralen *de novo* Synthese in der Abwesenheit der β-Propeller-Domaine. Wir schließen daraus, dass die Funktion des β-Propellers bei niedrigem pH auch dann signifikant ist, wenn der Ligand ein Rhinovirus ist. Er erleichtert die virale Konversion im Inneren von Endosomen, indem er den Virus-stabilisierenden Effekt des mit hoher Avidität bindenden *LDLR* reduziert. Dadurch begünstigt er die Infektion.

2. Introduction

2.1. Viruses

Viruses are sub-microscopic, obligate intracellular parasites, mobile genetic elements most probably of cellular origin, being engaged in a long co-evolution with their host. Viruses depend on specific host cells supplying the complex metabolic and biosynthetic machinery for their propagation. The viral nucleic acid contains the genetic information necessary to program the host cell for virus production. Because of their limited size, viral genomes code for only a few structural and some non-structural regulatory proteins which are necessary for their replication. The various viral components are synthesized separately within the cell and then they self-assemble to form progeny particles. A fully assembled infectious virus is called a virion. Its genome (DNA or RNA) is protected by a protein coat and eventually by an additional lipid bilayer (envelope) derived from host membrane, modified with virus encoded glycoproteins. The pathological symptoms are usually caused by the actions of the virus itself (e.g. killing the cells it infects), as well as by the immune response of the host. Since viruses depend on host survival for their own survival, they usually do not kill the host organism, at least not before they spread.

2.2. The family *Picornaviridae*

Human rhinoviruses (HRVs), the subjects of our investigations, belong to the family *Picornaviridae,* which name refers to the small size and the ribonucleic acid genome of these viruses. All members of the family are small, non-enveloped, icosahedral viruses with a single-stranded messenger-sense RNA genome (Stanway, 1990). With more than 200 serotypes this family comprises one of the largest groups of human and animal pathogens and has a considerable medical and economical importance. *Picornaviridae* is also one of the most diverse and oldest known virus families; poliomyelitis (caused by poliovirus) was reported already in Egyptian hieroglyphs, and foot-and mouth disease virus was the first animal virus discovered in 1898.

Picornavirus research has yielded numerous landmark discoveries in the development of modern virology and even biology in general, like the propagation of viruses in cultured cells, the development of inactivated and attenuated vaccines to prevent poliomyelitis, the demonstration of the first RNA-dependent RNA polymerase activity of an animal virus, the discovery of polyproteins as precursors of viral polypeptides, the first chemical structure of

the genome of an autonomously replicating RNA virus, the first 3D atomic resolution of an animal virus, the discovery of an internal ribosomal entry site to initiate translation of the uncapped picornavirus RNA, etc. (Semler and Wimmer, 2002).

Picornaviruses were originally classified on the basis of pathogenesis, biophysical properties (particle density, pH sensitivity), as well as serological relatedness. For example enteroviruses, cardioviruses, and hepatitis A viruses are acid stable surviving at pH 3, whereas rhinoviruses and aphthoviruses are labile at pH < 6. Due to the continuously increasing amounts of sequence and structural data, their classification is currently based on phylogenetic properties, and the family *Picornaviridae* is currently grouped into 8 genera (Table 1), *Enterovirus, Cardiovirus, Aphthovirus, Hepatovirus, Parechovirus, Erbovirus, Kobuvirus,* and *Teschovirus*.

Picornaviridae	
Genus	**Species**
Enterovirus	Human enterovirus A Human enterovirus B Human enterovirus C Human enterovirus D Simian enterovirus A Bovine enterovirus Porcine enterovirus A Porcine enterovirus B Human rhinovirus A Human rhinovirus B
Cardiovirus	Encephalomyocarditis virus (EMCV) Theliovirus (ThV)
Aphthovirus	Foot-and-mouth-disease virus (FMDV) Equine rhinitis A virus (ERAV)
Hepatovirus	Hepatitis A virus (HAV)
Parechovirus	Human parechovirus (HPeV) Ljungan virus (LV)
Erbovirus	Equine rhinitis B virus (ERBV)
Kobuvirus	Aichi virus (AiV) Bovine kobuvirus
Teschovirus	Porcine teschovirus (PTV)

Table 1. Classification of the family *Picornaviridae* based on the 8th International Committee for the Taxonomy of Viruses (ICTV) report (http://www.picornaviridae.com)

The taxonomy of *Picornaviridae* is continuously changing (http://www.picornaviridae.com). The Picornavirus Study Group has proposed some revisions including new genera, provisionally named "*Sapelovirus*", "*Senecavirus*", and "*Tremovirus*". The two human rhinovirus species have been moved to the genus *Enterovirus* which now also includes the recently discovered species C of HRVs (see below), and the former genus *Rhinovirus* does not exist any more. Three other picornaviruses, duck hepatitis virus 1, seal picornavirus 1**,** and human cosavirus**,** whose genomes have recently been sequenced, have been proposed to belong to novel genera.

The genus ***Enterovirus*** contains the most species and virus types. *Poliovirus*, which belongs to the human enterovirus C species and comprises 3 types, is the best studied member of the family. *Coxsackieviruses, echoviruses, human-, simian-, bovine-,* and *porcine-enteroviruses* also belong to this genus. These viruses infect mainly humans, spread through the faecal-oral route, and are transmitted directly from person to person. They are able to pass through the acidic environment of the stomach (they are stable at pH 3 or even below), and infect primarily cells of the intestinal epithelium and lymphoid cells of the gut. In addition to milder symptoms like common cold, intestinal disorders, and diarrhea, enteroviruses cause also severe illnesses as myositis, carditis, pharyngitis, pneumonitis, meningitis, and encephalitis. By entering the blood stream some strains can lead to systemic infections and sometimes even to infections of the central nervous system by crossing the blood-brain barrier. *Human rhinoviruses*, the most important etiologic agents of the common colds, have recently been integrated into this genus. They are adapted to replicate in the nasopharyngeal region, and especially during spring and autumn infect many people causing mild respiratory illness which often sets the stage for more severe infections by bacteria or other viruses.

Aphthoviruses infect the naso- and oropharyngeal regions of their hosts and they spread in the air. *Equine rhinitis A virus* is specific for horses. *Foot-and-mouth disease virus (FMDV)* infects cloven hoofed animals, especially cattle, goats, pigs, and sheep, causing the formation of blisters in the mouth and between the claws. It might lead to death of young animals through inflammation of the heart muscle, so it is of tremendous economic importance.

Cardioviruses, represented by *Encephalomyocarditis virus (EMCV)* and *Theilovirus (ThV)*, infect a number of different species, including humans, other primates, pigs, different rodents, birds, and even mosquitoes. Infection occurs orally and causes various symptoms depending on the particular virus and host, like gastrointestinal infections, acute myocarditis, encephalitis or abortions in sows. Human infection has been reported to involve the central nervous system but not to cause myocarditis (Scraba and Palmenberg, 1999).

Hepatoviruses include the *human hepatitis A virus* which causes roughly 50 % of acute viral hepatitis cases in humans. Transmission occurs via the faecal-oral route by uptake of

contaminated food or water. Replication occurs mainly in hepatocytes, but the virus is presumed to travel to the intestine via the bile duct.

Parechoviruses, comprising *human parechovirus (HPEV)* and *Ljungan virus (LV*), mainly cause diarrhea with eventual respiratory complications and are rarely associated with encephalitis and flaccid paralysis (Stanway and Hyypia, 1999).

The genus ***Kobuvirus*** consists of *Aichi virus*, *Bovine kobuvirus*, and a third candidate species that has recently been described in pigs (*Porcine kobuvirus*). Aichi virus was first recognised in 1989 as the cause of oyster-associated non-bacterial gastroenteritis in man (Yamashita et al., 1995).

The genus ***Erbovirus*** contains a single species, *Equine rhinitis B virus (ERBV)* with two serotypes, ERBV-1 and ERBV-2, causing acute respiratory disease in horses.

The genus ***Teschovirus*** consists of a single species, *Porcine teschovirus* causing encephalomyelitis in pigs.

2.3. Human rhinoviruses

HRVs account for more than 50 % of mild infections of the upper respiratory tract and thus are the major cause of the common cold in humans (Tyrrell and Parsons, 1960). The symptoms are sneezing, nasal obstruction, sore throat, headache, cough, and malaise. These viruses are sensitive to low pH (below pH 6) and require a temperature not exceeding 34°C; therefore, they grow best in the outer layer of the nasal mucosa. However, there are an increasing number of reports on replication of HRVs also in the lower airway system (Hayden, 2004; Mosser et al., 2002). Most of the respiratory illnesses caused by human rhinoviruses are benign, but symptoms may persist for several days, and the resultant interruption in school and work days may be substantial. Moreover, HRV infections can predispose to complications both in the upper and lower respiratory tract, and are connected with sinusitis, otitis media, exacerbation of asthma, chronic bronchitis, and cystic fibrosis (Heikkinen and Jarvinen, 2003; Pitkaranta and Hayden, 1998), especially in older adults and infants. HRVs spread from person to person, usually by direct contact or indirectly through the air.

HRVs are divided into two groups based on their receptor specificity. Most of the types (87; members of the major group) bind to human intercellular adhesion molecule 1 (ICAM-1) (Greve et al., 1989; Staunton et al., 1989; Tomassini et al., 1989). The remaining 12 types of the minor group attach to members of the low-density lipoprotein receptor (LDLR) family

including LDLR, very-LDLR (VLDLR), and LDLR-related protein (LRP) (Gruenberger et al., 1995; Hofer et al., 1994; Marlovits et al., 1998b; Marlovits et al., 1998c).

The 99 types of HRVs are phylogenetically classified into 2 species, HRV-A and HRV-B (Tidona and Darai, 2002). While the species HRV-A comprises both major and minor receptor group members, all types of the species HRV-B belong to the major receptor group.

Human rhinovirus A involves the following 74 types: HRV-1, 2, 7, 8, 9, 10, 11, 12, 13, 15, 16, 18, 19, 20, 21, 22, 23, 24, 25, 28, 29, 30, 31, 32, 33, 34, 36, 38, 39, 40, 41, 43, 44, 45, 46, 47, 49, 50, 51, 53, 54, 55, 56, 57, 58, 59, 60, 61, 62, 63, 64, 65, 66, 67, 68, 71, 73, 74, 75, 76, 77, 78, 80, 81, 82, 85, 88, 89, 90, 94, 96, 98 and 100.
Minor group viruses are underlined. HRV type 1 is divided into two subtypes, HRV-1A and HRV-1B.

Human rhinovirus B involves the following 25 types: HRV-3, 4, 5, 6, 14, 17, 26, 27, 35, 37, 42, 48, 52, 69, 70, 72, 79, 83, 84, 86, 91, 92, 93, 97 and 99.

Based on sequence analysis, human rhinovirus 87 turned out to be an enterovirus, most closely related to enterovirus 68 (Blomqvist et al., 2002; Savolainen et al., 2002). Recent observations showed that two serotypes, HRV23 and HRV25 earlier considered as major group viruses, rather behaved like minor group ones (Vlasak et al., 2005b). Furthermore, based on the high similarity in amino acid sequence of the capsid protein VP1 of HRV8 and HRV95, and of HRV-Hanks (H) and HRV21, the two pairs are now considered only two types.

Recently, a new phylogenetic group was identified but its properties with respect to receptor binding and entry have not been elucidated yet. These viruses have been called HRV-A2 due to their closer relationship with HRV-A in some analyses (Arden et al., 2006; McErlean et al., 2007) whereas others named them HRV-X (Kistler et al., 2007) or HRV-C (Lamson et al., 2006; Lau et al., 2007; Lee et al., 2007; McErlean et al., 2008). The taxonomic position of these viruses will be considered by the International Committee on Taxonomy of Viruses (ICTV) *Picornaviridae* Study Group in consultation with other HRV researchers.

2.4. The HRV genome

The first picornaviral RNA to be completely sequenced and cloned was that of type 1 poliovirus. Since then, sequence analyses of other species have shown that all picornaviruses share a similar genome organization. The single stranded RNA is infectious, as it is being directly translated after reaching the cytoplasm of the host cell. The central part of the ~7.1 kb

messenger sense HRV RNA encodes for a 2200 amino acid polyprotein in a single open reading frame (ORF). As shown in Fig.1, the coding region is flanked with substantially conserved untranslated regions (UTR), the 5' UTR (0.6-1.5 kb) containing an internal ribosome entry site (IRES) (Jackson, 2005; Pelletier and Sonenberg, 1988), regulatory sequences, and a small 3' UTR with poly-A tail. The IRES is about 400-450 nucleotides upstream of the translational start site (Andino et al., 1990). The *cis*-acting elements are required for translation, RNA replication and virulence. Instead of a cap structure well known for cellular mRNAs, a small virus encoded protein called VPg (virion protein genomic) is covalently linked via a phophodiester bond to the 5' UTR of the viral RNA. VPg has been shown to be essential for the protein-primed replication of both positive- and negative-stranded RNA (Nomoto, 1977; Wimmer, 1982).

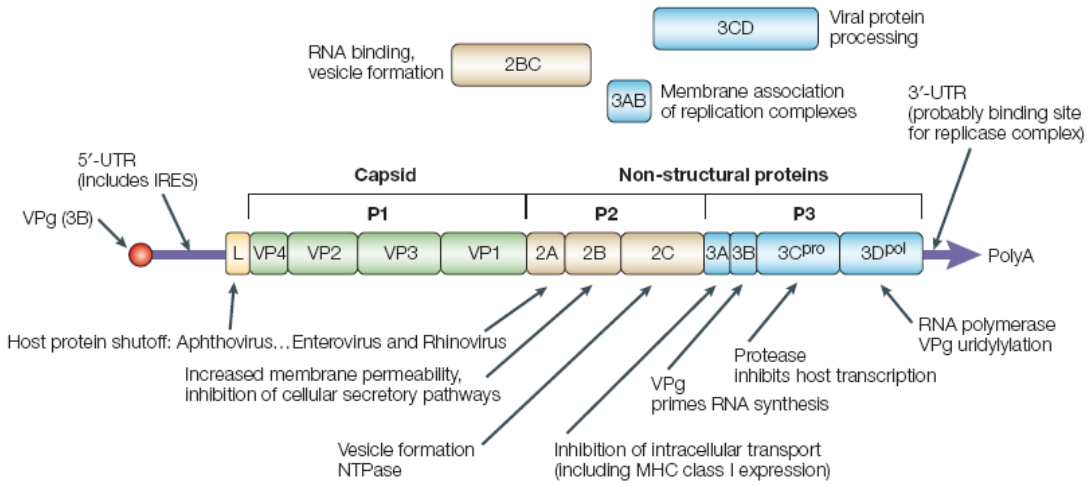

Figure 1. Genome organisation of picornaviruses. All structural and non-structural proteins and the 3 major cleavage intermediates together with their main biologic functions are shown (Whitton et al., 2005).

The central protein coding part of the picornavirus genome can be divided into three regions: P1, P2, and P3. The P1 region codes for the structural proteins (capsid proteins VP1 to VP4), while the P2 and P3 regions code non-structural proteins. The RNA is first translated into a polyprotein which is subsequently autocatalytically cleaved by viral proteases. Some intermediate cleavage products also have important functions in the replication cycle, usually different from that of the end products. The detailed functions of the different viral proteins are summarized in Fig. 1. Viral proteases such as 2A, 3C and the leader protein L in cardio-, aphtho-, erbo-, kobu-, and teschoviruses, are involved in the co-translational cleavage of the polyprotein and in the inhibition of host cell functions (Bernstein et al., 1985; Palmenberg et al., 1979; Toyoda et al., 1986). To promote the expression of the viral RNA, rhinoviruses inhibit the cellular cap-dependent translation via the cleavage of the cap binding protein eukaryotic initiation factor 4G (eIF4G) by the viral protease 2A. Proteins 2B and 2C determine the host range (Lomax and Yin, 1989; Yin and Lomax, 1983) and also play a role

in the rearrangement of the intracellular membrane network (Cho et al., 1994), while 2C, 3AB, VPg and RNA-polymerase $3D^{pol}$ are important for the replication of viral RNA (Flanegan et al., 1977; Li, 1988; Nomoto, 1977; Pallansch et al., 1980; Semler, 1981b; van Dyke et al., 1982). Recently, the complete sequences of all rhinoviruses and isolates known so far have been published, and are available in the GenBank (Palmenberg et al., 2009).

2.5. Capsid structure and functions

The protein coat of the non-enveloped rhinoviruses has several functions: it protects the RNA from environmental damages (such as nucleases), determines host range and tissue tropism by specific receptor recognition, delivers the viral RNA into the cytoplasm of host cells, selects and packs the viral genome during replication, and determines antigenicity.

The spherical capsids of human rhinoviruses are assembled from 60 protein subunits called protomers, each of which are composed of four structural proteins, viral protein 1 (VP1), VP2, VP3 and VP4 (Fig. 2). Five protomers build up a pentameric unit characterised by a five-fold axis, and twelve such pentamers form an icosahedral capsid with a diameter of ~30 nm. Three dimensional structures of five rhinoviruses at < 3 Å resolution have been determined by X-ray crystallography, HRV1A (Kim et al., 1989), HRV2 (Verdaguer et al., 2000), HRV3 (Zhao et al., 1996), HRV14 (Arnold and Rossmann, 1990; Rossmann et al., 1985) and HRV16 (Hadfield et al., 1997; Oliveira et al., 1993).

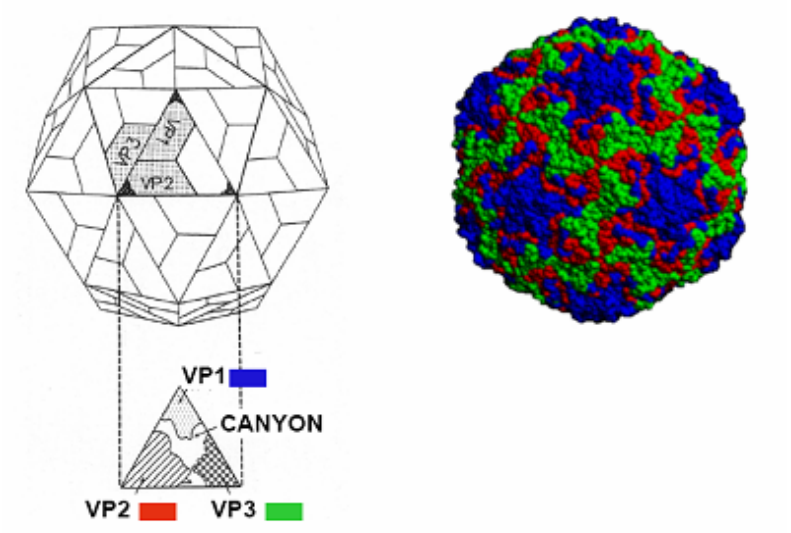

Figure 2. The icosahedral capsid of human rhinoviruses. Four viral proteins (VP1-VP3 external, VP4 internal) form a viral protomer, five such protomers are assembled into a pentamer, and twelve pentamers build up an icosahedral capsid. Around each five-fold axis there is a deep surface depression, called the canyon (Rueckert, 1996).

In the absence of significant sequence similarity, the proteins VP1 to VP3 share the same overall conformation, a wedge shaped β-barrel (the so-called "Swiss roll") built by eight antiparallel β-strands (Fig. 3) (Fields et al., 1996; Rossmann et al., 1985). The loops connecting the β-strands can accommodate extra segments leading to variations that give each subunit and each picornavirus its distinctive morphology and antigenicity. The external surface of the capsid is formed by VP1, VP2 and VP3, (molecular masses around 30 kD), VP1 being the immune-dominant and the most surface exposed one.

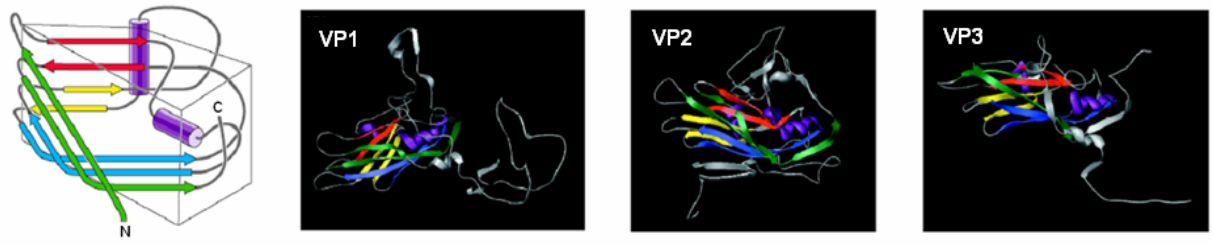

Figure 3. Structures of rhinovirus proteins. The topology of the polypeptide chain in a β-barrel jelly roll is shown at the left. The β-strands, indicated by arrows, form two antiparallel sheets juxtaposed in a wedge like structure. The two α-helices (purple cylinders) are also conserved in location and orientation. The loops connecting the β-strands in VP1, VP2 and VP3 vary considerably in length and conformation, particularly at the top of the β-barrel which corresponds to the outer surface of the capsid. (Flint et al., 2000)

While the carboxyl termini of these three proteins are at the surface of the virion, the amino termini face the interior. The smallest (7 kD) capsid protein VP4 lies at the inner surface close to the RNA and is in conjunction with the amino termini of VP1 and VP2. The picornavirus capsid is highly flexible, it temporarily exposes deeply buried parts of VP4 and the N-termini of VP1 proteins; this process is called viral „breathing" (Fricks and Hogle, 1990; Lewis et al., 1998; Li et al., 1994). The amino-terminal glycine of VP4 is linked to a myristic acid which is required for the assembly of the pentameric subunits and may also play a role in the release of VP4 during the uncoating process (Ansardi et al., 1992; Chow, 1987; Moscufo and Chow, 1992). The overall folding pattern is well preserved in proteins VP1, VP2 and VP3 in all studied rhinoviruses to date. The structural differences, determining the morphology and antigenicity of the types are mainly located at the external surface loops which connect the β-strands (Verdaguer et al., 2000).

2.5.1. The canyon and the hydrophobic pocket

In entero- and rhinoviruses each star-shaped plateau at the fivefold symmetry axes is surrounded by an about 15 Å deep and 12 Å wide cleft, called the „canyon" (Fig.4). It is formed by the junctions of VP1, VP2 and VP3. Conserved residues at the canyon floor constitute the attachment site for cellular receptors, as shown for major group rhinoviruses and ICAM-1 (Olson et al., 1993; Rossmann et al., 1985).

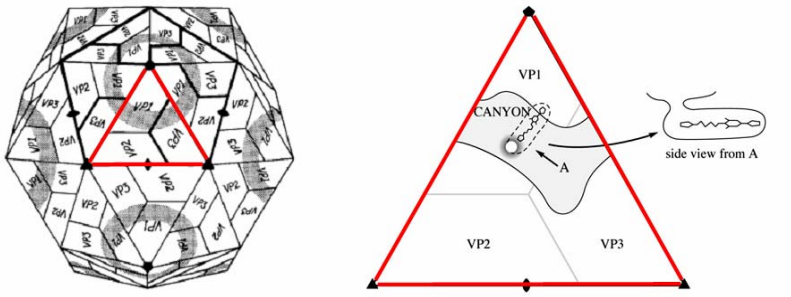

Figure 4. Schematic structure of the picornavirus capsid showing the canyons with grey circles. The enlarged view of a triangle shows the position of the pocket beneath the canyon floor. Modified after (Zhao et al., 1997).

In contrast, the minor group receptors bind at the star-shaped plateau at the fivefold axis, and not in the canyon (Hewat et al., 2000; Verdaguer et al., 2004). The function of the canyon was primarily proposed to hide the receptor binding site from the host immune surveillance (canyon hypothesis (Rossmann, 1989a, b)). However, the X-ray structure of an HRV14-Fab complex has challenged this hypothesis, showing that the antibody bound deep inside the canyon, to an epitope including conserved residues which also take part in receptor binding (Smith et al., 1996). Based on the present view, the canyon rather provides a conformationally sensitive region that may have a role in capsid destabilization during the uncoating process. It is also supported by the observation that ICAM-1 triggers viral uncoating and the subsequent RNA release (Rossmann et al., 2000).

Beneath the canyon floor there is a hydrophobic „pocket" (Fig.4). This area of the virus is fairly well conserved and is frequently found occupied by a sphingosine-like fatty acid or similar hydrophobic compound with a polar head group stemming from the cell (Rossmann et al., 2002). This so far chemically uncharacterized molecule is called natural pocket factor which is believed to play an important role in the viral life-cycle preventing premature RNA release by stabilization of the virion. The structures of a number of picornaviruses have been studied with different molecules bound within the pocket (Hogle et al., 1985; Oliveira et al., 1993; Smyth et al., 2003).

2.6. The HRV infection cycle

As depicted in Fig.5, after specific attachment and cell entry, HRVs of both receptor groups end up in endosomal compartments. For major group HRVs either ICAM-1 alone or in concert with the low pH environment triggers conversion into subviral particles and concomitantly RNA release (uncoating) (Bayer et al., 1999; Bayer et al., 1998; Brabec et al., 2003; Neubauer et al., 1987; Nurani et al., 2003). The replication takes place in the cytoplasm. The viral RNA is first translated into a polyprotein, and then structural and non-structural proteins are produced via autocatalytic cleavages. A viral protease ($2A^{pro}$) stops the cap-dependent translation of the host cell, cleaving eIF4G (this step is called host cell shut off). So the infected cell becomes a virus factory, producing viral proteins via IRES-dependent translation. The RNA replication takes place at virus induced membranous structures. First, a limited quantity of negative stranded RNA is produced. These serve as templates for the synthesis of positive strands. Finally, new viruses are assembled and leave the cell by lysis.

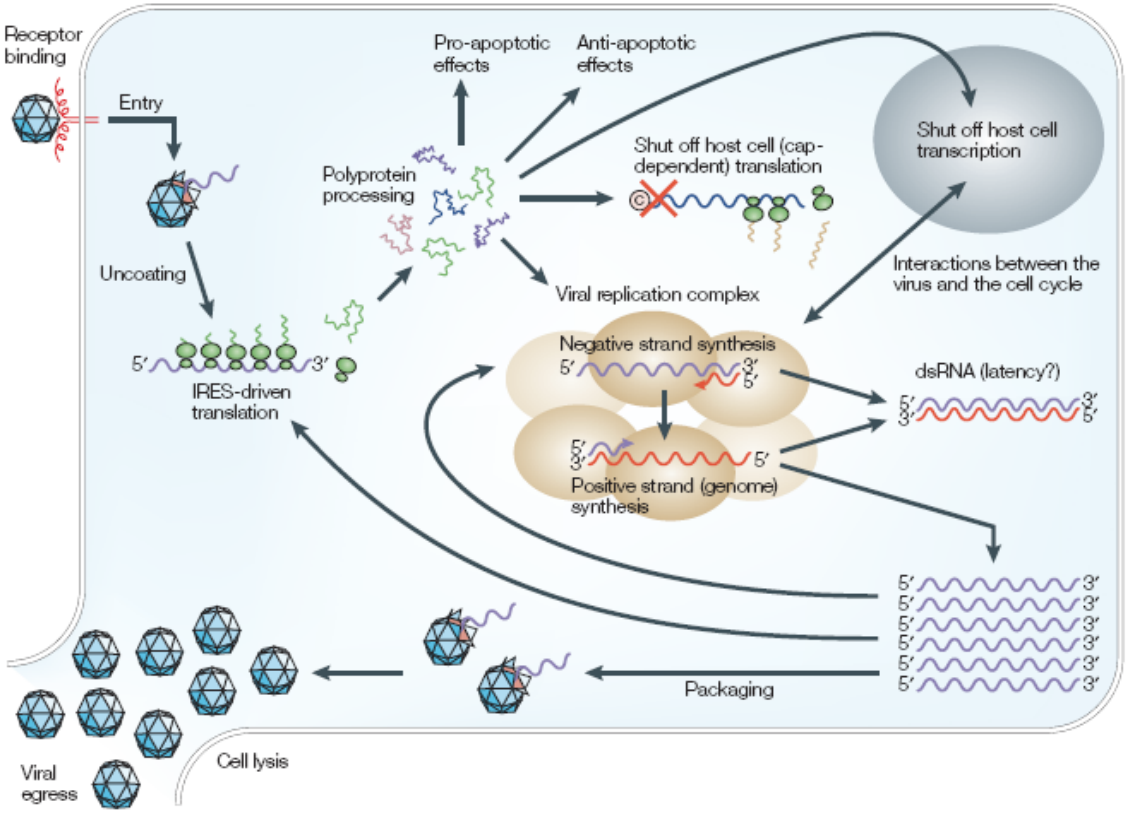

Figure 5. The infection cycle of picornaviruses. „©"represents the m7G cap, present on most host mRNAs. Positive-stranded viral RNA is shown in purple and negative-stranded RNA in red. dsRNA, double-stranded RNA; IRES, internal ribosome entry site. (Whitton et al., 2005)

2.6.1. Cell attachment and internalization

Human rhinoviruses (except of the types of HRV-C whose receptor is so far unknown) can be divided into two main groups based on receptor specificity (Abraham and Colonno, 1984; Uncapher et al., 1991): major group viruses bind to intercellular adhesion molecule 1 (ICAM-1) (Greve et al., 1989; Tomassini et al., 1989), whereas serotypes of the minor group were shown to bind various members of the low density lipoprotein (LDL) receptor family, like low-density lipoprotein receptor (LDLR), the LDLR-related protein (LRP), and the very-low-density lipoprotein receptor (VLDLR) (Hofer et al., 1994; Marlovits et al., 1998b; Marlovits et al., 1998d). Some major group HRV serotypes can also bind to heparan sulphate (Khan et al., 2007; Vlasak et al., 2005a).

While in major group HRVs the receptor binding site is located at the floor of the canyon, in minor group HRVs it is situated at the star-shaped dome of the five fold axis (Fig.6).

The binding site of ICAM-1 has been located at the base of the canyon by cryo-electron microscopy image reconstruction analysis of receptor-bound structures of HRV3 (Xing et al., 2003), HRV14 (Kolatkar et al., 1999) and HRV16 (Olson et al., 1993).

The VLDL receptor footprint in HRV2 is located at the star-shaped dome of the icosahedral fivefold axis, formed by the BC and HI loops of VP1 (Hewat et al., 2000). LDL-receptors, exemplified by V33333 (a concatemer of ligand-binding repeat 3 of human VLDLR), bind minor group rhinoviruses via multiple receptor modules by adopting a ring-like conformation around the vertices of the virion. As a result of this unique geometry, low-affinity interactions cooperate to achieve high avidity binding to twelve different HRV types featuring a single conserved lysine and a diffuse positive surface potential (Querol-Audi et al., 2009).

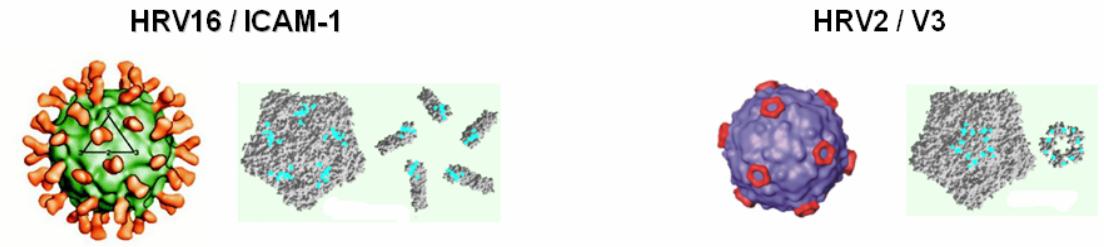

Figure 6. Comparison of the binding sites of V3 and ICAM-1 at the viral pentamer. Complexes between virus and soluble receptors were solved for HRV16 biding to a two-domain ICAM-1 by cryo-EM (PDB entry 1d3e) (Kolatkar et al., 1999), and for HRV2 binding to modules V2-3 of human VLDLR by X-ray (as V2 and V3 were undistinguishable, the model was done with V3; PDB entry 1v9u) (Hewat et al., 2000). The binding surface areas of both receptors are shown in cyan. Note that the binding modules of V2-3 molecules come so close to each other that they appear to form a ring (Fuchs and Blaas, 2008).

Cell entry by the minor group HRV2 occurs via clathrin-dependent endocytosis (DeTulleo and Kirchhausen, 1998; Snyers et al., 2003), however, when this pathway is blocked, HRV2 might also exploit other endocytosis routes (Bayer et al., 2001).

For the major group virus HRV14, DeTulleo and Kirchhausen demonstrated inhibition of entry upon expression of the dominant negative mutant dynamin^{K44A} (DeTulleo and Kirchhausen, 1998), and deduced that uptake was clathrin dependent. However, in view of the recent discovery of many pathways requiring dynamin function this is questionable. This is even more so as ICAM-1 does not possess clathrin entry motives and replacement of its cytoplasmic tail with a glycosylphosphatidylinositol anchor did not abrogate infection (Staunton et al., 1992). Investigations about HRV14 internalization presently ongoing in our lab also indicate that it is not clathrin dependent and rather appears to occur via a particular type of macropinocytosis (Khan et al., 2010).

2.6.2. Uncoating at low endosomal pH and RNA release into the cytoplasm

In vitro incubation at pH ≤ 3 inactivates all HRVs and this property was originally used for their classification (Tyrrell and Chanock, 1963). However, most HRVs already convert into subviral particles and thus lose infectivity at much higher pH values. For example, HRV2 readily experiences conformational modifications below a threshold pH of 5.6 *in vitro* and *in vivo* (Gruenberger et al., 1991; Prchla et al., 1994), and is inactivated within a range of about 0.6 pH units, following a sigmoid progression. On the other hand, some major group viruses were found to be more stable (Khan et al., 2007).

Following cell entry, HRVs of both receptor groups end up in endosomal compartments. For major group HRVs ICAM-1 (either alone or in concert with the low pH) triggers conversion into subviral particles and concomitantly uncoating and RNA release occurs (Nurani et al., 2003). In contrast, structural changes and infection of minor group HRVs, exemplified by HRV2, exclusively depend on the low endosomal pH, and it was believed that the function of LDL-receptors were limited to virus delivery (Baravalle et al., 2004; Brabec et al., 2003).

During infection native virus is first converted into subviral A-particles that still contain RNA but have lost the innermost capsid protein VP4. They no more attach to their respective receptors and are hydrophobic because of externalization of the amphipathic VP1 N-termini that are believed to insert into the lipid bilayer (Lonberg Holm et al., 1976). In a next step the RNA is transferred into the cytosol leaving empty hydrophilic subviral B particles behind. These processes happen at the endosomal membrane and are strongly coordinated. VP4 is able to induce membrane permeability (Davis et al., 2008), and most probably this protein is

responsible for pore formation observed during RNA release of minor group rhinoviruses. While the minor group virus HRV2 opens a pore in the membrane and the endosome remains largely intact, structural transition of the major group virus HRV14 results in disruption of the endosome (Fuchs and Blaas, 2008; Prchla et al., 1995; Schober et al., 1998). In case of HRV2 empty particles are left inside the endosome and are shuttled to lysosomes for degradation. Conversely, as HRV14 disrupts the endosome, not only the RNA but also viral proteins arrive into the cytosol. Therefore, the capsid of HRV14 is degraded to a much lesser extent, as it fails to reach the lysosomes.

The exact mechanism of RNA release and the exit point of RNA are not known. Since the uncoating intermediates (the 135S particles) are not stable for the long time needed for crystallization, no structural data about the RNA release are available. The present models for uncoating of the two rhinovirus groups (Hewat et al., 2002; Hewat and Blaas, 2004) are based on differences found between the 3D-structures of native and empty capsids of HRV2 and of HRV14 by cryo-electron microscopy, so there are still a lot of open questions.

2.6.3. Translation of the viral RNA, polyprotein processing and "host cell shut-off"

IRES

As the viral RNA is released into the cytoplasm, VPg is removed from its 5' end by cellular esterases (Gulevich et al., 2002), and translation is initiated by the protein synthesizing machinery of the host cell. In contrast to most cellular mRNAs, the translation of picornaviral RNA is not initiated in a cap-dependent manner, but at an internal ribosome entry site (IRES). This conserved region containing highly ordered secondary structures is situated in the 5' UTR of the viral RNA, and is about 450 nucleotides long.

Polyprotein processing

First, a large polyprotein precursor is synthesized which is then co-translationally processed into structural and non-structural viral proteins through a sequence of autocatalytic cleavages performed by virally encoded proteases. Figure 7 shows the processing events of rhino- and enteroviruses. Right after its translation, the 2A protease ($2A^{pro}$) adopts a three-dimensional structure competent for proteolytic processing. The first cleavage occurs between the C-terminus of VP1 and the N-terminus of $2A^{pro}$ in *cis,* at the P1/P2 junction, thereby separating the precursors of structural and non-structural proteins (Sommergruber et al., 1989; Toyoda et al., 1986). Further cleavages are performed by the protease $3C^{pro}$ and its precursor

3CD^{pro}. Precursor proteins (e.g., 2BC, 3AB, 3CD) have different functions as the mature cleavage products. The 3CD^{pro} undergoes an intramolecular self-cleavage (Palmenberg and Rueckert, 1982) which sets the 3C^{pro} and the RNA-dependent RNA-polymerase 3D^{pol} free. Then, 3C^{pro} cleaves in *trans* at all other cleavage sites (Palmenberg et al., 1979; Semler, 1981a) located within the P1, P2, and 3AB precursors. Finally, the cleavage of VP0 into VP4 and VP2 occurs upon virus assembly, which sets up the metastable state of the capsid. This maturation cleavage is thought to be autocatalytic and dependent on RNA encapsidation (Hindiyeh et al., 1999).

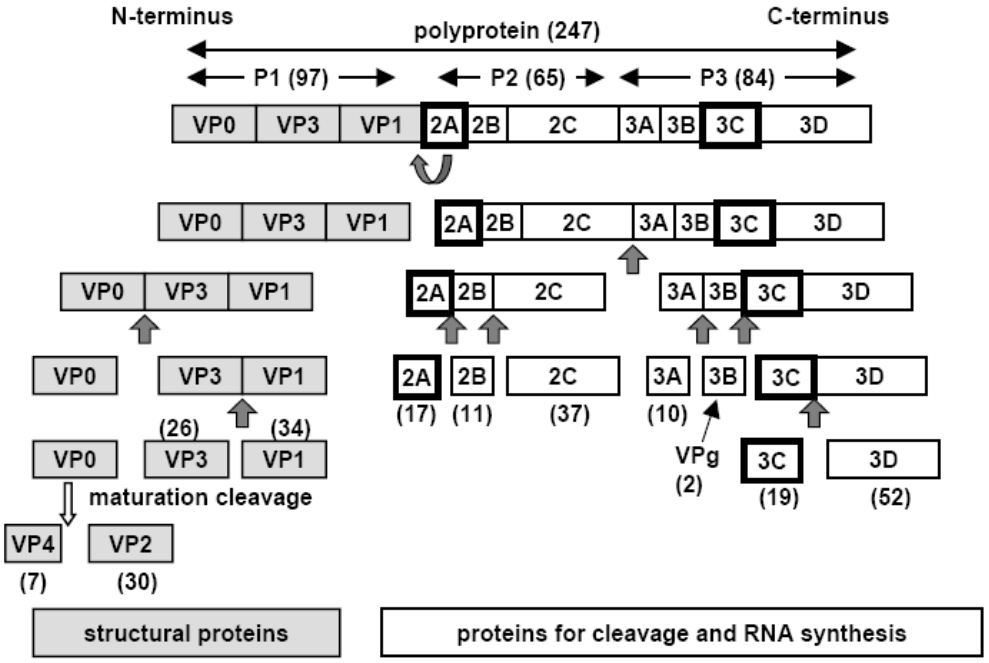

Figure 7. Cleavage pattern of picornaviral polyprotein processing. The primary cleavage is carried out by the 2A protease between its own N-terminus and the C-terminus of the P1 region. The viral protease responsible for the majority of polyprotein processing is the 3C protease, and its precursor 3CD. Numbers in brackets indicate the size of the proteins in kD (Figure adapted from B. Krenn).

Host cell shut off

The viral proteases also have several cellular targets; they cleave transcription and translation factors as well as cytoskeletal proteins (Joachims et al., 1999; Kuyumcu-Martinez et al., 2004; Neznanov et al., 2005; Seipelt et al., 2000). The cleavage of the cap-binding protein eukaryotic initiation factor 4G (eIF4G I, and its isoform eIF4G II) by 2A^{pro} leads to the inhibition of cap-dependent protein translation (Gradi et al., 1998; Haghighat et al., 1996; Kräusslich, 1987). This so called "host cell shut off" is a common strategy applied by viruses to facilitate the expression of their genomes by making the cellular translation factors available for virus production. Fig. 8 compares cap dependent and IRES dependent translation. After cleavage of eIF4G, its C-terminal fragment is no longer able to attach to the 5' cap, but instead it binds to the viral RNA with much higher affinity (Pestova et al., 1996).

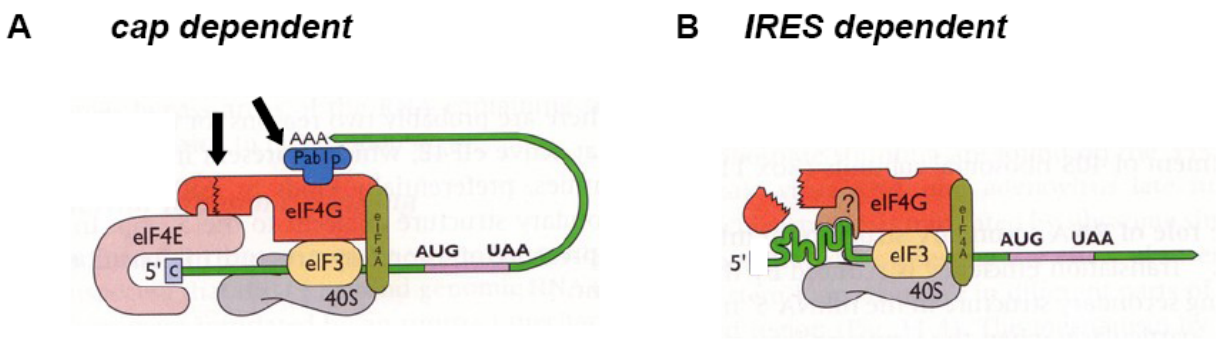

Figure 8. Cap-dependent (A) and IRES-dependent (B) initiation of translation. Arrows indicate the targets of the viral $2A^{pro}$ and $3C^{pro}$ [modified after (Flint et al., 2000)].

2.6.4. Viral RNA replication

For reviews see: (Agol et al., 1999; Andino et al., 1999). The positive-stranded HRV genome is amplified through a negative-stranded full-length RNA complement which serves as a template for the synthesis of new positive sense RNA strands. During the replication process three different forms of the viral RNA have been identified: ssRNAs with positive polarity, replicative intermediates with one positive and a few nascent negative strands, and full length double stranded replicative forms. In an infected cell, positive strands are present in vast excess over negative strands. Most of the non-structural viral proteins and several cellular proteins are involved in RNA replication. The virally encoded RNA-dependent RNA polymerase $3D^{pol}$ in conjunction with several other viral and cellular proteins performs the priming and synthesis of both positive and negative stranded progeny RNA molecules.

The replication occurs at the cytoplasmic surface of virus-induced membrane vesicles which build rosette-like structures around the replication complex (Bienz et al., 1992; Bienz et al., 1983; Egger et al., 2002). This compartmentalization helps to select the viral RNA out of the big pool of cellular RNA molecules, ensures a high local concentration of replicative proteins and RNA, and protects the templates even from nuclease attack. These membranes are thought to originate either from coat protein complex II-coated vesicles (Rust et al., 2001) or from autophagosomes (Jackson et al., 2005; Suhy et al., 2000). Phospholipid synthesis is also required for vesicle formation, which is triggered by the viral proteins 2BC and $2C^{ATPase}$ (Aldabe and Carrasco, 1995; Cho et al., 1994), and by a combination of 2BC and 3A (Suhy et al., 2000).

The assembly of the replication complex is driven by various *cis*-acting elements of the viral RNA. There is a cloverleaf structure at the 5' end which binds to 3CD and to the cellular poly-C binding protein, and is thought to have a regulatory role in the translation-to-

replication switch and in the assembly of the preinitiation complex (Gamarnik and Andino, 1998, 2000; Teterina et al., 2001). An internal RNA hairpin (*cis*-acting replication element (cre)) is involved in the recognition of viral RNA by the viral replicase complex. In the 3' UTR, sequences with conserved tertiary structures similar to "kissing" loops (Melchers et al., 1997; Pilipenko et al., 1996) or pseudoknots (Kusov et al., 1996) have been shown to interact with 3AB-3CD^{pro} (Harris et al., 1994). The preinitiation complex contains the RNA template and precursors of non-structural viral proteins (3AB, 3CD). 3AB anchors the viral protein VPg (3B) to virally induced membranes (Gerber et al., 2001; Towner et al., 1996). 3D^{pol} directly uridylates VPg which is then rapidly cleaved from its membrane-anchor by 3CD^{pro}. VPg-pU-pU-OH hybridizes with the 3' poly(A) tract of the RNA template and serves as a primer for 3D^{pol} (Paul et al., 1998), allowing for the synthesis of negative stranded RNA and the generation of a double stranded RNA intermediate. During elongation of negative strands, both homologous and non-homologous recombination events occur (Duggal and Wimmer, 1999; Jarvis and Kirkegaard, 1992). The genomic RNA must be first translated before it can serve as a template for replication (Novak and Kirkegaard, 1994). The reason for this is unknown; maybe the translation provides short-lived protein precursors (like 3AB and 3CD) which are necessary for replication.

Negative strand synthesis starts with the production of a short-lived intermediate containing the initial genomic RNA and its complementary negative-stranded RNA. Then, the new positive strands are synthesized whereby two adenines at the 3´ end of the negative stranded RNA serve as a VPg-pU-pU-OH primer binding site. RNA replication by the viral RNA-dependent RNA polymerase is error-prone and hence is accompanied by numerous mutations which result in an antigenic drift and a population of quasispecies, an important feature of viral evolution (Agol, 2006; Ward et al., 1988). As soon as positive strand synthesis has completed, the viral RNAs are released from the membrane-bound replication complexes. The new positive viral RNA strand can either be used as a template for further polyprotein synthesis or will be assembled into new virus particles.

2.6.5. Assembly, maturation, and release of new virus particles from the host cell

At later stages of infection, when the concentrations of both the newly synthesized genomic viral RNA and capsid proteins are high enough, assembly begins. First, VP1, VP3, and VP0 are assembled to 5S protomers. Then, five protomers form a 14S pentamer (Verlinden et al., 2000). Subsequently, the genomic VPg-RNA is packaged to form non-infectious 150S provirions, either via nucleation of 14S pentamers around the RNA genome or via threading the RNA into a preformed empty capsid; the underlying mechanism is not known. Finally, the short-lived provirion undergoes the maturation cleavage (Lee et al., 1993); VP0 is cleaved

into VP4 and VP2 by an autocatalytic mechanism (Bishop and Anderson, 1993; Basavappa et al., 1994). This cleavage sets up the metastable state of the capsid, thereby generating the infectious virion. While in cell culture the mature virus particles leave their host cells by lysis showing a cytopathic effect (CPE), in the nasal mucosa they are released by an unknown mechanism, without appreciable cell damage (Winther, 1994).

2.7. HRV and the common cold

2.7.1. Pathogenesis and clinical manifestations

Human rhinoviruses cause ~50 % of common colds and are a big economic burden in terms of lost working days. The incidence of infection is increased in fall and spring, with an average of 5 to 7 episodes per year in children, and 2 to 3 episodes per year in adults (Turner, 1997, 2001). HRV is transmitted by hand-to-hand contact or via aerosolization. The major entry point is normally the nose, and eventually the eyes (in this case drainage into the nasopharynx would occur through the nasolacrimal duct). In the nasal cavity the viruses target ciliated and non-ciliated epithelial cells by attachment to specific receptors. Lower respiratory epithelial cells are also susceptible to rhinovirus infection (Gern et al., 1997; Hayden, 2004; Mosser et al., 2002; Papadopoulos et al., 2000; Papadopoulos et al., 1999), however, the optimal growth temperature of most types (33°C) corresponds to the temperature of the nasal mucosa. The infection develops very quickly, after 8-10 hours progeny virus is already detectable (Heikkinen and Jarvinen, 2003). The first symptoms occur within 16 hours and peak on days 1-3 of infection. The median duration of illness is 9.5 to 11 days, but it can last even up to 16 days in certain populations such as young children and the elderly. The symptoms often start with a sore throat and continue with increased mucous secretion (runny nose) and sneezing caused by cholinergic stimulation. Nasal obstruction and rhinorrhea is caused by vasodilatation and increased vascular permeability of the mucosa (Heikkinen and Jarvinen, 2003). At later stages of the infection patients may suffer from facial pressure, headache and cough, caused by the big quantity of secreted mucus. Infants and young children may have even fever, which is not characteristic for adults. Although HRVs cause cytopathic effect (cell rounding, chromatin condensation, deformation of nuclei, detachment of the cells from their support, cell lysis) in cultured cells, no histopathological changes of the nasal epithelium has been observed in natural infections (Winther, 1994). The clinical symptoms are primarily caused by the inflammatory response of the host. While HRV infections are typically mild, they are associated with a number of upper and lower respiratory tract complications in both children and adults; see reviews (Heikkinen and Jarvinen, 2003; Monto et al., 2001; Pitkaranta and Hayden, 1998). Among bacterial

complications are acute otitis media (AOM), sinusitis, and pneumonia. Rhinovirus infections are associated with exacerbations of chronic respiratory diseases such as asthma (Gern, 2002), cystic fibrosis, and chronic obstructive pulmonary disease (COPD) (Anzueto and Niederman, 2003; Greenberg, 2002). Rhinovirus infection may have serious consequences for elderly people and for immunocompromised patients (Falsey et al., 2002).

2.7.2. Antiviral host defense mechanisms

Upon infection, viruses face powerful host defence mechanisms. First, at early time points of infection the secretion of type I interferons and proinflammatory cytokines and chemokines sets up the "antiviral state" in infected and non infected neighbouring cells. This inhibits viral replication, spread, and cell proliferation, and enhances the ability of natural killer cells to lyse virally infected cells (Samuel, 2001). Several immune mediators triggering inflammatory response have been identified in the context of rhinovirus infection. Among them are type I interferons (IFN-α, IFN-β), kinins, leukotrienes, histamine, interleukins (IL-1α, IL-1β, IL-6, IL-8, IL-11, IL-16), tumour necrosis factor-α (TNF-α), RANTES (regulated upon activation, normal T-cell expressed and secreted), granulocyte macrophage-colony stimulating factor (GM-CSF), growth-regulated oncogene-α (Gro-α), epithelial neutrophil-activating protein-78 (ENA-78), eotaxin 1/2, and macrophage inflammatory protein-1α (MIP-1α) (Donninger et al., 2003; Einarsson et al., 1996; Gern and Busse, 1999; Heikkinen and Jarvinen, 2003; Kim et al., 2000; Konno et al., 2002; Message and Johnston, 2004; Schroth et al., 1999; Subauste et al., 1995; Terajima et al., 1997; Zhu et al., 1996; Zhu et al., 1997). Different stress signals, such as increased levels of reactive oxygen intermediates (ROIs) and the presence of double stranded RNA, induce interferon production in the infected cells. DsRNA also increases the expression of Toll-like receptor 3 (TLR3) in infected host cells (Hewson et al., 2005), thereby enhancing the innate immune response. The cytokine production leads to increased endothelial cell permeability which allows the migration of immune cells to the site of infection. The clinical symptoms of rhinovirus infections are mainly caused by the activity of the host immune system; reviewed in (Kirchberger et al., 2007). The interferons released from infected cells diffuse to adjacent cells in the tissue, and activate the transcription of more than 30 genes via the JAK-STAT signal transduction pathway. Among these antivirally active proteins are the dsRNA-dependent protein kinase R (PKR), the 2'-5' oligoadenylate synthetase (OAS), endoribonuclease L (RNAse L), and a great number of other genes involved in the fundamental cellular metabolism. These proteins require also dsRNA as a co-factor to become activated, which is a characteristic condition for viral infections. Upon contact with dsRNA molecules PKR gets activated by autophosphorylation and gives rise to inhibition of both viral and cellular protein synthesis by phosphorylation of eIF2α (Kimball, 1999). OAS produces a series of short oligoadenylates containing an unusual 2’-5’-phosphodiester linkage (2’-5’-oligo(A)). These activate RNAseL which inhibits translation by efficient cleavage of

all types of ssRNAs (both viral and cellular RNAs including rRNA) (Castelli et al., 1998a; Castelli et al., 1998b).

Viral growth can also be limited by post-translational modifications; e.g. the IFN-inducible RNA-specific adenosine deaminase (ADAR1), a host RNA-editing enzyme, can introduce mutations into *de novo* synthesized viral genomes.

The immune response is mediated almost entirely by the innate system (e.g., complement, professional phagocytes, and natural killer cells) which removes viruses in a few days, still before the adaptive immune system becomes fully activated. Therefore, neutralizing antibodies are not made in sufficient amounts to effectively protect against the next rhinovirus infection, even by the same serotype. Moreover, the existence of more than 100 serotypes and the low level of antibody cross protection between them is a further reason for catching colds several times during our life.

2.7.3. Therapeutic treatments and antiviral strategies

Symptomatic treatments

There are a number of treatments focused on relieving the symptoms, increasing the comfort of the patient, and limiting complications (Anzueto and Niederman, 2003; Heikkinen and Jarvinen, 2003; Turner, 2001). In order to reduce fever and soreness of the throat non steroidal anti-inflammatory drugs such as aspirin or paracetamol, as well as localised versions targeting the throat (often delivered in lozenge form) are used. Nasal decongestants such as pseudoephedrine or oxymetazoline reduce the inflammation in the nasal passages and help to open the airways by constricting the dilatated blood vessels. First generation anti-histamines such as brompheniramine, chlorpheniramine, diphenhydramine and clemastine are frequently used for the reduction of sneezing and rhinorrhea. Ipratropium bromide, an anti-cholinergic nasal spray has been shown to reduce rhinorrhea by 30 % in natural colds. As cough medications, both mucolytic agents and cough suppressants are frequently used.

Antiviral treatment strategies

The large number of HRV serotypes is a great challenge for vaccine development. To date no vaccines against these viruses are available, because of little-to-no cross-protection between the different serotypes. Therefore, the strategy is to target specific steps of the infection cycle, like cell susceptibility, viral attachment, uncoating, RNA replication, and viral protein processing, to develop anti-HRV compounds; reviewed in (De Palma et al., 2008; Rotbart, 2002; Turner, 2001). The following section provides a brief overview about the different antiviral approaches against HRVs.

Inhibition of virus entry by different capsid binding agents

The determination of three-dimensional structures of rhinoviruses by X-ray crystallography has created the possibility to design several capsid-binding compounds. These chemicals block viral infection by inhibiting viral uncoating and/or viral attachment to host cell receptors.

The **WIN series of compounds** (Fig. 9) manufactured by the Sterling Winthrop Research Institute (McKinlay et al., 1992) played a remarkable role in the development of antiviral agents against both rhino- and enteroviruses. These small (~300 D) hydrophobic flexible organic compounds displace the natural pocket factor, bind inside the hydrophobic pocket with high affinity (Andries et al., 1991; Grant et al., 1994; Mosser and Rueckert, 1993; Smith et al., 1986), and make the virus more resistant to uncoating by increasing the stability of the capsid (Rombaut et al., 1991). These antiviral compounds block the attachment of major group HRVs and the uncoating of both major and minor group serotypes (Gruenberger et al., 1991; Pevear et al., 1989; Smith et al., 1986), and also stabilize rhinoviruses *in vitro* against denaturation by acidification and heat (Fox et al., 1986). However, clinical trials with WIN compounds (e.g. **Disoxaril**) or other capsid binders (e.g. **Pirodavir**) were not successful due to side effects (Rotbart, 2002; Turner et al., 1993) or the lack of clinical benefit (Hayden et al., 1995). Later, a new generation of capsid-binding drugs with better pharmacokinetics and metabolic stability with broad and potent antiviral activity were developed. The most successful agent in this series was **Pleconaril** which did not even show any adverse side effects (Florea et al., 2003; Hayden et al., 2002; Hayden et al., 2003a). However, due to interference with the pharmacokinetics of other drugs it was first rejected by the Food and Drug Administration (FDA) in 2001. Then, later in 2007, a phase II clinical trial was completed with this substance (De Palma et al., 2008).

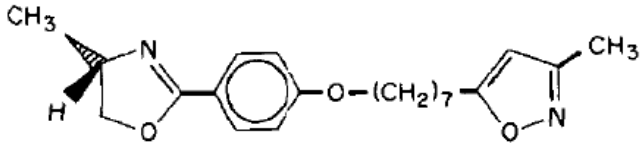

Figure 9. The chemical formula of the capsid binding agent I(S), also named WIN-52084, manufactured by the Sterling Winthrop Research Institute (Badger et al., 1989).

Infection can also be blocked by the inhibition of receptor attachment of virus particles using **soluble receptor fragments**. The **soluble ICAM-1, called Tremacamara**, reduced symptoms to some extent in experimentally induced HRV infections without significant side effects (Turner et al., 1999), but after a few passages *in vitro* viral resistance developed (Arruda et al., 1994). **Soluble VLDL receptor fragments** were also successfully applied to inhibit minor group infection *in vitro* (Marlovits et al., 1998c; Marlovits et al., 1998d).

Protease inhibitors

The viral 3C protease is a specific target for the development of antivirals, showing a great homology among HRV serotypes and several related picornaviruses, but not with cellular proteases. This unique structure together with its essential role in viral replication made $3C^{pro}$ an excellent target for the development of anti-picornavirus agents to inhibit viral polyprotein processing and protein synthesis (Patick and Potts, 1998; Wanga and Chen, 2007). The irreversible $3C^{pro}$ inhibitor **Rupintrivir (AG7088)** was the most promising drug candidate among the several substances synthesized, but recently it was halted from further development due to its inefficient antiviral activity when administered after 24 hours after virus inoculation (De Palma et al., 2008; Hayden et al., 2003b). However, novel protease inhibitors are still under development (Patick et al., 2005).

Inhibitors of viral RNA replication

Viral RNA replication is another specific target for antiviral therapy. **Enviroxime** inhibits the replication of rhino- and enteroviruses, even if it is administered several hours post infection. Initial studies suggested that it inhibits the initiation of positive-strand RNA synthesis by targeting 3A (Heinz and Vance, 1995), but its action turned out to be more complex and the exact molecular mechanism is still unclear (Brown-Augsburger et al., 1999). Unfortunately, it showed intolerance to oral dosing and only limited activity after intranasal administration despite its high potency in cell culture. Therefore its clinical development was discontinued (Anzueto and Niederman, 2003). Novel replication inhibitors keeping the properties of Enviroxime with a new chemical core structure were designed, however, so far no clinical trials have been reported (Hamdouchi et al., 2003).

Decreasing cell susceptibility to HRV infection

Nasal **interferon** was also tried as a therapeutic agent, since it is known to induce a cellular antiviral state. It could prevent rhinovirus infections, but showed just moderate effects when administered a day after experimental infection (Hayden and Gwaltney, 1984). Moreover, prolonged exposure induced side effects such as nasal irritation and stuffiness, mucosal ulceration, destruction of the nasal mucous membrane, and resistance against the drug (Hayden et al., 1986; Samo et al., 1983). A novel antiviral strategy is the search for natural or artificial **peptides or RNAs** that, upon expression, modify the cellular processes and thereby protect the cells against viral infection. A new peptide inhibitor identified by Poritz *et al.* by screening a high-complexity cDNA library, seems to interfere with the viral RNA-replication (Poritz et al., 2003).

Small interfering RNA

RNA silencing is also a new strategy to fight virus infection; see reviews (Gadkari, 2005; Tan and Yin, 2004). The appearance of double stranded RNA during viral replication would itself activate RNA interference, but viruses have evolved mechanisms to suppress this response. However, direct introduction of siRNA molecules (or vectors encoding them) into the cells were shown to specifically target the viral mRNA for degradation (Merl et al., 2005; Phipps et al., 2004). The next step towards clinical applications is the development of efficient siRNA delivery systems.

2.8. The major group receptor: ICAM-1

The 87 serotypes of the major group HRVs utilize the intercellular adhesion molecule 1 (ICAM-1, CD-54) as a receptor (Greve et al., 1989; Staunton et al., 1989; Tomassini et al., 1989). ICAM-1 is a transmembrane glycoprotein, a member of the immunoglobulin (Ig) supergene family (Simmons et al., 1988), composed of five glycosylated Ig domains at the N-terminus, a transmembrane region, and a short cytoplasmic tail at the C-terminus (Fig. 10). ICAM-1 is expressed by several cell types, e.g. at the surface of macrophages, B and T lymphocytes, fibroblasts, and cells of the vascular endothelium. It plays an important role in immune and inflammatory responses, as it is responsible for the adhesion between endothelial cells and leukocytes, allowing subsequent extravasation of leukocytes into the inflamed tissues. The ligands important in this process are two integrins, the lymphocyte function associated antigen-1 (LFA-1) and the macrophage-1 antigen (Mac-1) (Makgoba et al., 1988). The expression of ICAM-1 is regulated by cytokine signalling; it is normally present at the surface of cells at low concentrations (van de Stolpe and van der Saag, 1996), and cytokines like interleukin-1 (IL-1) and tumor necrosis factor alpha (TNFα) greatly increase its levels. Since an increased cytokine level is also a part of the host defense responding to rhinovirus infection, major group viruses increase the expression of their own receptor (Grunberg et al., 2000; Whiteman et al., 2003).

Residues important for HRV binding are located at the tip of domain 1 (D1), in the DE, BC and FG loops. Reconstruction of cryo-electron microscopy images of a soluble recombinant two-domain fragment of ICAM-1 (D1D2) in complex with HRV16 or HRV14 showed that the receptor binds at the bottom of the canyon (Rossmann et al., 1994). The natural pocket factor somewhat interferes with the major group receptor binding, by causing conformational changes in the canyon floor. However, due to its bigger affinity, ICAM-1 is able to replace this pocket factor and bind inside the canyon, by following a two-step kinetics (Rossmann et al., 2002). The interaction seems to be of electrostatic character, since the interacting surfaces

show a remarkable charge complementarity (Bella et al., 1999b; Giranda et al., 1990; Kolatkar et al., 1999; Olson et al., 1993). The binding site for Mac-1 is located in domain 3 whereas all other factors bind to domain 1 (Bella and Rossmann, 1999b; Rossmann et al., 2000) (Fig. 10). Major group HRVs bind exclusively to human ICAM-1, and they do not even recognize the homologous ICAM-2 or ICAM-3. ICAM-1 is also used as a receptor by other human pathogens like some coxsackievirus A family members (Shafren et al., 1997a), and erythrocytes infected by the malarial parasite *Plasmodium falciparum* (Berendt et al., 1992; Ockenhouse et al., 1992).

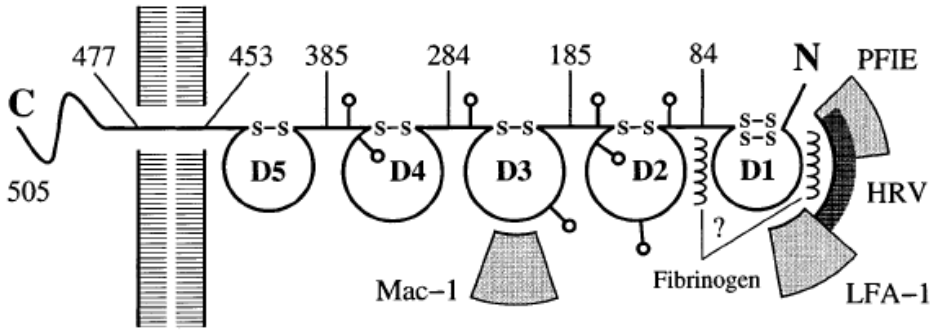

Figure 10. Schematic structure of ICAM-1. Each Ig domain is represented by a circle closed by one or two disulfide bonds. Amino acid numbers indicate the beginning and end of each domain. Lollipop-shaped structures indicate N-linked glycosylation sites. The approximate locations of binding sites of LFA-1, Mac-1, human rhinoviruses, fibrinogen, and *Plasmodium falciparum*-infected erythrocytes (PFIE) are indicated (Bella et al., 1999; Bella and Rossmann, 1999, 2000)

2.9. Minor group receptors: members of the LDLR family

2.9.1. Identification of the minor group receptors

Twelve HRV types, the minor group, use members of the low-density lipoprotein receptor (LDLR) family (Herz and Bock, 2002) for cell attachment and entry. The first minor group receptors identified were LDLR and the large subunit of the α_2-macroglobulin receptor/ LDLR-related protein (LRP) (Hofer et al., 1992). Further investigations showed that soluble recombinant fragments encompassing the binding repeats of human LDLR and of human very low-density lipoprotein receptor (VLDLR) bind minor group HRVs. Such soluble minireceptors interfere with attachment to natural cell surface receptors by competition, thus inhibiting viral infection in a concentration dependent manner (Marlovits et al., 1998a, b; Marlovits et al., 1998c).

2.9.2. Members of the LDLR family

The structurally closely related cell surface receptors belonging to the LDL receptor gene family fulfil diverse functions in different organs, tissues, and cell types; they are ubiquitously expressed and highly conserved throughout different species. **Family members** expressed in mammals (Fig. 11) include the low-density lipoprotein receptor (LDLR) (Brown and Goldstein, 1986; Yamamoto et al., 1984), the very low-density lipoprotein receptor (VLDLR) (Sakai et al., 1994), apolipoprotein E receptor 2 (apoER2) (Kim et al., 1996), the LDLR related protein (LRP) (Herz et al., 1988), LRP5, LRP6, megalin (also known as gp330 or LPR2) (Saito et al., 1994), LRP1b (Liu et al., 2000) and multiple epidermal growth factor containing protein 7 (MEGF7) (Nakayama et al., 1998).

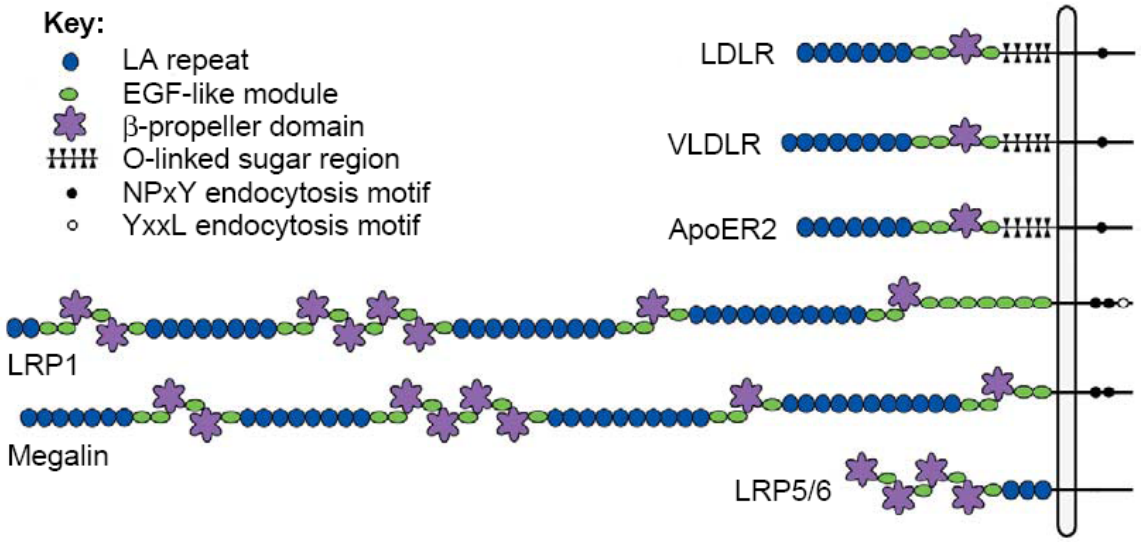

Figure 11. The LDLR family. The domain organization of the core family members is illustrated schematically. Abbreviations: LDLR, low-density lipoprotein receptor; VLDLR, very-low-density lipoprotein receptor; ApoER2, apolipoprotein E receptor 2; LRP, LDL-receptor-related protein (Beglova and Blacklow, 2005).

The **modular architecture** of these proteins has allowed the evolution of complex and highly specialized functions. All family members share common motifs: complement-type A repeats (ligand binding domains), epidermal growth factor (EGF) precursor homology domains, β-propeller domains, a single transmembrane region, and a short cytoplasmic tail with an internalization signal. The ligand binding domain(s) of these receptors is/are built by several **cysteine rich complement-type A repeats**, LDLR has 7, VLDLR has 8, and LRP contains 31 such repeats. They can bind many unrelated proteins, such as apolipoproteins, proteases, protease-inhibitor complexes, signaling molecules such as reelin, and several other types of proteins and low-molecular weight compounds. The ligand binding repeats are formed by roughly 40 residues arranged in two loops, held together by three disulfide bonds. The coordination of calcium is essential for the correct folding as well as for the maintenance of

the 3D structure of the repeats (Rudenko and Deisenhofer, 2003). The **EGF-like repeats** (named so because of their homology to the epidermal growth factor) are small, disulfide containing modules which also possess Ca^{2+} binding sites. The **YWTD β-propeller** is built of six blades, each made up of a β-sheet with four antiparallel strands. Its name comes from the characteristic YWTD (Tyr-Trp-Thr-Asp) consensus sequence found on the second strand of each blade. At the carboxy terminus of the extracellular portion of LDLR, VLDLR and ApoER2, there is a **highly O-glycosylated region** rich in serine and threonine residues. The intracellular regions of these receptors possess an internalization signal, an **NPxY** motif which directs the receptors into clathrin-coated pits.

2.9.3. The diverse functions of LDLR family members

The functions of LDLR family members (Fig. 12) are much more diverse than originally thought. They bind proteases, protease inhibitors, signaling molecules, heat shock proteins, vitamin carriers, toxins, antibiotics and many other molecules (Basu et al., 2001; Gliemann, 1998; Herz, 2001b; Howell and Herz, 2001; Schneider and Nimpf, 2003). These receptors are not only important in endocytic uptake of their ligands, but also in many cellular functions, including migration, pericellular proteolysis, signal transduction, antigen presentation and synaptic plasticity. The LDL-receptor-related protein (LRP) and megalin, two scavenging receptors produced in the liver and kidney, respectively, bind to more than two-dozen different ligands each (Nykjaer and Willnow, 2002).

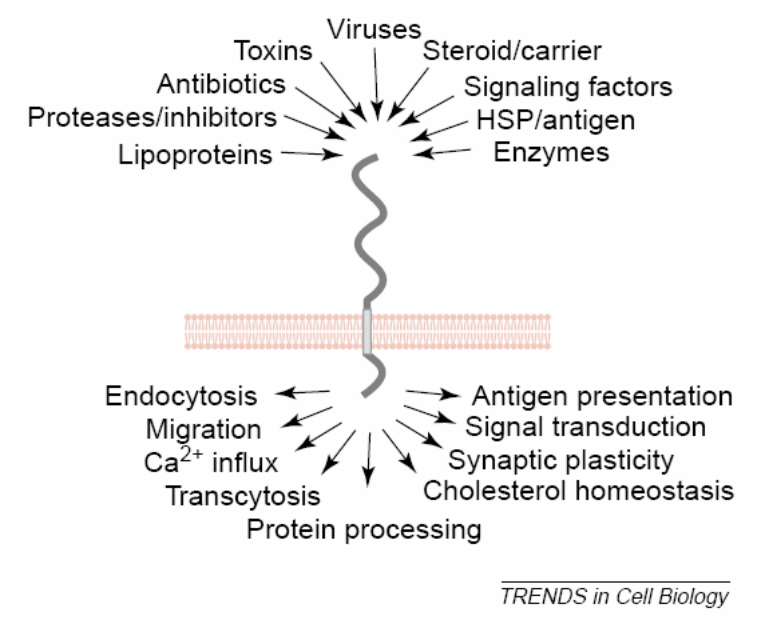

Figure 12. Cellular activities and putative functions of members of the LDLR family (Nykjaer and Willnow, 2002)

The multifunctionality of these receptors is achieved in part by the number of complement-type A repeats (e.g. 31 in LRP and 36 in megalin) and the use of co-receptors. Interaction with diverse cell-surface proteins such as seven-transmembrane-span receptors, ion channels, adhesion molecules or glycosylphosphatidylinositol (GPI)-anchored proteins provides activities not usually observed for endocytic receptors. The molecular interactions of this protein family with other cell-surface proteins are reviewed in (Nykjaer and Willnow, 2002).

2.9.4. LDL-receptor

The **LDL-receptor** is the prototype of the LDLR gene family; see a recent review (Jeon and Blacklow, 2005). This 120 kD cell-surface glycoprotein mediates the cellular uptake of cholesterol-containing lipoprotein particles, playing an important role in the homeostatic control of blood cholesterol level (Brown and Goldstein, 1986). This occurs in all nucleated cells but mainly in the liver which removes ~70 % of LDL from the circulation.

The LDLR gene and its expression

The LDL-receptor was originally identified by Brown and Goldstein in 1973, during their search for the molecular basis of familial hypercholesterolemia (Brown and Goldstein, 1986; Goldstein et al., 1985; Hobbs et al., 1990). A decade later its gene was cloned and sequenced. It is more than 45 kb long and contains 18 exons resulting in a 5.3 kb long mRNA (Russell et al., 1984; Yamamoto et al., 1984). The **expression of the LDL-receptor gene is regulated by the intracellular cholesterol level** (Sudhof et al., 1985; Zubay, 1998). The synthesised LDLR is co-translationally directed into the ER by its N-terminal hydrophobic signal sequence which is then cleaved off. In the ER receptor associated protein (RAP), a specific molecular chaperone, binds to the ligand binding repeats of LDLR and prevents its premature interaction with ligands. RAP dissociates from the receptors in early Golgi compartments and recycles back to the ER (Herz and Marschang, 2003). The LDL-receptor is subjected to **post-translational glycosylation** by the processing machineries of the ER and the Golgi. The final molecular mass is dependent on the degree of N- and O-glycosylation and ranges between 115 and 160 kD (Cummings et al., 1983; Tolleshaug et al., 1982; Yamamoto et al., 1984). Concomitantly with this maturation, the receptor travels through the secretory pathway and finally the mature protein appears at the cell surface in coated pits.

Ligand binding of LDLR

LDL-receptor binds to two proteins: to the 400 kD apolipoprotein B-100 (apoB-100) with a lower, and to the 34 kD apolipoprotein E (apoE) with a higher affinity. These are both essential components of plasma lipoproteins.

Approximately 65-70 % of plasma cholesterol in humans circulates in the form of **LDL** (Brown and Goldstein, 1974a, b) which is the most important physiologic ligand of the LDL-receptor. The ~180-250 Å LDL particle contains a single copy of the 4536 residues long glycoprotein **apoB-100** (Chen et al., 1986; Knott et al., 1986) that binds to LDLR with a stoichiometry of 1:1 (van Driel et al., 1989). For a review about the structure of apoB-100 in LDL particles see (Segrest et al., 2001).

LDLR also binds to lipoproteins that contain multiple copies of **apoE**, such as β-migrating forms of very low-density lipoprotein (**β-VLDL**) or certain intermediate- (**IDL**) and high-density lipoproteins (**HDL**) (Innerarity and Mahley, 1978; Innerarity et al., 1978; Mahley and Innerarity, 1983; Weisgraber et al., 1978). Lipoproteins containing ApoE recognize all the core members of the LDLR family possessing tandem repeats of LDL-A modules (LDLR, VLDLR, apoER2, LRP-1, and LRP-2). ApoE is a small two-domain protein (299 residues) (Aggerbeck et al., 1988; McLean et al., 1984; Rall et al., 1982; Wetterau et al., 1988) which has four known isoforms in humans. The E2 isoform is defective in receptor binding (Weisgraber et al., 1982), and the less common E4 allele is considered a risk factor for Alzheimer's disease (Strittmatter et al., 1993). The N-terminal domain of apoE takes part in LDLR binding, whereas the C-terminal domain is required for incorporation into lipoproteins (Innerarity et al., 1983; Wetterau et al., 1988). Complexation of apoE with lipid is a requirement for high-affinity interaction with its receptors; the delipidated apoE shows at least 500-fold lower affinity (Innerarity et al., 1979; Pitas et al., 1979; Weisgraber et al., 1994; Wilson et al., 1991).

Recycling of the LDLR

The same LDLR molecule can be used several times for internalization of ligands. Its recycling is shown in Fig. 13. Plasma lipoproteins bind to LDL receptors which cluster at the surface of cells in clathrin-coated pits. Subsequently, the lipoprotein-receptor complexes are taken up via endocytosis (Anderson et al., 1977; Anderson et al., 1976; Anderson et al., 1978). Within the lumen of endocytic vesicles the LDL-receptor undergoes conformational changes which lead to ligand release (Beglova et al., 2004b; Jeon and Blacklow, 2005). While the lipoproteins are delivered to lysosomes, the receptors are returned to the cell surface in a

process called receptor recycling (Brown and Goldstein, 1983; Goldstein et al., 1985; Jeon and Blacklow, 2005)

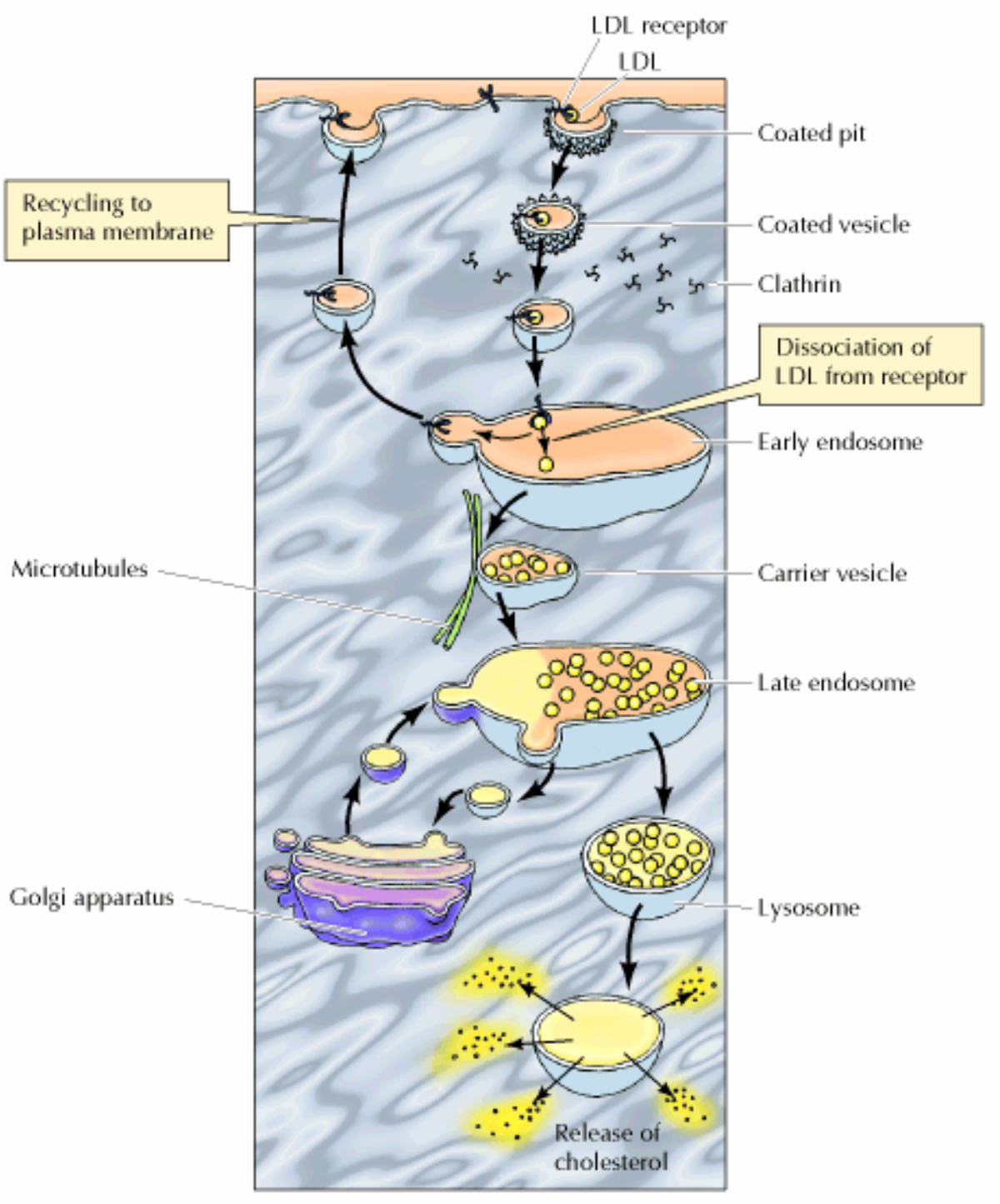

Figure 13. Endocytosis and intercellular routes of LDLR. The receptor-ligand complex is internalized via clathrin-coated vesicles which then fuse with early endosomes. At the low-pH environment of the early endosome LDL dissociates from the receptor and is transported to late endosomes in large carrier vesicles that move along microtubules. Transport vesicles carrying lysosomal hydrolases from the Golgi apparatus then fuse with late endosomes which mature to lysosomes where LDL is degraded and cholesterol is released. The LDL receptor is recycled from early endosomes to the plasma membrane (Cooper, 2000).

The modular architecture of LDLR

The mature 839 residues long human LDLR is a modular type 1 transmembrane protein, composed of various independently folded domains with different functions (Russell et al., 1984; Sudhof-TC et al., 1985; Sudhof et al., 1985; Yamamoto et al., 1984). Figure 14 shows the structural architecture of the receptor with molecular details elucidated by different research groups.

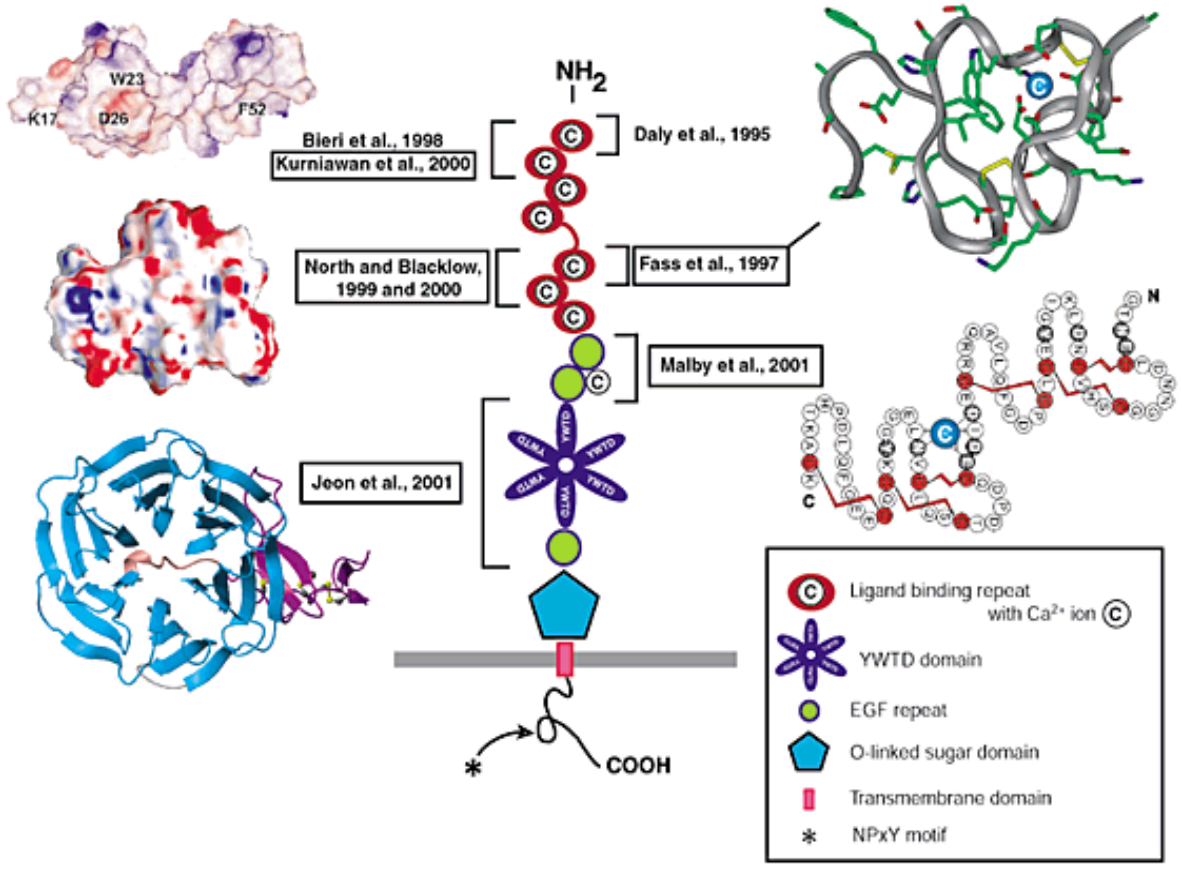

Figure 14. Domain organization of the LDLR. Boxed references next to structural representations indicate the cited publication from which the respective structure has been reproduced (Herz, 2001a).

The **ligand binding domain** (292 residues at the N-terminus) contains seven homologous cysteine rich repeats which are referred to as LDL receptor type A (LA) repeats or occasionally complement-type A repeats because such modules are also present in the terminal components of the complement cascade (Chakravarti et al., 1989; DiScipio et al., 1988; Haefliger et al., 1987; Howard et al., 1987; Rao et al., 1987; Stanley et al., 1985). The three-dimensional structure of the ligand binding repeats has been determined both by NMR-spectroscopy (Daly et al., 1995) and X-ray crystallography (Fass et al., 1997). Furthermore, the X-ray structure of the whole extracellular domain of human LDLR at low pH (Rudenko et al., 2002), and also the interdomain flexibility measured by NMR have been

reported (Beglova et al., 2004a). Each of ~40 residues long repeat is formed by two loops which are held together by three disulfide bonds in a conserved I-III, II-V, and IV-VI pattern (Bieri et al., 1995a; Bieri et al., 1995b). As shown in Fig. 15, each repeat coordinates a single Ca^{2+} ion which is essential for both correct folding and maintenance of the three-dimensional structure (Atkins et al., 1998; Bieri et al., 1998; Fass et al., 1997). The ligand binding repeats are connected with short flexible linkers (Bieri et al., 1998; Kurniawan et al., 2000; North and Blacklow, 1999) which allow for conformational rearrangements, and enable binding to many different ligands.

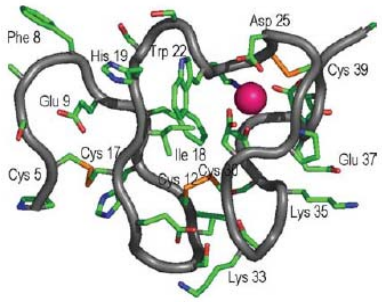

Figure 15. 3D X-ray structure of the fifth ligand-binding module of LDLR (PDB accession code 1AJJ). The critical bound calcium ion is illustrated as a (*red*) sphere. Side chains are superimposed on a (*grey*) ribbon trace of the module backbone. Cysteines and additional residues are labeled as reference points (Fass et al., 1997; Jeon and Blacklow, 2005).

The ligand binding repeats of LDLR are similar but not identical in their sequence. Conserved are the six cysteins, two hydrophobic residues near the N-termini, and an acidic cluster near the C-termini of the modules (Fig. 16). Mutagenesis studies of the seven LA modules have shown that the different repeats are not functionally equivalent in ligand binding. LA repeats 3-7 and also the first EGF-like repeat (EGF A) are essential for LDL (apoB-100) binding. In contrast, deletion of module five abrogates only high-affinity binding to β-VLDL (apoE) (Esser et al., 1988; Russell et al., 1989). The first two LA repeats contribute to LDL and β-VLDL binding only to a small extent (Sass et al., 1995).

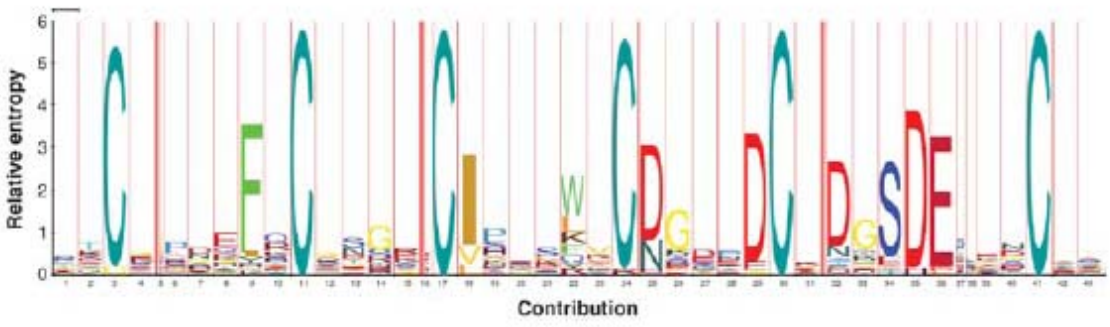

Figure 16. Sequence alignment of all LA modules from the database, illustrated using a sequence logo. The relative representation of each amino acid residue at every position in the sequence is proportional to the size of the letter at that site. Highly conserved are the six cysteines, two hydrophobic residues (Phe and Ile) in the N-terminal half of the module, and the cluster of acidic residues near the C-terminal end of the module (Crooks et al., 2004; Jeon and Blacklow, 2005).

Adjacent to the ligand binding domain there is a 400 residues long region with remarkable similarity to the epidermal growth factor (EGF) precursor, called **EGFP domain**. It is composed of two cysteine-rich calcium-binding EGF-like repeats (EGF-A and -B) (Malby et al., 2001), followed by a six bladed β-propeller containing a conserved YWTD (Tyr-Trp-Thr-Asp) motif (Springer, 1998), and a third EGF repeat (EGF-C). The EGFP domain controls the processes of lipoprotein release triggered by low endosomal pH, and the recycling of LDLR to the cell surface (Davis et al., 1987a).

The EGFP domain can be divided into two distinct parts: the EGF-AB domain pair (Kurniawan et al., 2001; Saha et al., 2001) and the β-propeller-EGF-C domain pair (Jeon et al., 2001; Rudenko et al., 2002) which both have a fixed interdomain relationship through the whole physiologic pH range. The structure of the EGF-AB pair shows an extended, rod-like conformation (Fig. 17), with an interdomain interface defined by calcium coordination and hydrophobic interactions.

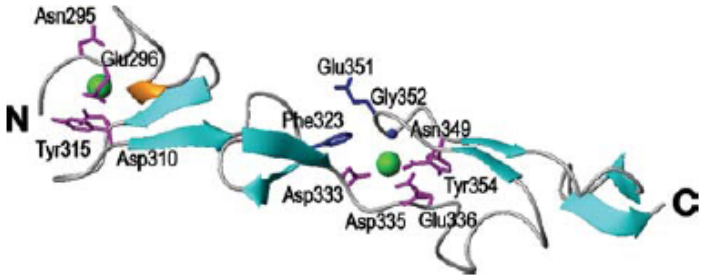

Figure 17. Structure of the EGF-AB domain pair [PDB accession code 1HJ7]. The intermodule interface is stabilized by a bound calcium ion (*green*) and hydrophobic packing of Phe 323 (*blue*) against the aliphatic portion of Glu 351 and the hole around Gly 352 (*blue*). The side chains of calcium-coordinating residues are illustrated (*purple*) (Jeon and Blacklow, 2005; Saha et al., 2001).

The YWTD domain, as confirmed by its 1.5 Å resolution X-ray structure (Jeon et al., 2001), is a six-bladed β-propeller, and shows an unexpected packing interface between the propeller and the third EGF module (E3 or EGF-C). Although the EGF-B module was also present, its position was disordered in the crystals (Fig. 18).

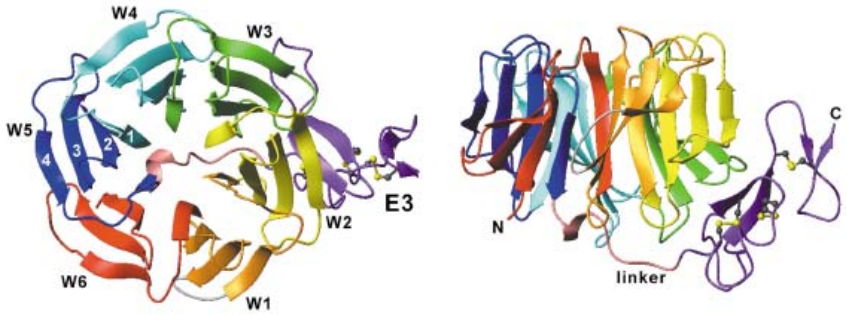

Figure 18. Structure of the YWTD β-propeller-EGF-C domain pair (PDB accession code 1IJQ). Ribbon representations of the YWTD domain and the adjacent C-terminal EGF-like module (E3) of the LDL receptor, coloured to point out the six YWTD repeats of the β-propeller (Jeon et al., 2001).

Downstream of the EGFP domain, at the C terminal end of the extracellular receptor region there is an **O-linked sugar domain,** a 58-residue sequence rich in serine and threonine that undergoes O-linked glycosylation (Cummings et al., 1983; Yamamoto et al., 1984). It is thought to function as a hydrophilic spacer that keeps lipophilic ligands (e.g. lipoproteins) away from the lipid bilayer of the plasma membrane. The deletion of this domain did not impair receptor function (Davis et al., 1986a). The receptor is anchored in the plasma membrane by a single **transmembrane region** composed of 25 hydrophobic amino acids (Yamamoto et al., 1984). The **intracellular portion** of LDLR is 50 residues long and contains a short **NPxY** (Asp-Pro-x-Tyr) sequence motif which is highly conserved in LDL receptors of several species (Chen et al., 1990). In the human LDL receptor this sequence is NPVY. It directs clustered receptors into clathrin-coated pits (Chen et al., 1990; Davis et al., 1986b) by mediating interaction of the receptor with the endocytosis machinery as well as with different cytoplasmic adaptor and scaffold proteins (Davis et al., 1987a; Davis et al., 1987b; Gotthardt et al., 2000; Herz and Bock, 2002; Rudenko and Deisenhofer, 2003).

Naturally occurring mutations in LDLR

Inherited loss of function mutations of the LDLR are the cause of the relatively common human genetic disease familial hypercholesterolemia (FH) (Hobbs et al., 1992; Ishibashi et al., 1993; Norman et al., 1999; Tolleshaug et al., 1983). It is characterized by the defective catabolism of LDL and elevated plasma lipoprotein and cholesterol levels, causing accelerated arteriosclerosis and coronary artery disease. More than 1000 mutant alleles causing FH have been already identified; (http://www.ucl.ac.uk/fh/ (Wilson et al., 1998) and http://www.umd.necker.fr/ LDLR/Home page.html (Villeger et al., 2002)). The frequency of heterozygotes carrying a defective or inactive allele is about 1 in every 500 persons worldwide; therefore FH is one of the most common human inborn errors of metabolism. Heterozygotes have a high plasma LDL concentration and a substantially increased risk for coronary artery disease while two defective copies cause severe premature atherosclerosis which typically leads to death at a very early age (Jeon and Blacklow, 2005). Many point mutations were found to be clustered in repeat 5 of the ligand binding domain (Blacklow and Kim, 1996; Fass et al., 1997), and also in the EGFP domain (Jeon et al., 2001). FH mutations have traditionally been separated into the following five classes depending on the nature of the receptor defect (Jeon and Blacklow, 2005): null alleles which synthesize no receptors (class 1), transport-defective alleles which are completely or partially defective in reaching the cell surface (class 2), binding-defective alleles (class 3), internalization-defective alleles which fail to cluster in coated pits (class 4) and recycling-defective alleles (class 5) (Hobbs et al., 1990). A sixth class of mutation exhibits a sorting defect in polarized epithelial cells (Koivisto et al., 2001).

2.9.5. VLDLR

The VLDL receptor shows the same domain organization as the LDL receptor, except that it has 8 ligand-binding repeats. The entire human VLDLR gene is approximately 40 kb long and contains 19 exons. The high sequence similarity between the genes of VLDLR and LDLR, and the almost complete conservation of exon and intron positions suggest that they have a common ancestor gene. VLDLR is much more conserved between different species than LDLR (Oka et al., 1994). It is most abundant in heart and skeletal muscle, and is also expressed in lower amounts in the kidney, brain, ovary, testis, lung, and adipose tissue, all of which utilize lipoprotein-derived free fatty acids as an energy source (Gafvels et al., 1993). VLDLR is a multi-ligand receptor and its ligand specificity partially overlaps with that of LRP. VLDLR is specific for apoE (Niemeier et al., 1996; Takahashi et al., 1996; Takahashi et al., 1995), and thus binds VLDL, β-VLDL and IDL, but not LDL. Additionally, VLDLR binds lipoprotein-A (Argraves et al., 1997), the ternary complex of the serine protease urokinase plasminogen activator with its inhibitor and receptor (Argraves et al., 1995; Heegaard et al., 1995), lipoprotein lipase (Argraves et al., 1995), thrombospondin-1 (Mikhailenko et al., 1997), and receptor associated protein (RAP) (Hiesberger et al., 1995; Simonsen et al., 1994), a chaperone responsible for proper folding and subcellular trafficking of LDLR family members (Battey et al., 1994; Savonen et al., 1999). Furthermore, VLDLR together with apoER2 plays an important role in mammalian brain development. Both receptors bind the large extracellular matrix protein reelin (Trommsdorff et al., 1999) which is required for neuronal migration and correct layer formation in the cerebellum and the cerebral cortex (D'Arcangelo et al., 1999; Hiesberger et al., 1999). Two isoforms of VLDLR have been reported, a cell surface expressed form possessing the O-linked sugar domain, and a secreted form lacking this domain (Iijima et al., 1998; Magrane et al., 1999; Magrane et al., 1998). The EGF-precursor domain is responsible for low pH induced release of ligands inside endosomes also in the case of VLDLR (Mikhailenko et al., 1999).

2.9.6. LRP-1

LDL receptor-related protein-1 (LRP-1), found to be identical with the α_2-macroglobulin receptor (Strickland et al., 1990) is expressed mainly in the liver, lung, and brain, also to significant amounts in the intestine and muscle, and at lower levels in the spleen, thymus, heart, kidney, and bone. This large (~600 kD) glycoprotein contains 31 complement-type and several epidermal growth factor-like repeats arranged in four clusters (Herz et al., 1988) (Fig. 12). The precursor of LRP-1 is post-translationally cleaved into two subunits, a large subunit (525 kD) containing the ligand binding domain, and a small subunit (85 kD) containing the transmembrane and cytoplasmic regions. The large subunit is non-covalently associated with

the small subunit which anchors the receptor in the plasma membrane. The 100 amino acid long cytoplasmic domain carries two NPxY, one YxxL, and two di-leucine motifs, the YxxL motif being the dominant signal for LRP-1 endocytosis (Li et al., 2000). The complexity of LRP-1 allows for its multifunctionality, binding many structurally and functionally unrelated ligands (Herz and Strickland, 2001; Strickland et al., 1994). LRP-1 plays a major role in hepatic uptake of lipoproteins such as β-VLDL and chylomicron remnants (Beisiegel et al., 1991; Beisiegel et al., 1989; Kowal et al., 1989; Willnow et al., 1992). As an endocytic receptor for proteases and protease inhibitors, LRP-1 regulates proteolytic processes in the blood circulation, including fibrinolysis and coagulation (Nykjaer and Willnow, 2002). It is also important for brain development and function by regulating neurite growth (Nathan et al., 1994) and calcium influx into neurons (Bacskai et al., 2000). Amongst other ligands LRP-1 internalizes α2-macroglobulin-protease complexes (Strickland et al., 1990), tissue-type plasminogen activator (tPA) complexed with plasminogen activator inhibitor type-1 (PAI-1) (Bu et al., 1993), urokinase plasminogen activator (uPA)-PAI-1 complexes (Herz et al., 1992), the protease factors IXa and Xa, factor VIII complexed with van Willebrand factor, Pseudomonas exotoxin A (Kounnas et al., 1992; Willnow and Herz, 1994), and lactoferrin (Willnow et al., 1992). Many of the LRP-1 ligands (including chylomicron remnants and factors VIII and IXa) adhere initially to heparan sulphate proteoglycans (HSPGs) which serve as low-affinity but high-capacity reservoirs acting as primary docking sites to sequester and present ligands to LRP-1 (Kolset and Salmivirta, 1999; Nykjaer and Willnow, 2002; Sarafanov et al., 2001). For normal processing of LRP-1 binding to the ER chaperone receptor associated protein (RAP) is necessary, which promotes proper folding, prevents premature binding to endogenously produced ligands (Bu et al., 1995; Bu and Rennke, 1996; Willnow et al., 1996), and allows for trafficking of the receptor to the *cis*-Golgi apparatus (Willnow, 1998).

2.9.7. Interactions of minor group HRVs with their cellular receptors

Cryo-electron microscopy reconstruction of a complex between HRV2 and a soluble VLDLR fragment encompassing the first three ligand binding repeats fused to maltose binding protein (MBP-V1-3) (Ronacher et al., 2000) revealed that the receptor binds at the small star-shaped dome of the icosahedral five-fold axis (Hewat et al., 2000). Somewhat later also the X-ray structure of HRV2 complexed with the VLDLR fragment V23 was solved, and the interacting residues at the binding interface were identified (Verdaguer et al., 2004). Since the conformations of V2 and V3 repeats are very similar and they could not be distinguished in the crystal structure, the sequence of repeat 3 was chosen to build the three dimensional model (Fig. 19).

The binding interface in the receptor includes an exposed tryptophan that is highly conserved, as well as acidic residues which are also necessary for the folding and maintenance of calcium coordination. The viral binding site is formed only by residues of the HI- and BC-loop of VP1, including a lysine which is conserved in all minor group serotypes. This lysine is the most important residue that forms ionic and hydrophobic interactions with the negatively charged cluster and the conserved tryptophan of the receptor. Additionally, the binding is stabilized by further hydrophobic (Ile1226 and Leu1132 of HRV2 with Trp22 of V3) and hydrophilic (Lys1228 and Thr1085 of HRV2 with Gln16 of V3) interactions.

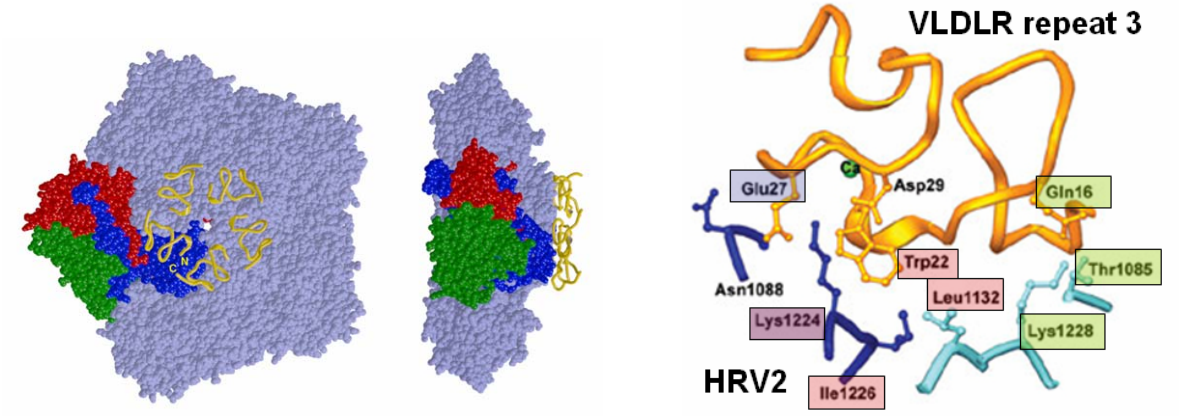

Figure 19. Ribbon diagram of HRV2-V3 interactions as determined by X-ray crystallography. Colour code: V3: yellow ribbon; VP1: blue ribbon; neighboring VP1: light blue ribbon. Interface residues are marked according to the mode of interaction, ionic interactions in blue, H-bonds in green, hydrophobic interactions in rose. Lys 1224 is marked in purple, because it establishes both ionic and hydrophobic contacts (Verdaguer et al., 2004).

VLDLR binding repeats V2, V3 and V5 have been experimentally shown to bind minor group rhinoviruses (Nizet et al., 2005). Based on sequence comparisons of all VLDLR and LDLR ligand binding repeats, virus binding of natural receptors was modelled as shown in Fig. 20. The repeats shown in red are considered to bind, thereby establishing high avidity multi-module attachment. Recently, the VP1 sequences of all HRVs have been determined, but except of the single lysine within the HI loop, no obviously conserved residues were found in the minor group (Palmenberg et al., 2009; Vlasak et al., 2003). Three dimensional modeling of the different VP1 proteins, based on the known 3D structures of 5 HRV types, suggests that the lysine together with an overall positive surface potential is crucial for the establishment of ionic interactions with negatively charged acidic residues of the receptors (LDLR, VLDLR, LRP-1). Despite the conserved lysine in all minor group HRVs, the exact mode of receptor binding probably differs from type to type due to the high variability of residues within the exposed loops. A good example for this is HRV1A which has even different receptor specificity, binding only to the murine homologue of the LDLR (Reithmayer et al., 2002).

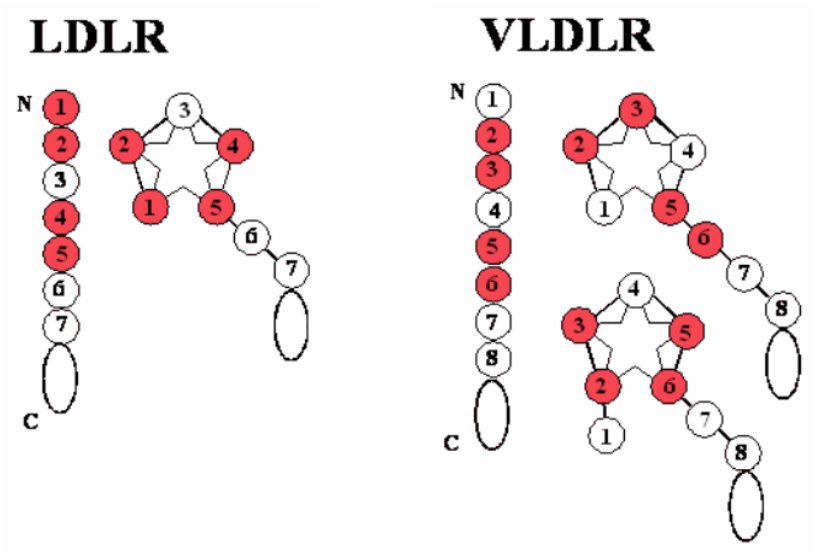

Figure 20. Model of virus binding by LDLR and VLDLR. The binding repeats are arranged around the star shaped dome of the 5-fold symmetry axes of the viral capsid. Repeats shown in red are considered binders, based on sequence comparisons with the VLDLR repeat V3 which has been resolved by X-ray crystallography in complex with HRV2. Such multi module attachment generally results in a high binding avidity. Modules without colour most probably do not bind because they lack residues known to be involved in interaction with virus.

2.10. The β-propeller of LDLR plays a central role in intracellular ligand release

Following lipoprotein binding, LDLR-lipoprotein complexes internalize through clathrin-coated pits and traffic to sorting endosomes, where lipoprotein release occurs (Anderson et al., 1977; Maxfield and McGraw, 2004). Lipoprotein release requires a functional EGFP homology domain and an acidic pH (Davis et al., 1987a). More than half (54 %) of human FH point mutations are located within the EGFP domain (Varret et al., 1998; Wilson et al., 1998). Mutant LDLR receptors with deleted EGFP homology domain (ΔEGFP) or EGF-AB domain pair (ΔAB) (which both are also naturally occurring FH mutations) are unable to release bound LDL or β-VLDL and show a recycling defect (Davis et al., 1987a; Boswell et al., 2004). The EGFP domain is also responsible for the acid-dependent ligand release by VLDLR (Mikhailenko et al., 1999). LDL-release occurs at ~pH 6, which corresponds to the luminal pH of sorting endosomes (Davis et al., 1987a; Maxfield and McGraw, 2004).

Several studies have been carried out to reveal the 3D structure of LDLR both at neutral and low pH to provide explanation for the molecular mechanism of ligand release. The β-propeller, a part of the EGFP domain, turned out to play the most important role in the process. There are three different hypotheses to date how it really happens.

I. The β-propeller competes for the lipoprotein binding sites on repeats LA4-LA5

Upon endosomal acidification LDLR adopts a closed conformation by establishing an intramolecular contact between its β-propeller domain and its LA repeats 4 and 5 (interface I, Fig. 21), as shown in the 3.7 Å resolution crystal structure solved at pH 5.3 (Rudenko et al., 2002). According to the intramolecular competition model (Beglova et al., 2004a) three histidines (H562 and H586 in the β-propeller and H190 in LA5) become protonated at their imidazole groups (p*Ka* of ~6), and subsequently establish van der Waals and ionic interactions between the β-propeller and the LA repeats. As a consequence, the β-propeller becomes a better ligand for the LA repeats, and induces the release of the LDL particle by competition. Various deletion and domain swap studies showing that the β-propeller and especially the mentioned His residues are necessary for the release of bound lipoproteins (Beglova et al., 2004a) have strengthened this hypothesis.

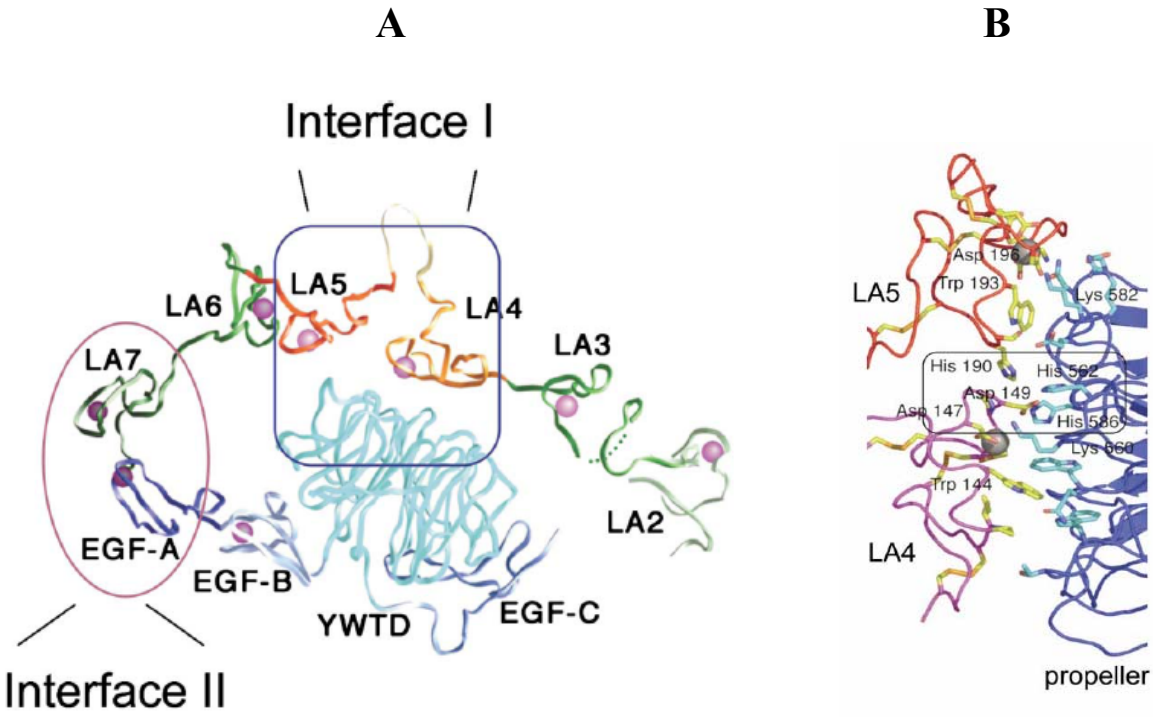

Figure 21. Ribbon trace of the LDL receptor structure determined at endosomal pH. A) The central ligand-binding modules, LA4 and LA5, form long-range contacts with the YWTD β-propeller domain and are highlighted in orange and red, respectively. The boxes enclose two interdomain interfaces that may be regulated by the change in pH that occurs upon moving from the cell surface to the endosome. The coordinates used for the figure are from PDB accession code 1N7D (Rudenko et al., 2002). B) Close-up view of interface I. The three interface histidines lie within the box at the centre of the interface (Beglova et al., 2004a).

A second, less extensive interface (interface II, Fig. 21) found in the low pH structure of LDLR was first thought to serve as a hinge allowing the ligand binding repeats to arc back over the propeller domain. However, it turned out that the conformation of the LA7-EGF-A-EGF-B domains is fixed throughout the whole physiologically relevant pH range, and it rather

constrains the flexible ligand-binding repeats to be in the neighbourhood of the propeller, so that receptor closure via intramolecular competition can readily occur at acidic pH (Fig. 22) (Beglova et al., 2004a).

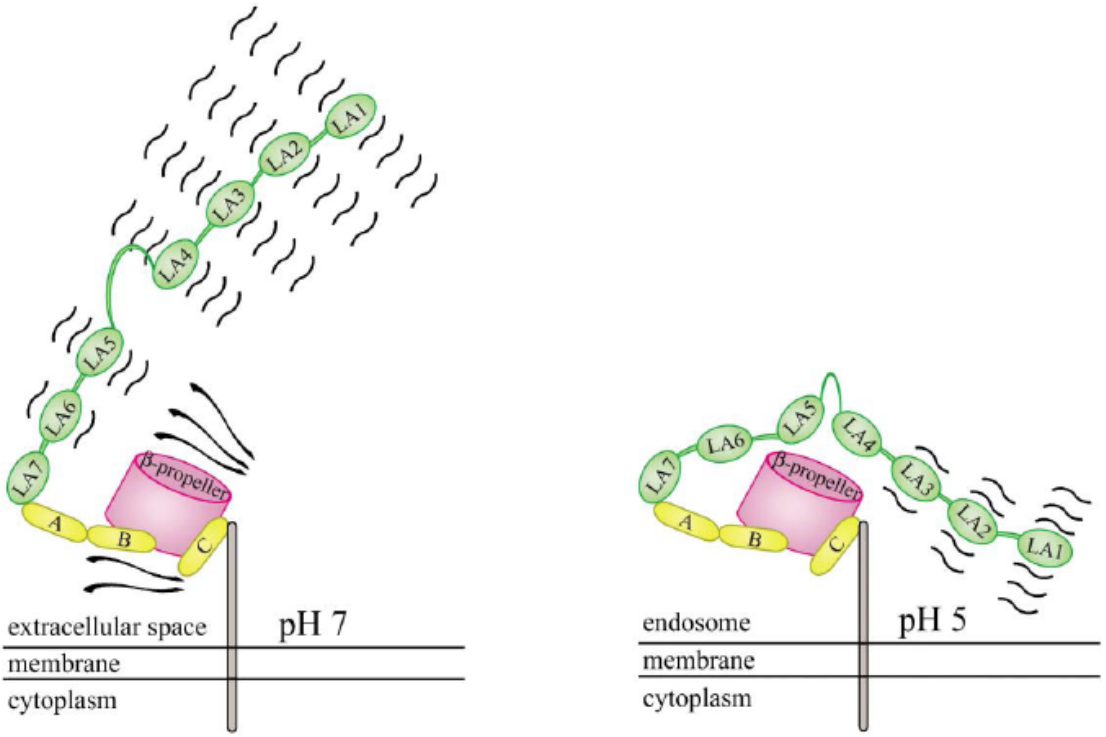

Figure 22. How fixed and flexible domain-connections permit interconversion between open and closed conformations. LA7, EGF-A, and EGF-B constitute a rigid scaffold that is invariant with pH. The numbers of small wavy lines correspond to the flexibility of LA modules (Beglova et al., 2004a).

II. The β-propeller causes lipoprotein release via an allosteric mechanism

The kinetics of lipoprotein dissociation showed that the EGFP homology domain rather interacts with LA 4 and 5 via binding to a site different from the lipoprotein binding site, and the three interface histidines have little impact on the acid-dependent transition between the open and closed state of the LDLR (Fig 23.) (Zhao and Michaely, 2008). The mutant protein with H190, H562, and H586 all substituted with alanine was defective in lipoprotein release but showed normal acid-dependent conformational change, suggesting that adoption of the closed conformation is not sufficient to drive lipoprotein release. In the allosteric model proposed by Zhao and colleagues the conformational change of the ligand binding repeats caused by their low pH induced engagement with the EGFP homology domain is responsible for lipoprotein release.

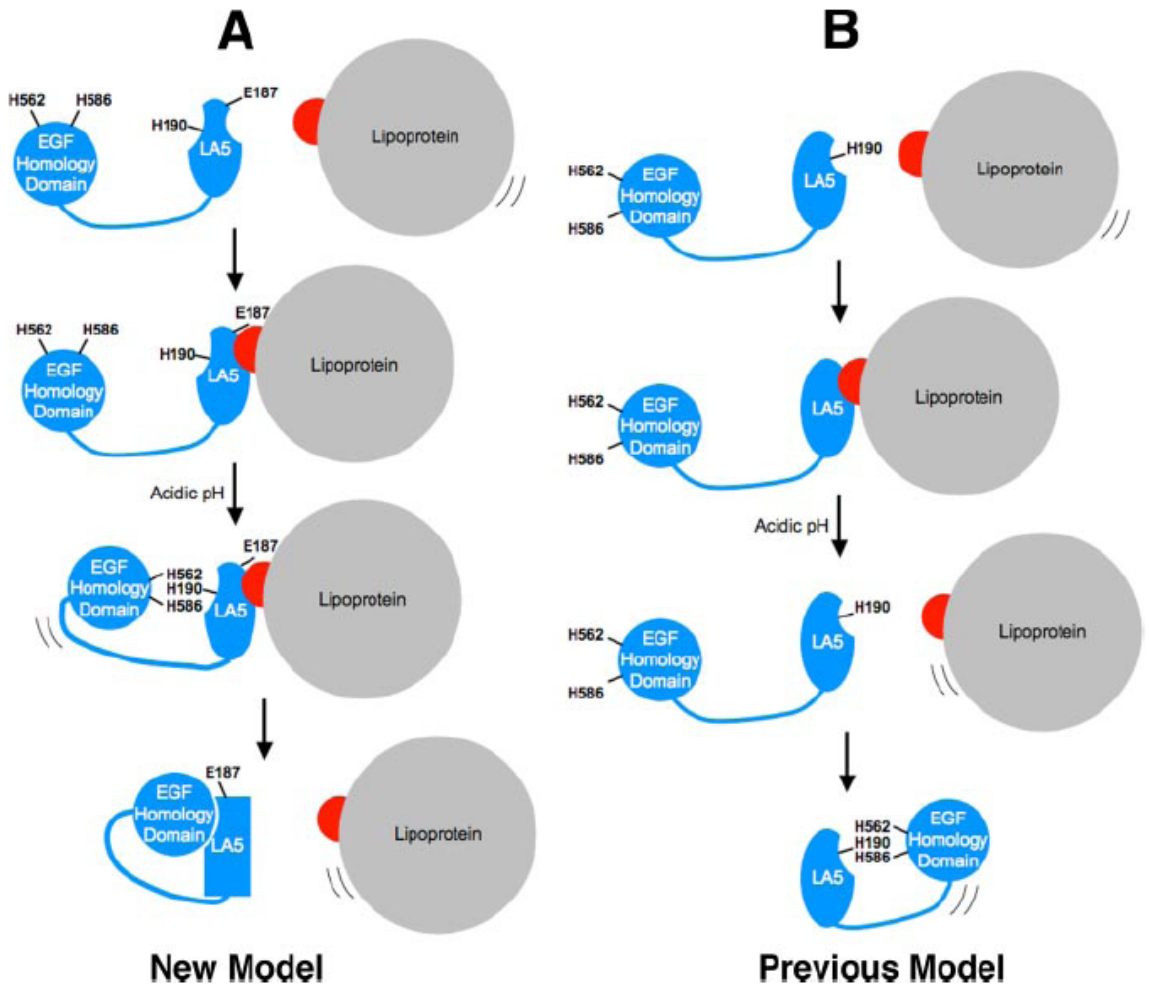

Figure 23. Model of lipoprotein release by LDLR conformational changes. LDLR is shown in *blue*, lipoprotein in *grey*, and apolipoprotein in *red*. Only the EGF homology domain and LA5 of the LDLR are depicted. In the proposed allosteric model (*A*), lipoproteins bind to the LDLR via E187, D203, and E208 (apoE) or via E187 (apoB100) (*1st and 2nd panels of A*). Upon acidification the EGF homology domain contacts LA5 (*3rd panel of A*), which drives a conformational change in LA5 that involves H190, H562, and H586. The conformational change in LA5 disrupts the binding sites for apolipoproteins, thereby driving release (*4th panel of A*). This new model stands in contrast to the previous model (*panel B*). In the previous model, lipoproteins bound to the same surface as the EGF homology domain (*top two panels of B*). The previous model also proposed that, as lipoprotein dissociates, the EGF homology domain replaces lipoprotein via an interaction that requires protonation of H190, H562, and H586 (*bottom two panels of B*) (Zhao and Michaely, 2008).

III. The decreaseing Ca^{2+} concentration within acidifying endosomes leads to partial unfolding of the ligand binding repeats

Recently, an additional mechanism for LDLR ligand release was proposed, namely the partial unfolding of ligand binding repeats due to the decrease of calcium concentrations within acidifying endosomes (Arias-Moreno et al., 2008). Upon acidification of the endosome Ca^{2+} is released to the cytoplasm, and the endosomal Ca^{2+} concentration drops from the extracellular level of 0.5-2 mM to 5 µM within 10 min (Gerasimenko et al., 1998). Previous *in vitro* experiments that led to the competition model (Beglova et al., 2004a; Rudenko et al., 2002)

were all carried out at extracellular Ca^{2+} concentrations. Arias-Moreno and colleagues, however, have shown that the affinity of LA5 for Ca^{2+} was markedly decreased at endosomal pH. As the isolated LA5 repeat is known to loose its stability when the coordinated Ca^{2+} is removed (Blacklow and Kim, 1996), its affinity for LDL must be also severely reduced. In their proposed model the unfolding of ligand binding repeats is the reason for LDL dissociation. This model does not necessarily exclude that the partially unfolded LA5 is still able to form the intramolecular complex with the β-propeller observed by X-ray crystallography (Rudenko et al., 2002), but it still remains to be tested. A similar mechanism was recently observed in the case of receptor associated protein (RAP); it dissociates from the receptors due to its partial unfolding triggered by histidine protonation at the acidic pH of the Golgi (Lee et al., 2006). It thus appears that acid-driven unfolding could be a general cellular mechanism to induce dissociation of protein complexes in acidic organelles (Arias-Moreno et al., 2008).

2.11. Early infection events of Picornaviruses

2.11.1. Receptor usage

The first step in the replication cycle is the attachment of infectious virus particles to host cell receptors. The specific recognition of cell surface molecules which are usually expressed by a restricted set of cell types and particular host organisms, determines tissue tropism and host range. Picornaviruses use a wide repertoire of cell surface molecules for attachment (Table 2), such as immunoglobulin-like, short consensus repeat (SCR)-like, low density lipoprotein (LRLR)-like molecules, integrins, heparane sulphate, etc. (Flint et al., 2000; Rossmann et al., 2002). Integrins used by foot-and-mouth disease virus (FMDV) and some echoviruses, are noncovalently linked, heterodimeric molecules consisting of a variety of α and β subunits, functioning in cell-cell interactions and signal transduction. Several immunoglobulin-like molecules are used as picornavirus receptors, such as intercellular adhesion molecule 1 (ICAM-1) used by major group HRVs and some coxackievirus A types, vascular cell adhesion molecule 1 (VCAM-1) used by encephalomyocarditis virus (EMCV), coxackievirus-adenovirus receptor (CAR) used by some coxackievirus B types, and poliovirus receptor (PVR/CD155). Some coxackieviruses end echoviruses bind to short consensus repeats (SCRs) of decay accelerating factor (DAF/CD55) which functions as a regulator of the complement activity protein family. Minor group HRVs attach to endocytic receptors of the LDLR superfamily (LDLR, LDLR-related protein and VLDLR).

Virus	Receptor	Type of molecule	Coreceptor
Foot-and-mouth disease virus	$\alpha_V\beta_3$ (vitronectin receptor)	integrin	
Foot-and-mouth disease virus (cell culture adapted)	Heparane sulphate	glycosaminoglycan	
Encephalomyocarditis virus	VCAM-1 Sialylated glycophorin A (for hemagglutination only)	Ig-like carbohydrate	
Poliovirus 1-3	PVR (CD155)	Ig-like	
Coxackievirus A13, A18, A21	ICAM-1	Ig-like	
Coxackievirus A21	DAF (CD55)	SCR-like	ICAM-1
Coxackievirus A9	$\alpha_V\beta_3$	integrin	
Coxackievirus B1-6	CAR	Ig-like	
Coxackievirus B1, B3, B5	DAF (CD55)	SCR-like	$\alpha_V\beta_6$ integrin
Echovirus 1, 8	$\alpha_V\beta_1$	integrin	β_2 microglobulin
Echovirus 22	$\alpha_V\beta_3$	integrin	
Echovirus 3, 6, 7,11,12, 13, 20, 21, 24, 29, 33	DAF (CD55)	SCR-like	β_2 microglobulin
Enterovirus 70	DAF (CD55)	SCR-like	
Bovie enterovirus	Sialic acid	carbohydrate	
Hepatitis A virus	HAVcr-1	Ig-like, mucin-like	
Major group HRV	ICAM-1	Ig-like	
Minor group HRV	LDLR-superfamily	signalling receptors	

Table 2. Receptors and coreceptors used by members of the Picornaviridae family, adapted from (Flint et al., 2000).

Some picornavirus receptors are used only as vehicles for virus delivery into the low pH environment of endosomes (e.g. integrins and heparane sulphate used by FMDV). Viruses which infect via the endosomal route but are not so sensitive to low pH need a receptor with a catalytic activity that uncoats the virus by itself (like PVR poliovirus) or in cooperation with the low pH (like ICAM-1 some major group HRV types).

There is a big variability in the receptor usage within the *Picornaviridae* family. Poliovirus is engaged with a single receptor type (all three types use CD155). Different types of coxackieviruses, echoviruses and HRVs attach to different, structurally and functionally unrelated receptors. The same receptors can also be used by different viruses, like the $\alpha_V\beta_3$ integrin (vitronectin receptor) by FMDV, coxackievirus A9 (CVA9) and echovirus (EV) 22; the decay accelerating factor by CVA21, CVB1, B3 and B5, enterovirus 70 and several

echovirus types; or ICAM-1 by major group HRVs and by coxackievirus A13, A18, and A21 (Flint et al., 2000).

2.11.2. Cell attachment via surface features: canyons and loops

Low resolution (15-25 Å) structures of several picornavirus-receptor complexes have been solved by image reconstruction analysis of cryo-electron micrographs, such as HRV 14 (Kolatkar et al., 1999; Olson et al., 1993), HRV 16 (Kolatkar et al., 1999), and coxsackievirus A12 (Xiao et al., 2001) with ICAM-1; poliovirus 1 with PVR (Belnap et al., 2000; He et al., 2000; Xing et al., 2000); coxsackievirus B3 with CAR (He et al., 2001); echovirus 7 (EV7) and EV12 with DAF (Bhella et al., 2004; He et al., 2001; Pettigrew et al., 2006) and HRV2 with the VLDL receptor (Hewat et al., 2000).

Picornavirus receptors bind either to exposed surface loops on the viral capsid or to structures deeply hidden at the bottom of the canyons surrounding the star-shaped mesa of each fivefold axis. The first binding mode is represented by integrins serving as receptors for foot-and-mouth disease virus, decay-accelerating factor binding to some coxackie A and B viruses, and LDL-receptors binding to minor group rhinoviruses. These receptors, binding to exposed structures of their viruses, only function as docking sites to increase virus concentration at the cell surface and/or as internalization vehicles. The viruses using such receptors either show a high sensitivity to low pH like minor group rhinoviruses and FMDV or they require an additional receptor for entry/conversion such as viruses binding to DAF but using CAR (coxackievirus B3) or ICAM1 (coxackievirus A21) in addition.

Several members of the Enterovirus genus like poliovirus, some coxackie A and B viruses, and major group rhinoviruses hide their receptor binding sites inside the canyon. The receptors of these viruses bind to conserved residues and trigger uncoating associated conformational changes of the viral capsid. In order to donate some of their binding energy to facilitate structural rearrangements, such receptors need to bind at a big surface area, and binding inside the canyon is a good strategy to do this (Hogle, 2002). ICAM-1, PVR, and CAR (Fig. 24) all bind via their N-terminal domain within the canyon of their cognate viruses, but their footprints and binding geometry differ greatly. The PVR has a bigger footprint area on the poliovirus surface than ICAM-1 on rhinovirus, and also shows a higher binding affinity (Xing et al., 2000). Consistent with this, poliovirus uncoating can be induced by receptor attachment itself whereas some major group rhinoviruses (e.g. HRV 16) (Hooverlitty and Greve, 1993) need an additional trigger by the low pH.

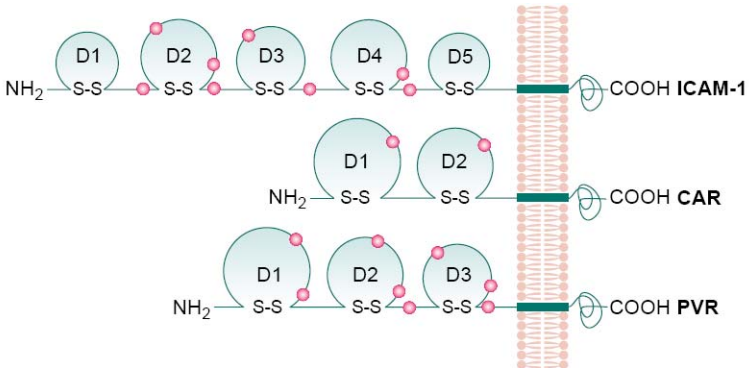

Figure 24. Members of the immunoglobulin superfamily used as picornavirus receptors. Intercellular adhesion molecule-1 (ICAM-1); coxsackievirus-adenovirus receptor (CAR); and poliovirus receptor (PVR) used as receptors by human rhinoviruses (HRVs) and coxsackievirus A21 (CAV21); coxsackie B viruses (CVB); and poliovirus (PV), respectively (Rossmann et al., 2002)

Viruses with structurally hidden, conserved receptor binding sites cannot tolerate big structural variability in their binding region, because they might easily lose binding specificity as well as their stability due to changes in deeply lying capsid structures. In contrast, viruses which bind to cell surface molecules via exposed loops continuously develop new binding properties due to the numerous mutations which occur during replication. Enteroviruses e.g. show variations in their DAF-binding sites; they bind to DAF at different SCRs, and even different regions of the same SCR can be utilized by different viruses (Hafenstein et al., 2007; Pettigrew et al., 2006). Changes in the receptor binding site might allow for attachment to new receptors, sometimes the virus might even gain the ability to infect new cell lines, which plays an important role in cell tropism.

2.11.3. Coreceptors and alternative receptors

Some picornaviruses use only a single type of receptor for cell attachment, entry, and uncoating, like the major group HRVs which use ICAM-1 or poliovirus which uses the poliovirus receptor (PVR)/CD155.

Other viruses need an interaction with more than one cell surface molecules for effective infection. Some coxackievirus B isolates (CB1, CB3, and CB5) can attach to cells using decay accelerating factor (DAF) (Bergelson et al., 1995; Shafren et al., 1995; Shafren et al., 1997b), but for cell entry and uncoating they need an additional interaction with the coxsackievirus and adenovirus receptor (CAR) (Bergelson et al., 1997; Martino et al., 2000; Milstone et al., 2005). The reason is that DAF binds to exposed surface structures outside of the canyon (Bhella et al., 2004; He et al., 2001; Pettigrew et al., 2006), where it cannot trigger conversion. However, in polarized epithelial cells CAR is concentrated at tight junctions, where it is relatively inaccessible for the viruses. Therefore DAF, which is present on the

apical surface, has also an important role in infection by capturing and concentrating the virus at the cell surface, and by inducing virus transport into the tight junctions (Marsh and Helenius, 2006; Shieh and Bergelson, 2002).

Heparan sulphate (HS) glucosaminoglycans are widely expressed at the surface of many cell lines and are used by several viruses for cell entry. It is not uncommon that viruses aqiure the ability to bind HS in cell culture, and infect cells lacking their original receptor. Examples are a mutant HRV89 (Vlasak et al., 2005a) which is able to infect cells lacking ICAM-1, a cell culture adapted FMDV which binds to HS additionally to integrins (Fry et al., 1999), and a coxackievirus variant CVB3 PD which is able to infect cells lacking both DAF and CAR (Zautner et al., 2003). While for FMDV the binding to HS is only the result of a cell culture adaptation, this is probably not the case for echoviruses, where also low passage clinical isolates of EV6 have this property (Goodfellow et al., 2001). HRV54 naturally has the ablity to bind both ICAM-1 and heparane sulphate (Khan et al., 2007).

2.11.4. Virus internalization via different pathways

Since viruses are obligate intracellular parasites, they must somehow internalize into their host cells. Most non-enveloped viruses hijack natural endocytosis routes by binding specific receptors used by cargos under physiologic conditions. Receptor choice is important in the selection of the entry route which allows for intracellular trafficking of the virus. Finally, at some point of the pathway genome release occurs, induced by specific triggers within appropriate organelles. Hijacking the endolysosomal route is a strategy used by several viruses, because endocytosis offers several advantages. After endocytosis no viral components remain at the cell surface for detection by the host immune system. Viruses are transferred deeply inside the cytoplasm exploiting the molecular motors of the infected cells. Acidification is generally a trigger for molecular conformational changes in many cellular processes, e.g. in ligand release from receptors (LDL from LDLR; the iron from transferrin) or in the release of freshly synthesized proteins from their chaperons (LRP from receptor-associated protein). Many viruses take the advantage of endosomal acidification as a trigger for membrane fusion and uncoating. Enveloped viruses generally infect via low-pH induced conversion of their envelope protein(s) (like hemagglutinin in the case of influenza (Cross et al., 2009)) which then insert(s) into the endosomal membrane assisting in viral fusion. Non-enveloped viruses (e.g. members of Picornaviruses) take advantage of the low pH for their capsid conversion and RNA release. Moreover, in this work we show that the low-pH induced conformational change of a virus receptor can also be beneficial for infection (namely the β-propeller switch of LDLR for minor group HRVs).

There are four **main endocytic routes used by viruses**: clathrin-mediated endocytosis, the caveolin dependent pathway, non-clathrin non-caveolae pathway and macropinocytosis.

Clathrin-mediated endocytosis (CME) is the best understood one among the different cellular entry pathways. Receptors possessing clathrin clustering signal sequences (as YXXφ and di-leucine) recruit their cargo into developing clathrin-coated pits (CCPs) which subsequently internalize and form small (approx. 100 nm in diameter) clathrin-coated vesicles (CCVs), found in all cell types. Clathrin interacts with a number of adaptor or accessory proteins, like AP-2 (adaptor protein-2), Eps 15 (epsin 15), SNX9 (sorting nexin 9), actin, actin-associated proteins, like N-WASP, Arp2/3 ARH and Dab2, amphiphysin, AP180, and dynamin. Receptors such as LDL-receptor, transferrin receptor, receptor tirosin kinases, G protein-coupled receptors, and many others are taken up by clathrin-mediated endocytosis. Clathrin mediated endocytosis is used by several viruses for cell entry such as Semliki Forest virus, vesicular stomatitis virus (Sieczkarski and Whittaker, 2002), adenovirus, (Meier et al., 2002), Sindbis virus (DeTulleo and Kirchhausen, 1998), canine parvovirus (Parker and Parrish, 2000), Hantaan virus (Jin et al., 2002), and certain picornaviruses, like the minor group human rhinoviruses (Snyers et al., 2003), FMDV (O'Donnell et al., 2005), and coxsackievirus B3 (Chung et al., 2005).

Endocytosis via caveolae (a special type of lipid rafts rich in proteins, cholesterol, sphingo- and glycolipids) happens in many, but not all cell types. These small, (~50-100 nm in diameter) flask-shaped pits resembling the shape of a cave are especially abundant in smooth muscle, type I pneumocytes, fibroblasts, adipocytes, and endothelial cells. The cholesterol-binding protein caveolin-1 is responsible for the formation and maintenance of caveolae. Caveolae are directly involved in the internalization of membrane components (glycosylphosphatidylinositol-anchored proteins and glycosphingolipids), extracellular ligands (folic acid, albumin, autocrine motility factor), bacterial toxins (cholera toxin, tetanus toxin), and several non-enveloped viruses (Simian virus 40, Polyoma virus) (Pelkmans, 2005; Pelkmans and Helenius, 2003). Simian virus 40 (SV40) is the best known virus entering cells through caveolae, and it is frequently used as a marker for the caveolar pathway. It enters via a two-step transport pathway, from plasma membrane caveolae through an intermediate organelle (termed the caveosome) to the smooth ER (Pelkmans et al., 2001). SV40 can also use a virus activated cholesterol and tyrosine kinase dependent endocytic pathway from the plasma membrane to the ER, that involves neither clathrin nor caveolae (Damm et al., 2005).

Macropinocytosis is the formation of vesicles of variable size (0.5-5μm in diameter) filled with large volumes of extracellular fluid. The cell membrane forms ruffles in an actin-dependent manner, which then enclose extracellular material non-specifically. Macropinosomes can become acidified by fusion with other vesicles such as endosomes and lysosomes (Hewlett et al., 1994). Although macropinocytosis is characteristic for specific cell

types such as macrophages and dendritic cells, it also happens in non-phagocytosing cell types, and occurs mainly upon stimulation by growth factors (Sieczkarski and Whittaker, 2002). Macropinocytosis is used for cell entry by vaccinia virus, a poxvirus which is too large to enter clathrin-coated pits (Mercer and Helenius, 2008). HIV1, which normally enters cells by direct fusion with the plasma membrane, can also fuse with the membrane of macropinosomes in macrophages, leading to a less efficient infection (Marechal et al., 2001).

It is not always easy to determine which entry route(s) a virus uses. Generally, the receptors define the entry pathways, but viruses which use alternative receptors for cell entry, can hijack different endocytosis routes. It is e.g. a well known phenomenon that viruses may develop the ability to bind heparane sulphate in cell culture, and enter into cells which are devoid of the virus receptor (Fry et al., 1999; Vlasak et al., 2005a). HRV54 generally uses ICAM-1, but it naturally has the ability to bind also heparane sulphate, and is able to infect RD cells that lack ICAM-1 (Khan et al., 2007). Moreover, the endocytic pathways are so interconnected that a virus might even use a combination of them, as the bovine papillomavirus 1 enters by clathrin-mediated endocytosis and then utilizes the caveolar pathway for infection (Laniosz et al., 2008). The knowledge about virus entry is continuously growing, and combined with sophisticated microscopic techniques, viruses are preferentially used as markers for the investigation of different entry pathways (Pelkmans and Helenius, 2003).

2.11.5. Cell entry of picornaviruses

Picornaviruses use various receptors for cell attachment, and also various endocytic pathways.

Poliovirus uses an entry pathway that requires energy, tyrosine kinases, an intact actin cytoskeleton, and cell signaling pathways, but is independent of clathrin, caveolin, flotillin or microtubules, and genome release occurs from vesicles that are very close to the cell surface (Brandenburg et al., 2007).

FMDV enters cells mainly via clathrin-dependent endocytosis when it binds to integrins (O'Donnell et al., 2005). The cell culture adapted variant using heparane sulphate was found to enter through a caveolae-mediated pathway which can associate and traffic with endosomes (O'Donnell et al., 2008).

Human rhinoviruses utilize different receptors and thus these viruses enter cells by different pathways. Members of the minor group use LDLR, VLDLR and LRP for internalization, which receptors follow clathrin mediated endocytosis (Snyers et al., 2003). The entry pathway

of major group rhinoviruses using ICAM-1 is not known in detail. Former times it was proposed that they follow a clathrin mediated endocytosis (DeTulleo and Kirchhausen, 1998). However, ICAM-1 lacks a typical clathrin localization signal, and even functions as a viral receptor when its cytoplasmic tail is replaced with a GPI-anchor (Staunton et al., 1992). Multivalent ICAM-1 ligands such as immunobeads have been shown to enter cells via macropinocytosis (Muro et al., 2003). It was recently shown that HRVs using ICAM1 enter rhabdomyosarcoma cells also by a particular type of macropinocytosis (Khan et al., 2010).

A number of enteroviruses use (DAF) as a receptor, which can be found in lipid rafts. Infection by a DAF-using strain of echovirus 11 (E11) is dependent on cholesterol and an intact cytoskeleton, which is an indication that this virus uses lipid rafts for cell attachment (Stuart et al., 2002). Coxsackievirus B4 also requires functional lipid rafts for attachment, and then it is delivered to the Golgi (Triantafilou and Triantafilou, 2004). The group B coxsackievirus receptor, CAR, is found in the epithelial tight junction. Coxsackievirus B entry needs a component of the tight junction called occludin, and occurs by a process that combines aspects of caveolar endocytosis with features of macropinocytosis (Coyne et al., 2007). Echovirus 1 enters cells using caveolin-mediated endocytosis, and apparently uncoats from the caveosome (Pietiainen et al., 2004).

2.11.6. Uncoating and RNA release to the cytoplasm

In order to protect the genome **viral capsids must be stable** enough to withstand extracellular conditions e.g. mechanical shearing, UV irradiation, dehydration, enzymatic attack, extremes of pH, ionic strength, and temperature, etc. For efficient infection however, once they reach their target cells and encounter **specific trigger(s)** wihin the appropriate cellular compartment, they **must become sufficiently unstable to allow for genome release**.

The final stage of assembly for many viruses involves proteolytic processing (**maturation cleavage**) of a structural protein (generally a surface glycoprotein for enveloped viruses or a capsid protein of a non-eveloped virus), which sets up a **metastable state**. Facing the appropriate trigger (receptor binding, endosomal acidification or both) the viral capsid proceeds to a **lower energy state** which is usually accompanied **by exposing hydrophobic sequences** that can attach to membranes. In enveloped viruses this membrane attachment facilitates fusion of the viral envelope with the cell membrane. In non-enveloped viruses the hydrophobic sequences must either generate a pore into a cellular membrane or disrupt it to facilitate entry and/or genome release (Hogle, 2002). In most picornaviruses the autocatalytic cleavage of VP0 into VP2 and V4, and the subsequent rearrangements of VP4 and the N-terminal extensions of VP1 and VP2 are responsible for locking the virus in the metastable

state. Mutations which prevent the maturation cleavage result in the production of non-infectious provirions as shown for poliovirus (Ansardi and Morrow, 1995), FMDV (Knipe et al., 1997), human rhinovirus 14 (Lee et al., 1993), hepatitis A virus (Bishop and Anderson, 1993) and Swine vesicular disease virus (Rebel et al., 2003). No maturation cleavage occurs in parechoviruses (Stanway et al., 2000). The present information about the RNA release of picornaviruses stems from the comparison of high resolution X-ray structures of different viral stages: the native virus, the immature provirion, virus-receptor complexes, and empty capsids. These are only snapshots of stable intermediates, which have to be then combined with genetic, biophysical, and biochemical observations to model the whole process. When facing the appropriate triggers (receptor binding and/or low pH), most picornaviruses undergo a capsid conversion by externalizing hydrophobic patches, like the myristoyl-VP4 and the N-terminal extensions of VP1 in poliovirus (Fricks and Hogle, 1990) and rhinovirus (Hewat and Neumann, 2002; Hewat and Blaas, 2004). While the conversion to **A-particle** is irreversible, transient and reversible exposure of VP4 and the N-terminal extension of VP1 occur at physiological temperatures in a process termed **"breathing"** (Li et al., 1994). In contrast to the stable virion, the generated hydrophobic A-particles are sensitive to proteases. The A-particle is infectious, as it still contains the RNA genome, and is hydrophobic which allows its association with cellular membranes.

The **role of receptor in virus conversion** depends on the stability of the virus, and on the nature of virus-receptor binding. Receptors binding at the viral surface, like LDL-receptors, integrins, heparane sulphate or decay accelerating factor (DAF) are not able to induce viral conversion; uncoating of viruses using such receptors exclusively depends on the low pH within endosomes. Receptors which bind deeply inside the canyon like ICAM-1, poliovirus receptor or CAR have the potential to induce conformational change of the viral capsid; whether they do, it depends on the certain virus. Receptor-sensitive viruses like poliovirus, HRV3, and HRV14 all can be converted by the attachment of their receptors at neutral pH. HRV16 however, is not converted by ICAM-1 binding alone, it also needs the low pH (Hoover-Litty and Greve, 1993).

After virus conversion the RNA leaves the capsid (uncoating) and penetrates through its surrounding membrane e.g. the plasma membrane (poliovirus) or the endosomal membrane (HRVs). Except of binding viruses and assisting in their conversion, picornavirus receptors also have additional roles in infection such as handing over the converting virus to the membrane or keeping the virus bound even during RNA egress. HRV2, the most investigated minor group HRV, loses the affinity to its receptors upon its low pH induced conversion, which can cause its dissotiation (Brabec et al., 2003). LDLR however, also undergoes conformational changes at low pH, which could be the reason for virus release as well. Modeling virus conversion at the plasma membrane of HeLa cells, which express LDLR, VLDLR, and LRP as receptor candidates, a big amount of native HRV2 was released from

the cells (Brabec et al., 2003). However, in our system using LDLR as the only virus receptor, HRV2 was found to be released upon its conversion and was directly handed over to the endosomal membrane (Konecsni et al., 2009). Whether in natural infectons the receptor keeps the virus bound until conversion occurs and subsequently hands it over to the membrane or it releases the virus still being native, influences the efficiency of infection greatly.

Picornaviruses, which depend on their receptor for conversion, remain bound, and their receptors also assist in RNA penetration, e.g. by holding the virus close to the plasma membrane (poliovirus receptor) or by disruption of the endosomal membrane (ICAM-1 in the case of major group rhinoviruses). The complex of poliovirus and the exodomain of its receptor linked to liposomes via a Ni-NTA anchor has been reconstructed by cryoelectron microscopy (Bubeck et al., 2005). The results suggest that binding via multiple receptors brings the viral 5-fold axis close to the membrane, allowing the insertion of multiple copies of VP4 and the N termini of VP1 proteins into the lipid bilayer upon conversion into the A-particle form. Cryo-EM pictures about HRV3-soluble ICAM-1 complexes formed at 4ºC followed by heating to 37ºC have shown that the receptor remains bound during, and even after RNA egress (Xing et al., 2003).

The low pH and/or the attachment to the receptor induce the conversion from native virus (150S) to A-particle (135S). Subviral particles can also be produced *in vitro*. Exposure of HRV2 to pH 5.0 primarily results in 135S particles, and heating to 50-56ºC for some minutes primarily generates empty 80S particles (Gruenberger et al., 1991; Korant et al., 1972) (Lonberg-Holm and Noble-Harvey, 1973; Lonberg-Holm and Yin, 1973; Noble and Lonberg-Holm, 1973). Poliovirus can be converted by warming in hypotonic buffers in the presence of millimolar levels of calcium ions (Curry et al., 1996; Wetz and Kucinski, 1991). In the absence of calcium the conversion proceeds directly to empty 80S particles, suggesting that calcium is required to stabilize the A-particle, and that depletion of calcium at some stage during the normal entry process may serve as a trigger for RNA release (Hogle, 2002).

Conversion from A-particle to empty B-particle, and penetration of the viral RNA into the cytosol

For efficient infection it is not enough that the RNA is released from the viral capsid, but it also has to penetrate through the membrane of the endosome/vesicle/organelle in which the virus has converted, to reach the cytosol, the place of replication. The RNA penetration of picornaviruses happens either by pore formation (minor group HRVs, poliovirus) or by disruption of the endosomal membrane (major group HRVs) (Brabec et al., 2005; Fuchs and Blaas, 2008; Tosteson et al., 2004).

The viruses which penetrate by pore formation (e.g. poliovirus and minor group rhinoviruses) previously attach to the membrane via their externaized hydrophobic patches, and via their VP4 proteins which have been released from the capsid upon conversion. Multiple copies of VP4 are believed to form channels in the membrane (Davis et al., 2008; Tosteson et al., 2004) which allow for RNA penetration. The situation is different for major group rhinoviruses which disrupt the endosomal membrane, as believed, via molecular constraints induced as the rigid ICAM-1 molecules follow the conformational changes of the bound virus (Fuchs and Blaas, 2008). It is interesting why major group HRVs disrupt the membrane but poliovirus forms pores, since their receptors belong to the same protein family. When the ICAM-1 molecules were not so long and rigid, which hinders the converted capsid to associate with the membrane, maybe also the major group HRVs could form pores.

FMDV is extremely sensitive to low pH, and its capsid is known to be disassembled to 12S pentamers still at the pH of early endosomes (Grubman and Baxt, 2004). A mutant FMDV which is unable to perform the maturation cleavage of VP0 into VP2 and VP4 is non-infectious, but also disassembles at low pH (Knipe et al., 1997). This indicates that a functional VP4 is necessary for infection, most probably for pore formation, to assist RNA penetration. Comparing the most investigated members of picornaviruses the A-particle seems to be an important intermediate, which, by associating with membranes, helps the RNA to be released vectorially into the cytosol and not into the lumen of the endosome. The quick disassembly of FMDV raises the question whether the A-particle is generally needed for RNA penetration or only the membrane-inserted VP4 proteins are really important. It is a further question whether FMDV has a short lived A-particle form which cannot be detected because of a rapid RNA penetration or the quick capsid disassembly (perhaps still in the receptor attached form) allows for a rapid pore formation by the soluble VP4s and for RNA penetration without a pre-existing A-particle. Recently it has been shown that another member of the Aphthovirus genus, the Equine rhinitis A virus, also dissociates to pentamers at mildly acidic pH but its dissociation is preceded by the transient formation of empty 80S particles (Tuthill et al., 2009). This suggests that also the A-particle form should exist but because of the quick uncoating process it could not be detected so far. Whether the A-particle, which is quite generally formed in many picornaviruses, is an indispensable intermediate to assist RNA penetration or the viral RNA itself has the potential to penetrate through the formed channels (e.g. by high affinity of VPg to membrane-inserted VP4) still remains a question.

3. Objectives

Human rhinoviruses use two different types of receptors for cell attachment and entry. Most of the viruses (87 types) belong to the major group, binding to the human intercellular adhesion molecule 1 (ICAM-1). The remaining 12 types of the minor group attach to members of the low-density lipoprotein receptor (LDLR) superfamily including LDLR, very-low-density lipoprotein receptor (VLDLR), and LDLR-related protein (LRP). Following attachment and internalization HRVs are transferred into endosomal compartments where the low pH and/or the virus-destabilizing activity of ICAM-1 trigger structural changes (conversion into subviral particles, i.e. virus uncoating) leading to RNA-delivery into the cytosol, where the replication takes place. While the major group receptor ICAM-1 actively induces virus uncoating, LDLR is considered to be just a vehicle for delivery of the virus into endosomes, where the low pH would be the unique trigger for uncoating. However, at the low pH prevailing in endosomes LDLR releases its bound natural ligand (LDL), and adopts a closed conformation via its β-propeller domain binding to the ligand-binding repeats LA 4 and LA 5. Since rhinoviruses are also sensitive to low pH, conformational modifications of both LDLR and minor group HRVs might take place concomitantly. Whether the virus is released by the receptor still in its native or its converted form might influence the efficiency of infection. While in the first case the virus would convert in the fluid phase of the endosome and diffuse back to the endosomal membrane for productive RNA release, in the second case it would be directly handed over from the receptor to the membrane upon its conversion. The latter is predicted to result in a higher efficiency of viral RNA release into the cytoplasm of the host cell. Since the β-propeller domain of LDLR is necessary for the release of bound LDL, we aimed at comparing the behaviour of wt and β-propeller deficient LDLR with respect to endosomal virus release and the efficiency of infection. As the virus should be also released from a propeller deficient receptor (due to its own conversion), differences between the two scenarios would point to the β-propeller having an impact on rhinovirus infection. This would indicate that LDLR is not just a simple vehicle for virus delivery. CHO *ldla7* cells that are deficient in endogenous LDLR (Krieger et al., 1981) and had been transfected to stably express either native or β-propeller-negative human LDLR (Beglova et al.) were used in the experiments, because no human cell line lacking both VLDLR and LRP is available. In order to separately consider virus-receptor interaction and later steps of the infection, low pH induced virus conversion and release was investigated by using the plasma membrane of the cells as a model for the inner side of the endosomal membrane. To assess the impact of the β-propeller in HRV infection, virus attachment, internalization, uncoating, capsid degradation, infection kinetics (using a CHO-adapted HRV2 variant), and the intracellular fate of LDLRs were investigated.

4. Materials and methods

4.1. Chemicals, reagents and buffer solutions

4.1.1. Chemicals

All chemicals were obtained from Sigma (Sigma, St. Louis, Mo.) or Merck (Darmstadt, Germany), unless specified otherwise. WIN 52084-2 was a kind gift of Dan Pevear, ViroPharma.

4.1.2. Cell culture materials, media and buffer solutions

Cell culture media and supplements were from Gibco BRL, cell culture dishes from Iwaki, T-175 flasks from Nunc^{TM}, T-162, T-75 and T-25 flasks, 6 well, 12 well and 24 well plates from Costar, and plastic tubes from Falcon.

HeLa-H1 cells were cultured in minimal essential medium (MEM) supplemented with 10 % heat-inactivated fetal calf serum (FCS), 2 mM L-glutamine, 100 U/ml penicillin, and 100 µg/ml streptomycin. For infection of HeLa cells MEM containing 30 mM $MgCl_2$ and 2 % FCS (infection medium) was used.

CHO cells were cultured in Ham's F-12 medium with 5 % FCS, 2 mM L-glutamine, 100 U/ml penicillin and 100 µg/ml streptomycin. Transfected CHO cells were maintained in the same medium containing the selection agent geneticin (G418) at 1 mg/ml. CHO-infection medium was Ham's F-12 containing 30 mM $MgCl_2$ and 2 % FCS, without geneticin.

Phosphate buffered saline (PBS) was 3.2 mM Na_2HPO_4, 0.5 mM KH_2PO_4, 1.3 mM KCl, 135 mM NaCl, pH 7.4.

Hank's balanced buffer solution (HBBS) was 137 mM NaCl, 5.4 mM KCl, 0.25 mM Na_2HPO_4, 0.44 mM KH_2PO_4, 1.3 mM $CaCl_2$, 1.0 mM $MgSO_4$, 4.2 mM $NaHCO_3$. It was used for washing and for incubation of CHO cells at 4°C during virus binding experiments and other cellular assays.

Radio-immunoprecipitation assay (RIPA) buffer (50 mM Tris-HCl (pH 7.5), 150 mM NaCl, 1 mM EDTA, 0.1 % Na-deoxycholate , 0.1 % SDS and 1 % Triton X-100) was used for cell lysis prior to radio-immunoprecipitation and/or scintillation counting.

Isotonic MES buffers of different pH. For virus binding/release experiments isotonic 30 mM MES buffers were made of a pH between 4.8 and 7 with increments of 0.2 pH units; to ensure isotonicity, the NaCl concentrations were calculated using the web tool „Recipe calculator for thermodynamically correct buffers" of the University of Liverpool, (http://www.liv.ac.uk/buffers/buffercalc.html). After adding the adequate amount of NaCl, the buffers were adjusted to the respective pH with NaOH at 0°C.

4.2. Cell lines

HeLa-H1 Ohio (American Type Culture Collection, Manassas, Va.), a subline supporting the replication of HRVs, was used for viral titre determination as well as for radiolabeling of virus with [S^{35}]-methionine/cysteine.

CHO cells overexpressing wild type and β-propeller negative human LDLR, a kind gift of Prof. Stephen Blacklow, Boston, USA, had been prepared by stable transfection of CHO-*ldla7* cells (a Chinese hamster ovary cell line that lacks functional endogenous LDL receptors (Kingsley and Krieger, 1984)) either with wild type human LDLR (termed RF3 cells) or with an LDLR in which the YWTD β-propeller and the EGF-C domains were deleted (termed ΔYC cells) (Beglova et al., 2004a, b).

4.3. Culturing and splitting of adherent cell lines

4.3.1. Growing cells

In order to ensure **sterile working conditions,** manipulations were performed in a laminar flow hood. Pipettes and buffers were autoclaved, media were sterile filtered through a micro filter (Cameo 25GAS) with a pore size of 0.22 µm.

Cells were cultured either as monolayers in tissue culture flasks, dishes, microtiter well plates or for special purposes in suspension at 37°C in a water-saturated atmosphere containing 5 % CO_2.

When **splitting monolayer cells**, medium was removed, cells were washed with PBS, than harvested with 10 mM EDTA in PBS (5 ml for a 162 cm^2 culture flask) incubating at 37°C for 3-5 min. EDTA chelates Ca^{2+}ions, weakening the interaction between the flask surface and

cell adhesion molecules. Detached cells from a 162 cm^2 flask were diluted to 14 ml with PBS, pelleted in a Heraeus Megafuge at 1200 rcf for 5 min to remove EDTA, and resuspended in the desired medium.

4.3.2. Freezing cells

After harvesting cells with 10 mM EDTA in PBS and pelleting, they were resuspended in freezing medium (10 v/v % DMSO in FCS) at a cell density corresponding to 54-56 cm^2 of monolayer cells per ml. The cells were transferred into cryo tubes (Nunc ^{TM}) (1 ml per each tube) which were placed in a freezing box containing isopropanol allowing slow cooling to -80°C. For long term storage at -196°C the tubes were transferred into liquid nitrogen the next day.

4.3.3. Thawing cells

Cells in cryo tubes were thawn in a water bath at 37°C until some few pieces of ice were still present. They were diluted to 10 ml with medium, and pelleted. The supernatant containing toxic DMSO used as a cryo-protectant was discarded, and the cell pellet was resuspended in growth medium and transferred into a culture flask.

4.3.4. Splitting cells and seeding them for different assays

Plastic ware	**Surface area**	**Number of HeLa cells**
T-225 flask	225 cm^2	360 x 10^5 cells
T-175 flask	175 cm^2	280 x 10^5 cells
T-162 flask	162 cm^2	260 x 10^5 cells
T-75 flask	75 cm^2	120 x 10^5 cells
T-25 flask	25 cm^2	40 x 10^5 cells
6-well plate	9.4 cm^2 / well	15 x 10^5 cells / well
12-well plate	4 cm^2 / well	6.4 x 10^5 cells / well
24-well plate	2 cm^2 / well	3.2 x 10^5 cells / well
48-well plate	0.8 cm^2 / well	1.3 x 10^5 cells / well
96-well plate	0.32 cm^2 / well	0.51 x 10^5 cells / well

Table 3. Cell numbers corresponding to the surface of culture flasks/plates used (1 cm^2 ~ 1.6 x 10^5 HeLa cells).

Seeding cells into 96-well plates for $TCID_{50}$

A day prior to infection 1/30 of the cells of a confluent 175 cm^2 flask were resuspended in 10 ml infection medium for each 96-well plate, and 100µl were seeded into each well. The plates were incubated at 37°C overnight; cells were ~60 % confluent the next day.

Seeding cells into 6-well plates for binding and infection assays

A day prior to infection 1/12 of the cells of a confluent 75 cm^2 flask or 1/25 of the cells of a confluent 162 cm^2 flask were resuspended and seeded in 4 ml F-12 infection medium per well. The cells were grown at 37°C and were ~60 % confluent the next day.

4.4. Viruses: wild type and CHO-adapted HRV2

HRV2 was originally obtained from the American Type Culture Collection (ATCC, Rockville, Md., USA). An HRV2 variant adapted to replicate in CHO cells was isolated by blind passages alternating between HeLa and CHO-RF3 cells. Cells in a 162 cm^2 flask were challenged with virus at 10 $TCID_{50}$/cell at 34°C for 30 min, medium with non-bound virus was replaced by fresh infection medium, and cells were incubated for 24 h to allow for infection. Virus eventually produced in the CHO cells was liberated by three consecutive freeze/thaw cycles and then HeLa cells were infected with the lysates. Whereas initially no CPE was seen in the CHO cells, HeLa cells usually lysed after 24 h. However, after 12 cycles CPE appeared in the CHO cells and persisted even upon CHO to CHO passaging for more than 5 times. The variant population, termed $HRV2_{CHO}$, replicated in both CHO cell lines but with different kinetics (see Results).

4.5. Infection

Infection with HRVs was performed at 34°C in infection medium (medium containing 2 % FCS, antibiotics, 2 mM glutamine, and 30 mM $MgCl_2$ for monolayer cultures; S-MEM supplemented with 2 % HS, antibiotics, 2 mM glutamine, 1 % non-essential amino acids, 1 % Pluronic F-68, and 1 mM $MgCl_2$ for suspension cultures) for 1.5 to 3 hours. Then, cells were washed twice with PBS to remove unbound virus and further incubated in infection medium to allow for virus replication.

In comparative infection experiments using CHO cells, viruses were allowed to bind for 1 h at 4°C, unbound virus was removed by washing with ice cold HBBS, than the cells were placed at 34°C in infection medium.

4.6. Preparation of seed virus

HeLa cells were grown to a density of $4x10^5$ cells/ml in a 2 l suspension culture. After transfer into 2 l infection medium for suspension cultures, the cells were infected with virus at MOI of 1 (one plaque forming unit per cell = 10 $TCID_{50}$/cell). The culture was incubated with stirring at 20 rpm for 16 hours at 34°C allowing for efficient virus production. After pelleting at 4.000 rpm (J6B rotor) for 20 min at 4°C, the cells were resuspended in 20 ml PBS and broken by Dounce homogenization on ice, than sonicated for 3 min to allow viral particles to be released. Cell debris was pelleted at 15,000 rpm (SS34 rotor) for 30 min at 4°C. Supernatants containing virus were stored at -80°C in aliquots.

4.7. Viral titre determination by $TCID_{50}$

A day before infection 1/30 of the cells of a confluent 175 cm^2 flask were resuspended in 10 ml infection medium for each 96-well plate, and 100 µl were seeded into each well. The plates were incubated at 37°C overnight, to be ~50-70 % dense on the day of infection. Serial 10-fold dilutions of the virus suspension of unknown titre were prepared, each in 2 ml infection medium. The cells were infected with 100 µl per well, using 12 wells for each of the 8 dilutions. Upon incubation at 34°C for five days, monolayers in wells containing infectious virus had lysed completely. The medium was removed and cells were stained with 0.1 % crystal violet in water (60-80 µl per well) for 10-15 min. The staining solution was discarded and the wells were rinsed with water. While wells containing intact cell monolayers appeared violet, empty wells remained unstained because lysed cells detached from the well surface and were washed away. From the numbers of infected and non-infected wells the tissue culture infectious dose, infecting 50 % of the culture per ml ($TCID_{50}$/ml), was calculated based on the method of Blake and O'Connell, 1993. It has been empirically determined that 10 $TCID_{50}$ is approximately equal to one plaque forming unit (pfu).

4.8. Radiolabeling of HRV2

HeLa cells were grown in a 162 cm^2 flask to about 80 % confluency, washed twice with PBS, and incubated with 20 ml methionine/cysteine-free DMEM supplemented with 2 % dialysed FCS, 100 U/ml penicillin, 100 µg/ml streptomycin, 2 mM L-glutamine, and 30 mM $MgCl_2$ for 4 h at 37°C. The medium was replaced by fresh methionine/cysteine-free medium, and virus was added at 1000 $TCID_{50}$/cell. The cells were incubated for 4 h at 34°C to allow for viral internalization and host cell shut off. Fifteen ml of the old medium were replaced by

fresh infection medium containing 2 % dialysed FCS. After addition of 1 mCi [^{35}S]-methionine/cysteine (Hartmann Analytic GmbH, Braunschweig, Germany) incubation was continued for 16 h. Cells were broken by 3 cycles of freezing/thawing, debris was removed by centrifugation at 20,000 rpm (Ty65 rotor) for 20 min at 4°C. Virus was pelleted at 50,000 rpm (Ty65 rotor) for 2 h, and resuspended in 1 ml HBBS supplemented with 2 % FCS overnight at 4°C. Insoluble material was removed by centrifugation in a table top centrifuge. Remaining free radiolabel was removed by 2x pelleting the virus in an Optima TLX (Beckman) table top ultracentrifuge (TLA 100.3 rotor) at 70,000 rpm for 1 h. The viral pellet was finally resuspended in 200 µl HBBS, 2 % FCS, and stored at 4°C. Incorporated radioactivity was quantified by liquid scintillation counting (Tricarb; Packard, Meriden, Connecticut, USA); only radiochemically pure virus preparations (i.e. only viral proteins visible in the autoradiogram), as checked on a reducing 15 % SDS-PAA gel, were used. To ensure the absence of eventually converted and/or damaged particles, the preparations were stored over *S. aureus*-2G2 immune-complexes which were removed by centrifugation before use.

4.9. FACS quantification of LDLR expression

CHO cells were detached from 162 cm^2 culture flasks by incubation in 5 ml 10 mM EDTA in PBS at 37°C for 5 min. The cells were washed with PBS and resuspended in Ham's F-12 growth medium to allow for re-saturation of cell surface LDL-receptors with Ca^{2+} at 37°C for 30 min. After 2 times washing in ice cold HBBS, the cells were resuspended in ice cold FACS-buffer (HBBS supplemented with 2 % FCS) at ~ 2x10^6 cells/ml, and incubated under slow rotation for 1 h at 4°C. Cells were dispensed in 2 ml Eppendorf tubes at ~2x10^6 cells/sample, pelleted at 1000 g for 5 min, resuspended in 200µl FACS-buffer containing chicken IgY directed against the ligand binding domain of human LDLR (prepared by standard techniques in our lab) at 2.5 µg/ml. The cells were then incubated on ice for 1 h by gently shaking the tubes every other 10 min. After 3 washes with 1 ml ice cold HBBS, phycoerythrin-conjugated donkey anti-chicken secondary antibody (Jackson Immuno Research) was added at 1:100 dilution in 200 µl FACS-buffer. After 30 min incubation, the cells were washed twice with cold HBBS, resuspended in 1 ml of cold HBBS, transferred into 5 ml polypropylene FACS tubes, and kept on ice until analyzed. Cell associated fluorescence corresponding to receptor expression was measured in a Becton-Dickinson LSR-I flow cytometer, using the CellQuest Pro software for data analysis.

4.10. FACS-sorting of highly expressing CHO cells

Cells were prepared the same way as for FACS quantification of LDLR expression. Sorting was carried out on a Becton-Dickinson FACS-Aria instrument, using two gates as indicated in Fig. 25. The gated cell populations were collected into F-12 growth medium, expanded in cell culture, and frozen for long term storage. Finally, the higher LDLR-expressing populations for both cell lines (shown in red) were expanded to a higher extent to prepare a stock of cells with identical receptor expression levels; these batches were used in all further assays.

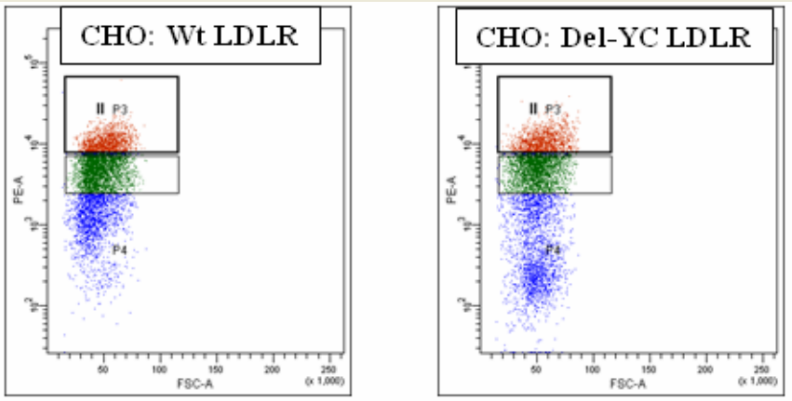

Figure 25. FACS-sorting of CHO cells to obtain highly expressing populations. Cells collected using the upper gate (shown in red) were finally expanded and used for further experiments.

4.11. Attachment of radiolabeled HRV2 to cell surface LDLRs

CHO cells expressing wt or truncated LDLR were grown in 6-well plates until about 80 % confluency. The growth medium was discarded, cells were washed with ice cold HBBS, 20,000 cpm of [^{35}S]-labeled HRV2 in ice cold infection medium was added per well, and the plates were incubated for 1 h at 4°C for virus binding. Non-bound virus was removed by washing 3 times with ice cold HBBS, the cells were lysed with 500 µl RIPA buffer on ice for 15 min, and transferred into scintillation vials. The wells were washed with 500 µl RIPA buffer and with 500 µl HBBS, and the washes were combined with the cell lysates. The required volumes of Filter Count scintillation cocktail (5-7 ml) were added to the lysates to obtain a clear suspension, and cell associated radioactivity was measured in a liquid scintillation counter (Tricarb; Packard, Meriden, Connecticut, USA).

4.12. Release of LDLR-bound HRV2 from CHO cells after low-pH treatment

CHO cells were grown in 6-well plates until confluent. The medium was removed, cells were incubated in cold HBBS for 10 min at 4°C, and challenged with 20,000 cpm of [^{35}S]-labelled HRV2 in ice cold CHO infection medium for 1 h at 4°C. Non-bound virus was removed by washing with ice cold HBBS, and cells were exposed to isotonic 30 mM MES buffers of pH 4.8 to 7 (with increments of 0.2 pH units) for 20 min at 4^{o}C. Samples were re-neutralized by addition of the adequate volumes of 1 M Tris-base. Virus released into the supernatant and remaining cell-associated was quantified separately by scintillation counting.

In a separate experiment the effect of the duration of low pH incubation and re-neutralization on virus dissociation was determined. Cells were incubated at pH 5, 6 and 7 for 20, 45 and 90 min, followed by re-neutralization to pH 7 for 0, 10, and 45 min.

4.13. Modelling endosomal virus conversion at the plasma membrane

4.13.1. Pre-treatment of virus with WIN-compound

In these experiments either untreated or WIN-compound treated radiolabeled viruses were used. WIN 52084-2 was dissolved at 0.5 mg/ml in 50 % dimethylsulfoxide (DMSO) and stored at -20°C. The working solutions contained WIN 52084-2 at 20 µg/ml and DMSO at 2 % final concentrations in 150 mM NaCl pH 7.5. For mock treated virus, 2 % DMSO in 150 mM NaCl pH 7.5 was used for incubation. For each sample to be assayed 30,000 cpm [^{35}S]-labelled HRV2 was pre-incubated in 20 µl of 150 mM NaCl pH 7.5 containing WIN 52084-2 at 20 µg/ml (final concentration) for 30 min at room temperature. Untreated virus was pre-incubated in the same buffer without the WIN-compound. Eventually present non-native virus was removed by immunoprecipitation with mAb 2G2 - *S. aureus* immunocomplexes.

4.13.2. Virus binding to cell surface LDLRs followed by low pH-induced release

CHO cells were grown in 6-well plates until confluent, and pre-incubated in cold HBBS for 10 min at 4°C. Then, 20,000 cpm of [^{35}S]-labelled HRV2 (untreated and pre-incubated with the antiviral, respectively) in ice cold infection medium was added to each well, and the plates

were incubated for 1 h at 4°C for virus binding. Non bound viruses were removed by washing 3 times with ice cold HBBS. The cells were then incubated in 1 ml cold isotonic buffers of pH 4.8, 5.2, 5.4, 5.6, 5.8 and 6.2 for 20 min at 4°C, to induce virus conversion at the plasma membrane. The low pH incubation was terminated by adding appropriate amounts (0-25 µl) of 1 M Tris base to the isotonic incubation buffers to adjust the pH values to neutral. The cells were further incubated in the re-neutralized buffers for 20 min at 4°C to allow for release of converted viruses. Supernatants (1 ml) were collected in 2 ml Eppendorf tubes, and the cells were washed twice with 250 µl HBBS. The washes were combined with the supernatants, and 300 µl of 6x RIPA buffer was added to each tube in order to accomplish 1x final concentration of RIPA buffer for immunoprecipitation. The cells were lysed on ice for 15 min by adding 500 µl RIPA buffer into each well, and the lysates were collected in 2 ml Eppendorf tubes. The wells were rinsed twice with 500 µl RIPA buffer, the washes were combined with the cell lysates, and debris was removed by centrifugation. The two samples (supernatants containing the incubation buffers, and the cleared cell lysates) belonging to each pH value, were processed separately for sequential immunoprecipitation.

4.13.3. Preparation of *Staphylococcus aureus* immunocomplexes

500 µl fixed, heat killed *S. aureus* cells from a 10 % stock suspension were pelleted at 10,000 rpm for 1 min in a table top Eppendorf centrifuge. The pellet was washed twice with 1 ml PBS and twice with 1 ml RIPA buffer. Bacteria were resuspended in 400 µl RIPA buffer and then incubated with 100 µl HRV2-antiserum for 1 h shaking at room temperature. Bacteria were pelleted, washed three times with RIPA buffer, and finally resuspended in 500 µl RIPA buffer containing 0.04 % sodium azide and stored at 4°C until used. Since protein-A binds rabbit IgG much better than mouse IgG, mAb 2G2 was bound via rabbit anti-mouse IgG by using the same procedure.

4.13.4. Immunoprecipitation and scintillation counting

Supernatants and cell lysates were processed separately for sequential immunoprecipitation. First subviral particles were recovered by addition of 20 µl MAb 2G2-*S. aureus* immunocomplexes and incubated for 2 h shaking at room temperature. Bacteria were pelleted and washed twice with 200 µl RIPA buffer. Supernatants and washes were combined, and remaining native virus was precipitated by 20 µl rabbit HRV2 antibody-*S. aureus* immunocomplexes. Pellets were washed twice with 200 µl RIPA buffer, resuspended in 200 µl HBBS, and transferred into scintillation vials. Remaining radioactive virus was collected from the Eppendorf tubes by washing 2 times with 200 µl HBBS, and added into the respective scintillation vials. The required volumes of Filter Count scintillation cocktail were

added (5-7 ml) to obtain a clear suspension, and radioactivity of the samples was determined in a liquid scintillation counter (Tricarb; Packard, Meriden, Connecticut, USA). Conversion of native virus into subviral particles was calculated by dividing the sum of 2G2-precipitated counts by the total counts (i.e. the sum of the counts in the 2G2 and anti-HRV2 precipitates). Conversion at pH 4.8 was set to 100 % and conversion at pH 7 to 0 %.

4.14. Internalization kinetics of LDLR-bound virus

CHO-*ldla7* cells expressing human wt LDLR (RF3) and cells expressing human LDLR without the β-propeller (ΔYC) were grown until confluent in 6-well plates. After removal of the medium and pre-incubation in HBBS for 10 min at 4°C the cells were challenged with HRV2 at 100, 50 and 10 $TCID_{50}$/cell in CHO-infection medium for 1 h at 4°C. Non-attached virus was washed away with ice cold HBBS, the medium was replaced with cold infection medium, and the cells were placed at 34°C for 0 (control for binding only), 1, 2, 3, 4, 5, 6 and 10 min. Viral entry was stopped by adding ice cold HBBS and placing the plates on ice. Following extensive washing with ice cold HBBS and blocking (in HBBS with 2 % FCS) for 1 h on ice, virus remaining surface-accessible was quantified in a cell-based ELISA type assay (performed on ice); mAb 8F5 (Skern et al., 1987) at 20 µg/ml in HBBS with 2 % FCS was added at 4°C for 1 h, cells were extensively washed and incubated with HRP-conjugated secondary antibody (diluted 1:20,000 in HBBS, 2 % FCS) at 4°C for 30 min. One ml of a solution of 100 µg/ml 3,3',5,5'-tetramethyl benzidine in 100 mM Na-acetate (pH 5.6), 0.03 % H_2O_2 was added to each well, and the colour reaction was allowed to develop on ice. After 20 min, 150 µl aliquots were transferred into a new 96-well plate, 75 µl of 1 M H_2SO_4 was added to each well, and A_{450} was measured in a Labsystem Multiscan RC plate reader. Values obtained for non-infected cells (background) were subtracted.

4.15. Kinetics of cellular protein synthesis

Protein synthesis rate was determined via time-dependent incorporation of [^{35}S]-labeled cysteine/methionine into cellular proteins. CHO cells were grown in 6 well plates to about 80 % confluence and incubated in methionine/cysteine-free medium (DMEM supplemented with 2 % dialysed FCS, 100 U/ml penicillin, 100 µg/ml streptomycin, 2 mM L-glutamine, and 30 mM $MgCl_2$) for 4 h at 37°C. The medium was replaced by 1 ml of fresh methionine/cysteine-free medium supplemented with 40 µCi of [^{35}S]-methionine/cysteine per well. Incorporation of radioactive amino acids into cellular proteins was monitored by incubating the cells at 37°C for 0, 1, 2, 3, and 4 h. After extensive washing with HBBS, cells

were lysed in 1 ml of 10 % trichloroacetic acid (TCA) in HBBS, and samples were transferred into 2 ml Eppendorf tubes. Wells were rinsed with 400 µl of 10 % TCA in HBBS, and the solutions combined. After incubation on ice for 20 min, precipitated cellular proteins were pelleted at 10,000 rpm for 2 min in a table top Eppendorf centrifuge. To avoid carry over of the pellet, 700 µl of the supernatant was siphoned off, and radioactivity of this half volume of total supernatant (S/2), and the pellet with the remaining half volume of supernatant (P+S/2) were scintillation counted separately, and pellet-associated counts were calculated.

4.16. Kinetics of intracellular virus conversion and degradation

CHO cells were grown in 6 well plates, pre-incubated in cold HBBS for 10 min at 4°C, and challenged with 20,000 cpm of [^{35}S]-labelled HRV2 at 4°C for 1 h. Unbound virus was removed by extensive washing with ice cold HBBS, and the cells were incubated in 1 ml CHO-infection medium at 34°C allowing for virus internalization and endosomal conversion. At the times given in the text the cells were lysed without removing the incubation medium by adding 200 µl of 6x RIPA buffer. Cell debris was removed by centrifugation. For monitoring uncoating, subviral particles were immunoprecipitated with mAb 2G2, and remaining native virus with HRV2 antiserum. Liquid scintillation counting was carried out as described above, and ratios of 2G2 precipitated counts and total counts were calculated.

Viral capsid degradation was measured the same way, except that only HRV2-antiserum was used for immunoprecipitation. Ratios of not precipitable counts and total counts were taken as a measure of degradation; set to 0 % at time 0.

4.17. Time-dependent co-localization of virus and LDLR

CHO cells were seeded onto 13 mm glass coverslips (Menzel, Braunschweig, Germany) and grown until 80 % confluent. Cells were washed with PBS containing 1 mM $CaCl_2$ and 1 mM $MgCl_2$ (PBS^{++}), pre-incubated in 200 µl CHO-infection medium for 30 min at 37 °C, cooled to 4°C, and challenged with HRV2 at 900 $TCID_{50}$/cell for 1 h. Unbound virus was removed by 3 washes with 2 ml ice-cold PBS^{++}, and the cells were incubated in 500 µl pre-warmed CHO-infection medium for 4, 20, and 60 min (chase). The cover slips were transferred into a 6 well plate on ice and washed with 2 ml of ice-cold PBS^{++} for 5 min. The cells were fixed for 30 min with 300 µl 4 % paraformaldehyde (PFA) in PBS^{++}, quenched with 300 µl 50 mM NH_4Cl in PBS for 10 min, washed 3 times and permeabilized with 300 µl of 0.2 % Triton X-100 in PBS for 5 min. Unspecific binding sites were blocked with 200 µl of 10 % goat

serum in PBS (Gibco Invitrogen Corp., Paisley, United Kingdom) for 30 min. All antibodies were diluted with PBS containing 10 % goat serum. HRV2 was detected with mAb 8F5 (Saito et al., 2007) (10 µg/ml) followed by Alexa 568-conjugated goat anti-mouse IgG (1:1000; Molecular Probes Incorp., Eugene, OR, USA), and LDLR was detected with chicken anti human LDLR IgY (10 µg/ml) and Alexa 488-conjugated goat anti-chicken IgG (1:1000) (Molecular Probes). Cells were washed 4 times for 10 min each with 5 ml PBS, and nuclei were stained with DRAQ5 (Biostatus, Shepshed Leicestershire, United Kingdom). Cover slips were briefly dipped in ddH_2O and mounted in Mowiol. Cells were viewed with a Zeiss Axiovert 200 microscope (Carl Zeiss, Jena, Germany) equipped with an UltraView ERS laser confocal system (PerkinElmer, Shelton, CT, USA). Twelve-bit images of highest resolution (1344 x 1024 pixels; no binning) were acquired through a 63x/ 1.4 Plan-Apochromat lens (Carl Zeiss, Jena, Germany). Images were taken with the same exposure time and emission was discriminated by sequential acquisition. For Z-stack analysis, at least 15 images were recorded at 0.2 µm intervals with a piezo-driven Z stage. UltraView software was used to correct for background fluorescence and to determine the extent of co-localization.

4.18. Kinetics of the infection of CHO cells with $HRV2_{CHO}$.

CHO cells grown in 6 well plates were challenged with $HRV2_{CHO}$ at 10 $TCID_{50}$/cell at 4°C for 1 h. Non-bound virus was removed by extensive washing with ice cold HBBS and the cells were incubated at 34°C in 2 ml CHO-infection medium. At time 0 (to determine bound virus) and after 3, 6, 9, 12, 16, 22, 26, 31, and 36 h post infection the cells were subjected to 3 freeze-thaw cycles, cell debris was removed and the viral titre was determined in HeLa cells.

4.19. Effect of HRV2 internalization on the expression and lysosomal degradation of LDLR

CHO RF3 and ΔYC cells were seeded onto 13 mm glass cover slips (Menzel, Braunschweig, Germany) and grown to 80 % confluence. Cells were washed with PBS^{++} (PBS containing 1 mM $CaCl_2$ and 1 mM $MgCl_2$) and pre-incubated in serum-free F12 medium for 1 h at 34ºC. HRV2 at 1,500 $TCID_{50}$/cell was internalized in serum-free F12 medium for 6 h. Cells were then cooled, washed, fixed and permeabilized with methanol at -20°C for 10 min, and processed for indirect immunofluorescence microscopy for detection of LDLR with chicken anti human LDLR IgY (10 µg/ml), and LAMP2 with anti-human CD107B mouse antibody (1:400 BD Biosciences, Pharmigen, USA), followed by Alexa-488-conjugated goat anti-chicken IgG and Alexa 568-conjugated goat anti-mouse IgG, respectively. Nuclei were

stained with Hoechst dye (1 µg/ml; for epifluorescence microscopy) and DRAQE5 (1:500; for confocal microscopy) and cells were embedded in Moviol. LDLR expression and the extent of co-localization with LAMP2 was investigated by epifluorescence microscopy using a Zeiss Axioplan 2 fluorescence microscope equipped with a C-Apochromat 40x lens and Axiovision software. Confocal microscopy was carried out as described above.

4.20. SDS-Polyacrylamide gel electrophoresis (SDS-PAGE)

The most widely used method to separate complex protein mixtures is the one-dimensional sodium dodecyl sulphate polyacrylamide gel electrophoresis (SDS-PAGE). This method utilizes the detergent SDS to solubilize, denature, and impart a uniform, strong negative charge to proteins. Thereby, the different proteins are separated according to their size rather than to their charge as they move through the polyacrylamide (PAA) matrix towards the anode. The migration rate and the separation range is determined by the pore size of the matrix and thus by the PAA concentration in the gel (Table 4).

Gel percentage	Separation range
6 %	70-500 kD
10 %	15-200 kD
15 %	5-50 kD

Table 4. Separation ranges of different PAA-gels

The recipes of all solutions are listed at the end of this section. The PAA gel is prepared and run in a Bio-Rad apparatus (Bio-Rad Laboratories GmbH, Vienna, Austria). A master mix for the resolving gel (Table 5.) is prepared by mixing the appropriate amounts of 4x resolving gel buffer, dd H_2O and acrylamide stock solution. Then APS (a radical starter for initiating polymerization) and TEMED (used as a catalyst) are added, the solution is mixed well, poured between two glass plates, overlaid with water and polymerized. After removing the water, 1.2 ml stacking gel solution is poured on top of the solid resolving gel. A comb is inserted immediately and the gel is allowed to polymerize. After removing the comb, the gel polymerized between the two glass plates is placed into an electrophoresis tank. The chamber is filled with electrophoresis buffer, and protein samples, mixed with 1/5 volume of 5x sample buffer and denatured at 95°C for 5 min, are loaded. For SDS-PAGE under non-reducing conditions, sample buffer lacking a reducing agent is used. A constant current of 25 mA per gel is applied until the front of the bromophenol blue marker reaches the bottom of the gel (~45 min). To estimate the molecular weight of samples, size standards are loaded onto the gel in parallel.

Proteins separated in SDS-PAA gels can be fixed and visualized by staining with Coomassie Brilliant Blue staining solution for 20 min (with a limit of detection of 200 ng protein). The acetic acid in the staining solution fixes the proteins in the gel. For identification of distinct bands the gel is destained either by boiling in H_2O or incubation in destaining solution until the background is sufficiently clear. Finally, the gel is dried on Whatman paper for 2 hours at 80°C.

resolving gel mixture	6 %	8 %	10 %	12 %	15 %	20 %
H_2O (ml)	2.75	2.4	2.1	1.75	1.25	0.4
4x resolving buffer stock (ml)	1.25	1.25	1.25	1.25	1.25	1.25
acrylamide stock (ml)	1.0	1.35	1.65	2.0	2.5	3.35
10 % APS (µl)	25	25	25	25	25	25
TEMED (µl)	2.5	2.5	2.5	2.5	2.5	2.5

Table 5. Composition of the resolving gel mixture to achieve the desired percentage

Stacking gel mixture: 2.5 ml stacking gel solution, 50 µl 10 % APS, 5 µl TEMED

4x resolving gel buffer stock: 1.5 M Tris-HCl, 0.4 % SDS pH 8.8

Acrylamide stock: 30 % acrylamide, 0.4 % bisacrylamide

Stacking gel solution: 12.5 ml 4x stacking gel buffer, 7.5 ml acrylamide solution, 30 ml H_2O

4x stacking gel buffer: 0.5 M Tris-HCl, 0.4 % SDS pH 6.8

10x electrophoresis running buffer: 250 mM Tris-base, 2 M glycine, 1 % SDS

10 % APS: 10 % ammonium persulfate in H_2O

5x sample buffer: 1.6 M Tris-HCl (pH 6.8), 15 % SDS (w/v), 50 % glycerol (v/v), 25 % β-mercaptoethanol (only for reducing gels), 0.15 mg/ml bromophenol blue

Coomassie Brilliant Blue solution: 45 % methanol, 10 % acetic acid, 0.4 % Coomassie Brilliant Blue R 250

Destaining solution: 40 % methanol, 10 % acetic acid

5. Results

Early infection events of human rhinoviruses are in the focus of our laboratory since many years. According to the present view (Brabec et al., 2003; Fuchs and Blaas, 2008), the minor group virus HRV2 is released from its receptors starting at ~pH 6 in early endosomes and is transferred in the fluid phase of endosomal carrier vesicles towards late endosomes while the receptors recycle. The gradually decreasing pH causes conversion of HRV2 into hydrophobic A-particles which then re-attach to the membrane of endosomal carrier vesicles and/or late endosomes and release their RNA into the cytosol through a pore. Therefore, minor group receptors (LDLR, VLDLR and LRP) are rather considered passive vehicles which deliver the virus to the low pH environment of endosomes. Within endosomes LDLR releases its bound natural ligand (LDL) by adopting a closed conformation via its β-propeller domain which binds to the ligand binding repeats LA4 and LA5 (Beglova et al., 2004a). As rhinoviruses are also sensitive to low pH, conformational modifications of both LDLR and minor group HRVs might take place concomitantly. We thus aimed to clarify whether the function of the β-propeller contributes to HRV infection by influencing viral conversion or virus release from the LDL-receptor.

Endosomal virus conversion can be modeled at the plasma membrane by binding virus to cell surface receptors at 4ºC (so internalization is blocked) and incubating the cells at acidic pH. In a previous work Brabec and colleagues used isotonic acetate-phosphate buffers between pH 7.4 and 5.4 to study the conversion of receptor-bound HRV2 at the membrane of HeLa cells (Brabec et al., 2003). We aimed to perform a similar experiment but instead of HeLa cells which express three different HRV receptors we wanted to work in a single receptor system. We have chosen LDLR because the most experimental data regarding the β-propeller are provided for this receptor. Since no human cell line expressing LDLR in the absence of VLDLR or LRP is available, CHO-*ldla7* cells, which are deficient in endogenous LDLR and are stably transfected to express either wild-type or β-propeller negative human LDLR (Beglova et al., 2004a), were used (Fig. 25).

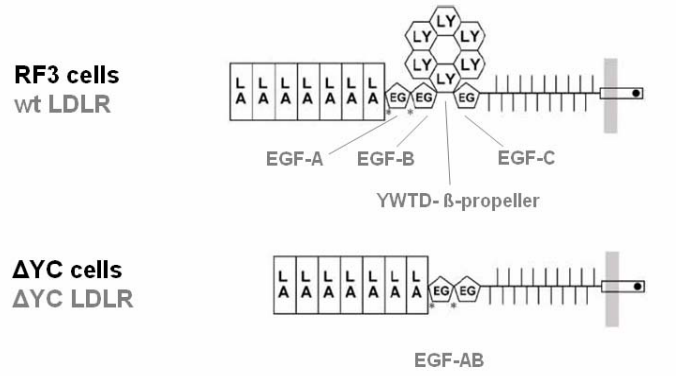

Figure 25. Schematic representation of the LDL-receptors expressed in stably transfected CHO-*ldla7* cells; modified after (Beglova et al., 2004a).

5.1. FACS-sorting and expansion yields homogenous populations of CHO cells highly expressing the respective LDLRs.

Immunofluorescence microscopy and fluorescence activated cell sorting (FACS) analysis revealed that the two transfected CHO cell lines were not homogenous in LDLR-expression. Despite being grown in the presence of the selecting agent geneticin, both RF3 and ΔYC cells had a tendency to lose the transfected LDLRs upon prolonged cultivation. In particular, the concentration of wt LDLR was comparatively low in most of the cells. Therefore, both cell lines were subjected to FACS-sorting, and cells expressing the respective receptors at similar levels were collected and expanded. This resulted in reasonably homogenous populations. Binding of radiolabeled HRV2 at 4°C was almost identical for both transfected cell lines with low background binding (3.9 % ± 0.7 % related to the mean binding of receptor-expressing cells) as determined for non-transfected CHO-*ldla7* cells that lack functional LDLR (Fig. 26). These cells were used for all experiments.

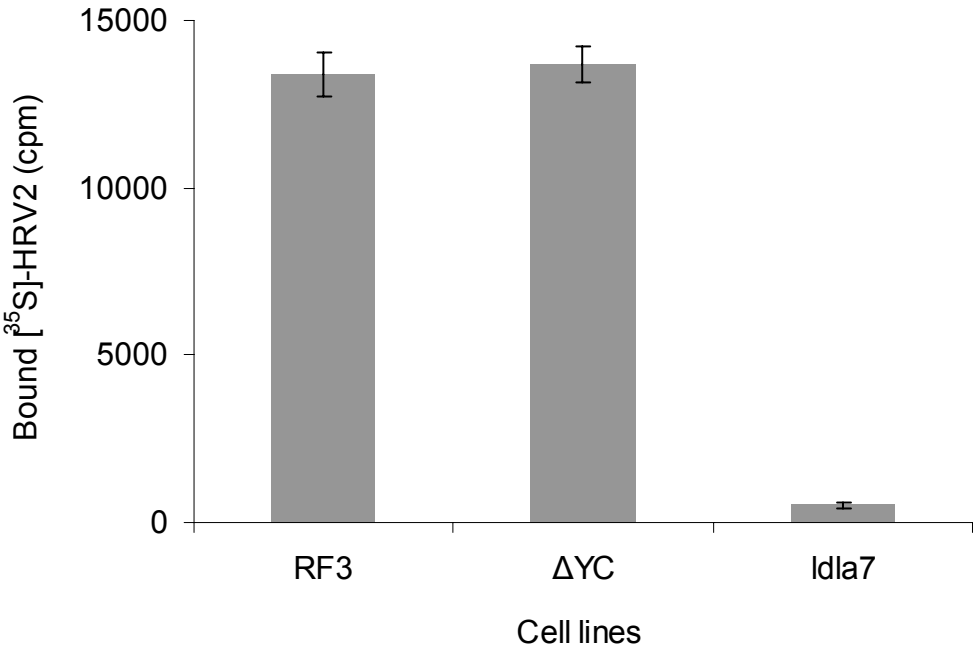

Figure 26. Virus binding to CHO cells transfected with wt or β-propeller negative human LDLR after FACS-sorting. Cells in 6-well plates were challenged with 20,000 cpm of radiolabeled virus at 4°C for 1 h. After removal of non-bound virus cells were lysed in RIPA buffer and associated counts were measured. The control *ldla7* cells are not transfected and lack functional LDLR. The same level of binding was observed for both transfected cell lines. Error bars show standard deviation (n=3).

5.2. Modeling endosomal conversion of HRV2 at the plasma membrane

The pH difference between the endosomal lumen and the cytosol is well maintained within the cell. The acetate buffer used by Brabec and colleagues is membrane permeable (Neubauer et al., 1987) and it rather equilibrates the pH at the two sides of the plasma membrane than establishes a pH difference. Moreover, the phosphate content of this buffer might deplete Ca^{2+} from the LA repeats of the receptor, reducing the strength of ligand binding by disturbing the active protein conformation. As mentioned earlier, partial unfolding of LA repeats due to decreasing endosomal Ca^{2+} concentration might indeed play an important role in ligand release from the LDLR (Arias-Moreno et al., 2008). Therefore, we decided to use another buffer system for low pH incubation of LDLR-bound virus. In order to better mimic the endosomal conditions we chose isotonic buffers based on MES (Good et al., 1966) which does not penetrate through biological membranes (www.sigmaaldrich.com) and therefore does not disturb the pH difference between the extra- and intracellular space. MES (p*Ka*=6.2) buffers well at pH values between 4.8 and 7, possessing the highest buffering capacity just within the range where structural changes of receptor and virus occur. Ca^{2+} was omitted from the buffer as decreasing Ca^{2+} concentration was found in acidifying endosomes (Arias-Moreno et al., 2008).

5.3. HRV2 is not released from CHO cells upon acidification but only after re-neutralization

Under the conditions used by Brabec and colleagues (HeLa cells with native receptor expression levels, incubation in acetate-phosphate buffers) about 50 % of receptor-bound HRV2 dissociated from the cells upon incubation at pH 6. In our experimental setup (CHO cells with ~10x higher receptor levels than HeLa cells; incubation in MES buffers) no release of receptor-bound HRV2 was observed at any pH, regardless of the kind of receptor (native or truncated) expressed. This was even so upon prolonged (90 min) incubation at pH 5. Unexpectedly however, substantial and rapid virus release was noticed upon re-neutralization of the cell-bound acidified viruses to pH 7 (which was applied for simultaneous termination of the low pH treatment in all samples). Therefore, in a separate experiment the effect of the duration of re-neutralization on virus dissociation was determined. In order to represent different stages of virus conversion, cells were exposed to isotonic 30 mM MES buffers of pH 5, 6 or 7 for 20 min at 4ºC, re-neutralized by addition of the required volumes of 1M Tris-base, and further incubated for 0, 10 and 45 min. Virus released into the supernatant and remaining cell-associated was quantified separately by scintillation counting.

Figure 27 shows the effect of re-neutralization on virus dissociation as a function of incubation time. The lack of virus release upon acidification suggests that HRV2 was directly handed over to the cell membrane as it has converted into hydrophobic A-particles. Since membrane-attached A-particles can only dissociate after their conversion into hydrophilic empty B-particles (Korant et al., 1972; Lonberg Holm et al., 1976), the re-neutralization (or some unknown factor associated with it) should have caused RNA release under our conditions. Whether the converted virus being attached to the endosomal membrane also experiences a re-neutralization effect in real infections (coming from the cytoplasm through virally opened membrane pores) still remains an open question.

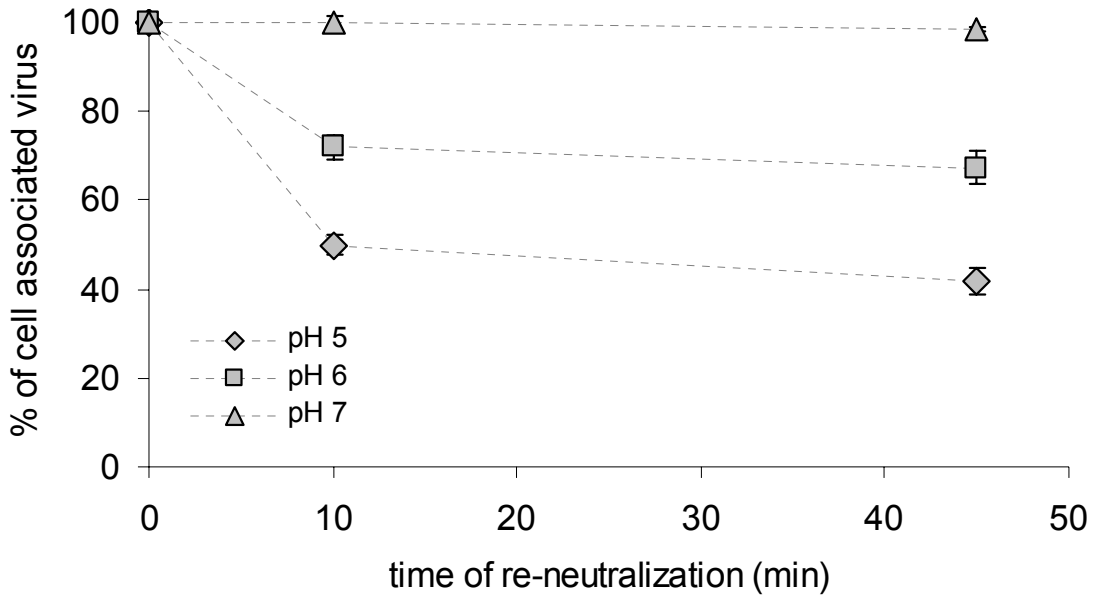

Fig. 27. Cell-attached HRV2 is not released from CHO cells upon incubation at low pH unless re-neutralized. Radiolabeled HRV2 was bound to CHO cells expressing wt LDLR at 4°C for 1 h. After removing non-bound virus, cells were exposed to isotonic 30 mM MES buffers of pH 5, 6, and 7 for 20 min at 4°C. Incubation buffers were then re-neutralized by addition of required volumes of 1 M Tris-base, and cells were further incubated for 0, 10, and 45 min. Cell-associated and released counts were measured. For three different stages of virus conversion (pre-treated at pH 5, 6, and 7) the effect of re-neutralization on virus dissociation is shown as a function of incubation time. Error bars show standard deviation (n=3).

5.4. The propeller deficient LDLR protects HRV2 against conversion similarly as a capsid-binding antiviral compound

The role of the β-propeller domain in virus conversion and release from LDLR was investigated by mimicking endosomal acidification at the plasma membrane. The

experimental setup of Brabec and colleagues was slightly modified. Briefly, [^{35}S]-labelled HRV2 was attached to the cells at 4^{o}C for 1 h, unbound virus was washed away with cold HBBS, and the cells were incubated in isotonic MES buffers of pH 4.8 to 7 (with increments of 0.2 pH units) at 4^{o}C for 20 min. The incubation buffers were then re-neutralized by adding the required volumes of Tris-base, and the cells were further incubated for 20 min. Radiolabel released into the medium in the form of subviral particles or of native virus was then determined by sequential immunoprecipitation. First, A- and B-subviral particles were precipitated with *Staphylococcus aureus*-bound monoclonal antibody 2G2 (Hewat and Blaas, 2006; Skern et al., 1987), then remaining native virus was recovered with rabbit HRV2 antiserum. The same procedure was carried out with the cellular fraction after cell lysis with RIPA buffer.

Low pH-induced virus conversion was quantified by liquid scintillation counting and is depicted as a percentage (total conversion in supernatant plus cell lysates) in Figure 28. Similarly to HRV2 bound to HeLa cells (Brabec et al., 2003), the conformational alterations of HRV2 bound to CHO cells expressing human wt LDLR (dark squares) also occurred within a pH range from < 6 to around 5.4, giving rise to a typical sigmoid curve. However, when the virus was bound to β-propeller negative LDLR (light diamonds) the curve was shifted towards lower pH values by an increment of about 0.3 pH units. This clearly shows that the β-propeller exerts a substantial effect on the conversion of HRV2. As not only the virus but also the LDLR undergoes conformational transitions between pH 6 and 5 (Rudenko et al., 2002), it is difficult to dissect the contribution of either one on virus-receptor dissociation. Capsid-binding drugs such as I(S), also named as WIN-52084 (from the Sterling Winthrop company that originally manufactured these compounds) displace fatty acids naturally present in the hydrophobic pocket of the capsid, and stabilize HRVs against low-pH induced conversion into subviral A-particles (Gruenberger et al., 1991; Kim et al., 1989). Therefore, the same experiment was carried out with HRV2 that had been pre-incubated with this drug. As also seen in Fig. 28, WIN-stabilization caused a shift in the conversion curve of wt LDLR-bound HRV2 (dark grey triangles) towards lower pH values. This shift was almost identical to the effect of the β-propeller deletion (light diamonds).

Apparently, in the absence of the β-propeller, the strong binding by the multi-modular receptor stabilizes the native virus conformation. This is in line with earlier data of Nicodemou *et al.*, demonstrating stabilization of HRV2 by the soluble concatemeric pentamer of module 3 of VLDLR (V33333) (Nicodemou et al., 2005). WIN-stabilization and binding to the truncated receptor had additive effects, shifting the sigmoid curve even more towards lower pH values (light grey circles).

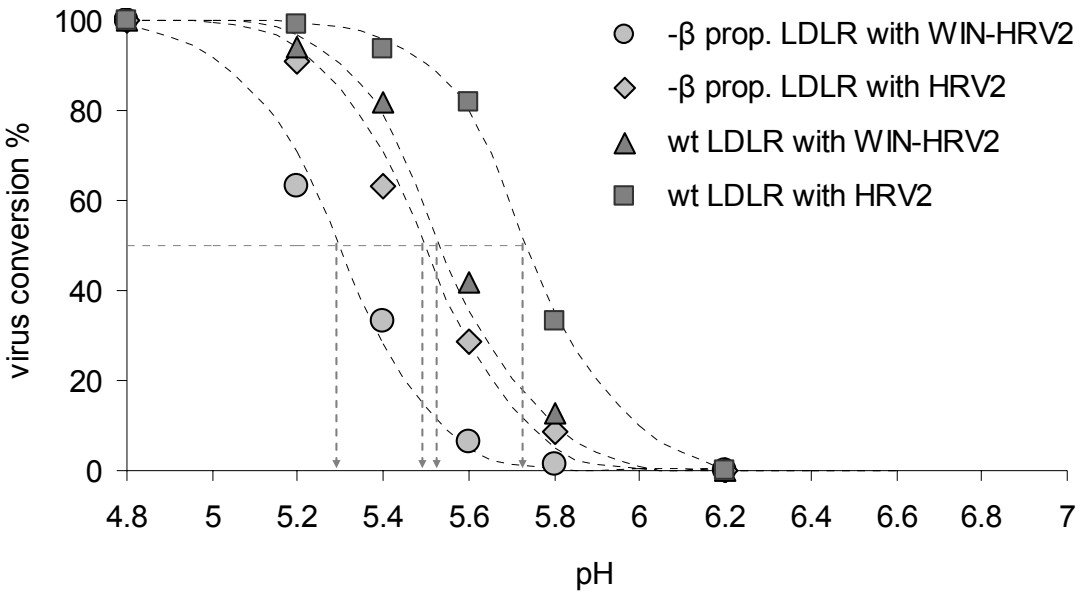

Figure 28. Conversion of LDLR-bound HRV2 at the plasma membrane induced by incubation in acidic buffers. Radiolabeled HRV2 either untreated or pre-incubated with the antiviral drug WIN-52084 was attached to the cells at 4°C for 1 h, non-bound virus was removed, and the cells were incubated at 4°C for 20 min in isotonic buffers of the pH values indicated. The buffers were re-neutralized by adding Tris-base, and the cells were further incubated for 20 min to allow for virus release. Converted virus was immunoprecipitated with mAb 2G2, and remaining native virus by anti-HRV2 antiserum from both the supernatants and cell lysates. Total conversion at pH 4.8 was set to 100 % and no conversion at pH 7 was set to 0 %. Note that the propeller-negative LDLR stabilizes the virus against conversion to a similar extent as the antiviral substance, and the two different types of protection effects are additive. The respective pH values causing 50 % conversion (inflexion points of the curves) under these conditions are projected to the X axis.

Virus particles released into the supernatant were found in 80-100 % as subviral particles at any pH value of incubation for all four experimental conditions (data not shown). This strongly suggests that the majority of virus particles remained receptor-bound until converted and native virus was not released to any significant extent. Most likely, the hydrophobic A-particles were directly handed over to the membrane upon their generation, where they remained bound until the RNA was released (triggered by re-neutralization of the incubation buffers), and only the remaining hydrophilic empty capsids fell off the cell surface.

5.5. Both CHO cell lines showed the same kinetics in uptake of HRV2

After modeling endosomal events at the plasma membrane, we turned to the investigation of intracellular steps of the infection. First, the kinetics of virus internalization was compared in the two transfected cell lines. This was derived from the time-dependent disappearance of surface-exposed virus. CHO-*ldla7* cells expressing human wt LDLR and human LDLR lacking the β-propeller were grown in 6-well plates until confluent. The medium was replaced

with fresh infection medium, and HRV2 at 100 $TCID_{50}$/cell was allowed to attach for 1 h at 4°C. Non-attached virus was washed away with cold HBBS, and the medium was replaced with fresh ice cold infection medium. Virus internalization was started in all samples simultaneously by placing them at 34°C. At the times indicated, receptor-bound virus remaining at the cell surface was quantified in a cell based ELISA type assay (performed on ice), using mAb 8F5 followed by HRP-conjugated secondary antibody. The kinetics of virus internalization was found to be identical in the two transfected cell lines, as shown in Fig. 29. The same experiment was carried out with 100, 50 and 10 $TCID_{50}$/cell of input virus, with essentially the same results.

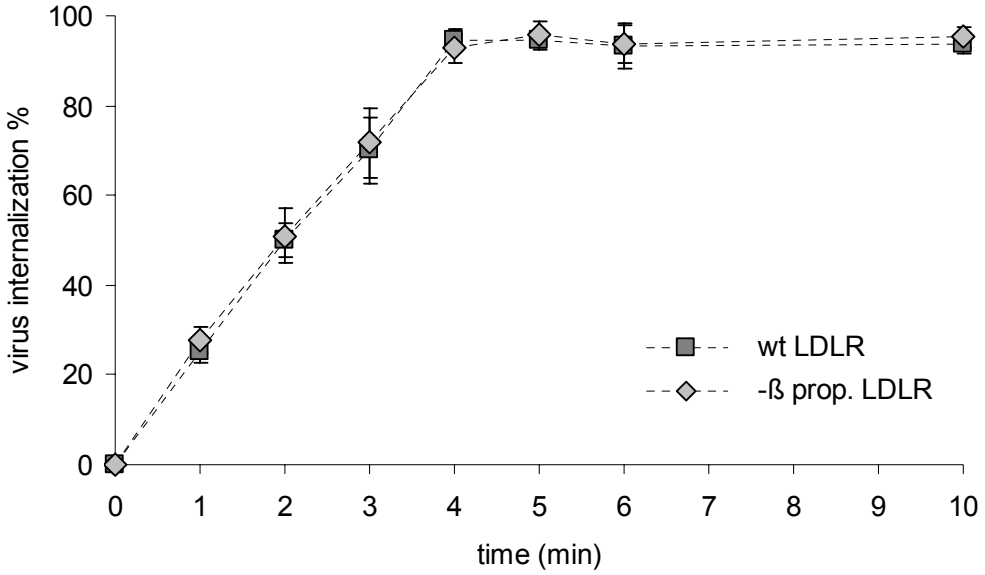

Figure 29. Internalization of HRV2 follows the same kinetics in CHO cells expressing wt and β-propeller deficient LDLR. CHO ldla7 cells expressing wt and β-propeller negative LDLR, respectively, were grown to confluency and challenged with HRV2 at 100 $TCID_{50}$/cell for 1 h at 4°C. Non-attached virus was removed and ice cold infection medium was added onto the cells. All samples were placed simultaneously at 34°C to start virus internalization. At the times indicated receptor-bound virus remaining at the cell surface was quantified by a cell based ELISA (performed on ice). Surface exposed virus at time 0 (i.e. prior to warming up) was set to 100 %. The y-axis was inverted for depiction of the percentage of virus internalization. Error bars show standard deviation (n=3).

5.6. Conversion of HRV2 to subviral particles is delayed when internalized via β-propeller deficient LDLR

We then asked whether the stronger virus-stabilizing effect of the β-propeller negative receptor (as revealed for virus bound to the plasma membrane) can also be observed during infection. Radiolabeled HRV2 was attached to the cells at 4°C for 1 h, unbound virus was washed away with cold HBBS, and the cells were incubated in 1 ml infection medium at 34°C to allow for virus internalization and uncoating. At various time points the cells were lysed

without removing the incubation medium, by adding 200 µl of 6x RIPA buffer. Sequential immunoprecipitation with mAb 2G2 and anti-HRV2 antiserum was carried out as described above, and radioactivity in the pellets was determined by scintillation counting. As seen in Fig. 30, a clear delay in virus conversion could be measured when the virus was internalized by the truncated receptor. This corresponds well with the virus protection effect observed in the experiments with plasma-membrane bound HRV2.

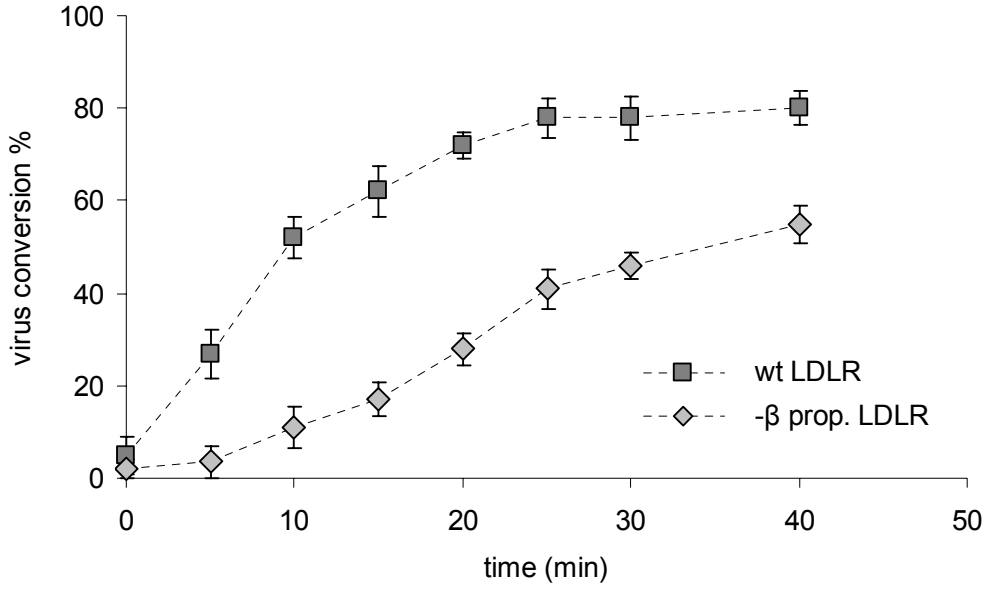

Figure 30. Endosomal virus conversion is delayed in CHO cells expressing β-propeller negative LDLR. Radiolabeled HRV2 was attached to cells grown in 6-well plates at 4°C for 1 h. After removal of unbound virus the cells were incubated in 1 ml infection medium at 34°C to allow for virus internalization and uncoating. At the time points indicated, the cells were lysed without removing the incubation medium. Converted virus was immunoprecipitated with mAb 2G2, and remaining native virus with anti-HRV2 antiserum. Ratios of 2G2 precipitated counts over all counts were calculated, native virus present at time 0 was set to 100 %. The y-axis was inverted for depiction to show the percentage of conversion. Error bars show standard deviation (n=3).

5.7. Dissociation of HRV2 from β-propeller deficient LDLR is delayed within endosomes

To assess whether wild type and mutant LDLR also exhibit distinct properties with respect to receptor-ligand dissociation, the time dependent co-localization of HRV2 and LDLR was determined by confocal immunofluorescence microscopy in collaboration with the group of Prof. Fuchs (Medical University of Vienna). HRV2 was bound at 4°C to the plasma membrane of CHO cells expressing wt or β-propeller negative LDLR that had been grown on coverslips. Virus entry was initiated by adding warm medium, and cells were further incubated at 34°C to allow for infection. At the times indicated in Fig. 31. cells were fixed, permeabilized, and LDLR and HRV2 were detected by specific antibodies followed by Alexa 488-conjugated goat anti-mouse IgG and Alexa 568-conjugated goat anti-chicken IgG,

respectively. The percentage of co-localization was calculated from immunofluorescence microscopy images, and showed a decrease over time in both cell lines. However, virus dissociation from the β-propeller negative receptor was clearly delayed and reduced. This again agrees well with the increased virus protecting effect observed for the truncated receptor. Apparently, the propeller negative receptor keeps the virus bound in its native state up to later time points of the infection.

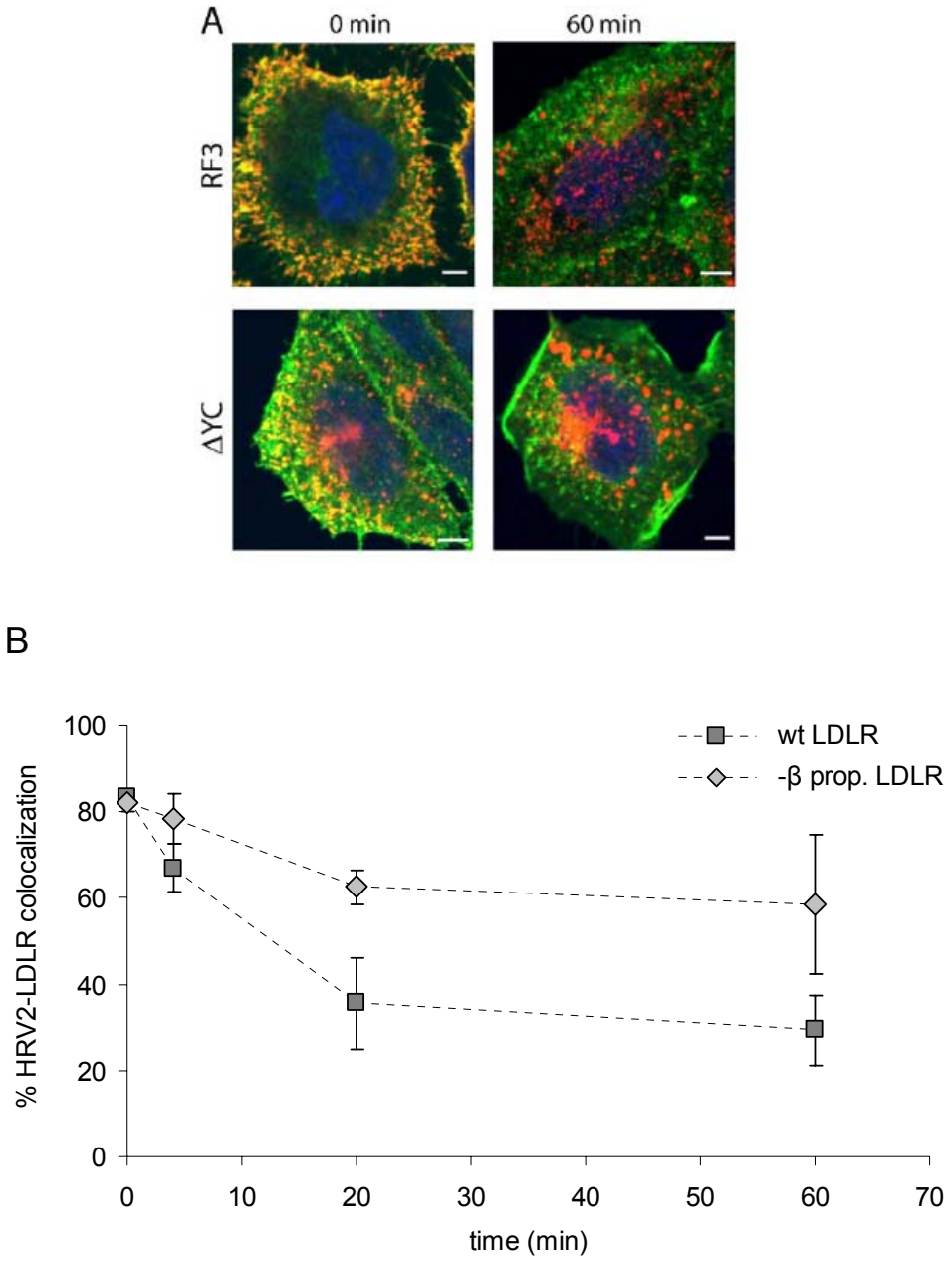

Figure 31. HRV2 dissociation from LDLR is delayed when the β-propeller is deleted. HRV2 was bound at 4°C to CHO cells grown on coverslips and entry was initiated by adding warm medium. At the times indicated, cells were fixed, permeabilized, and LDLR and HRV2 were detected by specific antibodies, followed by Alexa 488-conjugated goat anti-mouse IgG and Alexa 568-conjugated goat anti-chicken IgG, respectively. **(A)** Representative fluorescent images of one focal plane through the perinuclear region are shown after HRV2 binding (0 min) and 60 min after warming to 34°C. LDLR, green; HRV2, red. Bar: 2 µm. **(B)** The percent co-localization of virus and receptor was calculated from immunofluorescence microscopy images as in panel A. Co-localization at time zero was set to 100 %. Error bars show standard deviation (n=3).

5.8. Cellular protein synthesis is identical in the CHO cell lines expressing wt and truncated LDLR

Prior to performing infection kinetics experiments we compared the rate of cellular protein synthesis in the two transfected cell lines via incorporation of [^{35}S]-labeled cysteine/methionine. Cells were grown in 6-well plates until being subconfluent. The medium was replaced with infection medium lacking methionine/cysteine and incubation was continued for 4 h. Then, the medium was replaced with fresh infection medium supplemented with 40 µCi of [^{35}S]-methionine/cysteine. At the times indicated cells were extensively washed and radioactivity incorporated into cellular proteins was determined by TCA-precipitation followed by scintillation counting. Fig. 32 shows that the protein synthesis rates were identical in both cell lines. This excludes that eventually observed differences in virus growth were due to differences in the metabolic activity of the two cell lines.

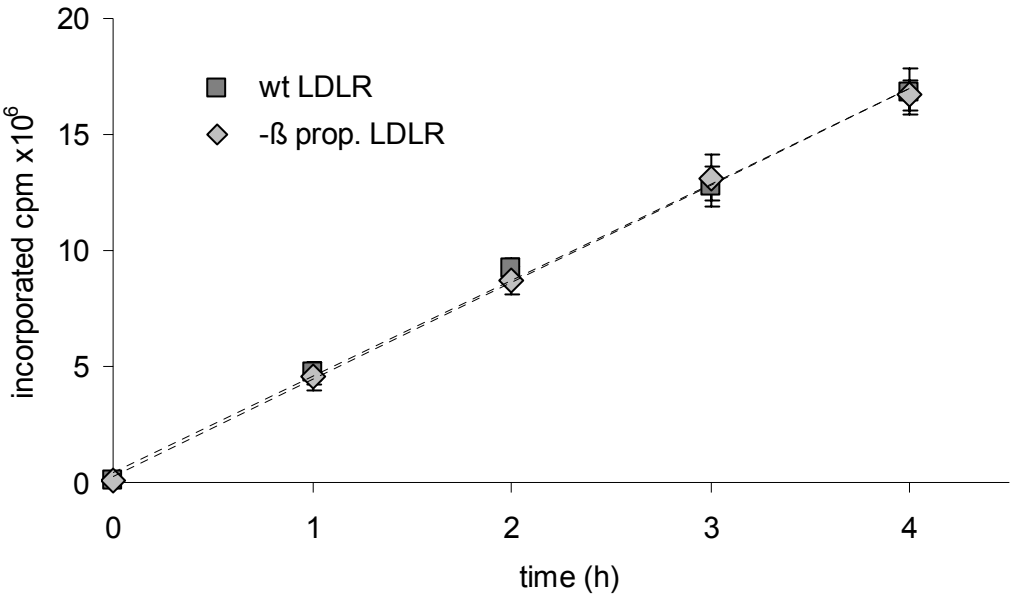

Figure 32. Protein synthesis rates are indistinguishable in CHO cells expressing wt and ß-propeller deficient LDLR. Subconfluent cells in 6-well plates were pre-incubated with infection medium lacking methionine/cysteine for 4 h. After incubation in fresh infection medium supplemented with 40 µCi of [^{35}S]-methionine/cysteine cells were extensively washed and radioactivity incorporated into cellular proteins was determined by TCA precipitation. Error bars show standard deviation (n=3).

5.9. HRV2 internalized via β-propeller deficient LDLR shows a delay in infection

Minor group rhinoviruses take advantage of the low endosomal pH for RNA release. Since the endosomal pathway terminates with lysosomal digestion of the endocytosed material, productive RNA release must happen within a defined time window. Due to the higher virus-stabilizing effect of the β-propeller deficient LDLR as compared to wt LDLR, the delay in virus conversion might limit the time for productive RNA release. In order to assess whether this is indeed the case, we compared the infection kinetics in the two CHO cell lines.

HRVs fail to replicate in non-human cells, complicating infection experiments in CHO cell lines. However, adaptation of HRV2 to mouse L cells has been reported (Yin and Lomax, 1983). The replicating virus variants showed mutations within non-structural proteins. We thus attempted the adaptation of HRV2 to grow in CHO cells by blind passages alternating between HeLa and CHO cells expressing human wt LDLR. After 12 such passages HRV2 variants, termed $HRV2_{CHO}$ appeared that replicated in both CHO cell lines. Figure 33 shows the corresponding infection kinetics.

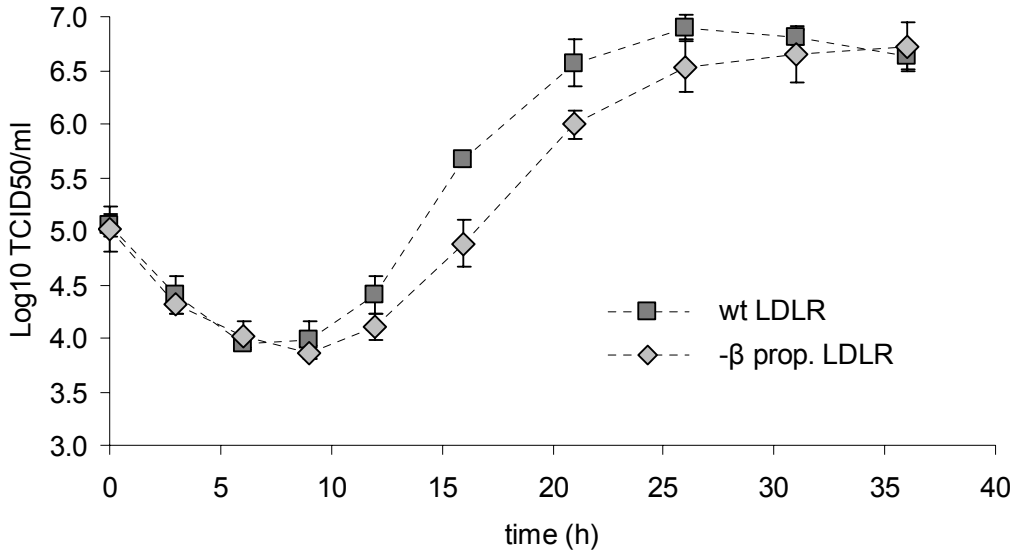

Figure 33. Infection kinetics of $HRV2_{CHO}$ in CHO cell lines expressing wt and truncated human LDLR. Cells seeded in 6-well plates were challenged with $HRV2_{CHO}$ at 10 $TCID_{50}$/cell at 4°C for 1 h. After removal of non-bound virus the cells were incubated at 34°C in 2 ml infection medium. At the times indicated, cells were broken by three cycles of freezing/thawing and virus titre was determined. Error bars show standard deviation (n=3).

There is a clear decrease in virus titre up to about 8 hours post infection, indicating uncoating of the internalized virus particles. From about 9 h onwards *de novo* viral synthesis is evident with the titre attaining a plateau after about 30 h. The most obvious difference between the two cell lines is manifested between 12 and 26 h; the cells expressing the wt receptor produced up to 6 times more virus at 16 h p.i. with a difference of about 5 h in reaching the plateau.

5.10. The ΔYC LDLR mutant is directed into lysosomes when internalizing HRV2

Deletion of the entire EGFP-homology domain of LDLR (ΔEGFP) inhibits the dissociation of bound LDL, impairs receptor recycling, and results in lysosomal degradation of the receptor-ligand complex (Davis et al., 1987a). Since the β-propeller is involved in the conformational changes of LDLR triggered at low pH (Beglova et al., 2004a; Rudenko et al., 2002), the same must be true also for the ΔYC deletion that was used in our experiments. However, contrarily to LDL, HRV2 is a low pH sensitive ligand, suffering conversion at pH ~5.8, a value encountered during passage through the endosomal pathway. Conformational changes of both the virus and the receptor should result in virus dissociation at a certain time during infection, regardless of the kind of receptor (wt or propeller-negative). In order to study whether this dissociation happens in time to allow for effective receptor recycling (LDLRs recycle from early endosomes) or too late for the receptor to be directed into the recycling pathway, fluorescence microscopy was employed to detect the extent of LDLR co-localization with the lysosomal marker LAMP2 (in collaboration with the group of Prof. Fuchs, Medical University of Vienna).

CHO cells expressing wt or β-propeller negative LDLR were grown on coverslips and pre-incubated for 30 min in serum-free medium. HRV2 at 1,500 $TCID_{50}$/cell in serum-free medium was added and internalized for 6 h at 34^{o}C (continuous internalization). The cells were cooled on ice, washed, fixed and permeabilized with methanol, washed, and incubated with monoclonal mouse anti-human LAMP-2 antibody (1:400), followed by Alexa-568 conjugated goat anti-mouse IgG. To visualize LDL-receptors, the cells were incubated with chicken anti-human LDLR IgY, followed by Alexa-488-conjugated goat anti-chicken IgG. Nuclei were stained blue with Hoechst dye (for epifluorescence) and Draqe5 (for confocal microscopy). As control mock infected cells incubated under the same conditions were used.

Internalization of HRV2 into RF3 cells had no significant influence on the total fluorescence and thus expression of wild-type LDLR (Fig. 34A, upper panels). Furthermore, little co-localization of LDLR with the lysosomal marker LAMP2 was seen both in the absence and

in the presence of HRV2 (Fig. 34B, upper panels). In contrast, in ΔYC cells HRV2 uptake resulted in a decrease of mutant LDLR fluorescence levels mainly at the plasma membrane (arrows) but not in the perinuclear area (Fig. 34A, lower panels, arrow heads). The decrease in plasma membrane expression of mutant receptors appears to be due to their lysosomal degradation, as deduced from the higher extent of co-localization of receptors with LAMP2 (Fig. 34B, lower panels). This means that virus conversion occurs too late for the β-propeller negative LDL-receptors to catch the recycling pathway.

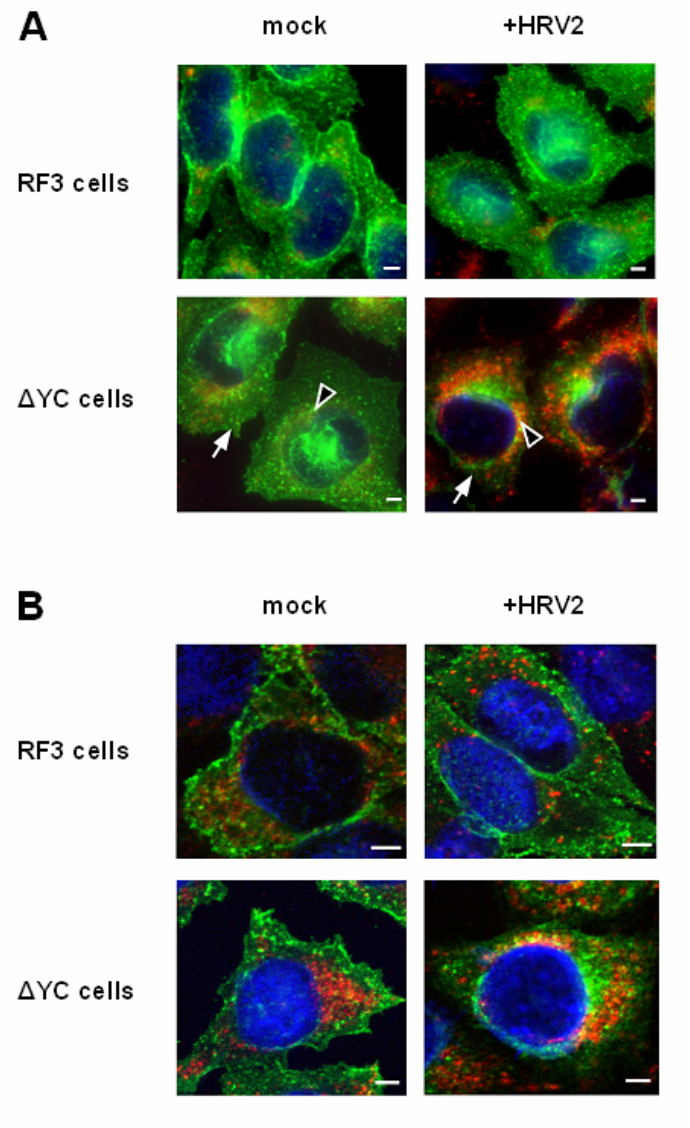

Figure 34. Continuous HRV2 internalization leads to degradation of mutant but not wild-type LDLR. CHO RF3 cells (expressing wt LDLR) and ΔYC cells (expressing β-propeller negative LDLR) were pre-incubated in serum-free Ham's F12 medium, and HRV2 at 1500 $TCID_{50}$/cell in serum-free medium was internalized for 6 h. Cells were then cooled, washed and processed for indirect immunofluorescence microscopy for detection of LDLR (green) and LAMP2 (red). Nuclei were stained blue with Hoechst dye (for epifluorescence) and Draqe5 (for confocal microscopy). **(A)** Conventional epifluorescence. All images were taken with the same exposure time in the respective channel and identical settings were used for illustration with the Axiovison software. Overlay images are shown. Arrow heads indicate perinuclear and arrows indicate plasma membrane localization of LDLR. **(B)** Confocal images were taken by using the same laser power and exposure time in the respective channel. Multicolour images shown were obtained with identical grey level settings in each channel. Out of 20 sections through the cells, the focal plane through the nucleus is depicted. Bar: 2 μm.

5.11. Capsid degradation of HRV2 is delayed in cells expressing propeller negative LDLR

As demonstrated above, the absence of the β-propeller leads to a delay in virus, uncoating and bound virus directs the truncated LDL-receptors to lysosomes for degradation. We thus asked whether virus degradation also differs in the two CHO cell lines. The experiment was carried out exactly as the uncoating assay (see section 5.6.), but longer incubation time was needed to detect viral degradation. Upon digestion the viral capsid loses epitopes recognized by the type-specific antiserum, therefore, we took the loss of immunoprecipitable material as a measure for capsid degradation. The data in Fig. 35 show that viral capsid degradation was delayed and substantially reduced in the cells expressing the truncated receptor.

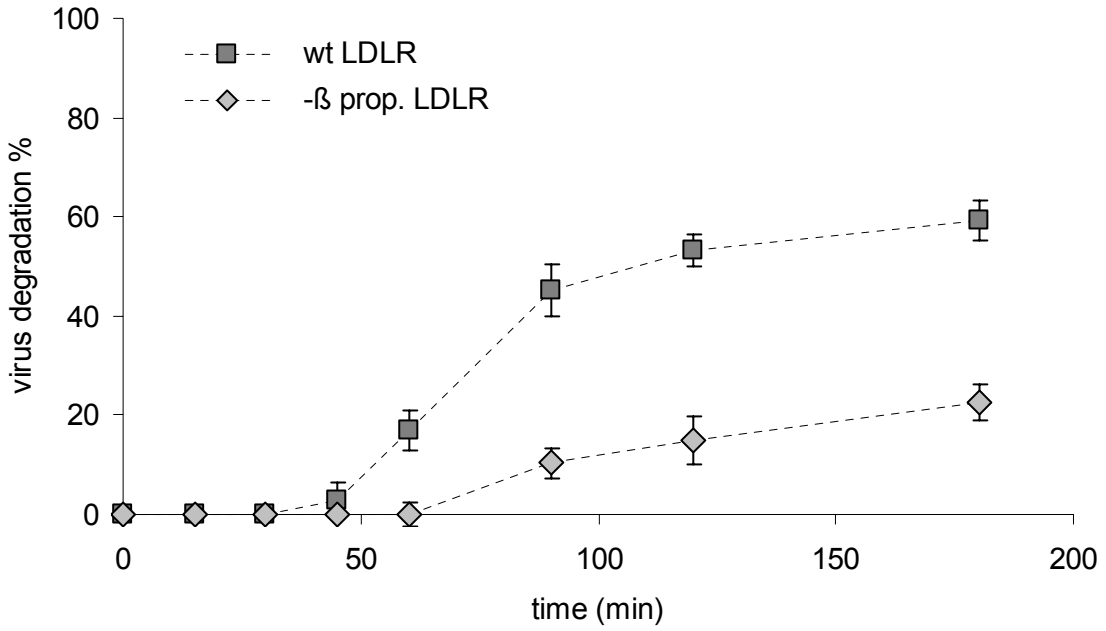

Figure 35. Virus degradation is delayed and reduced in CHO cells expressing β-propeller negative LDLR. Radiolabeled HRV2 was attached to the cells at 4°C for 1 h, unbound virus was washed away, and the cells were incubated in infection medium at 34°C to allow for virus internalization and uncoating. At the times indicated the cells were lysed. Remaining virus and viral protein fragments recognized by the HRV2 antiserum were immunoprecipitated and scintillation counted. Radioactivity precipitated at time 0 (corresponding intact virus) was set to 100 %, and the y-axis was inverted for depiction to show the percentage of degradation. Error bars show standard deviation (n=3).

6. Discussion

6.1. Function of the LDLR β-propeller in HRV2 infection

Minor group HRVs enter cells via clathrin-dependent endocytosis (Snyers et al., 2003) upon attaching to members of the LDLR superfamily including LDLR, VLDLR, and LDLR-related protein (LRP) (Hofer et al., 1994; Marlovits et al., 1998b; Marlovits et al., 1998d). The internalized virus then travels through the compartments of the endosomal route (early endosomes, endocytic carrier vesicles, late endosomes, lysosomes) and due to the activity of the vacuolar H^+-ATPase (V-ATPase) (Nishi and Forgac, 2002) experiences a continuously decreasing pH. A pH $\leq$ 5.6 attained in endocytic carrier vesicles and/or late endosomes triggers structural changes of the virion, which allow for its membrane-association via externalized VP1 N-terminal amphipathic helices. Concomitantly, the internal VP4 capsid proteins are released from the capsid (Hewat et al., 2002) and are believed to form pores in the endosomal membrane, which allow for RNA release as explicitly shown for HRV2 (Brabec et al., 2005; Fuchs and Blaas, 2008; Prchla et al., 1995; Schober et al., 1998). As structural changes of the virion and infection of HeLa cells can be brought about by the low endosomal pH alone when using a surrogate receptor (Baravalle et al., 2004), it was believed that the function of LDLR was limited to virus delivery.

However, LDL-receptors do not behave as passive vehicles when internalizing their natural ligands such as lipoproteins; their β-propeller domains (at least in cases of LDLR and VLDLR) were shown to actively participate in low pH induced ligand release (Beglova and Blacklow, 2005; Beglova et al., 2004a; Mikhailenko et al., 1999). Therefore, we decided to investigate whether the β-propeller also plays a role in minor group rhinovirus infection. We used CHO-*ldla7* cells deficient in endogenous LDLR (Krieger et al., 1981) that had been stably transfected to express either wild-type or β-propeller negative human LDLR (Beglova et al., 2004a). Untransfected *ldla7* cells did not show significant virus binding under our conditions, which allowed for the investigation of the propeller function in a single-receptor system.

The endosomal fate of internalized virus can be modeled at the plasma membrane under conditions when endocytosis is blocked (working at 4°C), by incubation of receptor-bound virus in acidic incubation buffers (Brabec et al., 2003). This experiment helps to investigate the influence of receptor-virus interactions on the efficiency of infection, dissecting these early events from later steps of the infection cycle. Clearly, this model experiment cannot completely mimic the situation within the endosomal lumen such as membrane curvature, kinetics of pH changes, volume ratio, and buffering capacity of intraendosomal and cytosolic spaces, therefore, one has to be careful when extrapolating the results to natural infections.

Nevertheless, when the conditions are well defined, such an experiment helps to elucidate distinct steps of the receptor-virus interaction during infection.

6.2. Low pH itself is not enough to trigger RNA release from membrane-attached HRV2 A-particles

Brabec and colleagues using HeLa cells for virus binding and acetate-phosphate buffers for low pH incubation observed substantial release of cell-bound HRV2 upon incubation at pH 6. This could not be reproduced with our CHO cells and MES buffers even at lower pH values; rather, re-neutralization of the incubation buffers was required for virus being shed into the supernatant. Furthermore, the vast majority (80-100 %) of the released particles were in their converted state regardless of the pH of acid-treatment. It thus appears that in our case the virus either remained receptor-bound in its native state (at pH values > 5.6) or it was directly transferred to the membrane upon its conversion (at pH values, < 5.6).

There are more possible reasons for the observed differences. One could be our choice to avoid phosphate-containing buffers for low pH incubation. It cannot be excluded that the interaction between virus and receptor was weakened via calcium depletion by the phosphate content of their buffer which could have caused a partial unfolding of the LA repeats (Arias-Moreno et al., 2008). This most probably did not happen with our MES buffers. An additional difference is that CHO cells express LDLR at much higher levels than HeLa cells. This might led to different virus-receptor stoichiometries of cell-bond virus, as much higher amounts of input virus was necessary for HeLa cells to achieve measurable levels of binding. It is possible that on average the virus particles were simultaneously docked by more receptor molecules with a higher binding strength on CHO cells than on HeLa cells. A further reason why the two systems cannot be directly compared is that HeLa cells express also VLDLR and LRP which might behave different from LDLR in binding and releasing HRV2.

Based on the present knowledge on HRV uncoating, the only way for the membrane-attached hydrophobic A-particles to become hydrophilic B-particles and dissociate from the membrane would be RNA release (Korant et al., 1972; Lonberg Holm et al., 1976). Our results thus strongly suggest that the low pH induces virus conversion only up to the A-particle form and RNA release needs an additional trigger. Whether it is indeed a re-neutralization step (which could come from the cytosol through virally opened pores) or another unknown factor which was induced by re-neutralization in our model conditions, needs to be further investigated. Since RNA release is a quick process and the short lived A-particle is difficult to investigate, there is only a little knowledge about this mechanism, based on differences in the 3D structures between native and empty capsids (Fuchs and Blaas, 2008; Hewat et al., 2002;

Hewat and Blaas, 2004). It also cannot be excluded with certainty that further, still unknown intermediates exist.

6.3. LDLR binding stabilizes HRV2 against low pH-induced conversion

The virus conversion follows a sigmoid curve with arbitrarily set end points of 0 % at pH 7 and 100 % at pH 5. The transition range for HRV2 is between pH 5.4 and 6.0. During infection there is a limited time window for effective RNA release into the cytoplasm of the host cell, which starts with capsid conversion and ends with enzymatic digestion and inactivation of the virion within lysosomes. In order to clarify whether the function of the LDLR β-propeller is important in minor group rhinovirus infection, we first compared the pH-dependence of HRV2 conversion bound either to wild type or β-propeller negative LDL-receptor.

The results clearly showed that virus bound to propeller deficient LDLR needed lower pH values for conversion into subviral particles than virus bound to wt receptor. This indicates that the β-propeller domain plays an important role in infection, via weakening the interaction between the virus and the ligand binding domain of the receptor. This also indicates that the native conformation of the virus is stabilized by the bound receptor. A similar effect has been already shown for a recombinant minireceptor composed of 5 copies of the third ligand binding repeat of VLDL-receptor (V33333) (Nicodemou et al., 2005). This concatemer exhibits much higher avidity for HRV2 as compared to LDLR and consequently might also exert a much stronger effect. In this work we could show that even the LDLR binds with sufficiently high avidity to protect HRV2 against conversion but this effect is naturally repressed by the function of the β-propeller. These results demonstrate that LDLR is indeed not just a simple vehicle transporting the virus into endosomes but it actively takes part in the uncoating process by tuning virus conversion; it balances high avidity binding against an intrinsic ligand-release function.

6.4. Is HRV2 released from LDLR in its native or converted state?

Within acidifying endosomes more factors can induce virus dissociation from the LDLR such as virus conversion, conformational change of the receptor, and maybe even LA-repeat unfolding due to the decrease of endosomal Ca^{2+} concentration. The virus might be released from LDLR either in its native form (and it converts subsequently in the fluid phase of the

endosome) or it might leave the receptor upon its conversion (then it is concomitantly handed over to the endosomal membrane). The latter case would result in higher infection efficiency.

The decreasing pH and the β-propeller act in concert and weaken the strength of virus-receptor binding. The various types of minor group HRVs show differences in their pH sensitivity (Khan et al., 2007) and most probably also in their binding avidity to LDLR. The higher is the pH stability of the virus, the longer the virus-receptor binding is maintained at decreasing pH passing through the endo-lysosomal pathway. Also, the higher is the binding avidity, the longer the virus remains receptor-bound and stabilized against conversion. As we have shown, high pH stability or too big stabilization effect by the receptor delays virus conversion and decreases the time window for effective RNA release.

Our data demonstrated that HRV2 was released from LDLR upon its conversion. However, generalization of our result for all minor group HRVs is not possible, since each virus type might have a different combination of pH sensitivity and binding avidity to LDLR. It is possible that minor group HRV types also exist with high pH stability and low receptor binding avidity which could be released from LDLR by the activity of the β-propeller still in their native state. In the case of HRV2 the decreasing pH and the β-propeller finally abrogated the virus-receptor binding but virus release happened only at a pH value which has already caused virus conversion as well.

6.5. The β-propeller accelerates the release of HRV2 from LDLR, which is essential for receptor recycling

Deletion of the entire EGFP-homology domain (ΔEGFP) of LDLR inhibits the dissociation of bound LDL. As ligand release is essential for LDLR recycling, the receptor-ligand complex is fated for lysosomal degradation (Davis et al., 1987a; Hobbs et al., 1992; Miyake et al., 1989). The X-ray structure of LDLR at acidic pH (Rudenko et al., 2002) confirmed that the function of the β-propeller domain is responsible for the low pH-associated conformational changes. Therefore, there is a strong reason to believe that the ΔYC mutant lacking both the propeller and the third EGF-homology domain (used in our experiments) behaves identically with respect to ligand release and receptor recycling as the ΔEGFP mutant of Davis and colleagues. In contrast to LDL, HRV2 is able to leave the β-propeller deficient receptor due to its low pH induced conversion. LDLR normally recycles from early endosomes (Maxfield and McGraw, 2004) but when virus remains bound due to the propeller deletion, recycling might be impaired. We thus asked whether HRV2 leaves the mutant receptor early enough to allow for efficient receptor recycling. Co-localization of LDLR with the lysosomal marker LAMP2 revealed that similarly to the natural ligands, HRV2 directs β-propeller deficient LDLR into

the degradative pathway. This indicates that the virus remains bound to the ΔYC-LDLR until bifurcation towards receptor recycling is no more possible.

6.6. Viral capsid degradation is delayed in cells expressing propeller negative LDLR

The propeller deficient LDLR is not able to release bound LDL and consequently the whole complex is degraded. Hijacking the endosomal route, HRV is anyhow destined for degradation; therefore it is extremely important to release its RNA into the cytoplasm before hydrolytic enzymes harm the capsid making it incompetent for RNA release. The β-propeller domain influencing virus conversion raised the question whether its deletion also affects virus degradation.

Our results showed that capsid degradation was delayed and substantially reduced when the propeller was deleted from the LDLR. This cannot be explained by increased recycling of virus-receptor complexes, since the truncated receptors are rather directed to lysosomes by the bound virus. We know that the virus leaves the mutant receptor at a time already late for receptor recycling, which suggests that virus conversion occurs either in endosomal carrier vesicles or late endosomes. This leads to a reduced time-window for the penetration of viral RNA into the cytosol, which starts later, at lower pH, and shortly before the degradative inactivation of the virus. Despite lysosomes are considered to be responsible for virus degradation, there are studies indicating that proteolytic digestion already starts in late endosomes (Pillay et al., 2002; Tjelle et al., 1996). Thus, the delayed virus conversion caused by the mutant receptor might have increased the amount of virus particles becoming inactivated before RNA release. The A-particle that fails to release its RNA remains membrane-associated, and might even more withstand enzymatic digestion, being protected by the membrane which wraps tightly around it. This could have been a possible reason for the observed delay in viral capsid degradation. Additionally, a part of the membrane-associated viral particles might have escaped from the lysosomal route, being associated with vesicles budding from late endosomes which communicate with the trans-Golgi network (Maxfield and McGraw, 2004). These assumptions still need to be verified.

6.7. The role of LDLR in minor group rhinovirus infection

The infection efficiency of minor group HRVs depends on complex molecular mechanisms composed of several interconnected factors, such as the time window available for effective RNA release, the correct orientation of viral RNA release (into the cytoplasm versus the inner space of multivesicular endosomes), the compatibility of viral replication with the molecular mechanisms of the infected cell, success in evading host defence mechanisms, etc.

The time window available for RNA release of minor group rhinoviruses is defined by the relation of viral pH sensitivity and virus-receptor binding avidity. Both factors depend on the capsid properties of the particular virus type. Thus, the balance between the optimal receptor-virus interaction and infection efficiency is an important factor driving viral evolution.

The main result of our studies was the clear proof that the LDLR is not just a simple vehicle for delivery of minor group rhinoviruses into endosomes. This receptor rather actively contributes to the efficiency of infection. The virus is endowed with the capacity for high-avidity multi-module binding that combines with an intrinsic ligand release mechanism of the receptor. High-avidity binding allows for infection at low virus concentrations, which is often the case in natural infections. However, as we have demonstrated, too strong receptor binding decreases infection efficiency by maintaining the virus in its native conformation and reducing the time window for effective RNA release. Altogether, using LDLR, which integrates high avidity binding with an intrinsic ligand release mechanism, is a better choice for the virus as using a receptor with a simply lower binding avidity.

7. Appendix

7.1. Abbreviations

µg	microgram
µl	microliter
°C	Celcius centigrade
3D	3 dimensional
Å	Angstöm
ADAR	adenosine deaminase
AOM	acute otitis media
AP	alkaline phosphatase
apoB-100	apolipoprotein B-100
apoE	apolipoprotein E
ApoER2	apolipoprotein E receptor 2
APS	ammonium persulfate
ATP	adenosine triphosphate
bp	base pairs
BSA	bovine serum albumin
CAR	coxackie-adenovirus receptor
CD-54	cluster of differentiation 54, identical molecule with ICAM-1
cDNA	complementary desoxiribonucleic acid
CHO-cell	Chinese hamster ovary cell
CHO-*ldla7*	mutant of CHO cell lacking functional LDL-receptor
COPD	chronic obstructive pulmonary disease
CPE	cytopathic effect
cpm	radioactive counts per minute
C-terminus	carboxy-terminus of a peptide/protein
D	Dalton
ddH_2O	double distilled water
DAF	decay accelerating factor
DMEM	Dulbecco's modified essential medium
DMSO	dimethyl sulfoxide
DNA	desoxyribonucleic acid
dsRNA	double stranded ribonucleic acid

DTT	dithiothreitol
EDTA	ethylenediamine tetraacetate
EGF	epidermal growth factor
EGFP	epidermal growth factor precursor
eIF2α	eukaryotic translation initiation factor 2α
eIF4G	eukaryotic translation initiation factor 4G
ELISA	enzyme-linked immunosorbent assay
EM	electron microscopy
ENA	epithelial neutrophil-activating protein
ER	endoplasmatic reticulum
FACS	fluorescence activated cell sorter
FCS	fetal calf serum
FDA	Food and Drug Administration
FH	familial hypercholesterolaemia
G418	geneticin
GM-CSF	granulocyte macrophage-colony stimulating factor
gp330	glycoprotein 330
GPI	glycosylphosphatidylinositol
Gro	growth-regulated oncogene
h	hour
HBBS	Hank's balanced buffer solution
HDL	high-density lipoprotein
HRV	human rhinovirus
$HRV2_{CHO}$	human rhinovirus adapted to replicate in CHO cells
HS	horse serum
HSPG	heparane sulfate proteoglycan
ICAM-1	intercellular adhesion molecule 1
IDL	intermediate density lipoprotein
IFN	interferon
Ig	immunoglobulin
IL	interleukin
IRES	internal ribosomal entry site
JAK-STAT	Janus kinase - Signal Transducers and Activators of Transcription
kb	kilobase
kD	kilodalton
LAMP	lysosome associated membrane protein
LA-repeat	LDL receptor type A repeat
LDL	low-density lipoprotein
LDLR	low-density lipoprotein receptor

LFA	lymphocyte function associated antigen
Lp	lipoprotein
LRP	LDL-receptor related protein
MAb	monoclonal antibody
MAb-2G2	monoclonal antibody 2G2
Mac–1	macrophage–1 antigen
MBP	maltose binding protein
mCi	milliCurie
MEGF7	multiple epidermal growth factor containing protein 7
MEM	minimal essential medium
MES	morpholinoethanesulphonic acid
mg	milligram
min	minute
MIP	macrophage inflammatory protein
ml	milliliter
MOI	multiplicity of infection
mRNA	messenger RNA
ng	nanogram
nm	nanometer
NMR	nuclear magnetic resonance
NPVY	peptide motif with asparagine-proline-valine-tyrosine
NPxY	peptide motif with asparagine-proline-any aminoacid-tyrosine
N-terminus	amino-terminus of a peptide/protein
OAS	oligoadenylate synthetase
ORF	open reading frame
P1, P2, P3	regions of the viral polyprotein
PAA	polyacrylamide
PAGE	polyacrylamide gel electrophoresis
PAI-1	plasminogen activator inhibitor type-1
PBS	phosphate buffered saline
PDB	protein database
PFA	paraformaldehyde
pH	negative logarithm of the H-ion concentration
pKa	negative logarithm of the acid dissociation constant
PKR	protein kinase R
PVR	poliovirus receptor
RANTES	regulated upon activation, normal T-cell expressed and secreted
RAP	receptor associated protein
RF3 cells	CHO-*ldla7* cells expressing human wt LDLR
RIPA	radio-immunoprecipitation assay

RNA	ribonucleic acid
RNAi	ribonucleic acid interference
RNAse L	endoribonuclease L
ROI	reactive oxygen intermediate
rpm	revolutions per minute
s	seconds
S	Svedberg constant
S. aureus	Staphylococcus aureus
SDS	sodium dodecyl sulphate
SDS-PAGE	sodium dodecyl sulphate polyacrylamide gel electrophoresis
siRNA	silencing ribonucleic acid
ssRNA	single stranded ribonucleic acid
TCA	trichloroacetic acid
$TCID_{50}$	tissue culture infectious dose 50
TEMED	tetramethylethylenediamine
TNF	tumor necrosis factor
TLR3	Toll-like receptor 3
tPA	tissue-type plasminogen activator
U/ml	enzymatic unit / milliliter
uPA	urokinase plasminogen activator
UTR	untranslated region
V repeats	ligand binding repeats of VLDL-receptor
V33333	concatemeric pentamer of module 3 of VLDLR
VLDL	very low-density lipoprotein
VLDLR	very low-density lipoprotein receptor
VP	viral protein
VPg	viral protein genome-linked
WIN	name of an antiviral compound
X-ray	Röntgen radiation
YWTD	peptide motif with tyrosine-tryptophane-threonine-asparagine
β-VLDL	β-migrating forms of very low-density lipoprotein
ΔAB-LDLR	LDLR with deleted EGF-AB domain pair
ΔEGFP-LDLR	LDLR with deleted EGFP homology domain
ΔYC-LDLR	LDLR with deleted YWTD β-propeller and EGF-C domains

7.2. Taxonomy of picornaviruses

The data are taken from www.picornaviridae.com

The family **Picornaviridae** belongs to the order **Picornavirales** and consists of 8 genera: **Enterovirus**, **Cardiovirus**, **Aphthovirus**, **Hepatovirus**, **Parechovirus**, **Erbovirus**, **Kobuvirus** and **Teschovirus**, plus three proposed genera named "**Sapelovirus**", "**Senecavirus**" and **"Tremovirus"**. The two human rhinovirus species have been moved to the genus **Enterovirus**; the genus **Rhinovirus** no longer exists.

The genus **Enterovirus** consists of 10 species: **Human enterovirus A, Human enterovirus B, Human enterovirus C, Human enterovirus D, Simian enterovirus A, Bovine enterovirus, Porcine enterovirus A, Porcine enterovirus B, Human rhinovirus A** and **Human rhinovirus B**.

The species **Human enterovirus A** consists of 21 serotypes: coxsackievirus A2 (CV-A2), CV-A3, CV-A4, CV-A5, CV-A6, CV-A7, CV-A8, CV-A10, CV-A12, CV-A14, CV-A16, enterovirus 71 (EV-71), EV-76, EV-89, EV-90, EV-91 and the simian enteroviruses EV-92, SV19, SV43, SV46 and A13.

The species **Human enterovirus B** consists of 59 serotypes: coxsackievirus B1 (CV-B1), CV-B2, CV-B3, CV-B4, CV-B5 (incl. swine vesicular disease virus [SVDV]), CV-B6, CV-A9, echovirus 1 (E-1; incl. E-8), E-2, E-3, E-4, E-5, E-6, E-7, E-9 (incl. CV-A23), E-11, E-12, E-13, E-14, E-15, E-16, E-17, E-18, E-19, E-20, E-21, E-24, E-25, E-26, E-27, E-29, E-30, E-31, E-32, E-33, enterovirus 69 (EV-69), EV-73, EV-74, EV-75, EV-77, EV-78, EV-79, EV-80, EV-81, EV-82, EV-83, EV-84, EV-85, EV-86, EV-87, EV-88, EV-93, EV-97, EV-98, EV-100, EV-101, EV-106, EV-107 and the simian enterovirus SA5.

The species **Human enterovirus C** consists of 18 serotypes: poliovirus (PV) 1, PV-2, PV-3, coxsackievirus A1 (CV-A1), CV-A11, CV-A13, CV-A17, CV-A19, CV-A20, CV-A21, CV-A22, CV-A24, EV-95, EV-96, EV-99, EV-102, EV-104 and EV-105. Human enterovirus C is the type species of the genus Enterovirus**.**

The species **Human enterovirus D** consists of three serotypes, EV-68, EV-70 & EV-94. Human rhinovirus (HRV) 87 has been reclassified as a strain of EV-68.

The species **Simian enterovirus A** consists of three simian viruses isolated during the 1950's (SV4, SV28 and SA4) and A-2 plaque virus. The close molecular relationships of all four viruses suggests that they all belong to a single serotype, simian enterovirus A1 (SEV-A1).

The species **Bovine enterovirus** consists of at least two serotypes: bovine enterovirus (BEV) 1 and BEV-2. However, it has recently been proposed that the bovine enteroviruses should be divided into two distinct species, each containing a number of types (Knowles, 2005; Zell *et al*., 2006).

The species **Porcine enterovirus B (PEV-B)** consists of a two serotypes: porcine enterovirus 9 (PEV-9) and PEV-10. Serotypes 1 to 7 and 11 to 13 have been reclassified and assigned to a new genus, Teschovirus.

The species **Human rhinovirus A** consists of the following 74 serotypes: HRV-1, 2, 7, 8, 9, 10, 11, 12, 13, 15, 16, 18, 19, 20, 21, 22, 23, 24, 25, 28, 29, 30, 31, 32, 33, 34, 36, 38, 39, 40, 41, 43, 44, 45, 46, 47, 49, 50, 51, 53, 54, 55, 56, 57, 58, 59, 60, 61, 62, 63, 64, 65, 66, 67, 68, 71, 73, 74, 75, 76, 77, 78, 80, 81, 82, 85, 88, 89, 90, 94, 95, 96, 98 and 100.

The recently reported candidate new HRV serotype, Hanks2102, is a HRV-21 by VP1 sequencing.

The species **Human rhinovirus B** consists of the following 25 serotypes: HRV-3, 4, 5, 6, 14, 17, 26, 27, 35, 37, 42, 48, 52, 69, 70, 72, 79, 83, 84, 86, 91, 92, 93, 97 and 99.

The genus **Cardiovirus** consists two species, **Encephalomyocarditis virus** and **Theilovirus**. EMCV is represented by a single serotype of the same name while the theiloviruses are comprised of Theiler's murine encephalomyelitis virus (TMEV), Vilyuisk human encephalomyelitis virus (VHEV), Thera virus (TRV; isolated from rats), Saffold virus (SAFV; isolated from humans) 1-8. The cardioviruses are most closely related to members of the genera Senecavirus, Aphthovirus and Erbovirus and to the recently recognised cosaviruses.

The genus **Aphthovirus** consists of two species, **Foot-and-mouth disease virus** and **Equine rhinitis A virus**. Recent nucleotide sequence data has shown that **bovine rhinoviruses** (three serotypes previously classified as tentative members of the now defunct genus *Rhinovirus*) should be re-classified in the genus **Aphthovirus**.

The genus **Hepatovirus** consists of two species, **Hepatitis A virus** and (the as yet unnamed) **"Avian encephalomyelitis-like viruses"**. The later is a tentative member of the genus. A proposal is currently being considered by the ICTV to formally name **"Avian encephalomyelitis-like viruses"** as **"Avian encephalomyelitis virus"** and to place it in a new genus with the provisional name **"Tremovirus"**.

The genus Parechovirus is comprised of two species, **Human parechovirus** and **Ljungan virus**.

Erbovirus, a genus within the family **Picornaviridae** containing a single species, **Equine rhinitis B virus (ERBV)** with two serotypes, ERBV-1 and ERBV-2. These two viruses were formerly known as equine rhinovirus 2 and equine rhinovirus 3, respectively.

The genus **Kobuvirus** consists of two species, **Aichi virus** and **Bovine kobuvirus**. A third candidate species has recently been described in pigs (**Porcine kobuvirus**).

The genus **Teschovirus** consists of a single species, **Porcine teschovirus**.

7.3. References

Abraham, G., and Colonno, R.J. (1984). Many rhinovirus serotypes share the same cellular receptor. J Virol *51*, 340-345.

Aggerbeck, L.P., Wetterau, J.R., Weisgraber, K.H., Wu, C.S., and Lindgren, F.T. (1988). Human apolipoprotein E3 in aqueous solution. II. Properties of the amino- and carboxyl-terminal domains. J Biol Chem *263*, 6249-6258.

Agol, V.I. (2006). Molecular mechanisms of poliovirus variation and evolution. Curr Top Microbiol Immunol *299*, 211-259.

Agol, V.I., Paul, A.V., and Wimmer, E. (1999). Paradoxes of the replication of picornaviral genomes. Virus Research *62*, 129-147.

Aldabe, R., and Carrasco, L. (1995). Induction of membrane proliferation by poliovirus proteins 2C and 2BC. Biochemical and Biophysical Research Communications *206*, 64-76.

Anderson, R.G., Brown, M.S., and Goldstein, J.L. (1977). Role of the coated endocytic vesicle in the uptake of receptor-bound low density lipoprotein in human fibroblasts. Cell *10*, 351-364.

Anderson, R.G., Goldstein, J.L., and Brown, M.S. (1976). Localization of low density lipoprotein receptors on plasma membrane of normal human fibroblasts and their absence in cells from a familial hypercholesterolemia homozygote. Proc Natl Acad Sci U S A *73*, 2434-2438.

Anderson, R.G., Vasile, E., Mello, R.J., Brown, M.S., and Goldstein, J.L. (1978). Immunocytochemical visualization of coated pits and vesicles in human fibroblasts: relation to low density lipoprotein receptor distribution. Cell *15*, 919-933.

Andino, R., Boddeker, N., Silvera, D., and Gamarnik, A.V. (1999). Intracellular determinants of picornavirus replication. Trends Microbiol *7*, 76-82.

Andino, R., Rieckhof, G.E., and Baltimore, D. (1990). A Functional Ribonucleoprotein Complex Forms Around the 5' End of Poliovirus RNA. Cell *63*, 369-380.

Andries, K., Dewindt, B., Snoeks, J., Willebrords, R., Stokbroekx, R., and Lewi, P.J. (1991). A comparative test of fifteen compounds against all known human rhinovirus serotypes as a basis for a more rational screening program - mini-review. Antiviral Research *16*, 213-225.

Ansardi, D.C., and Morrow, C.D. (1995). Amino acid substitutions in the poliovirus maturation cleavage site affect assembly and result in accumulation of provirions. Journal of Virology *69*, 1540-1547.

Ansardi, D.C., Porter, D.C., and Morrow, C.D. (1992). Myristylation of Poliovirus Capsid Precursor-P1 Is Required for Assembly of Subviral Particles. Journal of Virology *66*, 4556-4563.

Anzueto, A., and Niederman, M.S. (2003). Diagnosis and treatment of rhinovirus respiratory infections. Chest *123*, 1664-1672.

Arden, K.E., McErlean, P., Nissen, M.D., Sloots, T.P., and Mackay, I.M. (2006). Frequent detection of human rhinoviruses, paramyxoviruses, coronaviruses, and bocavirus during acute respiratory tract infections. J Med Virol *78*, 1232-1240.

Argraves, K.M., Battey, F.D., Maccalman, C.D., McCrae, K.R., Gafvels, M., Kozarsky, K.F., Chappell, D.A., Strauss, J.F., and Strickland, D.K. (1995). The very low density lipoprotein receptor mediates the cellular catabolism of lipoprotein lipase and urokinase- plasminogen activator inhibitor type I complexes. J Biol Chem *270*, 26550-26557.

Argraves, K.M., Kozarsky, K.F., Fallon, J.T., Harpel, P.C., and Strickland, D.K. (1997). The atherogenic lipoprotein Lp(a) is internalized and degraded in a process mediated by the VLDL receptor. J Clin Invest *100*, 2170-2181.

Arias-Moreno, X., Velazquez-Campoy, A., Rodriguez, J.C., Pocovi, M., and Sancho, J. (2008). The mechanism of LDL release in the endosome:implications of the stability and Ca++ affinity of the fifth binding module of the LDL receptor. J Biol Chem.

Arnold, E., and Rossmann, M.G. (1990). Analysis of the structure of a common cold virus, human rhinovirus 14, refined at a resolution of 3.0 A. J Mol Biol *211*, 763-801.

Arruda, E., Crump, C.E., and Hayden, F.G. (1994). In vitro selection of human rhinovirus relatively resistant to soluble intercellular adhesion molecule-1. Antimicrob Agents Chemother *38*, 66-70.

Atkins, A.R., Brereton, I.M., Kroon, P.A., Lee, H.T., and Smith, R. (1998). Calcium is essential for the structural integrity of the cysteine-rich, ligand-binding repeat of the low-density lipoprotein receptor. Biochemistry *37*, 1662-1670.

Bacskai, B.J., Xia, M.Q., Strickland, D.K., Rebeck, G.W., and Hyman, B.T. (2000). The endocytic receptor protein LRP also mediates neuronal calcium signaling via N-methyl-D-aspartate receptors. Proceedings of the National Academy of Sciences of the United States of America *97*, 11551-11556.

Badger, J., Minor, I., Oliveira, M.A., Smith, T.J., and Rossmann, M.G. (1989). Structural analysis of antiviral agents that interact with the capsid of human rhinoviruses. Proteins *6*, 1-19.

Baravalle, G., Brabec, M., Snyers, L., Blaas, D., and Fuchs, R. (2004). Human rhinovirus type 2-antibody complexes enter and infect cells via Fc-gamma receptor IIB1. J Virol *78*, 2729-2737.

Basavappa, R., Syed, R., Flore, O., Icenogle, J.P., Filman, D.J., and Hogle, J.M. (1994). Role and mechanism of the maturation cleavage of VPO in poliovirus assembly: Structure of the empty capsid assembly intermediate at 2.9 angstrom resolution. Protein Science *3*, 1651-1669.

Basu, S., Binder, R.J., Ramalingam, T., and Srivastava, P.K. (2001). CD91 is a common receptor for heat shock proteins gp96, hsp90, hsp70, and calreticulin. Immunity *14*, 303-313.

Battey, F.D., Gafvels, M.E., Fitzgerald, D.J., Argraves, W.S., Chappell, D.A., Strauss, J.F., and Strickland, D.K. (1994). The 39-kDa receptor-associated protein regulates ligand binding by the very low density lipoprotein receptor. J Biol Chem *269*, 23268-23273.

Bayer, N., Prchla, E., Schwab, M., Blaas, D., and Fuchs, R. (1999). Human rhinovirus HRV14 uncoats from early endosomes in the presence of bafilomycin. FEBS Lett *463*, 175-178.

Bayer, N., Schober, D., Huttinger, M., Blaas, D., and Fuchs, R. (2001). Inhibition of clathrin-dependent endocytosis has multiple effects on human rhinovirus serotype 2 cell entry. J Biol Chem *276*, 3952-3962.

Bayer, N., Schober, D., Prchla, E., Murphy, R.F., Blaas, D., and Fuchs, R. (1998). Effect of bafilomycin A1 and nocodazole on endocytic transport in HeLa cells: Implications for viral uncoating and infection. Journal of Virology *72*, 9645-9655.

Beglova, N., and Blacklow, S.C. (2005). The LDL receptor: how acid pulls the trigger. Trends Biochem Sci *30*, 309-317.

Beglova, N., Jeon, H., Fisher, C., and Blacklow, S.C. (2004a). Cooperation between fixed and low pH-inducible interfaces controls lipoprotein release by the LDL receptor. Mol Cell *16*, 281-292.

Beglova, N., Jeon, H., Fisher, C., and Blacklow, S.C. (2004b). Structural features of the low-density lipoprotein receptor facilitating ligand binding and release. Biochem Soc Trans *32*, 721-723.

Beisiegel, U., Weber, W., and Bengtsson Olivecrona, G. (1991). Lipoprotein lipase enhances the binding of chylomicrons to low density lipoprotein receptor-related protein. Proc Natl Acad Sci U S A *88*, 8342-8346.

Beisiegel, U., Weber, W., Ihrke, G., Herz, J., and Stanley, K.K. (1989). The LDL-receptor-related protein, LRP, is an apolipoprotein E-binding protein. Nature *341*, 162-164.

Bella, J., Kolatkar, P.R., Marlor, C.W., Greve, J.M., and Rossmann, M.G. (1999). The structure of the two amino-terminal domains of human intercellular adhesion molecule-1 suggests how it functions as a rhinovirus receptor. Virus Research *62*, 107-117.

Bella, J., and Rossmann, M.G. (1999). Review: rhinoviruses and their ICAM receptors. Journal of structural biology *128*, 69-74.

Bella, J., and Rossmann, M.G. (2000). ICAM-1 receptors and cold viruses. Pharmaceutica acta Helvetiae *74*, 291-297.

Belnap, D.M., McDermott, B.M., Jr., Filman, D.J., Cheng, N., Trus, B.L., Zuccola, H.J., Racaniello, V.R., Hogle, J.M., and Steven, A.C. (2000). Three-dimensional structure of poliovirus receptor bound to poliovirus. Proc Natl Acad Sci U S A *97*, 73-78.

Berendt, A.R., Mcdowall, A., Craig, A.G., Bates, P.A., Sternberg, M.J.E., Marsh, K., Newbold, C.I., and Hogg, N. (1992). The Binding Site on ICAM-1 for Plasmodium Falciparum Infected Erythrocytes Overlaps, But Is Distinct from, the LFA-1-Binding Site. Cell *68*, 71-81.

Bergelson, J.M., Cunningham, J.A., Droguett, G., Kurt-Jones, E.A., Krithivas, A., Hong, J.S., Horwitz, M.S., Crowell, R.L., and Finberg, R.W. (1997). Isolation of a common receptor for Coxsackie B viruses and adenoviruses 2 and 5. Science *275*, 1320-1323.

Bergelson, J.M., Mohanty, J.G., Crowell, R.L., John, N.F.S., Lublin, D.M., and Finberg, R.W. (1995). Coxsackievirus B3 adapted to growth in RD cells binds to decay-accelerating factor (CD55). Journal of Virology *69*, 1903-1906.

Bernstein, H.D., Sonenberg, N., and Baltimore, D. (1985). Poliovirus mutant that does not selectively inhibit host cell protein synthesis. Mol Cell Biol *5*, 2913-2923.

Bhella, D., Goodfellow, I.G., Roversi, P., Pettigrew, D., Chaudhry, Y., Evans, D.J., and Lea, S.M. (2004). The structure of echovirus type 12 bound to a two-domain fragment of its cellular attachment protein decay-accelerating factor (CD 55). J Biol Chem *279*, 8325-8332.

Bienz, K., Egger, D., Pfister, T., and Troxler, M. (1992). Structural and functional characterization of the poliovirus replication complex. J Virol *66*, 2740-2747.

Bienz, K., Egger, D., Rasser, Y., and Bossart, W. (1983). Intracellular distribution of poliovirus proteins and the induction of virus-specific cytoplasmic structures. Virology *131*, 39-48.

Bieri, S., Atkins, A.R., Lee, H.T., Winzor, D.J., Smith, R., and Kroon, P.A. (1998). Folding, calcium binding, and structural characterization of a concatemer of the first and second ligand-binding modules of the low-density lipoprotein receptor. Biochemistry *37*, 10994-11002.

Bieri, S., Djordjevic, J.T., Daly, N.L., Smith, R., and Kroon, P.A. (1995a). Disulfide bridges of a cysteine-rich repeat of the LDL receptor ligand-binding domain. Biochemistry *34*, 13059-13065.

Bieri, S., Djordjevic, J.T., Jamshidi, N., Smith, R., and Kroon, P.A. (1995b). Expression and disulfide-bond connectivity of the second ligand-binding repeat of the human LDL receptor. FEBS Lett *371*, 341-344.

Bishop, N.E., and Anderson, D.A. (1993). RNA-Dependent Cleavage of VP0 Capsid Protein in Provirions of Hepatitis-A Virus. Virology *197*, 616-623.

Blacklow, S.C., and Kim, P.S. (1996). Protein folding and calcium binding defects arising from familial hypercholesterolemia mutations of the LDL receptor. Nature Struct Biology *3*, 758-762.

Blomqvist, S., Savolainen, C., Raman, L., Roivainen, M., and Hovi, T. (2002). Human rhinovirus 87 and enterovirus 68 represent a unique serotype with rhinovirus and enterovirus features. J Clin Microbiol *40*, 4218-4223.

Boswell, E.J., Jeon, H., Blacklow, S.C., and Downing, A.K. (2004). Global defects in the expression and function of the low density lipoprotein receptor (LDLR) associated with two familial hypercholesterolemia mutations resulting in misfolding of the LDLR epidermal growth factor-AB pair. J Biol Chem *279*, 30611-30621.

Brabec, M., Baravalle, G., Blaas, D., and Fuchs, R. (2003). Conformational changes, plasma membrane penetration, and infection by human rhinovirus type 2: Role of receptors and low pH. J Virol *77*, 5370-5377.

Brabec, M., Schober, D., Wagner, E., Bayer, N., Murphy, R.F., Blaas, D., and Fuchs, R. (2005). Opening of size-selective pores in endosomes during human rhinovirus serotype 2 in vivo uncoating monitored by single-organelle flow analysis. J Virol *79*, 1008-1016.

Brandenburg, B., Lee, L.Y., Lakadamyali, M., Rust, M.J., Zhuang, X., and Hogle, J.M. (2007). Imaging Poliovirus Entry in Live Cells. PLoS Biol *5*, e183.

Brown-Augsburger, P., Vance, L.M., Malcolm, S.K., Hsiung, H., Smith, D.P., and Heinz, B.A. (1999). Evidence that enviroxime targets multiple components of the rhinovirus 14 replication complex. Archives of virology *144*, 1569-1585.

Brown, M.S., and Goldstein, J.L. (1974a). Expression of the familial hypercholesterolemia gene in heterozygotes: mechanism for a dominant disorder in man. Science *185*, 61-63.

Brown, M.S., and Goldstein, J.L. (1974b). Familial hypercholesterolemia: defective binding of lipoproteins to cultured fibroblasts associated with impaired regulation of 3-hydroxy-3-methylglutaryl coenzyme A reductase activity. Proc Natl Acad Sci U S A *71*, 788-792.

Brown, M.S., and Goldstein, J.L. (1983). Lipoprotein receptors in the liver. Control signals for plasma cholesterol traffic. J Clin Invest *72*, 743-747.

Brown, M.S., and Goldstein, J.L. (1986). A receptor-mediated pathway for cholesterol homeostasis. Science *232*, 34-47.

Bu, G.J., Geuze, H.J., Strous, G.J., and Schwartz, A.L. (1995). 39 kDa receptor-associated protein is an ER resident protein and molecular chaperone for LDL receptor-related protein. EMBO Journal *14*, 2269-2280.

Bu, G.J., Maksymovitch, E.A., and Schwartz, A.L. (1993). Receptor-mediated endocytosis of tissue-type plasminogen activator by low density lipoprotein receptor-related protein on human hepatoma HepG2 cells. Journal of Biological Chemistry *268*, 13002-13009.

Bu, G.J., and Rennke, S. (1996). Receptor-associated protein is a folding chaperone for low density lipoprotein receptor-related protein. J Biol Chem *271*, 22218-22224.

Bubeck, D., Filman, D.J., and Hogle, J.M. (2005). Cryo-electron microscopy reconstruction of a poliovirus-receptor-membrane complex. Nat Struct Mol Biol *12*, 615-618.

Castelli, J., Wood, K.A., and Youle, R.J. (1998a). The 2-5A system in viral infection and apoptosis. Biomed Pharmacother *52*, 386-390.

Castelli, J.C., Hassel, B.A., Maran, A., Paranjape, J., Hewitt, J.A., Li, X.L., Hsu, Y.T., Silverman, R.H., and Youle, R.J. (1998b). The role of 2'-5' oligoadenylate-activated ribonuclease L in apoptosis. Cell Death Differ *5*, 313-320.

Chakravarti, D.N., Chakravarti, B., Parra, C.A., and Muller-Eberhard, H.J. (1989). Structural homology of complement protein C6 with other channel-forming proteins of complement. Proc Natl Acad Sci U S A *86*, 2799-2803.

Chen, S.H., Yang, C.Y., Chen, P.F., Setzer, D., Tanimura, M., Li, W.H., Gotto, A.M., Jr., and Chan, L. (1986). The complete cDNA and amino acid sequence of human apolipoprotein B-100. J Biol Chem *261*, 12918-12921.

Chen, W.J., Goldstein, J.L., and Brown, M.S. (1990). NPXY, a sequence often found in cytoplasmic tails, is required for coated pit-mediated internalization of the low density lipoprotein receptor. J Biol Chem *265*, 3116-3123.

Cho, M.W., Teterina, N., Egger, D., Bienz, K., and Ehrenfeld, E. (1994). Membrane rearrangement and vesicle induction by recombinant poliovirus 2C and 2BC in human cells. Virology *202*, 129-145.

Chow, M., Newman, J. F. E., Filman, D., Hogle, J. M., Rowlands, D. J., and Brown, F. (1987). Myristoylation of picornavirus capsid protein VP4 and its structural significance. Nature *327*, 482-486.

Chung, S.K., Kim, J.Y., Kim, I.B., Park, S.I., Paek, K.H., and Nam, J.H. (2005). Internalization and trafficking mechanisms of coxsackievirus B3 in HeLa cells. Virology *333*, 31-40.

Cooper, G.M. (2000). The cell – a molecular approach (Sinauer Associates, Inc.).

Coyne, C.B., Shen, L., Turner, J.R., and Bergelson, J.M. (2007). Coxsackievirus entry across epithelial tight junctions requires occludin and the small GTPases Rab34 and Rab5. Cell host & microbe *2*, 181-192.

Crooks, G.E., Hon, G., Chandonia, J.M., and Brenner, S.E. (2004). WebLogo: a sequence logo generator. Genome Res *14*, 1188-1190.

Cross, K.J., Langley, W.A., Russell, R.J., Skehel, J.J., and Steinhauer, D.A. (2009). Composition and functions of the influenza fusion peptide. Protein and peptide letters *16*, 766-778.

Cummings, R.D., Kornfeld, S., Schneider, W.J., Hobgood, K.K., Tolleshaug, H., Brown, M.S., and Goldstein, J.L. (1983). Biosynthesis of N- and O-linked oligosaccharides of the low density lipoprotein receptor. J Biol Chem *258*, 15261-15273.

Curry, S., Chow, M., and Hogle, J.M. (1996). The poliovirus 135S particle is infectious. J Virol *70*, 7125-7131.
D'Arcangelo, G., Homayouni, R., Keshvara, L., Rice, D.S., Sheldon, M., and Curran, T. (1999). Reelin is a ligand for lipoprotein receptors. Neuron *24*, 471-479.

Daly, N.L., Djordjevic, J.T., Kroon, P.A., and Smith, R. (1995). Three-dimensional structure of the second cysteine-rich repeat from the human low-density lipoprotein receptor. Biochemistry *34*, 14474-14481.

Damm, E.M., Pelkmans, L., Kartenbeck, J., Mezzacasa, A., Kurzchalia, T., and Helenius, A. (2005). Clathrin- and caveolin-1-independent endocytosis: entry of simian virus 40 into cells devoid of caveolae. The Journal of cell biology *168*, 477-488.

Davis, C.G., Elhammer, A., Russell, D.W., Schneider, W.J., Kornfeld, S., Brown, M.S., and Goldstein, J.L. (1986a). Deletion of clustered O-linked carbohydrates does not impair function of low density lipoprotein receptor in transfected fibroblasts. J Biol Chem *261*, 2828-2838.

Davis, C.G., Goldstein, J.L., Sudhof, T.C., Anderson, R.G., Russell, D.W., and Brown, M.S. (1987a). Acid-dependent ligand dissociation and recycling of LDL receptor mediated by growth factor homology region. Nature *326*, 760-765.

Davis, C.G., Lehrman, M.A., Russell, D.W., Anderson, R.G., Brown, M.S., and Goldstein, J.L. (1986b). The J.D. mutation in familial hypercholesterolemia: amino acid substitution in cytoplasmic domain impedes internalization of LDL receptors. Cell *45*, 15-24.

Davis, C.G., van Driel, I.R., Russell, D.W., Brown, M.S., and Goldstein, J.L. (1987b). The low density lipoprotein receptor. Identification of amino acids in cytoplasmic domain required for rapid endocytosis. J Biol Chem *262*, 4075-4082.

Davis, M.P., Bottley, G., Beales, L.P., Killington, R.A., Rowlands, D.J., and Tuthill, T.J. (2008). Recombinant VP4 of human rhinovirus induces permeability in model membranes. J Virol.

De Palma, A.M., Vliegen, I., De Clercq, E., and Neyts, J. (2008). Selective inhibitors of picornavirus replication. Med Res Rev.

DeTulleo, L., and Kirchhausen, T. (1998). The clathrin endocytic pathway in viral infection. Embo J *17*, 4585-4593.

DiScipio, R.G., Chakravarti, D.N., Muller-Eberhard, H.J., and Fey, G.H. (1988). The structure of human complement component C7 and the C5b-7 complex. J Biol Chem *263*, 549-560.

Donninger, H., Glashoff, R., Haitchi, H.M., Syce, J.A., Ghildyal, R., van Rensburg, E., and Bardin, P.G. (2003). Rhinovirus induction of the CXC chemokine epithelial-neutrophil activating peptide-78 in bronchial epithelium. J Infect Dis *187*, 1809-1817.

Duggal, R., and Wimmer, E. (1999). Genetic recombination of poliovirus in vitro and in vivo: Temperature-dependent alteration of crossover sites. Virology *258*, 30-41 FTXT: Full text from Academic Press IDEAL Full text from Academic Press IDEAL (European Mirror).

Egger, D., Wolk, B., Gosert, R., Bianchi, L., Blum, H.E., Moradpour, D., and Bienz, K. (2002). Expression of hepatitis C virus proteins induces distinct membrane alterations including a candidate viral replication complex. J Virol *76*, 5974-5984.

Einarsson, O., Geba, G.P., Zhu, Z., Landry, M., and Elias, J.A. (1996). Interleukin-11: stimulation in vivo and in vitro by respiratory viruses and induction of airways hyperresponsiveness. J Clin Invest *97*, 915-924.

Esser, V., Limbird, L.E., Brown, M.S., Goldstein, J.L., and Russell, D.W. (1988). Mutational analysis of the ligand binding domain of the low density lipoprotein receptor. J Biol Chem *263*, 13282-13290.

Falsey, A.R., Walsh, E.E., and Hayden, F.G. (2002). Rhinovirus and coronavirus infection-associated hospitalizations among older adults. J Infect Dis *185*, 1338-1341.

Fass, D., Blacklow, S., Kim, P.S., and Berger, J.M. (1997). Molecular basis of familial hypercholesterolaemia from structure of LDL receptor module. Nature *388*, 691-693.

Fields, B.N., Knipe, M.D., and Howley, P.M. (1996). Virology. Third Edition, Lipincott-Raven Publishers, Philadelphia, New York.

Flanegan, J.B., Petterson, R.F., Ambros, V., Hewlett, N.J., and Baltimore, D. (1977). Covalent linkage of a protein to a defined nucleotide sequence at the 5'-terminus of virion and replicative intermediate RNAs of poliovirus. Proc Natl Acad Sci U S A *74*, 961-965.

Flint, S.J., Enquist, L.W., Krug, R.M., Racaniello, V.R., and Skalka, A.M. (2000). Principles of Virology: Molecular Biology, Pathogenesis and Control. ASM Press, Washington, DC.

Florea, N.R., Maglio, D., and Nicolau, D.P. (2003). Pleconaril, a novel antipicornaviral agent. Pharmacotherapy *23*, 339-348.

Fox, M.P., Otto, M.J., and McKinlay, M.A. (1986). Prevention of rhinovirus and poliovirus uncoating by WIN 51711, a new antiviral drug. Antimicrob Agents Chemother *30*, 110-116.

Fricks, C.E., and Hogle, J.M. (1990). Cell-induced conformational change in poliovirus - externalization of the amino terminus of Vp1 is responsible for liposome binding. J Virol *64*, 1934-1945.

Fry, E.E., Lea, S.M., Jackson, T., Newman, J.W.I., Ellard, F.M., Blakemore, W.E., Abu Ghazaleh, R., Samuel, A., King, A.M.Q., and Stuart, D.I. (1999). The structure and function of a foot-and-mouth disease virus-oligosaccharide receptor complex. Embo Journal *18*, 543-554.

Fuchs, R., and Blaas, D. (2008). Human rhinovirus cell entry and uncoating In Structure-based Study of Viral Replication, H.C.a.T. Miyamura, ed. (World Scientific and Imperial College Press), pp. 1-42.

Gadkari, D.A. (2005). RNA interference & inhibition of viruses. Indian J Med Res *121*, 147-150.

Gafvels, M.E., Caird, M., Britt, D., Jackson, C.L., Patterson, D., and Strauss, J.F., 3rd (1993). Cloning of a cDNA encoding a putative human very low density lipoprotein/apolipoprotein E receptor and assignment of the gene to chromosome 9pter-p23. Somat Cell Mol Genet *19*, 557-569.

Gamarnik, A.V., and Andino, R. (1998). Switch from translation to RNA replication in a positive-stranded RNA virus. Genes and Development *12*, 2293-2304.

Gamarnik, A.V., and Andino, R. (2000). Interactions of viral protein 3CD and poly(rC) binding protein with the 5 ' untranslated region of the poliovirus genome. Journal of Virology *74*, 2219-2226.

Gerasimenko, J.V., Tepikin, A.V., Petersen, O.H., and Gerasimenko, O.V. (1998). Calcium uptake via endocytosis with rapid release from acidifying endosomes. Curr Biol *8*, 1335-1338.

Gerber, K., Wimmer, E., and Paul, A.V. (2001). Biochemical and genetic studies of the initiation of human rhinovirus 2 RNA replication: purification and enzymatic analysis of the RNA-dependent RNA polymerase 3D(pol). J Virol *75*, 10969-10978.

Gern, J.E. (2002). Rhinovirus respiratory infections and asthma. Am J Med *112 Suppl 6A*, 19S-27S.

Gern, J.E., and Busse, W.W. (1999). Association of rhinovirus infections with asthma. Clin Microb Rev *12*, 9-18.

Gern, J.E., Galagan, D.M., Jarjour, N.N., Dick, E.C., and Busse, W.W. (1997). Detection of rhinovirus RNA in lower airway cells during experimentally induced infection. Amer J Respir Crit Care Med *155*, 1159-1161
.

Giranda, V.L., Chapman, M.S., and Rossmann, M.G. (1990). Modeling of the human intercellular adhesion molecule-1, the human rhinovirus major group receptor. Proteins *7*, 227-233.

Gliemann, J. (1998). Receptors of the low density lipoprotein (LDL) receptor family in man. Multiple functions of the large family members via interaction with complex ligands. Biological Chemistry *379*, 951-964.

Goldstein, J.L., Brown, M.S., Anderson, R.G., Russell, D.W., and Schneider, W.J. (1985). Receptor-mediated endocytosis: concepts emerging from the LDL receptor system. Annu Rev Cell Biol *1*, 1-39.

Good, N.E., Winget, G.D., Winter, W., Connolly, T.N., Izawa, S., and Singh, R.M. (1966). Hydrogen ion buffers for biological research. Biochemistry *5*, 467-477.

Goodfellow, I.G., Sioofy, A.B., Powell, R.M., and Evans, D.J. (2001). Echoviruses bind heparan sulfate at the cell surface. J Virol *75*, 4918-4921.

Gotthardt, M., Trommsdorff, M., Nevitt, M.F., Shelton, J., Richardson, J.A., Stockinger, W., Nimpf, J., and Herz, J. (2000). Interactions of the low density lipoprotein receptor gene family with cytosolic adaptor and scaffold proteins suggest diverse biological functions in cellular communication and signal transduction. Journal of Biological Chemistry *275*, 25616-25624.

Gradi, A., Svitkin, Y.V., Imataka, H., and Sonenberg, N. (1998). Proteolysis of human eukaryotic translation initiation factor eIF4GII, but not eIF4GI, coincides with the shutoff of host protein synthesis after poliovirus infection. Proceedings Of the National Academy Of Sciences Of the United States Of America *95*, 11089-11094.

Grant, R.A., Hiremath, C.N., Filman, D.J., Syed, R., Andries, K., and Hogle, J.M. (1994). Structures of poliovirus complexes with anti-viral drugs: Implications for viral stability and drug design. Current Biology *4*, 784-797.

Greenberg, S.B. (2002). Respiratory viral infections in adults. Curr Opin Pulm Med *8*, 201-208.

Greve, J.M., Davis, G., Meyer, A.M., Forte, C.P., Yost, S.C., Marlor, C.W., Kamarck, M.E., and McClelland, A. (1989). The major human rhinovirus receptor is ICAM-1. Cell *56*, 839-847.

Grubman, M.J., and Baxt, B. (2004). Foot-and-mouth disease. Clin Microbiol Rev *17*, 465-493.

Gruenberger, M., Pevear, D., Diana, G.D., Kuechler, E., and Blaas, D. (1991). Stabilization of human rhinovirus serotype-2 against pH-induced conformational change by antiviral compounds. Journal of General Virology *72*, 431-433.

Gruenberger, M., Wandl, R., Nimpf, J., Hiesberger, T., Schneider, W.J., Kuechler, E., and Blaas, D. (1995). Avian homologs of the mammalian low-density lipoprotein receptor family bind minor receptor group human rhinovirus. J Virol *69*, 7244-7247.

Grunberg, K., Sharon, R.F., Hiltermann, T.J.N., Brahim, J.J., Dick, E.C., Sterk, P.J., and Van Krieken, J. (2000). Experimental rhinovirus 16 infection increases intercellular adhesion molecule-1 expression in bronchial epithelium of asthmatics regardless of inhaled steroid treatment. Clinical & Experimental Allergy *30*, 1015-1023.

Gulevich, A.Y., Yusupova, R.A., and Drygin, Y.F. (2002). VPg Unlinkase, the Phosphodiesterase That Hydrolyzes the Bond between VPg and Picornavirus RNA: a Minimal Nucleic Moiety of the Substrate. Biochemistry (Mosc) *67*, 615-621.

Hadfield, A.T., Lee, W.M., Zhao, R., Oliveira, M.A., Minor, I., Rueckert, R.R., and Rossmann, M.G. (1997). The refined structure of human rhinovirus 16 at 2.15 angstrom resolution: Implications for the viral life cycle. Structure *5*, 427-441.

Haefliger, J.A., Tschopp, J., Nardelli, D., Wahli, W., Kocher, H.P., Tosi, M., and Stanley, K.K. (1987). Complementary DNA cloning of complement C8 beta and its sequence homology to C9. Biochemistry *26*, 3551-3556.

Hafenstein, S., Bowman, V.D., Chipman, P.R., Bator Kelly, C.M., Lin, F., Medof, M.E., and Rossmann, M.G. (2007). Interaction of decay-accelerating factor with coxsackievirus B3. J Virol *81*, 12927-12935.

Haghighat, A., Svitkin, Y., Novoa, I., Kuechler, E., Skern, T., and Sonenberg, N. (1996). The eIF4G eIF4E complex is the target for direct cleavage by the rhinovirus 2A proteinase. Journal Of Virology *70*, 8444-8450.

Hamdouchi, C., Sanchez-Martinez, C., Gruber, J., Del Prado, M., Lopez, J., Rubio, A., and Heinz, B.A. (2003). Imidazo[1,2-b]pyridazines, novel nucleus with potent and broad spectrum activity against human picornaviruses: design, synthesis, and biological evaluation. J Med Chem *46*, 4333-4341.

Harris, K.S., Xiang, W.K., Alexander, L., Lane, W.S., Paul, A.V., and Wimmer, E. (1994). Interaction of poliovirus polypeptide 3CD(pro) with the 5' and 3' termini of the poliovirus genome - Identification of viral and cellular cofactors needed for efficient binding. Journal of Biological Chemistry *269*, 27004-27014.

Hayden, F.G. (2004). Rhinovirus and the lower respiratory tract. Reviews in medical virology *14*, 17-31.

Hayden, F.G., Albrecht, J.K., Kaiser, D.L., and Gwaltney, J.M., Jr. (1986). Prevention of natural colds by contact prophylaxis with intranasal alpha 2-interferon. N Engl J Med *314*, 71-75.

Hayden, F.G., Coats, T., Kim, K., Hassman, H.A., Blatter, M.M., Zhang, B., and Liu, S. (2002). Oral pleconaril treatment of picornavirus-associated viral respiratory illness in adults: efficacy and tolerability in phase II clinical trials. Antivir Ther *7*, 53-65.

Hayden, F.G., and Gwaltney, J.M., Jr. (1984). Intranasal interferon-alpha 2 treatment of experimental rhinoviral colds. J Infect Dis *150*, 174-180.

Hayden, F.G., Herrington, D.T., Coats, T.L., Kim, K., Cooper, E.C., Villano, S.A., Liu, S., Hudson, S., Pevear, D.C., Collett, M.*, et al.* (2003a). Efficacy and safety of oral pleconaril for treatment of colds due to picornaviruses in adults: results of 2 double-blind, randomized, placebo-controlled trials. Clin Infect Dis *36*, 1523-1532.

Hayden, F.G., Hipskind, G.J., Woerner, D.H., Eisen, G.F., Janssens, M., Janssen, P.A., and Andries, K. (1995). Intranasal pirodavir (R77,975) treatment of rhinovirus colds. Antimicrob Agents Chemother *39*, 290-294.

Hayden, F.G., Turner, R.B., Gwaltney, J.M., Chi-Burris, K., Gersten, M., Hsyu, P., Patick, A.K., Smith, G.J., 3rd, and Zalman, L.S. (2003b). Phase II, randomized, double-blind, placebo-controlled studies of ruprintrivir nasal spray 2-percent suspension for prevention and treatment of experimentally induced rhinovirus colds in healthy volunteers. Antimicrob Agents Chemother *47*, 3907-3916.

He, Y., Bowman, V.D., Mueller, S., Bator, C.M., Bella, J., Peng, X., Baker, T.S., Wimmer, E., Kuhn, R.J., and Rossmann, M.G. (2000). Interaction of the poliovirus receptor with poliovirus. Proc Natl Acad Sci U S A *97*, 79-84.

He, Y., Chipman, P.R., Howitt, J., Bator, C.M., Whitt, M.A., Baker, T.S., Kuhn, R.J., Anderson, C.W., Freimuth, P., and Rossmann, M.G. (2001). Interaction of coxsackievirus B3 with the full length coxsackievirus- adenovirus receptor. Nat Struct Biol *8*, 874-878.

Heegaard, C.W., Simonsen, A.C., Oka, K., Kjoller, L., Christensen, A., Madsen, B., Ellgaard, L., Chan, L., and Andreasen, P.A. (1995). Very low density lipoprotein receptor binds and mediates endocytosis of urokinase-type plasminogen activator-type-1 plasminogen activator inhibitor complex. J Biol Chem *270*, 20855-20861.

Heikkinen, T., and Jarvinen, A. (2003). The common cold. Lancet *361*, 51-59.

Heinz, B.A., and Vance, L.M. (1995). The antiviral compound enviroxime targets the 3A coding region of rhinovirus and poliovirus. Journal of Virology *69*, 4189-4197.

Herz, J. (2001a). Deconstructing the LDL receptor - a rhapsody in pieces. Nat Struct Biol *8*, 476-478.

Herz, J. (2001b). The LDL receptor gene family: (un)expected signal transducers in the brain. Neuron *29*, 571-581.

Herz, J., and Bock, H.H. (2002). Lipoprotein receptors in the nervous system. Annu Rev Biochem *71*, 405-434.

Herz, J., Clouthier, D.E., and Hammer, R.E. (1992). LDL receptor-related protein internalizes and degrades uPA-PAI-1 complexes and is essential for embryo implantation. Cell *71*, 411-421.

Herz, J., Hamann, U., Rogne, S., Myklebost, O., Gausepohl, H., and Stanley, K.K. (1988). Surface location and high affinity for calcium of a 500-kd liver membrane protein closely related to the LDL-receptor suggest a physiological role as lipoprotein receptor. Embo J *7*, 4119-4127.

Herz, J., and Marschang, P. (2003). Coaxing the LDL Receptor Family into the Fold. Cell *112*, 289-292.

Herz, J., and Strickland, D.K. (2001). LRP: a multifunctional scavenger and signaling receptor. J Clin Invest *108*, 779-784.

Hewat, E., and Neumann, E. (2002). Characterization of the performance of a 200-kV field emission gun for cryo-electron microscopy of biological molecules. Journal of structural biology *139*, 60.

Hewat, E., Neumann, E., and Blaas, D. (2002). The concerted conformational changes during human rhinovirus 2 uncoating. Mol Cell *10*, 317-326.

Hewat, E.A., and Blaas, D. (2004). Cryoelectron microscopy analysis of the structural changes associated with human rhinovirus type 14 uncoating. J Virol *78*, 2935-2942.

Hewat, E.A., and Blaas, D. (2006). Nonneutralizing Human Rhinovirus Serotype 2-Specific Monoclonal Antibody 2G2 Attaches to the Region That Undergoes the Most Dramatic Changes upon Release of the Viral RNA. J Virol *80*, 12398-12401.

Hewat, E.A., Neumann, E., Conway, J.F., Moser, R., Ronacher, B., Marlovits, T.C., and Blaas, D. (2000). The cellular receptor to human rhinovirus 2 binds around the 5-fold axis and not in the canyon: a structural view. Embo J *19*, 6317-6325.

Hewlett, L.J., Prescott, A.R., and Watts, C. (1994). The Coated Pit and Macropinocytic Pathways Serve Distinct Endosome Populations. Journal of Cell Biology *124*, 689-703.

Hewson, C.A., Jardine, A., Edwards, M.R., Laza-Stanca, V., and Johnston, S.L. (2005). Toll-like receptor 3 is induced by and mediates antiviral activity against rhinovirus infection of human bronchial epithelial cells. J Virol *79*, 12273-12279.

Hiesberger, T., Hermann, M., Jacobsen, L., Novak, S., Hodits, R.A., Bujo, H., Meilinger, M., Huttinger, M., Schneider, W.J., and Nimpf, J. (1995). The chicken oocyte receptor for yolk precursors as a model for studying the action of receptor-associated protein and lactoferrin. J Biol Chem *270*, 18219-18226.

Hiesberger, T., Trommsdorff, M., Howell, B.W., Goffinet, A., Mumby, M.C., Cooper, J.A., and Herz, J. (1999). Direct binding of Reelin to VLDL receptor and ApoE receptor 2 induces tyrosine phosphorylation of disabled-1 and modulates tau phosphorylation. Neuron *24*, 481-489.

Hindiyeh, M., Li, Q.H., Basavappa, R., Hogle, J.M., and Chow, M. (1999). Poliovirus mutants at histidine 195 of VP2 do not cleave VP0 into VP2 and VP4. Journal of Virology *73*, 9072-9079.

Hobbs, H.H., Brown, M.S., and Goldstein, J.L. (1992). Molecular genetics of the LDL receptor gene in familial hypercholesterolemia. Hum Mutat *1*, 445-466.

Hobbs, H.H., Russell, D.W., Brown, M.S., and Goldstein, J.L. (1990). The LDL receptor locus in familial hypercholesterolemia: mutational analysis of a membrane protein. Annu Rev Genet *24*, 133-170.

Hofer, F., Berger, B., Gruenberger, M., Machat, H., Dernick, R., Tessmer, U., Kuechler, E., and Blaas, D. (1992). Shedding of a rhinovirus minor group binding protein - Evidence for a Ca^{2+}-dependent process. Journal of General Virology *73*, 627-632.

Hofer, F., Gruenberger, M., Kowalski, H., Machat, H., Huettinger, M., Kuechler, E., and Blaas, D. (1994). Members of the low density lipoprotein receptor family mediate cell entry of a minor-group common cold virus. Proc Natl Acad ScieUSA *91*, 1839-1842.

Hogle, J., M., Chow, M., and Filman, D.J. (1985). Three-Dimensional Structure of Poliovirus at 2.9 A Resolution. Science *229*, 1358-1365.

Hogle, J.M. (2002). POLIOVIRUS CELL ENTRY: Common Structural Themes in Viral Cell Entry Pathways. Annu Rev Microbiol *56*, 677-702.

Hoover-Litty, H., and Greve, J.M. (1993). Formation of rhinovirus-soluble ICAM-1 complexes and conformational changes in the virion. J Virol *67*, 390-397.

Hooverlitty, H., and Greve, J.M. (1993). Formation of rhinovirus-soluble ICAM-1 complexes and conformational changes in the virion. Journal of Virology *67*, 390-397.

Howard, O.M., Rao, A.G., and Sodetz, J.M. (1987). Complementary DNA and derived amino acid sequence of the beta subunit of human complement protein C8: identification of a close structural and ancestral relationship to the alpha subunit and C9. Biochemistry *26*, 3565-3570.

Howell, B.W., and Herz, J. (2001). The LDL receptor gene family: signaling functions during development. Curr Opin Neurobiol *11*, 74-81.

Iijima, H., Miyazawa, M., Sakai, J., Magoori, K., Ito, M.R., Suzuki, H., Nose, M., Kawarabayasi, Y., and Yamamoto, T.T. (1998). Expression and characterization of a very low density lipoprotein receptor variant lacking the O-linked sugar region generated by alternative splicing. J Biochem *124*, 747-755.

Innerarity, T.L., Friedlander, E.J., Rall, S.C., Jr., Weisgraber, K.H., and Mahley, R.W. (1983). The receptor-binding domain of human apolipoprotein E. Binding of apolipoprotein E fragments. J Biol Chem *258*, 12341-12347.

Innerarity, T.L., and Mahley, R.W. (1978). Enhanced binding by cultured human fibroblasts of apo-E-containing lipoproteins as compared with low density lipoproteins. Biochemistry *17*, 1440-1447.

Innerarity, T.L., Mahley, R.W., Weisgraber, K.H., and Bersot, T.P. (1978). Apoprotein (E--A-II) complex of human plasma lipoproteins. II. Receptor binding activity of a high density lipoprotein subfraction modulated by the apo(E--A-II) complex. J Biol Chem *253*, 6289-6295.

Innerarity, T.L., Pitas, R.E., and Mahley, R.W. (1979). Binding of arginine-rich (E) apoprotein after recombination with phospholipid vesicles to the low density lipoprotein receptors of fibroblasts. J Biol Chem *254*, 4186-4190.

Ishibashi, S., Brown, M.S., Goldstein, J.L., Gerard, R.D., Hammer, R.E., and Herz, J. (1993). Hypercholesterolemia in low density lipoprotein receptor knockout mice and its reversal by adenovirus-mediated gene delivery. J Clin Invest *92*, 883-893.

Jackson, R.J. (2005). Alternative mechanisms of initiating translation of mammalian mRNAs. Biochem Soc Trans *33*, 1231-1241.

Jackson, W.T., Giddings, T.H., Jr., Taylor, M.P., Mulinyawe, S., Rabinovitch, M., Kopito, R.R., and Kirkegaard, K. (2005). Subversion of cellular autophagosomal machinery by RNA viruses. PLoS Biol *3*, e156.

Jarvis, T.C., and Kirkegaard, K. (1992). Poliovirus RNA Recombination - Mechanistic Studies in the Absence of Selection. EMBO Journal *11*, 3135-3145.

Jeon, H., and Blacklow, S.C. (2005). Structure and Physiologic Function of the Low-Density Lipoprotein Receptor. Annu Rev Biochem *74*, 535-562.

Jeon, H., Meng, W., Takagi, J., Eck, M.J., Springer, T.A., and Blacklow, S.C. (2001). Implications for familial hypercholesterolemia from the structure of the LDL receptor YWTD-EGF domain pair. Nat Struct Biol *8*, 499-504.

Jin, M., Park, J., Lee, S., Park, B., Shin, J., Song, K.J., Ahn, T.I., Hwang, S.Y., Ahn, B.Y., and Ahn, K. (2002). Hantaan virus enters cells by clathrin-dependent receptor-mediated endocytosis. Virology *294*, 60-69.

Joachims, M., Van Breugel, P.C., and Lloyd, R.E. (1999). Cleavage of poly(A)-binding protein by enterovirus proteases concurrent with inhibition of translation in vitro. J Virol *73*, 718-727.

Khan, A.G., Pichler, J., Rosemann, A., and Blaas, D. (2007). Human rhinovirus type 54 infection via heparan sulfate is less efficient and strictly dependent on low endosomal pH. J Virol *81*, 4625-4632.

Khan, A.G., Pickl-Herk, A., Marlovits, T., Fuchs R., Blaas, D. (2010). Human Rhinovirus 14 Enters Rhabdomyosarcoma Cells Expressing ICAM-1 by a Clathrin, Caveolin, and Flotillin independent Pathway. J Virol, Epub 2010 Feb 3.

Kim, D.H., Iijima, H., Goto, K., Sakai, J., Ishii, H., Kim, H.J., Suzuki, H., Kondo, H., Saeki, S., and Yamamoto, T. (1996). Human apolipoprotein E receptor 2. A novel lipoprotein receptor of the low density lipoprotein receptor family predominantly expressed in brain. J Biol Chem *271*, 8373-8380.

Kim, J., Sanders, S.P., Siekierski, E.S., Casolaro, V., and Proud, D. (2000). Role of NF-kappa B in cytokine production induced from human airway epithelial cells by rhinovirus infection. J Immunol *165*, 3384-3392.

Kim, S., Smith, T.J., Chapman, M.S., Rossmann, M.G., Pevear, D.C., Dutko, F.J., Felock, P.J., Diana, G.D., and McKinlay, M.A. (1989). Crystal structure of human rhinovirus serotype-1A (Hrv1A). J Mol Biol *210*, 91-111.

Kimball, S.R. (1999). Eukaryotic initiation factor eIF2. Int J Biochem Cell Biol *31*, 25-29.

Kingsley, D.M., and Krieger, M. (1984). Receptor-mediated endocytosis of low density lipoprotein: somatic cell mutants define multiple genes required for expression of surface-receptor activity. Proc Natl Acad Sci U S A *81*, 5454-5458.

Kirchberger, S., Majdic, O., and Stockl, J. (2007). Modulation of the immune system by human rhinoviruses. Int Arch Allergy Immunol *142*, 1-10.

Kistler, A., Avila, P.C., Rouskin, S., Wang, D., Ward, T., Yagi, S., Schnurr, D., Ganem, D., Derisi, J.L., and Boushey, H.A. (2007). Pan-viral screening of respiratory tract infections in adults with and without asthma reveals unexpected human coronavirus and human rhinovirus diversity. J Infect Dis *196*, 817-825.

Knipe, T., Rieder, E., Baxt, B., Ward, G., and Mason, P.W. (1997). Characterization of synthetic foot-and-mouth disease virus provirions separates acid-mediated disassembly from infectivity. J Virol *71*, 2851-2856.

Knott, T.J., Pease, R.J., Powell, L.M., Wallis, S.C., Rall, S.C., Jr., Innerarity, T.L., Blackhart, B., Taylor, W.H., Marcel, Y., Milne, R.*, et al.* (1986). Complete protein sequence and identification of structural domains of human apolipoprotein B. Nature *323*, 734-738.

Koivisto, U.M., Hubbard, A.L., and Mellman, I. (2001). A novel cellular phenotype for familial hypercholesterolemia due to a defect in polarized targeting of LDL receptor. Cell *105*, 575-585.

Kolatkar, P.R., Bella, J., Olson, N.H., Bator, C.M., Baker, T.S., and Rossmann, M.G. (1999). Structural studies of two rhinovirus serotypes complexed with fragments of their cellular receptor. EMBO J *18*, 6249-6259.

Kolset, S.O., and Salmivirta, M. (1999). Cell surface heparan sulfate proteoglycans and lipoprotein metabolism. Cell Mol Life Sci *56*, 857-870.

Konecsni, T., Berka, U., Pickl-Herk, A., Bilek, G., Khan, A.G., Gajdzig, L., Fuchs, R., and Blaas, D. (2009). Low pH-triggered beta-propeller switch of the low-density lipoprotein receptor assists rhinovirus infection. J Virol *83*, 10922-10930.

Konno, S., Grindle, K.A., Lee, W.M., Schroth, M.K., Mosser, A.G., Brockman-Schneider, R.A., Busse, W.W., and Gern, J.E. (2002). Interferon-gamma enhances rhinovirus-induced RANTES secretion by airway epithelial cells. Am J Respir Cell Mol Biol *26*, 594-601.

Korant, B.D., Lonberg Holm, K., Noble, J., and Stasny, J.T. (1972). Naturally occurring and artificially produced components of three rhinoviruses. Virology *48*, 71-86.

Kounnas, M.Z., Morris, R.E., Thompson, M.R., Fitzgerald, D.J., Strickland, D.K., and Saelinger, C.B. (1992). The alpha2-macroglobulin receptor low density lipoprotein receptor-related protein binds and internalizes Pseudomonas Exotoxin-A. Journal of Biological Chemistry *267*, 12420-12423.

Kowal, R.C., Herz, J., Goldstein, J.L., Esser, V., and Brown, M.S. (1989). Low density lipoprotein receptor-related protein mediates uptake of cholesteryl esters derived from apoprotein E-enriched lipoproteins. Proc Natl Acad Sci U S A *86*, 5810-5814.

Kräusslich, H.G., Nicklin, M. J., Toyoda, H., Etchison, D., and Wimmer, E. (1987). Poliovirus proteinase 2A induces cleavage of eucaryotic initiation factor 4F polypeptide p220. J Virol *61*, 2711-2718.

Krieger, M., Brown, M.S., and Goldstein, J.L. (1981). Isolation of Chinese hamster cell mutants defective in the receptor-mediated endocytosis of low density lipoprotein. J Mol Biol *150*, 167-184.

Kurniawan, N.D., Aliabadizadeh, K., Brereton, I.M., Kroon, P.A., and Smith, R. (2001). NMR structure and backbone dynamics of a concatemer of epidermal growth factor homology modules of the human low-density lipoprotein receptor. J Mol Biol *311*, 341-356.

Kurniawan, N.D., Atkins, A.R., Bieri, S., Brown, C.J., Brereton, I.M., Kroon, P.A., and Smith, R. (2000). NMR structure of a concatemer of the first and second ligand-binding modules of the human low-density lipoprotein receptor. Protein Science *9*, 1282-1293.

Kusov, Y., Weitz, M., Dollenmeier, G., Gaussmuller, V., and Siegl, G. (1996). RNA-protein interactions at the 3' end of the hepatitis A virus RNA. J Virol *70*, 1890-1897.

Kuyumcu-Martinez, N.M., Van Eden, M.E., Younan, P., and Lloyd, R.E. (2004). Cleavage of poly(A)-binding protein by poliovirus 3C protease inhibits host cell translation: a novel mechanism for host translation shutoff. Mol Cell Biol *24*, 1779-1790.

Lamson, D., Renwick, N., Kapoor, V., Liu, Z., Palacios, G., Ju, J., Dean, A., St George, K., Briese, T., and Ian Lipkin, W. (2006). MassTag Polymerase-Chain-Reaction Detection of Respiratory Pathogens, Including a New Rhinovirus Genotype, That Caused Influenza-Like Illness in New York State during 2004-2005. J Infect Dis *194*, 1398-1402.

Laniosz, V., Holthusen, K.A., and Meneses, P.I. (2008). Bovine papillomavirus type 1: from clathrin to caveolin. J Virol *82*, 6288-6298.

Lau, S.K., Yip, C.C., Tsoi, H.W., Lee, R.A., So, L.Y., Lau, Y.L., Chan, K.H., Woo, P.C., and Yuen, K.Y. (2007). Clinical Features and Complete Genome Characterization of a Distinct Human Rhinovirus (HRV) Genetic Cluster, Probably Representing a Previously Undetected HRV Species, HRV-C, Associated with Acute Respiratory Illness in Children. J Clin Microbiol *45*, 3655-3664.

Lee, D., Walsh, J.D., Mikhailenko, I., Yu, P., Migliorini, M., Wu, Y., Krueger, S., Curtis, J.E., Harris, B., Lockett, S.*, et al.* (2006). RAP uses a histidine switch to regulate its interaction with LRP in the ER and Golgi. Mol Cell *22*, 423-430.

Lee, W.M., Kiesner, C., Pappas, T., Lee, I., Grindle, K., Jartti, T., Jakiela, B., Lemanske, R.F., Shult, P.A., and Gern, J.E. (2007). A diverse group of previously unrecognized human rhinoviruses are common causes of respiratory illnesses in infants. PLoS ONE *2*, e966.

Lee, W.M., Monroe, S.S., and Rueckert, R.R. (1993). Role of maturation cleavage in infectivity of picornaviruses: activation of an infectosome. J Virol *67*, 2110-2122.

Lewis, J.K., Bothner, B., Smith, T.J., and Siuzdak, G. (1998). Antiviral agent blocks breathing of the common cold virus. Proc Natl Acad Sci U S A *95*, 6774-6778.

Li, J.-P., and Baltimore, D. (1988). Isolation of poliovirus 2C mutants defective in viral RNA synthesis. J Virol *62*, 4016-4021.

Li, Q., Yafal, A.G., Lee, Y.M., Hogle, J., and Chow, M. (1994). Poliovirus neutralization by antibodies to internal epitopes of VP4 and VP1 results from reversible exposure of these sequences at physiological temperature. J Virol *68*, 3965-3970.

Li, Y.H., Marzolo, M.P., van Kerkhof, P., Strous, G.J., and Bu, G.J. (2000). The YXXL motif, but not the two NPXY motifs, serves as the dominant endocytosis signal for low density lipoprotein receptor-related protein. Journal of Biological Chemistry *275*, 17187-17194.

Liu, C.X., Musco, S., Lisitsina, N.M., Yaklichkin, S.Y., and Lisitsyn, N.A. (2000). Genomic organization of a new candidate tumor suppressor gene, LRP1B. Genomics *69*, 271-274.

Lomax, N.B., and Yin, F.H. (1989). Evidence for the role of the P2 protein of human rhinovirus in its host range change. J Virol *63*, 2396-2399.

Lonberg-Holm, K., and Noble-Harvey, J. (1973). Comparison of in vitro and cell-mediated alteration of a human Rhinovirus and its inhibition by sodium dodecyl sulfate. J Virol *12*, 819-826.

Lonberg-Holm, K., and Yin, F.H. (1973). Antigenic determinants of infective and inactivated human rhinovirus type 2. J Virol *12*, 114-123.

Lonberg Holm, K., Gosser, L.B., and Shimshick, E.J. (1976). Interaction of liposomes with subviral particles of poliovirus type 2 and rhinovirus type 2. J Virol *19*, 746-749.

Magrane, J., Casaroli-Marano, R.P., Reina, M., Gafvels, M., and Vilaro, S. (1999). The role of O-linked sugars in determining the very low density lipoprotein receptor stability or release from the cell. FEBS Lett *451*, 56-62.

Magrane, J., Reina, M., Pagan, R., Luna, A., Casaroli-Marano, R.P., Angelin, B., Gafvels, M., and Vilaro, S. (1998). Bovine aortic endothelial cells express a variant of the very low density lipoprotein receptor that lacks the O-linked sugar domain. J Lipid Res *39*, 2172-2181.

Mahley, R.W., and Innerarity, T.L. (1983). Lipoprotein receptors and cholesterol homeostasis. Biochimica et biophysica acta *737*, 197-222.

Makgoba, M.W., Sanders, M.E., Ginther Luce, G.E., Dustin, M.L., Springer, T.A., Clark, E.A., Mannoni, P., and Shaw, S. (1988). ICAM-1 a ligand for LFA-1-dependent adhesion of B, T and myeloid cells. Nature *331*, 86-88.

Malby, S., Pickering, R., Saha, S., Smallridge, R., Linse, S., and Downing, A.K. (2001). The first epidermal growth factor-like domain of the low-density lipoprotein receptor contains a noncanonical calcium binding site. Biochemistry *40*, 2555-2563.

Marechal, V., Prevost, M.C., Petit, C., Perret, E., Heard, J.M., and Schwartz, O. (2001). Human immunodeficiency virus type 1 entry into macrophages mediated by macropinocytosis. J Virol *75*, 11166-11177.

Marlovits, T.C., Abrahamsberg, C., and Blaas, D. (1998a). Soluble LDL minireceptors - Minimal structure requirements for recognition of minor group human rhinovirus. Journal of Biological Chemistry *273*, 33835-33840.

Marlovits, T.C., Abrahamsberg, C., and Blaas, D. (1998b). Very-low-density lipoprotein receptor fragment shed from HeLa cells inhibits human rhinovirus infection. Journal of Virology *72*, 10246-10250.

Marlovits, T.C., Zechmeister, T., Gruenberger, M., Ronacher, B., Schwihla, H., and Blaas, D. (1998c). Recombinant soluble low density lipoprotein receptor fragment inhibits minor group rhinovirus infection in vitro. FASEB J *12*, 695-703.

Marlovits, T.C., Zechmeister, T., Schwihla, H., Ronacher, B., and Blaas, D. (1998d). Recombinant soluble low-density lipoprotein receptor fragment inhibits common cold infection. J Mol Recognit *11*, 49-51.

Marsh, M., and Helenius, A. (2006). Virus entry: open sesame. Cell *124*, 729-740.

Martino, T.A., Petric, M., Weingartl, H., Bergelson, J.M., Opavsky, M.A., Richardson, C.D., Modlin, J.F., Finberg, R.W., Kain, K.C., Willis, N.*, et al.* (2000). The coxsackie-adenovirus receptor (CAR) is used by reference strains and clinical isolates representing all six serotypes of coxsackievirus group B and by swine vesicular disease virus. Virology *271*, 99-108.

Maxfield, F.R., and McGraw, T.E. (2004). Endocytic recycling. Nat Rev Mol Cell Biol *5*, 121-132.

McErlean, P., Shackelton, L.A., Andrews, E., Webster, D.R., Lambert, S.B., Nissen, M.D., Sloots, T.P., and Mackay, I.M. (2008). Distinguishing molecular features and clinical characteristics of a putative new rhinovirus species, human rhinovirus C (HRV C). PLoS ONE *3*, e1847.

McErlean, P., Shackelton, L.A., Lambert, S.B., Nissen, M.D., Sloots, T.P., and Mackay, I.M. (2007). Characterisation of a newly identified human rhinovirus, HRV-QPM, discovered in infants with bronchiolitis. J Clin Virol *39*, 67-75.

McKinlay, M.A., Pevear, D.C., and Rossmann, M.G. (1992). Treatment of the picornavirus common cold by inhibitors of viral uncoating and attachment. Annual Review of Microbiology *46*, 635-654.

McLean, J.W., Elshourbagy, N.A., Chang, D.J., Mahley, R.W., and Taylor, J.M. (1984). Human apolipoprotein E mRNA. cDNA cloning and nucleotide sequencing of a new variant. J Biol Chem *259*, 6498-6504.

Meier, O., Boucke, K., Hammer, S.V., Keller, S., Stidwill, R.P., Hemmi, S., and Greber, U.F. (2002). Adenovirus triggers macropinocytosis and endosomal leakage together with its clathrin-mediated uptake. The Journal of cell biology *158*, 1119-1131.

Melchers, W.J.G., Hoenderop, J.G.J., Slot, H.J.B., Pleij, C.W.A., Pilipenko, E.V., Agol, V.I., and Galama, J.M.D. (1997). Kissing of the two predominant hairpin loops in the coxsackie B virus 3' untranslated region is the essential structural feature of the origin of replication required for negative-strand RNA synthesis. J Virol *71*, 686-696.

Mercer, J., and Helenius, A. (2008). Vaccinia virus uses macropinocytosis and apoptotic mimicry to enter host cells. Science *320*, 531-535.

Merl, S., Michaelis, C., Jaschke, B., Vorpahl, M., Seidl, S., and Wessely, R. (2005). Targeting 2A protease by RNA interference attenuates coxsackieviral cytopathogenicity and promotes survival in highly susceptible mice. Circulation *111*, 1583-1592.

Message, S.D., and Johnston, S.L. (2004). Host defense function of the airway epithelium in health and disease: clinical background. J Leukoc Biol *75*, 5-17.

Mikhailenko, I., Considine, W., Argraves, K.M., Loukinov, D., Hyman, B.T., and Strickland, D.K. (1999). Functional domains of the very low density lipoprotein receptor: molecular analysis of ligand binding and acid-dependent ligand dissociation mechanisms. Journal of Cell Science *112*, 3269-3281.

Mikhailenko, I., Krylov, D., Argraves, K.M., Roberts, D.D., Liau, G., and Strickland, D.K. (1997). Cellular internalization and degradation of thrombospondin- 1 is mediated by the amino-terminal heparin binding domain (HBD) - High affinity interaction of dimeric HBD with the low density lipoprotein receptor-related protein. J Biol Chem *272*, 6784-6791.

Milstone, A.M., Petrella, J., Sanchez, M.D., Mahmud, M., Whitbeck, J.C., and Bergelson, J.M. (2005). Interaction with coxsackievirus and adenovirus receptor, but not with decay-accelerating factor (DAF), induces A-particle formation in a DAF-binding coxsackievirus B3 isolate. J Virol *79*, 655-660.

Miyake, Y., Tajima, S., Funahashi, T., and Yamamoto, A. (1989). Analysis of a recycling-impaired mutant of low density lipoprotein receptor in familial hypercholesterolemia. J Biol Chem *264*, 16584-16590.

Monto, A.S., Fendrick, A.M., and Sarnes, M.W. (2001). Respiratory illness caused by picornavirus infection: a review of clinical outcomes. Clin Ther *23*, 1615-1627.

Moscufo, N., and Chow, M. (1992). Myristate-protein interactions in poliovirus: interactions of VP4 threonine 28 contribute to the structural conformation of assembly intermediates and the stability of assembled virions. J Virol *66*, 6849-6857.

Mosser, A.G., Brockman-Schneider, R., Amineva, S., Burchell, L., Sedgwick, J.B., Busse, W.W., and Gern, J.E. (2002). Similar frequency of rhinovirus-infectible cells in upper and lower airway epithelium. J Infect Dis *185*, 734-743.

Mosser, A.G., and Rueckert, R.R. (1993). WIN 51711-dependent mutants of poliovirus type 3: evidence that virions decay after release from cells unless drug is present. J Virol *67*, 1246-1254.

Muro, S., Wiewrodt, R., Thomas, A., Koniaris, L., Albelda, S.M., Muzykantov, V.R., and Koval, M. (2003). A novel endocytic pathway induced by clustering endothelial ICAM-1 or PECAM-1. J Cell Sci *116*, 1599-1609.

Nakayama, M., Nakajima, D., Nagase, T., Nomura, N., Seki, N., and Ohara, O. (1998). Identification of high-molecular-weight proteins with multiple EGF-like motifs by motif-trap screening. Genomics *51*, 27-34.

Nathan, B.P., Bellosta, S., Sanan, D.A., Weisgraber, K.H., Mahley, R.W., and Pitas, R.E. (1994). Differential effects of apolipoproteins E3 and E4 on neuronal growth in vitro. Science *264*, 850-852.

Neubauer, C., Frasel, L., Kuechler, E., and Blaas, D. (1987). Mechanism of entry of human rhinovirus 2 into HeLa cells. Virology *158*, 255-258.

Neznanov, N., Chumakov, K.M., Neznanova, L., Almasan, A., Banerjee, A.K., and Gudkov, A.V. (2005). Proteolytic cleavage of the p65-RelA subunit of NF-kappaB during poliovirus infection. J Biol Chem *280*, 24153-24158.

Nicodemou, A., Petsch, M., Konecsni, T., Kremser, L., Kenndler, E., Casasnovas, J.M., and Blaas, D. (2005). Rhinovirus-stabilizing activity of artificial VLDL-receptor variants defines a new mechanism for virus neutralization by soluble receptors. FEBS Lett *579*, 5507-5511.

Niemeier, A., Gafvels, M., Heeren, J., Meyer, N., Angelin, B., and Beisiegel, U. (1996). VLDL receptor mediates the uptake of human chylomicron remnants in vitro. J Lipid Res *37*, 1733-1742.

Nishi, T., and Forgac, M. (2002). The vacuolar (H+)-ATPases--nature's most versatile proton pumps. Nat Rev Mol Cell Biol *3*, 94-103.

Nizet, S., Wruss, J., Landstetter, N., Snyers, L., and Blaas, D. (2005). A mutation in the first ligand-binding repeat of the human very-low-density lipoprotein receptor results in high-affinity binding of the single V1 module to human rhinovirus 2. J Virol *79*, 14730-14736.

Noble, J.N., and Lonberg-Holm, K. (1973). Interactions of components of human rhinovirus type 2 with HeLa cells. Virology *51*, 270-278.

Nomoto, A., Detjen, B., Pozzati, R., and Wimmer, E. (1977). The location of the poliovirus genome protein in viral RNAs and its implication for RNA syntheses. Nature *268*, 208-213.

Norman, D., Sun, X.M., Bourbon, M., Knight, B.L., Naoumova, R.P., and Soutar, A.K. (1999). Characterization of a novel cellular defect in patients with phenotypic homozygous familial hypercholesterolemia. J Clin Invest *104*, 619-628.

North, C.L., and Blacklow, S.C. (1999). Structural independence of ligand-binding modules five and six of the LDL receptor. Biochemistry *38*, 3926-3935.

Novak, J.E., and Kirkegaard, K. (1994). Coupling between genome translation and replication in an RNA virus. Genes Dev *8*, 1726-1737.

Nurani, G., Lindqvist, B., and Casasnovas, J.M. (2003). Receptor priming of major group human rhinoviruses for uncoating and entry at mild low-pH environments. J Virol *77*, 11985-11991.

Nykjaer, A., and Willnow, T.E. (2002). The low-density lipoprotein receptor gene family: a cellular Swiss army knife? Trends Cell Biol *12*, 273-280.

O'Donnell, V., Larocco, M., and Baxt, B. (2008). Heparan sulfate-binding foot-and-mouth disease virus enters cells via caveola-mediated endocytosis. J Virol *82*, 9075-9085.

O'Donnell, V., Larocco, M., Duque, H., and Baxt, B. (2005). Analysis of Foot-and-Mouth Disease Virus Internalization Events in Cultured Cells. J Virol *79*, 8506-8518.

Ockenhouse, C.F., Betageri, R., Springer, T.A., and Staunton, D.E. (1992). Plasmodium Falciparum-Infected Erythrocytes Bind ICAM-1 at a Site Distinct from LFA-1, Mac-1, and Human Rhinovirus. Cell *68*, 63-69.

Oka, K., Ishimuraoka, K., Chu, M.J., Sullivan, M., Krushkal, J., Li, W.H., and Chan, L. (1994). Mouse very-low-density-lipoprotein receptor (VLDLR) cDNA cloning, tissue-specific expression and evolutionary relationship with the low-density-lipoprotein receptor. European Journal of Biochemistry *224*, 975-982.

Oliveira, M.A., Zhao, R., Lee, W.M., Kremer, M.J., Minor, I., Rueckert, R.R., Diana, G.D., Pevear, D.C., Dutko, F.J., McKinlay, M.A.*, et al.* (1993). The structure of human rhinovirus 16. Structure *1*, 51-68.

Olson, N.H., Kolatkar, P.R., Oliveira, M.A., Cheng, R.H., Greve, J.M., McClelland, A., Baker, T.S., and Rossmann, M.G. (1993). Structure of a human rhinovirus complexed with its receptor molecule. Proc Natl Acad Scie USA *90*, 507-511.

Pallansch, M.A., Kew, O.M., Palmenberg, A.C., Golini, F., Wimmer, E., and Rueckert, R.R. (1980). Picornaviral VPg sequences are contained in the replicase precursor. J Virol *35*, 414-419.

Palmenberg, A.C., Pallansch, M.A., and Rueckert, R.R. (1979). Protease required for processing picornaviral coat protein resides in the viral replicase gene. J Virol *32*, 770-778.

Palmenberg, A.C., and Rueckert, R.R. (1982). Evidence for intramolecular self-cleavage of picornaviral replicase precursors. J Virol *41*, 244-249.

Palmenberg, A.C., Spiro, D., Kuzmickas, R., Wang, S., Djikeng, A., Rathe, J.A., Fraser-Liggett, C.M., and Liggett, S.B. (2009). Sequencing and Analyses of All Known Human Rhinovirus Genomes Reveals Structure and Evolution. Science.

Papadopoulos, N.G., Bates, P.J., Bardin, P.G., Papi, A., Leir, S.H., Fraenkel, D.J., Meyer, J., Lackie, P.M., Sanderson, G., Holgate, S.T.*, et al.* (2000). Rhinoviruses infect the lower airways. Journal of Infectious Diseases *181*, 1875-1884.

Papadopoulos, N.G., Sanderson, G., Hunter, J., and Johnston, S.L. (1999). Rhinoviruses replicate effectively at lower airway temperatures. Journal of Medical Virology *58*, 100-104.

Parker, J.S., and Parrish, C.R. (2000). Cellular uptake and infection by canine parvovirus involves rapid dynamin-regulated clathrin-mediated endocytosis, followed by slower intracellular trafficking. J Virol *74*, 1919-1930.

Patick, A.K., Brothers, M.A., Maldonado, F., Binford, S., Maldonado, O., Fuhrman, S., Petersen, A., Smith, G.J., 3rd, Zalman, L.S., Burns-Naas, L.A.*, et al.* (2005). In vitro antiviral activity and single-dose pharmacokinetics in humans of a novel, orally bioavailable inhibitor of human rhinovirus 3C protease. Antimicrob Agents Chemother *49*, 2267-2275.

Patick, A.K., and Potts, K.E. (1998). Protease inhibitors as antiviral agents. Clinical Microbiology Reviews *11*, 614&.

Paul, A.V., van Boom, J.H., Filippov, D., and Wimmer, E. (1998). Protein-primed RNA synthesis by purified poliovirus RNA polymerase. Nature *393 (6682)*, 280-284.

Pelkmans, L. (2005). Secrets of caveolae- and lipid raft-mediated endocytosis revealed by mammalian viruses. Biochimica et biophysica acta *1746*, 295-304.

Pelkmans, L., and Helenius, A. (2003). Insider information: what viruses tell us about endocytosis. Curr Opin Cell Biol *15*, 414-422.

Pelkmans, L., Kartenbeck, J., and Helenius, A. (2001). Caveolar endocytosis of simian virus 40 reveals a new two-step vesicular-transport pathway to the ER. Nat Cell Biol *3*, 473-483.

Pelletier, J., and Sonenberg, N. (1988). Internal initiation of translation of eukaryotic mRNA directed by a sequence derived from poliovirus RNA. Nature *334*, 320-325.

Pestova, T.V., Shatsky, I.N., and Hellen, C.U. (1996). Functional dissection of eukaryotic initiation factor 4F: the 4A subunit and the central domain of the 4G subunit are sufficient to mediate internal entry of 43S preinitiation complexes. Mol Cell Biol *16*, 6870-6878.

Pettigrew, D.M., Williams, D.T., Kerrigan, D., Evans, D.J., Lea, S.M., and Bhella, D. (2006). Structural and functional insights into the interaction of echoviruses and decay-accelerating factor. J Biol Chem *281*, 5169-5177.

Pevear, D.C., Fancher, M.J., Felock, P.J., Rossmann, M.G., Miller, M.S., Diana, G., Treasurywala, A.M., McKinlay, M.A., and Dutko, F.J. (1989). Conformational change in the floor of the human rhinovirus canyon blocks adsorption to HeLa cell receptors. J Virol *63*, 2002-2007.

Phipps, K.M., Martinez, A., Lu, J., Heinz, B.A., and Zhao, G. (2004). Small interfering RNA molecules as potential anti-human rhinovirus agents: in vitro potency, specificity, and mechanism. Antiviral Res *61*, 49-55.

Pietiainen, V., Marjomaki, V., Upla, P., Pelkmans, L., Helenius, A., and Hyypia, T. (2004). Echovirus 1 endocytosis into caveosomes requires lipid rafts, dynamin II, and signaling events. Molecular biology of the cell *15*, 4911-4925.

Pilipenko, E.V., Poperechny, K.V., Maslova, S.V., Melchers, W.J., Slot, H.J., and Agol, V.I. (1996). Cis-element, oriR, involved in the initiation of (-) strand poliovirus RNA: a quasi-globular multi-domain RNA structure maintained by tertiary ('kissing') interactions. Embo J *15*, 5428-5436.

Pillay, C.S., Elliott, E., and Dennison, C. (2002). Endolysosomal proteolysis and its regulation. Biochem J *363*, 417-429.

Pitas, R.E., Innerarity, T.L., Arnold, K.S., and Mahley, R.W. (1979). Rate and equilibrium constants for binding of apo-E HDLc (a cholesterol-induced lipoprotein) and low density lipoproteins to human fibroblasts: evidence for multiple receptor binding of apo-E HDLc. Proc Natl Acad Sci U S A *76*, 2311-2315.

Pitkaranta, A., and Hayden, F.G. (1998). Rhinoviruses: important respiratory pathogens. Annals of Medicine *30*, 529-537.

Poritz, M.A., Malmstrom, S., Schmitt, A., Kim, M.K., Zharkikh, L., Kamb, A., and Teng, D.H. (2003). Isolation of a peptide inhibitor of human rhinovirus. Virology *313*, 170-183.

Prchla, E., Kuechler, E., Blaas, D., and Fuchs, R. (1994). Uncoating of human rhinovirus serotype 2 from late endosomes. Journal of Virology *68*, 3713-3723.

Prchla, E., Plank, C., Wagner, E., Blaas, D., and Fuchs, R. (1995). Virus-mediated release of endosomal content in vitro: Different behavior of adenovirus and rhinovirus serotype 2. The Journal of cell biology *131*, 111-123.

Querol-Audi, J., Konecsni, T., Pous, J., Carugo, O., Fita, I., Verdaguer, N., and Blaas, D. (2009). Minor group human rhinovirus-receptor interactions: geometry of multimodular attachment and basis of recognition. FEBS Lett *583*, 235-240.

Rall, S.C., Jr., Weisgraber, K.H., and Mahley, R.W. (1982). Human apolipoprotein E. The complete amino acid sequence. J Biol Chem *257*, 4171-4178.

Rao, A.G., Howard, O.M., Ng, S.C., Whitehead, A.S., Colten, H.R., and Sodetz, J.M. (1987). Complementary DNA and derived amino acid sequence of the alpha subunit of human complement protein C8: evidence for the existence of a separate alpha subunit messenger RNA. Biochemistry *26*, 3556-3564.

Rebel, J.M., Leendertse, C.H., Dekker, A., and Moormann, R.J. (2003). Effects of mutations in the VP2/VP4 cleavage site of Swine vesicular disease virus on RNA encapsidation and viral infectivity. Archives of virology *148*, 1747-1756.

Reithmayer, M., Reischl, A., Snyers, L., and Blaas, D. (2002). Species-specific receptor recognition by a minor-group human rhinovirus (HRV): HRV serotype 1A distinguishes between the murine and the human low-density lipoprotein receptor. J Virol *76*, 6957-6965.

Rombaut, B., Andries, K., and Boeye, A. (1991). A Comparison of WIN-51711 and R-78206 As Stabilizers of Poliovirus Virions and Procapsids. Journal of General Virology *72*, 2153-2157.

Ronacher, B., Marlovits, T.C., Moser, R., and Blaas, D. (2000). Expression and folding of human very-low-density lipoprotein receptor fragments: neutralization capacity toward human rhinovirus HRV2. Virology *278*, 541-550.

Rossmann, M.G. (1989a). The canyon hypothesis. Viral Immunol *2*, 143-161.

Rossmann, M.G. (1989b). The canyon hypothesis. Hiding the host cell receptor attachment site on a viral surface from immune surveillance. J Biol Chem *264*, 14587-14590.

Rossmann, M.G., Arnold, E., Erickson, J.W., Frankenberger, E.A., Griffith, J.P., Hecht, H.J., Johnson, J.E., Kamer, G., Luo, M., Mosser, A.G*., et al.* (1985). Structure of a human common cold virus and functional relationship to other picornaviruses. Nature *317*, 145-153.

Rossmann, M.G., Bella, J., Kolatkar, P.R., He, Y.N., Wimmer, E., Kuhn, R.J., and Baker, T.S. (2000). Cell recognition and entry by rhino- and enteroviruses. Virology *269*, 239-247.

Rossmann, M.G., He, Y., and Kuhn, R.J. (2002). Picornavirus-receptor interactions. Trends Microbiol *10*, 324-331.

Rossmann, M.G., Olson, N.H., Kolatkar, P.R., Oliveira, M.A., Cheng, R.H., Greve, J.M., McClelland, A., and Baker, T.S. (1994). Crystallographic and cryo EM analysis of virion-receptor interactions. Arch Virol Suppl *9*, 531-541.

Rotbart, H.A. (2002). Treatment of picornavirus infections. Antiviral Res *53*, 83-98.

Rudenko, G., and Deisenhofer, J. (2003). The low-density lipoprotein receptor: ligands, debates and lore. Curr Opin Struct Biol *13*, 683-689.

Rudenko, G., Henry, L., Henderson, K., Ichtchenko, K., Brown, M.S., Goldstein, J.L., and Deisenhofer, J. (2002). Structure of the LDL receptor extracellular domain at endosomal pH. Science *298*, 2353-2358.

Rueckert, R.R. (1996). Picornaviridae: The Viruses and Their Replication. In Fields Virology, B.N. Fields, D.M. Kipe, and P.M. Howley, eds. (Philadelphia, Lippincott - Raven Publishers), pp. 609-654.

Russell, D.W., Brown, M.S., and Goldstein, J.L. (1989). Different combinations of cysteine-rich repeats mediate binding of low density lipoprotein receptor to two different proteins. J Biol Chem *264*, 21682-21688.

Russell, D.W., Schneider, W.J., Yamamoto, T., Luskey, K.L., Brown, M.S., and Goldstein, J.L. (1984). Domain map of the LDL receptor: sequence homology with the epidermal growth factor precursor. Cell *37*, 577-585.

Rust, R.C., Landmann, L., Gosert, R., Tang, B.L., Hong, W., Hauri, H.P., Egger, D., and Bienz, K. (2001). Cellular COPII proteins are involved in production of the vesicles that form the poliovirus replication complex. J Virol *75*, 9808-9818.

Saha, S., Boyd, J., Werner, J.M., Knott, V., Handford, P.A., Campbell, I.D., and Downing, A.K. (2001). Solution structure of the LDL receptor EGF-AB pair: a paradigm for the assembly of tandem calcium binding EGF domains. Structure *9*, 451-456.

Saito, A., Pietromonaco, S., Loo, A.K.C., and Farquhar, M.G. (1994). Complete cloning and sequencing of rat gp330/"megalin," a distinctive member of the low density lipoprotein receptor gene family. Proceedings of the National Academy of Sciences of the United States of America *91*, 9725-9729.

Saito, M., Hanson, P.I., and Schlesinger, P. (2007). Luminal chloride-dependent activation of endosome calcium channels: patch clamp study of enlarged endosomes. J Biol Chem *282*, 27327-27333.

Sakai, J., Hoshino, A., Takahashi, S., Miura, Y., Ishii, H., Suzuki, H., Kawarabayasi, Y., and Yamamoto, T. (1994). Structure, chromosome location, and expression of the human very low density lipoprotein receptor gene. J Biol Chem *269*, 2173-2182.

Samo, T.C., Greenberg, S.B., Couch, R.B., Quarles, J., Johnson, P.E., Hook, S., and Harmon, M.W. (1983). Efficacy and tolerance of intranasally applied recombinant leukocyte A interferon in normal volunteers. J Infect Dis *148*, 535-542.

Samuel, C.E. (2001). Antiviral actions of interferons. Clin Microbiol Rev *14*, 778-809, table of contents.

Sarafanov, A.G., Ananyeva, N.M., Shima, M., and Saenko, E.L. (2001). Cell surface heparan sulfate proteoglycans participate in factor VIII catabolism mediated by low density lipoprotein receptor-related protein. J Biol Chem *276*, 11970-11979.

Sass, C., Giroux, L.M., Lussiercacan, S., Davignon, J., and Minnich, A. (1995). Unexpected consequences of deletion of the first two repeats of the ligand-binding domain from the low density lipoprotein receptor - Evidence from a human mutation. J Biol Chem *270*, 25166-25171.

Savolainen, C., Blomqvist, S., Mulders, M.N., and Hovi, T. (2002). Genetic clustering of all 102 human rhinovirus prototype strains: serotype 87 is close to human enterovirus 70. J Gen Virol *83*, 333-340.

Savonen, R., Obermoeller, L.M., Trausch-Azar, J.S., Schwartz, A.L., and Bu, G. (1999). The carboxyl-terminal domain of receptor-associated protein facilitates proper folding and trafficking of the very low density lipoprotein receptor by interaction with the three amino-terminal ligand-binding repeats of the receptor. J Biol Chem *274*, 25877-25882.

Schneider, W.J., and Nimpf, J. (2003). LDL receptor relatives at the crossroad of endocytosis and signaling. Cell Mol Life Sci *60*, 892-903.

Schober, D., Kronenberger, P., Prchla, E., Blaas, D., and Fuchs, R. (1998). Major and minor-receptor group human rhinoviruses penetrate from endosomes by different mechanisms. J Virol *72*, 1354-1364.

Schroth, M.K., Grimm, E., Frindt, P., Galagan, D.M., Konno, S., Love, R., and Gern, J.E. (1999). Rhinovirus replication causes RANTES production in primary bronchial epithelial cells. American Journal of Respiratory Cell and Molecular Biology *20*, 1220-1228.

Scraba, D.G., and Palmenberg, A.C. (1999). Cardioviruses (Picornaviridae). Encyclopedia of Virology, 2nd edition, RG Webseter and A Granoff Eds *Academic Press, London*.

Segrest, J.P., Jones, M.K., De Loof, H., and Dashti, N. (2001). Structure of apolipoprotein B-100 in low density lipoproteins. J Lipid Res *42*, 1346-1367.

Seipelt, J., Liebig, H.D., Sommergruber, W., Gerner, C., and Kuechler, E. (2000). 2A proteinase of human rhinovirus cleaves cytokeratin 8 in infected HeLa cells. J Biol Chem *275*, 20084-20089.

Semler, B., Hanecak, R., Anderson, C.W., and Wimmer, E. (1981a). Cleavage sites in the polypeptide precursors of poliovirus protein P2-X. Virology *114*, 598-594.

Semler, B.L., Anderson, C. W., Kitamura, N., Rothberg, P. G., Wishart, W. L. and Wimmer, E. (1981b). Poliovirus replication proteins: RNA sequence encoding P3-1b and the sites of proteolytic processing. Proc Natl Acad Sci USA *78*, 3464-3468.

Semler, B.L., and Wimmer, E. (2002). Molecular Biology of Picornaviruses (Washington, DC 20036-2904, ASM Press).

Shafren, D.R., Bates, R.C., Agrez, M.V., Herd, R.L., Burns, G.F., and Barry, R.D. (1995). Coxsackieviruses B1, B3, and B5 use decay accelerating factor as a receptor for cell attachment. J Virol *69*, 3873-3877.

Shafren, D.R., Dorahy, D.J., Greive, S.J., Burns, G.F., and Barry, R.D. (1997a). Mouse cells expressing human intercellular adhesion molecule-1 are susceptible to infection by coxsackievirus A21. J Virol *71*, 785-789.

Shafren, D.R., Williams, D.T., and Barry, R.D. (1997b). A decay accelerating factor binding strain of coxsackievirus B3 requires the coxsackievirus adenovirus receptor protein to mediate lytic infection of rhabdomyosarcoma cells. Journal Of Virology *71*, 9844-9848.

Shieh, J.T., and Bergelson, J.M. (2002). Interaction with decay-accelerating factor facilitates coxsackievirus B infection of polarized epithelial cells. J Virol *76*, 9474-9480.

Sieczkarski, S.B., and Whittaker, G.R. (2002). Dissecting virus entry via endocytosis. J Gen Virol *83*, 1535-1545.

Simmons, D., Makgoba, M.W., and Seed, B. (1988). ICAM, an adhesion ligand of LFA-1, is homologous to the neural cell adhesion molecule NCAM. Nature *331*, 624-627.

Simonsen, A.C.W., Heegaard, C.W., Rasmussen, L.K., Ellgaard, L., Kjoller, L., Christensen, A., Etzerodt, M., and Andreasen, P.A. (1994). Very low density lipoprotein receptor from mammary gland and mammary epithelial cell lines binds and mediates endocytosis of M(r) 40,000 receptor associated protein. FEBS Letters *354*, 279-283.

Skern, T., Neubauer, C., Frasel, L., Gruendler, P., Sommergruber, W., Zorn, W., Kuechler, E., and Blaas, D. (1987). A neutralizing epitope on human rhinovirus type 2 includes amino acid residues between 153 and 164 of virus capsid protein VP2. J Gen Virol *68*, 315-323.

Smith, T.J., Chase, E.S., Schmidt, T.J., Olson, N.H., and Baker, T.S. (1996). Neutralizing antibody to human rhinovirus 14 penetrates the receptor-binding canyon. Nature *383*, 350-354.

Smith, T.J., Kremer, M.J., Luo, M., Vriend, G., Arnold, E., Kamer, G., Rossman, M.G., McKinlay, M.A., Diana, G.D., and Otto, M.J. (1986). The site of attachment in human rhinovirus 14 for antiviral agents that inhibit uncoating. Science *233*, 1286-1293.

Smyth, M., Pettitt, T., Symonds, A., and Martin, J. (2003). Identification of the pocket factors in a picornavirus. Archives of virology *148*, 1225-1233.

Snyers, L., Zwickl, H., and Blaas, D. (2003). Human rhinovirus type 2 is internalized by clathrin-mediated endocytosis. J Virol *77*, 5360-5369.

Sommergruber, W., Zorn, M., Blaas, D., Fessl, F., Volkmann, P., Maurer Fogy, I., Pallai, P., Merluzzi, V., Matteo, M., Skern, T.*, et al.* (1989). Polypeptide 2A of human rhinovirus type 2: identification as a protease and characterization by mutational analysis. Virology *169*, 68-77.

Springer, T.A. (1998). An extracellular beta-propeller module predicted in lipoprotein and scavenger receptors, tyrosine kinases, epidermal growth factor precursor, and extracellular matrix components. J Mol Biol *283*, 837-862.

Stanley, K.K., Kocher, H.P., Luzio, J.P., Jackson, P., and Tschopp, J. (1985). The sequence and topology of human complement component C9. Embo J *4*, 375-382.

Stanway, G. (1990). Structure, Function and Evolution of Picornaviruses. Journal of General Virology *71*, 2483-2501.

Stanway, G., and Hyypia, T. (1999). Parechoviruses. Journal of Virology *73*, 5249-5254.

Stanway, G., Joki-Korpela, P., and Hyypia, T. (2000). Human parechoviruses--biology and clinical significance. Reviews in medical virology *10*, 57-69.

Staunton, D.E., Gaur, A., Chan, P.Y., and Springer, T.A. (1992). Internalization of a major group human rhinovirus does not require cytoplasmic or transmembrane domains of ICAM-1. J Immunol *148*, 3271-3274.

Staunton, D.E., Merluzzi, V.J., Rothlein, R., Barton, R., Marlin, S.D., and Springer, T.A. (1989). A cell adhesion molecule, ICAM-1, is the major surface receptor for rhinoviruses. Cell *56*, 849-853.

Strickland, D.K., Ashcom, J.D., Williams, S., Burgess, W.H., Migliorini, M., and Argraves, W.S. (1990). Sequence identity between the alpha 2-macroglobulin receptor and low density lipoprotein receptor-related protein suggests that this molecule is a multifunctional receptor. J Biol Chem *265*, 17401-17404.

Strickland, D.K., Kounnas, M.Z., Williams, S.E., and Argraves, W.S. (1994). LDL receptor-related protein (LRP): A multiligand receptor. Fibrinolysis *8*, 204-215.

Strittmatter, W.J., Saunders, A.M., Schmechel, D., Pericak-Vance, M., Enghild, J., Salvesen, G.S., and Roses, A.D. (1993). Apolipoprotein E: high-avidity binding to beta-amyloid and increased frequency of type 4 allele in late-onset familial Alzheimer disease. Proc Natl Acad Sci U S A *90*, 1977-1981.

Stuart, A.D., Eustace, H.E., McKee, T.A., and Brown, T.D. (2002). A novel cell entry pathway for a DAF-using human enterovirus is dependent on lipid rafts. J Virol *76*, 9307-9322.

Subauste, M.C., Jacoby, D.B., Richards, S.M., and Proud, D. (1995). Infection of a human respiratory epithelial cell line with rhinovirus - Induction of cytokine release and modulation of susceptibility to infection by cytokine exposure. J Clin Invest *96*, 549-557.

Sudhof-TC, Russell-DW, Goldstein-JL, Brown-MS, Sanchez-Pescador-R, and Bell-GI (1985). Cassette of eight exons shared by genes for LDL receptor and EGF precursor. Science *288*, 893-895.

Sudhof, T.C., Goldstein, J.L., Brown, M.S., and Russell, D.W. (1985). The LDL receptor gene: a mosaic of exons shared with different proteins. Science *228*, 815-822.

Suhy, D.A., Giddings, T.H., and Kirkegaard, K. (2000). Remodeling the endoplasmic reticulum by poliovirus infection and by individual viral proteins: an autophagy-like origin for virus-induced vesicles. Journal of Virology *74*, 8953-8965.

Takahashi, S., Oida, K., Ookubo, M., Suzuki, J., Kohno, M., Murase, T., Yamamoto, T., and Nakai, T. (1996). Very low density lipoprotein receptor binds apolipoprotein E2/2 as well as apolipoprotein E3/3. FEBS Lett *386*, 197-200.

Takahashi, S., Suzuki, J., Kohno, M., Oida, K., Tamai, T., Miyabo, S., Yamamoto, T., and Nakai, T. (1995). Enhancement of the binding of triglyceride-rich lipoproteins to the very low density lipoprotein receptor by apolipoprotein E and lipoprotein lipase. Journal of Biological Chemistry *270*, 15747-15754.

Tan, F.L., and Yin, J.Q. (2004). RNAi, a new therapeutic strategy against viral infection. Cell Res *14*, 460-466.

Terajima, M., Yamaya, M., Sekizawa, K., Okinaga, S., Suzuki, T., Yamada, N., Nakayama, K., Ohrui, T., Oshima, T., Numazaki, Y.*, et al.* (1997). Rhinovirus infection of primary cultures of human tracheal epithelium: role of ICAM-1 and IL-1beta. The American journal of physiology *273*, L749-759.

Teterina, N.L., Egger, D., Bienz, K., Brown, D.M., Semler, B.L., and Ehrenfeld, E. (2001). Requirements for Assembly of Poliovirus Replication Complexes and Negative-Strand RNA Synthesis. J Virol *75*, 3841-3850.

Tidona, C.A., and Darai, G. (2002). The Springer Index of Viruses. Springer-Verlag, Berlin, Heidelberg.

Tjelle, T.E., Brech, A., Juvet, L.K., Griffiths, G., and Berg, T. (1996). Isolation and characterization of early endosomes, late endosomes and terminal lysosomes: their role in protein degradation. J Cell Sci *109 (Pt 12)*, 2905-2914.

Tolleshaug, H., Goldstein, J.L., Schneider, W.J., and Brown, M.S. (1982). Posttranslational processing of the LDL receptor and its genetic disruption in familial hypercholesterolemia. Cell *30*, 715-724.

Tolleshaug, H., Hobgood, K.K., Brown, M.S., and Goldstein, J.L. (1983). The LDL receptor locus in familial hypercholesterolemia: multiple mutations disrupt transport and processing of a membrane receptor. Cell *32*, 941-951.

Tomassini, E., Graham, T., DeWitt, C., Lineberger, D., Rodkey, J., and Colonno, R. (1989). cDNA cloning reveals that the major group rhinovirus receptor on HeLa cells is intercellular adhesion molecule 1. Proc Natl Acad Sci USA *86*, 4907-4911.

Tosteson, M.T., Wang, H., Naumov, A., and Chow, M. (2004). Poliovirus binding to its receptor in lipid bilayers results in particle-specific, temperature-sensitive channels. J Gen Virol *85*, 1581-1589.

Towner, J.S., Ho, T.V., and Semler, B.L. (1996). Determinants of membrane association for poliovirus protein RAB. J Biol Chem *271*, 26810-26818.

Toyoda, H., Nicklin, M.J.H., Murray, M.G., Anderson, C.W., Dunn, J.J., Studier, F.W., and Wimmer, E. (1986). A second virus-encoded proteinase involved in proteolytic processing of poliovirus polyprotein. Cell *45*, 761-770.

Triantafilou, K., and Triantafilou, M. (2004). Lipid-raft-dependent Coxsackievirus B4 internalization and rapid targeting to the Golgi. Virology *326*, 6-19.

Trommsdorff, M., Gotthardt, M., Hiesberger, T., Shelton, J., Stockinger, W., Nimpf, J., Hammer, R.E., Richardson, J.A., and Herz, J. (1999). Reeler/Disabled-like disruption of neuronal migration in knockout mice lacking the VLDL receptor and ApoE receptor 2. Cell *97*, 689-701.

Turner, R.B. (1997). Epidemiology, Pathogenesis, and Treatment Of the Common Cold. Annals Of Allergy Asthma and Immunology *78 (6)*, 531-539.

Turner, R.B. (2001). The treatment of rhinovirus infections: progress and potential. Antiviral Res *49*, 1-14.

Turner, R.B., Dutko, F.J., Goldstein, N.H., Lockwood, G., and Hayden, F.G. (1993). Efficacy of oral WIN 54954 for prophylaxis of experimental rhinovirus infection. Antimicrob Agents Chemother *37*, 297-300.

Turner, R.B., Wecker, M.T., Pohl, G., Witek, T.J., McNally, E., St George, R., Winther, B., and Hayden, F.G. (1999). Efficacy of tremacamra, a soluble intercellular adhesion molecule 1, for experimental rhinovirus infection - A randomized clinical trial. Jama Journal of the American Medical Association *281*, 1797-1804.

Tuthill, T.J., Harlos, K., Walter, T.S., Knowles, N.J., Groppelli, E., Rowlands, D.J., Stuart, D.I., and Fry, E.E. (2009). Equine rhinitis A virus and its low pH empty particle: clues towards an aphthovirus entry mechanism? PLoS pathogens *5*, e1000620.

Tyrrell, D.A.J., and Chanock, R.M. (1963). Rhinoviruses: A Description. Science *141*, 152-153.

Tyrrell, D.A.J., and Parsons, R. (1960). Some virus isolations from common colds: III. cytopathic effects in tissue culture. Lancet *Jan. 30*, 239-242.

Uncapher, C.R., Dewitt, C.M., and Colonno, R.J. (1991). The major and minor group receptor families contain all but one human rhinovirus serotype. Virology *180*, 814-817.

van de Stolpe, A., and van der Saag, P.T. (1996). Intercellular adhesion molecule-1. J Mol Med *74*, 13-33.

van Driel, I.R., Brown, M.S., and Goldstein, J.L. (1989). Stoichiometric binding of low density lipoprotein (LDL) and monoclonal antibodies to LDL receptors in a solid phase assay. J Biol Chem *264*, 9533-9538.

van Dyke, T.A., Rickles, J.R., and Flanegan, J.B. (1982). Genome-length copies of poliovirion RNA are synthesized in vitro by the poliovirus RNA-dependent RNA polymerase. J Biol Chem *257*, 4610-4617.

Varret, M., Rabes, J.P., Thiart, R., Kotze, M.J., Baron, H., Cenarro, A., Descamps, O., Ebhardt, M., Hondelijn, J.C., Kostner, G.M.*, et al.* (1998). LDLR Database (second edition): new additions to the database and the software, and results of the first molecular analysis. Nucleic Acids Research *26 (1)*, 248-252.

Verdaguer, N., Blaas, D., and Fita, I. (2000). Structure of human rhinovirus serotype 2 (HRV2). Journal of Molecular Biology *300*, 1179-1194.

Verdaguer, N., Fita, I., Reithmayer, M., Moser, R., and Blaas, D. (2004). X-ray structure of a minor group human rhinovirus bound to a fragment of its cellular receptor protein. Nature Struct Mol Biol *11*, 429-434.

Verlinden, Y., Cuconati, A., Wimmer, E., and Rombaut, B. (2000). Cell-free synthesis of poliovirus: 14S subunits are the key intermediates in the encapsidation of poliovirus RNA. J Gen Virol *81 Pt 11*, 2751-2754.

Villeger, L., Abifadel, M., Allard, D., Rabes, J.P., Thiart, R., Kotze, M.J., Beroud, C., Junien, C., Boileau, C., and Varret, M. (2002). The UMD-LDLR database: additions to the software and 490 new entries to the database. Hum Mutat *20*, 81-87.

Vlasak, M., Blomqvist, S., Hovi, T., Hewat, E., and Blaas, D. (2003). Sequence and structure of human rhinoviruses reveal the basis of receptor discrimination. J Virol *77*, 6923-6930.

Vlasak, M., Goesler, I., and Blaas, D. (2005a). Human rhinovirus type 89 variants use heparan sulfate proteoglycan for cell attachment. J Virol *79*, 5963-5970.

Vlasak, M., Roivainen, M., Reithmayer, M., Goesler, I., Laine, P., Snyers, L., Hovi, T., and Blaas, D. (2005b). The minor receptor group of human rhinovirus (HRV) includes HRV23 and HRV25, but the presence of a lysine in the VP1 HI loop Is not sufficient for receptor binding. J Virol *79*, 7389-7395.

Wanga, Q.M., and Chen, S.H. (2007). Human rhinovirus 3C protease as a potential target for the development of antiviral agents. Curr Protein Pept Sci *8*, 19-27.

Ward, C.D., Stokes, M.A., and Flanegan, J.B. (1988). Direct measurement of the poliovirus RNA polymerase error frequency in vitro. J Virol *62*, 558-562.

Weisgraber, K.H., Innerarity, T.L., and Mahley, R.W. (1978). Role of lysine residues of plasma lipoproteins in high affinity binding to cell surface receptors on human fibroblasts. J Biol Chem *253*, 9053-9062.

Weisgraber, K.H., Innerarity, T.L., and Mahley, R.W. (1982). Abnormal lipoprotein receptor-binding activity of the human E apoprotein due to cysteine-arginine interchange at a single site. J Biol Chem *257*, 2518-2521.

Weisgraber, K.H., Roses, A.D., and Strittmatter, W.J. (1994). The role of apolipoprotein E in the nervous system. Curr Opin Lipidol *5*, 110-116.

Wetterau, J.R., Aggerbeck, L.P., Rall, S.C., Jr., and Weisgraber, K.H. (1988). Human apolipoprotein E3 in aqueous solution. I. Evidence for two structural domains. J Biol Chem *263*, 6240-6248.

Wetz, K., and Kucinski, T. (1991). Influence of different ionic and pH environments on structural alterations of poliovirus and their possible relation to virus uncoating. Journal of General Virology *72*, 2541-2544.

Whiteman, S.C., Bianco, A., Knight, R.A., and Spiteri, M.A. (2003). Human Rhinovirus Selectively Modulates Membranous and Soluble Forms of Its Intercellular Adhesion Molecule-1 (ICAM-1) Receptor to Promote Epithelial Cell Infectivity. J Biol Chem *278*, 11954-11961.

Whitton, J.L., Cornell, C.T., and Feuer, R. (2005). Host and virus determinants of picornavirus pathogenesis and tropism. Nat Rev Microbiol *3*, 765-776.

Willnow, T.E. (1998). Receptor-associated protein (RAP): A specialized chaperone for endocytic receptors. Biological Chemistry *379*, 1025-1031.

Willnow, T.E., Goldstein, J.L., Orth, K., Brown, M.S., and Herz, J. (1992). Low density lipoprotein receptor-related protein and gp330 bind similar ligands, including plasminogen activator-inhibitor complexes and lactoferrin, an inhibitor of chylomicron remnant clearance. Journal of Biological Chemistry *267*, 26172-26180.

Willnow, T.E., and Herz, J. (1994). Genetic deficiency in low density lipoprotein receptor-related protein confers cellular resistance to Pseudomonas exotoxin A. Evidence that this protein is required for uptake and degradation of multiple ligands. J Cell Sci *107*, 719-726.

Willnow, T.E., Rohlmann, A., Horton, J., Otani, H., and Herz, J. (1996). RAP, a specialized chaperone, prevents ligand-induced ER retention and degradation of LDL receptor-related endocytic receptors. EMBO J *15*, 2632 - 2639.

Wilson, C., Wardell, M.R., Weisgraber, K.H., Mahley, R.W., and Agard, D.A. (1991). Three-dimensional structure of the LDL receptor-binding domain of human apolipoprotein E. Science *252*, 1817-1822.

Wilson, D.J., Gahan, M., Haddad, L., Heath, K., Whittall, R.A., Williams, R.R., Humphries, S.E., and Day, I.N. (1998). A World Wide Web site for low-density lipoprotein receptor gene mutations in familial hypercholesterolemia: sequence-based, tabular, and direct submission data handling. Am J Cardiol *81*, 1509-1511.

Wimmer, E. (1982). Genome-linked proteins of viruses. Cell *28*, 199-201.

Winther, B. (1994). Effects on the Nasal Mucosa of Upper Respiratory Viruses (Common Cold). Danish Medical Bulletin *41*, 193-204.

Xiao, C., Bator, C.M., Bowman, V.D., Rieder, E., He, Y., Hebert, B., Bella, J., Baker, T.S., Wimmer, E., Kuhn, R.J.*, et al.* (2001). Interaction of Coxsackievirus A21 with Its Cellular Receptor, ICAM-1. J Virol *75*, 2444-2451.

Xing, L., Casasnovas, J.M., and Cheng, R.H. (2003). Structural analysis of human rhinovirus complexed with icam-1 reveals the dynamics of receptor-mediated virus uncoating. J Virol *77*, 6101-6107.

Xing, L., Tjarnlund, K., Lindqvist, B., Kaplan, G.G., Feigelstock, D., Cheng, R.H., and Casasnovas, J.M. (2000). Distinct cellular receptor interactions in poliovirus and rhinoviruses. Embo J *19*, 1207-1216.

Yamamoto, T., Davis, C.G., Brown, M.S., Schneider, W.J., Casey, M.L., Goldstein, J.L., and Russell, D.W. (1984). The human LDL receptor: a cysteine-rich protein with multiple Alu sequences in its mRNA. Cell *39*, 27-38.

Yamashita, T., Sakae, K., Kobayashi, S., Ishihara, Y., Miyake, T., Mubina, A., and Isomura, S. (1995). Isolation of cytopathic small round virus (Aichi virus) from Pakistani children and Japanese travelers from Southeast Asia. Microbiol Immunol *39*, 433-435.

Yin, F.H., and Lomax, N.B. (1983). Host range mutants of human rhinovirus in which nonstructural proteins are altered. J Virol *48*, 410-418.

Zautner, A.E., Korner, U., Henke, A., Badorff, C., and Schmidtke, M. (2003). Heparan sulfates and coxsackievirus-adenovirus receptor: each one mediates coxsackievirus B3 PD infection. J Virol *77*, 10071-10077.

Zhao, R., Hadfield, A.T., Kremer, M.J., and Rossmann, M.G. (1997). Cations in human rhinoviruses. Virology *227*, 13-23.

Zhao, R., Pevear, D.C., Kremer, M.J., Giranda, V.L., Kofron, J.A., Kuhn, R.J., and Rossmann, M.G. (1996). Human rhinovirus 3 at 3.0 angstrom resolution. Structure *4*, 1205-1220.

Zhao, Z., and Michaely, P. (2008). The epidermal growth factor homology domain of the LDL receptor drives lipoprotein release through an allosteric mechanism involving H190, H562, and H586. J Biol Chem *283*, 26528-26537.

Zhu, Z., Tang, W., Ray, A., Wu, Y., Einarsson, O., Landry, M.L., Gwaltney, J., Jr., and Elias, J.A. (1996). Rhinovirus stimulation of interleukin-6 in vivo and in vitro. Evidence for nuclear factor kappa B-dependent transcriptional activation. J Clin Invest *97*, 421-430.

Zhu, Z., Tang, W.L., Gwaltney, J.M., Wu, Y., and Elias, J.A. (1997). Rhinovirus Stimulation Of Interleukin 8 In Vivo and In Vitro: Role Of Nf Kappa B. American Journal Of Physiology Lung Cellular and Molecular Physiology *17 (4)*, L814-L824.

Zubay, G. (1998). Biochemistry. Biochemistry 4th edition.

7.4. Curriculum vitae

Personal data:

Name:	**Konecsni, Tünde**
Date of birth:	22.09.1977
Address:	36/1/22 Schlachthausgasse, 1030, Vienna, Austria
Telephone:	0650 / 6410237
E-mail:	tuende.konecsni@univie.ac.at
Nationality:	Hungarian

Education:

10.2004 -

PhD-student in Molecular Biology (Vienna Biocenter International PhD Program)

Max F. Perutz Laboratories, University Departments of the Vienna Biocenter, Vienna, Austria

Human rhinovirus-receptor interactions and viral uncoating:

- Mutagenesis, cloning and expression of recombinant VLDL-minireceptors

- Role of the β-propeller module of LDL-receptor in human rhinovirus infection (Prof.Dr.D. Blaas)

10.2001 - 10.2004

PhD-student in Analytical Chemistry

Institute of Bioanalysis, University of Pécs, Hungary

Applications of capillary electrophoresis in bioanalytical aspects *(Prof.Dr.F. Kilár)*

1996-2002

MSc in Biology, BSc in Chemistry, Teacher

University of Pécs, Faculty of Life Sciences, Pécs, Hungary

International research scholarships:

04.2004 - 07.2004 AKTION ÖSTERREICH-UNGARN

02-04, 08-10. 2003 CEEPUS

University of Vienna, Institute of Analytcal Chemistry

Capillary electrophoresis of virus-receptor complexes *(Prof. Dr. E. Kenndler)*

03.2001- 05. 2001 ERASMUS

Karl Franzens-University Graz, Institute of Pharmaceutical Chemistry

Reverse phase HPLC of drugs *(Prof. Dr. G. Gübitz)*

Personal skills: English (fluent), German (good), teaching and supervising experience

7.5. Publications

Konecsni, T., Berka, U., Pickl-Herk, A., Bilek, G., Khan, A.G., Gajdzig, L., Fuchs, R., and Blaas, D. (2009). Low pH-triggered beta-propeller switch of the low-density lipoprotein receptor assists rhinovirus infection. J Virol *83*, 10922-10930.

Querol-Audi, J., **Konecsni, T.**, Pous, J., Carugo, O., Fita, I., Verdaguer, N., and Blaas, D. (2009). Minor group human rhinovirus-receptor interactions: geometry of multimodular attachment and basis of recognition. FEBS Lett *583*, 235-240.

Nicodemou, A., Petsch, M., **Konecsni, T.**, Kremser, L., Kenndler, E., Casasnovas, J. M., and Blaas, D. (2005). Rhinovirus-stabilizing activity of artificial VLDL-receptor variants defines a new mechanism for virus neutralization by soluble receptors. FEBS Lett *579*, 5507-5511.

Kremser, L., **Konecsni, T.**, Blaas, D., and Kenndler, E. (2004). Fluorescence labeling of human rhinovirus capsid and analysis by capillary electrophoresis. Anal Chem *76*, 4175-4181.

Konecsni, T., Kremser, L., Snyers, L., Rankl, C., Kilar, F., Kenndler, E., and Blaas, D. (2004). Twelve receptor molecules attach per viral particle of human rhinovirus serotype 2 via multiple modules. FEBS Lett *568*, 99-104.

Konecsni, T., and Kilar, F. (2004). Monitoring of the conjugation reaction between human serum transferrin and fluorescein isothiocyanate by capillary electrophoresis. J Chromatogr A *1051*, 135-139.

Visegrady, B., **Konecsni, T**., Grobuschek, N., Schmid, M. G., Kilar, F., Aboul-Enein, H. Y., and Gubitz, G. (2002). Chiral separation of thiazide diuretics by HPLC on Chiralcel OD-RH, Chiralcel OJ-R and Chirobiotic-T phases. J Biochem Biophys Methods *53*, 15-24.

JOURNAL OF VIROLOGY, Nov. 2009, p. 10922–10930 Vol. 83, No. 21
0022-538X/09/$12.00 doi:10.1128/JVI.01312-09

Low pH-Triggered Beta-Propeller Switch of the Low-Density Lipoprotein Receptor Assists Rhinovirus Infection▽

Tuende Konecsni,[1] Ursula Berka,[2] Angela Pickl-Herk,[1] Gerhard Bilek,[1] Abdul Ghafoor Khan,[1] Leszek Gajdzig,[2] Renate Fuchs,[2] and Dieter Blaas[1]*

Max F. Perutz Laboratories, University Departments at the Vienna Biocenter, Department of Medical Biochemistry, Medical University of Vienna, Vienna, Austria,[1] and Department of Pathophysiology, Medical University of Vienna, Vienna, Austria[2]

Received 26 June 2009/Accepted 5 August 2009

Minor group human rhinoviruses (HRVs) bind three members of the low-density lipoprotein receptor (LDLR) family: LDLR proper, very-LDLR (VLDLR) and LDLR-related protein (LRP). Whereas ICAM-1, the receptor of major group HRVs actively contributes to viral uncoating, LDLRs are rather considered passive vehicles for cargo delivery to the low-pH environment of endosomes. Since the Tyr-Trp-Thr-Asp β-propeller domain of LDLR has been shown to be involved in the dissociation of bound LDL via intramolecular competition at low pH, we studied whether it also plays a role in HRV infection. Human cell lines deficient in LDLR family proteins are not available. Therefore, we used CHO-*ldla7* cells that lack endogenous LDLR. These were stably transfected to express either wild-type (wt) human LDLR or a mutant with a deletion of the β-propeller. When HRV2 was attached to the propeller-negative LDLR, a lower pH was required for conversion to subviral particles than when attached to wt LDLR. This indicates that high-avidity receptor binding maintains the virus in its native conformation. HRV2 internalization directed the mutant LDLR but not wt LDLR to lysosomes, resulting in reduced plasma membrane expression of propeller-negative LDLR. Infection assays using a CHO-adapted HRV2 variant showed a delay in intracellular viral conversion and de novo viral synthesis in cells expressing the truncated LDLR. Our data indicate that the β-propeller attenuates the virus-stabilizing effect of LDLR binding and thereby facilitates RNA release from endosomes, resulting in the enhancement of infection. This is a nice example of a virus exploiting high-avidity multimodule receptor binding with an intrinsic release mechanism.

Human rhinoviruses (HRVs), members of the picornavirus family of nonenveloped, single-stranded positive-sense RNA viruses, are the major cause of the common cold. Based on phylogeny, they are divided into two species, HRV-A and HRV-B. For cell entry, HRVs use two different types of receptors; 87 major group viruses bind human intercellular adhesion molecule 1 (ICAM-1) (44), while 12 types (the minor group) attach to members of the low-density lipoprotein receptor (LDLR) family, including LDLR, very-LDLR (VLDLR), and LDLR-related protein (LRP) (46). All minor group HRVs are HRV-A, but major group HRVs belong to either species. Recently, a new clade tentatively termed HRV-C was identified (23), but its properties with respect to receptor binding and entry have not been elucidated.

The minor group virus HRV2 enters via clathrin-dependent endocytosis (41). This is not unexpected since LDLRs possess a clathrin localization signal in their C-terminal cytoplasmic domains. However, when the clathrin-dependent pathway is blocked, similar to physiologic ligands, HRV2 might also exploit other endocytosis routes (3). After cell entry, HRVs of both receptor groups end up in endosomal compartments. For major group HRVs either ICAM-1 alone or in concert with the low-pH environment triggers conversion into subviral particles; concomitantly, the virion is uncoated, and the genomic RNA is released (33). In contrast, structural changes and infection of the minor group viruses exclusively depend on the low endosomal pH, and it was believed that the function of LDLRs was limited to virus delivery (8).

Exposure to pH ≤3 inactivates all HRVs, and this property was originally used as a means for their classification (43). However, most HRVs already convert into subviral particles and thereby lose infectivity at much higher pH values. For example, HRV2 readily experiences conformational modifications below a threshold pH of 5.6 in vitro and in vivo (16, 34), and inactivation occurs within a range of ~0.6 pH units according to a sigmoid progression. On the other hand, some major group viruses were found to be more stable (20).

During infection, native virus is first converted into subviral A-particles that still contain RNA but have lost the innermost capsid protein VP4. They no longer attach to their respective receptors but are hydrophobic because of externalization of the amphipathic N termini of VP1 that are believed to insert into the lipid bilayer of the endosomal membrane (28). In a next step, the RNA is transferred into the cytosol, leaving behind empty hydrophilic subviral B particles. These processes are strongly coordinated, as indicated by the in vitro membrane-disrupting activity of VP4 (11). VP4 appears to also play an essential role in RNA transfer. Furthermore, when VP0 is not cleaved into VP2 and VP4 during viral maturation, the virions bind to their receptors and undergo all structural tran-

* Corresponding author. Mailing address: Max F. Perutz Laboratories, University Departments at the Vienna Biocenter, Department of Medical Biochemistry, Medical University of Vienna, Dr. Bohr Gasse 9/3, A-1030 Vienna, Austria. Phone: 43 1 4277 61630. Fax: 43 1 4277 9616. E-mail: dieter.blaas@meduniwien.ac.at.

▽ Published ahead of print on 12 August 2009.

sitions but fail to initiate infection most probably because the RNA does not arrive in the cytosol (26).

The conformational modifications of the major group virus HRV14 result in disruption of the endosome; on the other hand, the minor group virus HRV2 opens a pore in the membrane for the RNA to enter the cytosol and the endosome remains largely intact (35, 39). In the latter case, empty particles are left and are shuttled to lysosomes for degradation. Conversely, HRV14 capsid proteins arrive, together with the viral RNA in the cytosol. Therefore, the capsid is degraded to a much lesser extent since it fails to reach the lysosomes.

C-terminal from the ligand-binding domain, LDLR possesses an epidermal growth factor (EGF)-precursor homology (EGFP) domain with two cysteine-rich EGF-like repeats (EGF-A and -B), a six-bladed β-propeller with characteristic Tyr-Trp-Thr-Asp (YWTD) motives, and a third EGF repeat (EGF-C). The three-dimensional structure of LDLR at pH 5.3 shows a closed conformation, in which ligand binding repeats L4 and L5 fold back toward the β-propeller, establishing an intramolecular interaction (37). This involves lysine and tryptophan residues similar to those conferring binding of VLDLR to HRV2 (45) and LDLR to receptor-associated protein at neutral pH (13). Moreover, a number of histidine residues in the propeller become partly protonated and establish additional ionic interactions with buried negatively charged residues of the two ligand binding repeats. This intramolecular competition for the ligand-binding repeats is believed to be responsible for the release of bound LDL at low pH. However, recent mutagenesis experiments suggest that the three histidines supposed to participate in this competition are rather involved in an allosteric mechanism lowering the affinity of the ligand for the receptor at the low endosomal pH (48).

Since virus conversion and release from the receptor is triggered by acid pH in any case, we sought to determine whether competition by the β-propeller played any role in viral infection. Comparing the behavior of wild-type (wt) and propeller-deficient LDLR in HRV2 infection, we demonstrate that the β-propeller promotes infection by facilitating virus conversion and RNA release in the appropriate endosomal compartments within a suitable time window. These results show that minor group receptors are not just passive vehicles for virus delivery but actively contribute to infection.

MATERIALS AND METHODS

Chemicals. All chemicals were obtained from Sigma (St. Louis, MO) or Merck (Darmstadt, Germany) unless specified otherwise. WIN-52084-2 (kindly provided by Dan Pevear, ViroPharma) was dissolved at 0.5 mg/ml in 50% dimethyl sulfoxide and stored at −20°C. Tissue culture plates and flasks were from Iwaki (Bibby Sterilin, Stone, Staffordshire, United Kingdom).

Buffer solutions. Isotonic 30 mM MES (morpholinoethanesulfonic acid) buffers were adjusted to a pH between 4.8 and 7.0 with 0.2 increments. To ensure isotonicity, the NaCl concentrations were calculated by using the web tool "Recipe Calculator for Thermodynamically Correct Buffers," of the University of Liverpool, (http://www.liv.ac.uk/buffers/buffercalc.html). After addition of the adequate amount of NaCl, the buffers were brought to the respective pH with NaOH at 0°C. Hanks balanced buffer solution (HBBS; 0.137 M NaCl, 5.4 mM KCl, 0.25 mM Na_2HPO_4, 0.44 mM KH_2PO_4, 1.3 mM $CaCl_2$, 1.0 mM $MgSO_4$, 4.2 mM $NaHCO_3$) was used for washes, as well as for incubation of CHO cells at 4°C as specified in the text. Radioimmunoprecipitation assay (RIPA) buffer (50 mM Tris-HCl [pH 7.5], 150 mM NaCl, 1 mM EDTA, 1% sodium deoxycholate, 0.1% sodium dodecyl sulfate, 1% Triton X-100) was used for cell lysis prior to radioimmunoprecipitation and/or scintillation counting.

Cell lines. HeLa-H1 Ohio cells (American Type Culture Collection, Manassas, VA), a subline supporting the replication of HRVs, were used for HRV2 production and labeling with [^{35}S]methionine-cysteine, as well as for titer determination. CHO-*ldla7* Chinese hamster ovary cells lacking functional endogenous LDLRs (22) but stably transfected to overexpress native human LDLR (termed RF3 cells) or LDLR in which the YWTD β-propeller domain and the EGF-C domain are deleted (termed ΔYC cells) (5, 6), kindly provided by Stephen Blacklow (Boston, MA), were used in all other experiments.

Cell culture medium. HeLa-H1 cells (for short HeLa) were cultured in minimal essential medium (MEM) supplemented with 10% heat-inactivated fetal calf serum (FCS), 2 mM L-glutamine, 100 U of penicillin/ml, and 100 μg of streptomycin/ml (Gibco/Invitrogen Corp., Paisley, United Kingdom). For infection of HeLa cells, MEM containing 30 mM $MgCl_2$ and 2% FCS (infection medium) was used. CHO cells were cultured in Ham F-12 medium with 5% FCS, 2 mM L-glutamine, 100 U of penicillin/ml, and 100 μg of streptomycin/ml. RF3 and ΔYC cells were maintained in the same medium containing 1 mg of Geneticin (G418)/ml. CHO-infection medium was Ham F-12 containing 30 mM $MgCl_2$ and 2% FCS, without Geneticin. Cells were grown at 37°C, and infection was carried out at 34°C under a 5% CO_2 atmosphere.

Virus. HRV2 was originally obtained from the American Type Culture Collection. An HRV2 variant adapted to replicate in CHO cells was isolated by blind passages alternating between HeLa and CHO-RF3 cells. Cells in a 162-cm^2 flask were challenged with virus at 10 50% tissue culture infective doses ($TCID_{50}$)/cell at 34°C for 30 min, medium with nonbound virus was replaced by fresh infection medium, and cells were incubated for 24 h to allow for infection. Virus eventually produced in the CHO cells was liberated by three consecutive freeze-thaw cycles, and HeLa cells were infected with the lysates. Whereas initially no cytopathic effect (CPE) was seen in the CHO cells, HeLa cells were usually lysed after 24 h. However, after 12 cycles CPE appeared in the CHO cells and persisted even upon CHO to CHO passaging for more than five times. The variant population, termed $HRV2_{CHO}$, replicated in both CHO cell lines but with different kinetics (see below).

Radiolabeling of HRV2. HeLa cells were grown in a 162-cm^2 flask until ca. 80% confluent, washed twice with phosphate-buffered saline (PBS), and incubated with 20 ml of methionine-cysteine-free Dulbecco modified Eagle medium supplemented with 2% dialyzed FCS, 100 U of penicillin/ml, 100 μg of streptomycin/ml, 2 mM L-glutamine, and 30 mM $MgCl_2$ for 4 h at 37°C. The medium was replaced by fresh methionine-cysteine-free medium, and virus was added at 1,000 $TCID_{50}$/cell. The cells were incubated for 4 h at 34°C to allow for viral internalization and host cell shutoff. Portions (15 ml) of the old medium were replaced by fresh infection medium containing 2% dialyzed FCS. After the addition of 1 mCi of [^{35}S]methionine-cysteine (Hartmann Analytic GmbH, Braunschweig, Germany), incubation was continued for 16 h. Cells were broken by three cycles of freezing-thawing, and debris was removed by centrifugation at 20,000 rpm (Ty65 rotor) for 20 min at 4°C. Virus was pelleted at 50,000 rpm (Ty65 rotor) for 2 h and suspended in 1 ml of HBBS supplemented with 2% FCS overnight at 4°C. Insoluble material was removed by centrifugation in a benchtop centrifuge. Remaining free radiolabel was removed by pelleting two times in a Beckman Optima TLX benchtop ultracentrifuge (TLA 100.3 rotor) at 70,000 rpm for 1 h. The viral pellet was finally resuspended in 200 μl of HBBS–2% FCS and stored at 4°C. Incorporated radioactivity was quantified by liquid scintillation counting (Tricarb; Packard, Meriden, CT); only radiochemically pure virus preparations (i.e., only viral proteins visible in the autoradiogram), as checked on a reducing 15% sodium dodecyl sulfate-polyacrylamide gel, were used. To ensure the absence of subviral particles, the preparations were stored over *S. aureus*-2G2 immunocomplexes that were removed by centrifugation before using the virus. The monoclonal antibody (MAb) 2G2 specifically recognizes subviral particles (31).

FACS quantification of LDLR expression. CHO cells were detached from 162-cm^2 culture flasks by incubation in 5 ml of 10 mM EDTA in PBS at 37°C for 5 min. The cells were washed with PBS and resuspended in Ham F-12 growth medium to allow for resaturation of cell surface LDLRs with Ca^{2+} at 37°C for 30 min. After two washes in ice-cold HBBS, the cells were resuspended in ice-cold fluorescence-activated cell sorting (FACS) buffer (HBBS supplemented with 2% FCS) at $\sim 2 \times 10^6$ cells/ml, followed by incubation under slow rotation for 1 h at 4°C. The cells were dispensed in 2-ml Eppendorf tubes at $\sim 2 \times 10^6$ cells/sample, pelleted at 1,000 × *g* for 5 min, resuspended in 200 μl of FACS buffer containing chicken immunoglobulin Y (IgY) directed against the ligand-binding domain of human LDLR (prepared by standard techniques) at 2.5 μg/ml. The cells were then incubated on ice for 1 h by gently shaking the tubes every other 10 min. After three washes with 1 ml of ice-cold HBBS, phycoerythrin-conjugated donkey anti-chicken secondary antibody (Jackson Immunoresearch) was added at 1:100 in 200 μl of FACS buffer. After 30 min of incubation, the cells were washed

twice with cold HBBS, resuspended in 1 ml of cold HBBS, transferred into 5-ml polypropylene FACS tubes, and kept on ice until analyzed. Cell-associated fluorescence corresponding to receptor expression was measured in a Becton Dickinson LSR-I flow cytometer, using the CellQuest Pro software for data analysis.

Quantification of cell attachment of HRV2. CHO cells expressing wt or truncated LDLR were grown in six-well plates until ca. 80% confluent. The growth medium was discarded, the cells were washed with ice-cold HBBS, 20,000 cpm of ^{35}S-labeled HRV2 in ice-cold infection medium was added per well, and the plates were incubated for 1 h at 4°C for virus binding. Unbound virus was removed by three washes with ice-cold HBBS, and the cells were lysed in 500 μl of RIPA buffer on ice for 15 min and transferred into scintillation vials. The wells were washed with 500 μl of RIPA buffer and with 500 μl of HBBS, the washes were combined with the cell lysates, and the cell-associated radioactivity was measured in a liquid scintillation counter (Tricarb).

Release of LDLR-bound HRV2 from CHO cells after low-pH treatment. CHO cells were grown in six-well plates until confluent. The medium was removed, and the cells were incubated in cold HBBS for 10 min at 4°C and challenged with 20,000 cpm of ^{35}S-labeled HRV2 in ice-cold CHO infection medium for 1 h at 4°C. Unbound virus was removed by washing the samples with ice-cold HBBS, and the cells were exposed to isotonic 30 mM MES buffers of pH 4.8 to 7.0 (with increments of 0.2 pH units) for 20 min at 4°C. Samples were reneutralized by the addition of the adequate volumes of 1 M Tris base. The virus released into the supernatant and remaining cell-associated virus were quantified separately by scintillation counting as described above. In a separate experiment, the effect of the duration of low-pH incubation and reneutralization on virus dissociation was determined. Cells were incubated at pH 5.0, 6.0, and 7.0 for 20, 45, and 90 min, followed by reneutralization to pH 7.0 for 0, 10, and 45 min.

Modeling endosomal virus conversion at the plasma membrane and influence of WIN-52084-2. The capsid-binding drug was dissolved at 0.5 mg/ml in 50% dimethyl sulfoxide. For each assay 30,000 cpm of ^{35}S-labeled HRV2 was preincubated in 20 μl of 150 mM NaCl (pH 7.5) containing WIN-52084-2 at a final concentration of 20 μg/ml for 30 min at room temperature. As a control, the virus was preincubated in the same solution without the WIN compound. Eventually, the non-native virus was removed by immunoprecipitation with MAb 2G2-*S. aureus* immunocomplexes prepared as follows. A 500-μl portion of fixed, heat-killed *S. aureus* cells from a 10% stock suspension was pelleted at 10,000 rpm for 1 min in a benchtop Eppendorf centrifuge. The pellet was washed twice with 1 ml of PBS and twice with 1 ml of RIPA buffer. Bacteria were resuspended in 400 μl of RIPA buffer, and 100 μl of rabbit HRV2-antiserum was added, followed by incubation for 1 h at room temperature. Bacteria were pelleted, washed three times with RIPA buffer, and finally resuspended in 500 μl of RIPA buffer containing 0.04% sodium azide. Since protein A binds rabbit IgG much better than mouse IgG, MAb 2G2 was bound via rabbit anti-mouse IgG by using the same procedure.

CHO cells were grown in six-well plates until confluent and preincubated in cold HBBS for 10 min at 4°C. After challenge with 20,000 cpm of ^{35}S-labeled HRV2 (untreated and preincubated with the antiviral, respectively) in CHO infection medium at 4°C for 1 h, unbound virus was removed, and the cells were further incubated in isotonic buffers of pH 4.8 to 7.0 for 20 min at 4°C as described above. The buffers were reneutralized, and the cells were further incubated for 20 min at 4°C to allow for virus release. Supernatants (1 ml) were collected in 2-ml Eppendorf tubes, the cells were washed twice with 250 μl of HBBS, the washes were combined with the supernatants, and 300 μl of 6× RIPA buffer was added. The cells were lysed in 500 μl of RIPA buffer on ice for 15 min and collected in 2-ml Eppendorf tubes. The wells were rinsed twice with 500 μl of RIPA buffer, and the washes were combined with the cell lysates. Debris was removed by centrifugation. Supernatants and cell lysates were processed separately for sequential immunoprecipitation. First, subviral particles were recovered by the addition of 20 μl of MAb 2G2-*S. aureus* immunocomplexes, followed by incubation for 2 h at room temperature. Bacteria were pelleted and washed twice with 200 μl of RIPA buffer. Remaining native virus in supernatants and washes was precipitated with 20 μl of rabbit HRV2 antibody-*S. aureus* immunocomplexes. Pellets were washed twice with 200 μl of RIPA buffer and scintillation counted. Conversion of native virus into subviral particles was calculated by dividing the sum of 2G2-precipitated counts by the total counts (i.e., the sum of 2G2 and anti-HRV2 precipitated counts). Conversion at pH 4.8 was set to 100% and conversion at pH 7.0 to 0%.

Kinetics of virus conversion. CHO cells were grown in six-well plates, preincubated in cold HBBS for 10 min at 4°C, and challenged with 20,000 cpm of ^{35}S-labeled HRV2 at 4°C for 1 h. Unbound virus was removed by extensive washing with ice-cold HBBS, and the cells were incubated in 1 ml of CHO infection medium at 34°C, allowing for virus internalization and uncoating. At the times given in the text, the cells were lysed without removing the incubation medium by adding 200 μl of 6× RIPA buffer. Cell debris was removed by centrifugation. To monitor the uncoating, subviral particles were immunoprecipitated with MAb 2G2, and the remaining native virus was immunoprecipitated with HRV2 antiserum, followed by quantification by liquid scintillation counting as described above, and the ratios of 2G2 precipitated counts over total counts were calculated.

Time-dependent colocalization of virus and LDLR. CHO cells were seeded onto 13-mm glass coverslips (Menzel, Braunschweig, Germany) and grown until 80% confluent. Cells were washed with PBS containing 1 mM $CaCl_2$ and 1 mM $MgCl_2$ (PBS^{++}), preincubated in 200 μl of CHO infection medium for 30 min at 37°C, cooled to 4°C, and challenged with HRV2 at 900 $TCID_{50}$/cell for 1 h. Unbound virus was removed by three washes with 2 ml of ice-cold PBS^{++}, and the cells were incubated in 500 μl of prewarmed CHO infection medium for 4, 20, and 60 min (chase). The coverslips were transferred into a six-well plate on ice and washed with 2 ml of ice-cold PBS^{++} for 5 min. The cells were fixed for 30 min with 300 μl of 4% paraformaldehyde in PBS^{++}, quenched with 300 μl of 50 mM NH_4Cl in PBS for 10 min, washed three times, and permeabilized with 300 μl of 0.2% Triton X-100 in PBS for 5 min. Nonspecific binding sites were blocked with 200 μl of 10% goat serum in PBS (Gibco/Invitrogen) for 30 min. All antibodies were diluted with PBS containing 10% goat serum. HRV2 was detected with MAb 8F5 (40) at 10 μg/ml, followed by Alexa 568-conjugated goat anti-mouse IgG (1:1,000; Molecular Probes, Eugene, OR), and LDLR was detected with chicken anti-human LDLR IgY (10 μg/ml) and Alexa 488-conjugated goat anti-chicken IgG (1:1,000; Molecular Probes). Cells were washed four times for 10 min each time with 5 ml of PBS, and nuclei were stained with DRAQ5 (Biostatus, Shepshed, Leicestershire, United Kingdom). Coverslips were briefly dipped in double-distilled H_2O and mounted in Mowiol. Cells were viewed with a Zeiss Axiovert 200 microscope (Carl Zeiss, Jena, Germany) equipped with an UltraView ERS laser confocal system (Perkin-Elmer, Shelton, CT). Twelve-bit images of highest resolution (1,344 × 1,024 pixels; no binning) were acquired through a 63×/1.4 Plan-Apochromat lens (Carl Zeiss). Images were taken with the same exposure time, and emission was discriminated by sequential acquisition. For Z-stack analysis, at least 15 images were recorded at 0.2-μm intervals with a piezo-driven Z stage. UltraView software was used to correct for background fluorescence and to determine the extent of colocalization.

Effect of HRV2 internalization on LDLR expression. RF3 and ΔYC cells were preincubated in serum-free Ham F-12 medium for 1 h at 34°C. HRV2 at 1,500 $TCID_{50}$/cell was internalized in serum-free Ham F-12 medium for 6 h. Cells were then cooled, washed, fixed, and permeabilized with methanol at −20°C for 10 min and processed for indirect immunofluorescence microscopy for the detection of LDLR (see above) and LAMP2 (anti-human CD107B mouse antibody 1:400; BD Biosciences/Pharmingen), followed by Alexa 488-conjugated goat anti-chicken IgG and Alexa 568-conjugated goat anti-mouse IgG, respectively. Nuclei were stained with Hoechst dye (1 μg/ml; for epifluorescence microscopy) and DRAQE5 (1:500; for confocal microscopy), and cells were embedded in Mowiol. LDLR expression and the extent of colocalization with LAMP2 was investigated by epifluorescence microscopy using a Zeiss Axioplan 2 fluorescence microscope equipped with a C-Apochromat 40× lens and Axiovision software. Confocal microscopy was carried out as described above.

Kinetics of the infection of CHO cells with $HRV2_{CHO}$. CHO cells grown in six-well plates were challenged with $HRV2_{CHO}$ at 10 $TCID_{50}$/cell at 4°C for 1 h. Unbound virus was removed by extensive washing with ice-cold HBBS, and the cells were incubated at 34°C in 2 ml of CHO infection medium. At time zero (to determine bound virus) and at 3, 6, 9, 12, 16, 22, 26, 31, and 36 h, the cells were subjected to three freeze-thaw cycles, cell debris was removed, and the virus titers were determined in HeLa cells.

RESULTS

At pH 5.3 LDLR releases LDL via intramolecular competition of its β-propeller domain for the ligand binding repeats L4 and L5 (5, 6, 37) or, as more recently suggested, via allosteric conformational changes (48). Since conversion of HRV2 into subviral particles during infection also occurs at similar pH values in late endosomes (16), structural changes of receptor and virus might take place concomitantly. Therefore, we sought to determine whether the β-propeller function was also important for minor group rhinovirus infection. Since human cells defective in expression of the receptors recognized by minor group HRVs are not available, all experiments were

carried out using CHO cells lacking endogenous LDLR as a consequence of a mutation (*ldla7* cells) (25). These cells were transfected to stably express human wt LDLR (RF3 cells) or a mutant receptor lacking the YWTD–β-propeller and the EGF-C domain (ΔYC cells).

Immunofluorescence microscopy and FACS analysis revealed that the expression levels of the LDLRs in the two cell lines were not identical (not shown). In particular, despite being grown in the presence of the selecting agent Geneticin, the concentration of wt LDLR was comparatively low in most of the cells. Therefore, both cell lines were subjected to FACS sorting, and cells expressing the respective receptors at similar levels were collected and expanded. This resulted in reasonably homogeneous populations; binding of radiolabeled HRV2 at 4°C was almost identical for both cell lines (ca. 70% ± 3.5% of total input virus) with low background binding (3.9% ± 0.7% related to the receptor-expressing cells) as determined for non-transfected CHO-*ldla7* control cells that lack functional LDLR. These cells were used for all experiments.

Structural changes and uncoating of HRV2 at the low endosomal pH can be mimicked at the plasma membrane by incubation of receptor-bound virus in acidic buffers (8). Since dissociation of the virus from its receptor when still in its native conformation might strongly decrease productive infection, we first investigated the possible role of the β-propeller domain in this process. The experiments were carried out with the two CHO cell lines by incubation of plasma membrane-bound virus in low-pH buffer. To avoid depletion of the Ca ions that are necessary to maintain the receptor in its native conformation, we used MES buffer instead of the acetate-phosphate buffers applied in the previous study (8).

HRV2 remains attached to CHO cells upon acidification unless reneutralized. ^{35}S-labeled HRV2 was bound to wt LDLR and mutant LDLR expressed on the respective CHO cell line for 1 h at 4°C. Unbound virus was washed away with ice-cold HBBS, and bound virus was exposed to a series of isotonic MES buffers of pH 4.8 to 7.0 for 20 min. In contrast to the previous results with HeLa cells (8), we found that the CHO cells did not release bound virus at any pH value, not even from the cells expressing wt LDLR on prolonged incubation at the lowest pH. This is most probably the result of the ~10-fold-higher LDLR expression level in the transfected cells than in HeLa cells. It suggests that HRV2 either remained receptor bound in its native form or had converted to subviral particles that were handed over to the cell membrane. However, substantial and rapid virus release was noticed after reneutralization to pH 7.0 (data not shown). The hydrophobic A-particles associate with liposomes (28), whereas the hydrophilic empty B-particles do not (24, 28). Therefore, these data imply that HRV2, when bound to CHO cells and exposed to low pH, dissociates from the cells uniquely upon reneutralization in the form of empty capsids.

LDLR binding stabilizes HRV2 against low pH-induced conversion. We next set out to identify the nature of the viral material remaining bound and being released. The experiment above was repeated, and subviral particles and native virus in the supernatant were determined by sequential immunoprecipitation with MAb 2G2 that specifically recognizes subviral particles (18, 31) and rabbit anti-HRV2 IgG. This method has been extensively used previously for quantification of the conversion of HRV2 into subviral particles (3, 19, 34). The same procedure was carried out with the cellular fraction after cell lysis with RIPA buffer. Immunoprecipitates were quantified by liquid scintillation counting (Fig. 1). Similar to the results with HeLa cells (8), the conformational alterations of HRV2 bound to CHO cells expressing wt LDLR occurred within a pH range from <6.0 to ~5.4, following a typical sigmoid curve. However, when virus was bound to β-propeller-negative LDLR, the curve was shifted toward lower pH values by ~0.3 pH units.

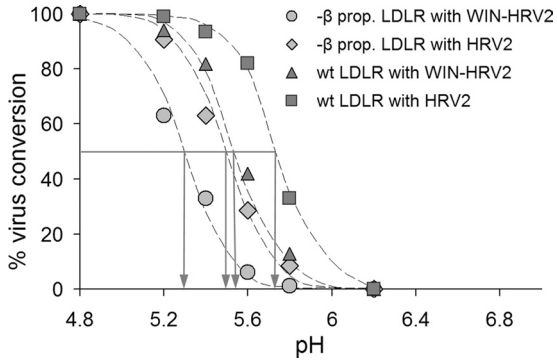

FIG. 1. Conversion of LDLR-bound HRV2 at the plasma membrane by incubation in isotonic buffers of different pH. Radiolabeled HRV2 either untreated or preincubated with the antiviral capsid-binder WIN-52084 was attached to the cells at 4°C for 1 h, unbound virus was removed, and the cells were incubated at 4°C for 20 min in isotonic buffers with the pH values indicated. The buffers were reneutralized by adding Tris base, and the cells were further incubated for 20 min to allow for virus release. Converted virus was immunoprecipitated with MAb 2G2 and remaining native virus with anti-HRV2 antiserum from both the supernatants and cell lysates. Total conversion at pH 4.8 was set to 100%, and no conversion at pH 7.0 was set to 0%. Note that the propeller-negative LDLR stabilizes the virus against its conversion to a similar extent as the antiviral substance; the two different types of protection effects were additive.

Capsid-binding drugs, such as I(S), also named WIN-52084 (from the Sterling Winthrop company that originally manufactured them), displace fatty acids naturally present in the hydrophobic pocket of the capsid and protect HRVs against low pH-induced conversion into subviral A-particles (16, 21). Therefore, the same experiment was carried out with HRV2 that had been preincubated with this drug. Stabilization by the compound also resulted in a shift of the conversion curve of wt LDLR-bound HRV2 toward lower pH values. This increase in stability at low pH was almost identical to that caused by truncated LDLR. Apparently, in the absence of the β-propeller domain the high-avidity attachment of the receptor via several ligand-binding modules stabilizes the native conformation of the virus. This is in line with earlier data of Nicodemou et al. (32), who demonstrated stabilization of HRV2 by the soluble concatemeric pentamer of module 3 (V33333) of VLDLR in vitro. Stabilization by WIN-52084 and the β-propeller negative receptor were additive, shifting the sigmoid curve even more toward lower pH values (Fig. 1). Under our experimental conditions virtually no virus was released from the cells upon acidification. However, upon reneutralization, a large percentage was found in the cell supernatant, and 80 to 100% of it was in the form of subviral particles at any pH value for all four experimental conditions (data not shown).

Upon endocytosis in HeLa cells, HRV2 is shuttled from

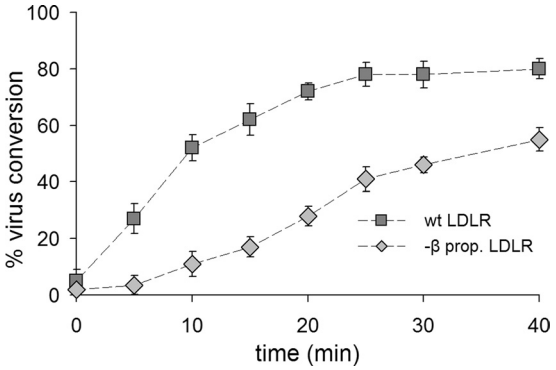

FIG. 2. Viral conversion is delayed and reduced in CHO cells expressing the β-propeller-negative LDLR compared to wt LDLR. Radiolabeled HRV2 was attached to cells grown in six-well plates at 4°C for 1 h, unbound virus was washed away, and the cells were incubated in 1 ml of infection medium at 34°C, allowing for virus internalization and uncoating. At the time points indicated, the cells were lysed without removing the incubation medium. Converted virus was immunoprecipitated with MAb 2G2 and remaining native virus was immunoprecipitated with anti-HRV2 antiserum and scintillation counted. The percentage of virus conversion was calculated as 2G2-precipitated counts divided by total precipitated counts and set to 0% at time zero. Note the delay and lower extent of uncoating when the virus enters via the truncated receptor. Error bars indicate the means ± the standard deviations (SD) ($n = 3$).

early to late endosomes within endosomal carrier vesicles (ECV). The RNA is released from the virus either in ECV or in late endosomes (4), and the remaining empty capsids move on to lysosomes, where they are degraded. Therefore, productive RNA release must happen within a window of opportunity in the correct compartment. The experiments mimicking the situation in endosomes at the plasma membrane suggest that the β-propeller might facilitate virus conversion at comparatively higher pH values at earlier times. Thereby, the time window for RNA release would be longer, which could influence the efficiency of infection. Therefore, we investigated viral conformational changes during cell entry.

Conversion of native HRV2 to subviral particles is delayed when internalized via β-propeller-deficient LDLR. Radiolabeled HRV2 was attached to the cells at 4°C for 1 h, unbound virus was washed away with cold HBBS, and the cells were incubated in infection medium at 34°C to allow for virus internalization and conversion in endosomes. At various times, the cells were lysed by adding RIPA buffer without removing the incubation medium. Subviral particles and remaining native virus were recovered by sequential immunoprecipitation with MAb 2G2 and anti-HRV2 antiserum and determined by liquid scintillation counting. The percentage of virus conversion was calculated as the ratio of 2G2-precipitated counts over total precipitated counts and set to 0% at time zero. As seen in Fig. 2, virus conversion was strongly delayed and reduced when entry occurred via the truncated receptor.

The dissociation of HRV2 from the two forms of LDLR within endosomes was also assessed via the time-dependent colocalization of HRV2 and LDLR by confocal immunofluorescence microscopy. HRV2 was bound to the plasma membrane of CHO cells expressing the respective receptor on ice, and the cells were further incubated at 34°C for the times

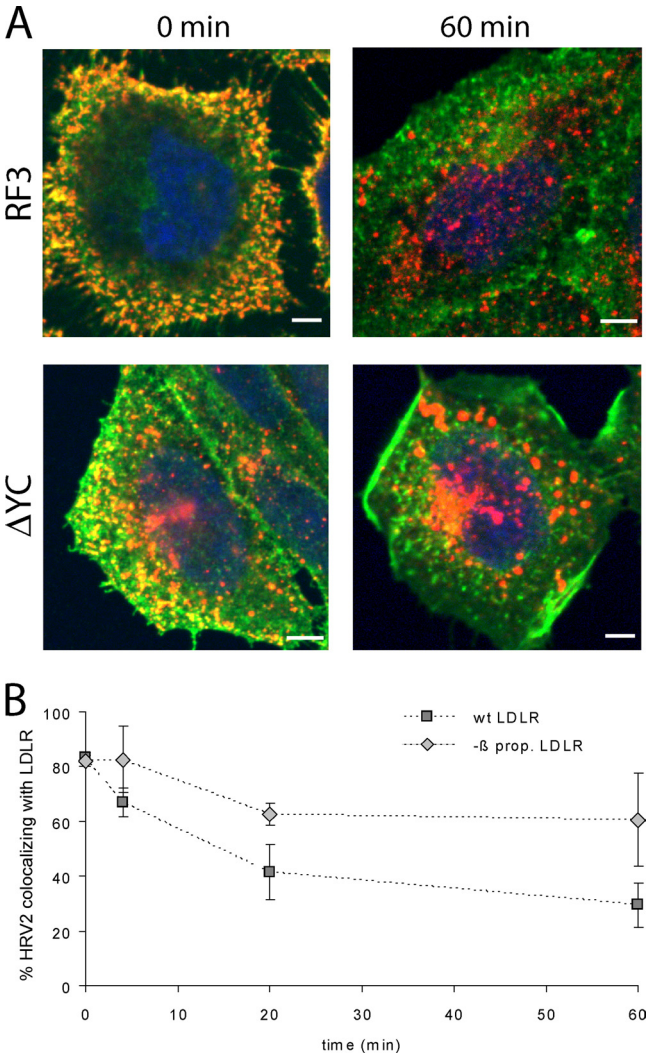

FIG. 3. HRV2 dissociation from LDLR is delayed when the β-propeller is deleted. HRV2 was bound at 4°C to CHO cells grown on coverslips, and entry was initiated by adding warm medium. At the times indicated, the cells were fixed and permeabilized, and LDLR and HRV2 were detected by specific antibodies, followed by Alexa 488-conjugated goat anti-mouse IgG and Alexa 568-conjugated goat anti-chicken IgG, respectively. (A) Representative fluorescent images of one focal plane through the perinuclear region are shown after HRV2 binding (0 min) and 60 min after warming to 34°C. LDLR, green; HRV2, red. (B) The percent colocalization of virus and receptor was calculated from immunofluorescence microscopy images as in panel A. Colocalization at time zero was set to 100%. Error bars indicate the means ± the SD ($n = 3$).

indicated in Fig. 3. Virus and receptor were differentially labeled with suitable specific antibodies and visualized (Fig. 3A). Colocalization was determined by using UltraView software (Fig. 3B). In agreement with virus-receptor dissociation in early endosomes (8), colocalization of HRV2 and receptor rapidly decreased in time. Furthermore, when the virus entered via the β-propeller-negative receptor, this dissociation occurred at a substantially slower rate and only to a minor extent.

Infection is delayed when HRV2 is internalized via β-propeller-deficient LDLR. Most HRVs fail to replicate in nonhu-

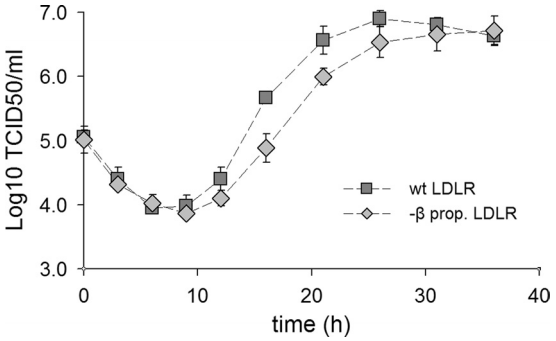

FIG. 4. Infection kinetics of CHO cell-adapted HRV2 in cells expressing wt and β-propeller-negative LDLR. Cells seeded in six-well plates were challenged with $HRV2_{CHO}$ at 10 $TCID_{50}$/cell at 4°C for 1 h. After the removal of unbound virus, the cells were incubated at 34°C. At the times indicated, the cells were broken by three cycles of freeze-thawing, and the virus titer was determined. Note the significant delay in virus production in the cells expressing the truncated receptor. Error bars indicate means ± the SD ($n = 3$).

man cells, and challenge of the CHO cell lines with HRV2 did not result in productive infection. However, adaptation of HRV2 to mouse L cells has been reported (47). The variants showed mutations within nonstructural viral proteins, indicating that receptor binding was not affected. We thus used the same strategy for adapting HRV2 to replicate in hamster cells. After 12 blind passages alternating between RF3-CHO cells and HeLa cells, a population of HRV2 variants, termed $HRV2_{CHO}$, was selected that caused CPE and multiplied in both CHO lines. Figure 4 depicts the infection kinetics of $HRV2_{CHO}$ in the two lines. The virus titer decreased at the early times after challenge, indicating uncoating of incoming virus. From about 9 h onward, replication was evident with the virus titer attaining a plateau after about 30 h. The most obvious difference between the two cell lines is seen between 12 and 26 h; the cells expressing the wt receptor produced up to 6 times more virus at 16 h postinfection, with a difference of ~5 h in reaching the plateau.

HRV2 directs the β-propeller-deficient LDLR to lysosomes. Deletion of the entire EGFP-homology domain of LDLR has been shown to inhibit dissociation of bound LDL, impairs receptor recycling, and results in lysosomal degradation of the receptor-ligand complex (10). Since the β-propeller is the main player in the conformational changes at low pH (5, 37), we thought it likely that the ΔYC deletion mutant used in our experiments behaves identically. To assess whether HRV2 internalization results in degradation of the mutant LDLR, we studied colocalization of LDLR with the lysosomal marker LAMP2 by fluorescence microscopy. CHO cells expressing wt or β-propeller-negative LDLR were grown on coverslips and incubated for 30 min in serum-free medium, and HRV2 at 1,500 $TCID_{50}$/cell was continuously internalized for 6 h at 34°C. The cells were chilled, washed, fixed, permeabilized, and incubated with mouse anti-LAMP2 antibody, followed by Alexa 568-conjugated goat anti-mouse IgG. LDLRs were revealed with chicken anti-LDLR IgY, followed by Alexa 488-conjugated goat anti-chicken IgG. For control purposes, mock-infected cells were incubated under the same conditions. Internalization of HRV2 into RF3 cells had no significant

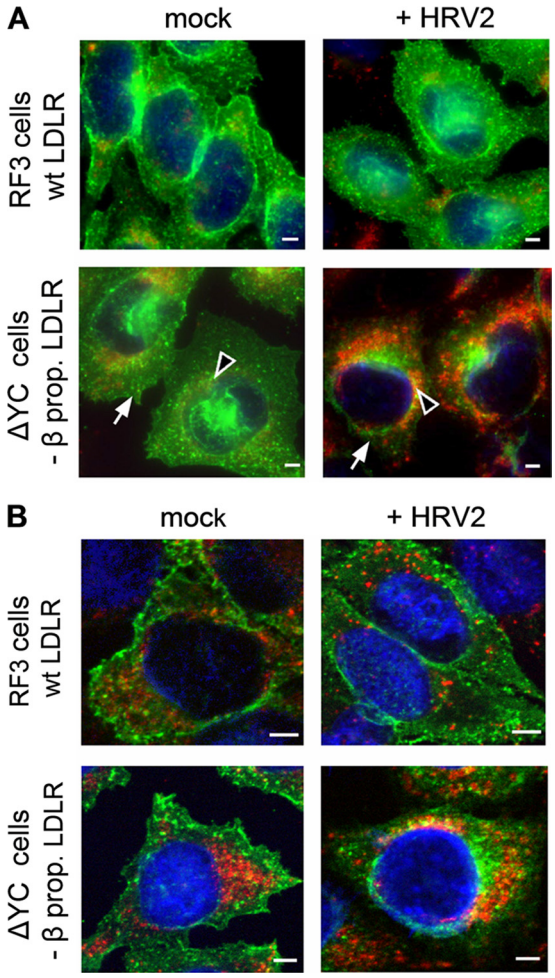

FIG. 5. Continuous HRV2 internalization leads to degradation of mutant but not wt LDLR. RF3 and ΔYC cells were preincubated in serum-free Ham F-12 medium, and HRV2 at 1,500 $TCID_{50}$/cell was internalized for 6 h. Cells were cooled, washed, and processed for indirect immunofluorescence microscopy for the detection of LDLR (green) and LAMP2 (red). Nuclei were stained with Hoechst dye (for epifluorescence) and DRAQE5 (for confocal microscopy). (A) Conventional epifluorescence microscopy. All images were taken with the same exposure time in the respective channel and identical settings were used for illustration with the Axiovision software. Overlay images are shown. Arrowheads indicate perinuclear and arrows indicate plasma membrane localization of the receptors. (B) Confocal images were taken by using the same laser power and exposure time in the respective channel. Multicolor images shown were obtained with identical gray level settings in each channel. Of 20 sections through the cells, the focal plane through the nucleus is depicted. Bar, 2 μm.

influence on the total fluorescence and thus on the concentration of wt LDLR (Fig. 5A, upper panels). Furthermore, little colocalization of LDLR with the late endosome/lysosome marker LAMP2 was seen in the absence and in the presence of HRV2 (Fig. 5B, upper panels). In contrast, in ΔYC cells HRV2 uptake resulted in decreased LDLR levels mainly at the plasma membrane (arrows) but not in the perinuclear area (Fig. 5A, lower panels, arrowheads). The decrease in plasma membrane localization of the mutant receptors appears to be due to their lysosomal degradation as deduced from the higher extent of colocalization of receptors with LAMP2 (Fig. 5B,

lower panels). Collectively, this indicates that the virus directs the truncated receptor to lysosomes.

DISCUSSION

LDL has been shown to dissociate from plasma membrane LDLR at pH <5.5 (10); if the entire EGFP-domain or the β-propeller together with the EGF-C domain is absent from the receptor, LDL release is reduced to 10% compared to 100% for wt LDLR (6, 7). The 3D X-ray structure of LDLR determined at pH 5.3 revealed an intramolecular interaction between modules LA4 and LA5 and the β-propeller and thereby nicely explained the underlying mechanism at the molecular level (37). In the present study we took advantage of CHO-*ldla7* cells that are deficient in the endogenous receptor but had been stably transfected to overexpress human wt LDLR (RF3 cells) and LDLR lacking the β-propeller, together with the EGF-C domain (ΔYC cells). We demonstrated that the β-propeller domain is not only important for the LDL metabolism but also exerts a similar function in the conversion and release of minor group HRVs, exemplified by HRV2. LDLR is thus not only a vehicle for virus delivery, but it also fine-tunes the location and timeliness of RNA transfer into the cytosol. By comparing cells expressing either wt LDLR (RF3) or LDLR whose β-propeller was deleted (ΔYC cells), it became clear that, in the absence of this latter domain, HRV2 was less readily released from the receptor and the structural changes associated with uncoating and required for RNA release were only observed at a lower pH. The final conversion to 80S particles appears to be facilitated by reneutralization. We are currently investigating whether this could also occur in vivo via pores in the endosomal membrane, allowing for the exit of protons. We also compared the two forms of the receptor with respect to infection and virus production. Since HRV2 fails to replicate in rodent cells, it was adapted to grow in these cells by a series of blind passages alternating between RF3 and HeLa cells. The resultant HRV2 variant (termed $HRV2_{CHO}$) grew to roughly one-fifth of the titer attained in HeLa cells. It was previously shown that adaptation to mouse cells by a similar protocol does not modify the viral capsid but rather introduces mutations into nonstructural proteins (17, 27). Therefore, it is highly unlikely that receptor interaction is modified in this variant, and it was legitimate to use it for our analyses. As a consequence of β-propeller deletion, the infection was delayed and less efficient. Stabilization of HRV2 by a receptor construct carrying five copies of V3, the third module of VLDLR arranged in tandem, has been noted earlier (32). This effect is most probably due to the strong multivalent attachment of the receptor modules around the fivefold axes of icosahedral symmetry (36). It appears that even LDLR, in which only repeats 1, 2, 4, and 5 possess the tryptophan essential for virus binding (45), exhibits sufficient avidity for protecting the virus against conformational changes at low pH.

Conversion of the virus to subviral particles in endosomes and viral de novo synthesis were delayed in ΔYC cells compared to RF3 cells. These data indicate that wt LDLR facilitates viral conformational modification and subsequent steps such as virus release from the receptor, RNA uncoating, and RNA transfer into the cytoplasm. This is brought about by the β-propeller that supposedly competes with the virus for ligand-binding repeats LA4 and LA5. Our data correlate well with the results for LDL release mentioned above; only ca. 15% of HRV2 was released from the mutated receptor in ΔYC cells and 70% of HRV2 was released from the wt receptor in RF3 cells after 60 min internalization.

Endocytosed ligands are transported through the endocytic pathway to lysosomes and thereby become exposed to an increasingly lower pH; pH 6.5 to 6.0 in early endosomes, pH 5.5 to 5.0 in late endosomes, and pH 4.5 to 4.0 in lysosomes. Sorting of LDL from transferrin, a marker of the recycling pathway, occurs in early (sorting) endosomes within 2 to 4 min (12, 15, 30). However, the low-pH structure of LDLR was analyzed at pH 5.3 (5, 6, 37). This raises the question of which additional factors may aid ligand release in early endosomes. Since binding of ligands to the LDLR family is Ca^{2+} dependent (9), a mildly acidic pH and a low endosomal Ca ion concentration could cooperatively facilitate ligand dissociation as shown in in vitro experiments (1). Since the V-ATPase is electrogenic, inward proton transport has to be balanced by inward chloride and/or outward cation (K^+, Na^+, and Ca^{2+}) movement. Indeed, upon pinching-off the plasma membrane, endocytic vesicles rapidly alter their internal milieu from one corresponding to the extracellular environment (pH neutral and high concentrations of chloride, sodium, and calcium ions) to an acidic pH. Although the endosomal chloride concentration is lowered to ~17 mM within 3 min, it subsequently increases to 60 mM as the pH decreases to 5.3 along the lysosomal pathway (42). In contrast, a continuous decrease in endosomal Ca^{2+} was observed; its concentration dropped within 3 min to 29 μM and to ~3 μM after 20 min (14). Indeed, various calcium channels (e.g., a "transient receptor potential-like Ca-channel" [38]) and various mucolipin calcium channels (29) were identified in endosomal subcompartments that exhibit distinct properties and therefore may contribute to low endosomal calcium as well as to endosomal pH regulation.

Lack of ligand dissociation from LDLR affects receptor trafficking. For β-VLDL, the EGFP domain had no influence on binding, internalization, and degradation, but the mutant LDLRs failed to recycle. This resulted in a time-dependent loss of mutant receptors, presumably due to their lysosomal degradation (10). Taken together, the failure to dissociate ligand from LDLR results in receptor trafficking to lysosomes (2). This is in line with our results that demonstrate that HRV2 directs the mutant receptor to lysosomes.

Based on the earlier finding that virus is released from its receptor in the native state at the pH prevailing in early endosomes (8), we rather expected that propeller-deficient LDLR would increase the efficiency of infection by holding the virus close to the endosomal membrane until conversion occurs. In contrast, our conversion assays showed that the virus was not released at any pH values, unless the incubation buffers were reneutralized. These results do not necessarily contradict previous data on HeLa cells (8), where release of native HRV2 at pH 6.0 was shown, for the following reasons. (i) HeLa cells express, in addition to LDLR, LRP and VLDLR. Infection of HeLa cells is inhibited to 80 to 90% by receptor-associated protein (M. Brabec et al., unpublished results), which is indicative for a preferential role of LRP1 and/or VLDLR in HRV2 entry. (ii) Intracellular trafficking of HRV2 bound to LRP1 may be distinct from LDLR. (iii) The low-pH

buffers used by Brabec et al. contained phosphate but lacked calcium and thus facilitated release of native virus (see above). Whether the virus dissociates from the receptor when still in its native state or just upon conversion most probably depends on the interrelation of multiple factors, such as the avidity of virus-receptor binding and the pH range of virus conversion compared to that of the receptor switch.

Taken together, our results underscore the role of the β-propeller in LDLR for minor group HRV infection. LDLR is thus not just a simple vehicle for delivery of the virus into endosomes but is also a well-chosen carrier combining high-avidity multimodule binding with an intrinsic release mechanism. If the release mechanism is impaired, the virus fails to undergo conversion at the correct time, and the correct intracellular compartment and infection is less efficient.

ACKNOWLEDGMENTS

We thank Stephen Blacklow for the gift of the recombinant CHO cells and Irene Goesler for virus production.

This study was supported by the Austrian Science Foundation (FWF) grant P17516-B10.

REFERENCES

1. **Arias-Moreno, X., A. Velazquez-Campoy, J. C. Rodriguez, M. Pocovi, and J. Sancho.** 2008. Mechanism of low density lipoprotein (LDL) release in the endosome: implications of the stability and Ca^{2+} affinity of the fifth binding module of the LDL receptor. J. Biol. Chem. **283:**22670–22679.
2. **Basu, S. K., J. L. Goldstein, R. G. Anderson, and M. S. Brown.** 1981. Monensin interrupts the recycling of low density lipoprotein receptors in human fibroblasts. Cell **24:**493–502.
3. **Bayer, N., D. Schober, M. Huttinger, D. Blaas, and R. Fuchs.** 2001. Inhibition of clathrin-dependent endocytosis has multiple effects on human rhinovirus serotype 2 cell entry. J. Biol. Chem. **276:**3952–3962.
4. **Bayer, N., D. Schober, E. Prchla, R. F. Murphy, D. Blaas, and R. Fuchs.** 1998. Effect of bafilomycin A1 and nocodazole on endocytic transport in HeLa cells: implications for viral uncoating and infection. J. Virol. **72:**9645–9655.
5. **Beglova, N., H. Jeon, C. Fisher, and S. C. Blacklow.** 2004. Cooperation between fixed and low pH-inducible interfaces controls lipoprotein release by the LDL receptor. Mol. Cell **16:**281–292.
6. **Beglova, N., H. Jeon, C. Fisher, and S. C. Blacklow.** 2004. Structural features of the low-density lipoprotein receptor facilitating ligand binding and release. Biochem. Soc. Trans. **32:**721–723.
7. **Boswell, E. J., H. Jeon, S. C. Blacklow, and A. K. Downing.** 2004. Global defects in the expression and function of the low density lipoprotein receptor (LDLR) associated with two familial hypercholesterolemia mutations resulting in misfolding of the LDLR epidermal growth factor-AB pair. J. Biol. Chem. **279:**30611–30621.
8. **Brabec, M., G. Baravalle, D. Blaas, and R. Fuchs.** 2003. Conformational changes, plasma membrane penetration, and infection by human rhinovirus type 2: role of receptors and low pH. J. Virol. **77:**5370–5377.
9. **Brown, M. S., J. Herz, and J. L. Goldstein.** 1997. LDL receptor structure: calcium cages, acid baths and recycling receptors. Nature **388:**629–630.
10. **Davis, C. G., J. L. Goldstein, T. C. Sudhof, R. G. Anderson, D. W. Russell, and M. S. Brown.** 1987. Acid-dependent ligand dissociation and recycling of LDL receptor mediated by growth factor homology region. Nature **326:**760–765.
11. **Davis, M. P., G. Bottley, L. P. Beales, R. A. Killington, D. J. Rowlands, and T. J. Tuthill.** 2008. Recombinant VP4 of human rhinovirus induces permeability in model membranes. J. Virol. **82:**4169–4174.
12. **Dunn, K. W., and F. R. Maxfield.** 1992. Delivery of ligands from sorting endosomes to late endosomes occurs by maturation of sorting endosomes. J. Cell Biol. **117:**301–310.
13. **Fisher, C., N. Beglova, and S. C. Blacklow.** 2006. Structure of an LDLR-RAP complex reveals a general mode for ligand recognition by lipoprotein receptors. Mol. Cell **22:**277–283.
14. **Gerasimenko, J. V., A. V. Tepikin, O. H. Petersen, and O. V. Gerasimenko.** 1998. Calcium uptake via endocytosis with rapid release from acidifying endosomes. Curr. Biol. **8:**1335–1338.
15. **Ghosh, R. N., D. L. Gelman, and F. R. Maxfield.** 1994. Quantification of low density lipoprotein and transferrin endocytic sorting HEp2 cells using confocal microscopy. J. Cell Sci. **107:**2177–2189.
16. **Gruenberger, M., D. Pevear, G. D. Diana, E. Kuechler, and D. Blaas.** 1991. Stabilization of human rhinovirus serotype-2 against pH-induced conformational change by antiviral compounds. J. Gen. Virol. **72:**431–433.
17. **Harris, J. R., and V. R. Racaniello.** 2005. Amino acid changes in proteins 2B and 3A mediate rhinovirus type 39 growth in mouse cells. J. Virol. **79:**5363–5373.
18. **Hewat, E. A., and D. Blaas.** 2006. Nonneutralizing human rhinovirus serotype 2-specific monoclonal antibody 2G2 attaches to the region that undergoes the most dramatic changes upon release of the viral RNA. J. Virol. **80:**12398–12401.
19. **Huber, M., M. Brabec, N. Bayer, D. Blaas, and R. Fuchs.** 2001. Elevated endosomal pH in HeLa cells overexpressing mutant dynamin can affect infection by pH-sensitive viruses. Traffic **2:**727–736.
20. **Khan, A. G., J. Pichler, A. Rosemann, and D. Blaas.** 2007. Human rhinovirus type 54 infection via heparan sulfate is less efficient and strictly dependent on low endosomal pH. J. Virol. **81:**4625–4632.
21. **Kim, S., T. J. Smith, M. S. Chapman, M. G. Rossmann, D. C. Pevear, F. J. Dutko, P. J. Felock, G. D. Diana, and M. A. McKinlay.** 1989. Crystal structure of human rhinovirus serotype-1A (Hrv1A). J. Mol. Biol. **210:**91–111.
22. **Kingsley, D. M., and M. Krieger.** 1984. Receptor-mediated endocytosis of low density lipoprotein: somatic cell mutants define multiple genes required for expression of surface-receptor activity. Proc. Natl. Acad. Sci. USA **81:**5454–5458.
23. **Kistler, A., P. C. Avila, S. Rouskin, D. Wang, T. Ward, S. Yagi, D. Schnurr, D. Ganem, J. L. Derisi, and H. A. Boushey.** 2007. Pan-viral screening of respiratory tract infections in adults with and without asthma reveals unexpected human coronavirus and human rhinovirus diversity. J. Infect. Dis. **196:**817–825.
24. **Korant, B. D., K. Lonberg Holm, J. Noble, and J. T. Stasny.** 1972. Naturally occurring and artificially produced components of three rhinoviruses. Virology **48:**71–86.
25. **Krieger, M., M. S. Brown, and J. L. Goldstein.** 1981. Isolation of Chinese hamster cell mutants defective in the receptor-mediated endocytosis of low density lipoprotein. J. Mol. Biol. **150:**167–184.
26. **Lee, W. M., S. S. Monroe, and R. R. Rueckert.** 1993. Role of maturation cleavage in infectivity of picornaviruses: activation of an infectosome. J. Virol. **67:**2110–2122.
27. **Lomax, N. B., and F. H. Yin.** 1989. Evidence for the role of the P2 protein of human rhinovirus in its host range change. J. Virol. **63:**2396–2399.
28. **Lonberg Holm, K., L. B. Gosser, and E. J. Shimshick.** 1976. Interaction of liposomes with subviral particles of poliovirus type 2 and rhinovirus type 2. J. Virol. **19:**746–749.
29. **Martina, J. A., B. Lelouvier, and R. Puertollano.** 2009. The calcium channel mucolipin-3 is a novel regulator of trafficking along the endosomal pathway. Traffic **10:**1143–1156.
30. **Mayor, S., J. F. Presley, and F. R. Maxfield.** 1993. Sorting of membrane components from endosomes and subsequent recycling to the cell surface occurs by a bulk flow process. J. Cell Biol. **121:**1257–1269.
31. **Neubauer, C., L. Frasel, E. Kuechler, and D. Blaas.** 1987. Mechanism of entry of human rhinovirus 2 into HeLa cells. Virology **158:**255–258.
32. **Nicodemou, A., M. Petsch, T. Konecsni, L. Kremser, E. Kenndler, J. M. Casasnovas, and D. Blaas.** 2005. Rhinovirus-stabilizing activity of artificial VLDL-receptor variants defines a new mechanism for virus neutralization by soluble receptors. FEBS Lett. **579:**5507–5511.
33. **Nurani, G., B. Lindqvist, and J. M. Casasnovas.** 2003. Receptor priming of major group human rhinoviruses for uncoating and entry at mild low-pH environments. J. Virol. **77:**11985–11991.
34. **Prchla, E., E. Kuechler, D. Blaas, and R. Fuchs.** 1994. Uncoating of human rhinovirus serotype 2 from late endosomes. J. Virol. **68:**3713–3723.
35. **Prchla, E., C. Plank, E. Wagner, D. Blaas, and R. Fuchs.** 1995. Virus-mediated release of endosomal content in vitro: different behavior of adenovirus and rhinovirus serotype 2. J. Cell Biol. **131:**111–123.
36. **Querol-Audi, J., T. Konecsni, J. Pous, O. Carugo, I. Fita, N. Verdaguer, and D. Blaas.** 2009. Minor group human rhinovirus-receptor interactions: geometry of multimodular attachment and basis of recognition. FEBS Lett. **583:**235–240.
37. **Rudenko, G., L. Henry, K. Henderson, K. Ichtchenko, M. S. Brown, J. L. Goldstein, and J. Deisenhofer.** 2002. Structure of the LDL receptor extracellular domain at endosomal pH. Science **298:**2353–2358.
38. **Saito, M., P. I. Hanson, and P. Schlesinger.** 2007. Luminal chloride-dependent activation of endosome calcium channels: patch clamp study of enlarged endosomes. J. Biol. Chem. **282:**27327–27333.
39. **Schober, D., P. Kronenberger, E. Prchla, D. Blaas, and R. Fuchs.** 1998. Major and minor-receptor group human rhinoviruses penetrate from endosomes by different mechanisms. J. Virol. **72:**1354–1364.
40. **Skern, T., C. Neubauer, L. Frasel, P. Gruendler, W. Sommergruber, W. Zorn, E. Kuechler, and D. Blaas.** 1987. A neutralizing epitope on human rhinovirus type 2 includes amino acid residues between 153 and 164 of virus capsid protein VP2. J. Gen. Virol. **68:**315–323.
41. **Snyers, L., H. Zwickl, and D. Blaas.** 2003. Human rhinovirus type 2 is internalized by clathrin-mediated endocytosis. J. Virol. **77:**5360–5369.
42. **Sonawane, N. D., and A. S. Verkman.** 2003. Determinants of [Cl−] in recycling and late endosomes and Golgi complex measured using fluorescent ligands. J. Cell Biol. **160:**1129–1138.

43. **Tyrrell, D. A. J., and R. M. Chanock.** 1963. Rhinoviruses: a description. Science **141:**152–153.
44. **Uncapher, C. R., C. M. Dewitt, and R. J. Colonno.** 1991. The major and minor group receptor families contain all but one human rhinovirus serotype. Virology **180:**814–817.
45. **Verdaguer, N., I. Fita, M. Reithmayer, R. Moser, and D. Blaas.** 2004. X-ray structure of a minor group human rhinovirus bound to a fragment of its cellular receptor protein. Nat. Struct. Mol. Biol. **11:**429–434.
46. **Vlasak, M., M. Roivainen, M. Reithmayer, I. Goesler, P. Laine, L. Snyers, T. Hovi, and D. Blaas.** 2005. The minor receptor group of human rhinovirus (HRV) includes HRV23 and HRV25, but the presence of a lysine in the VP1 HI loop is not sufficient for receptor binding. J. Virol. **79:**7389–7395.
47. **Yin, F. H., and N. B. Lomax.** 1983. Host range mutants of human rhinovirus in which nonstructural proteins are altered. J. Virol. **48:**410–418.
48. **Zhao, Z., and P. Michaely.** 2008. The epidermal growth factor homology domain of the LDL receptor drives lipoprotein release through an allosteric mechanism involving H190, H562, and H586. J. Biol. Chem. **283:**26528–26537.